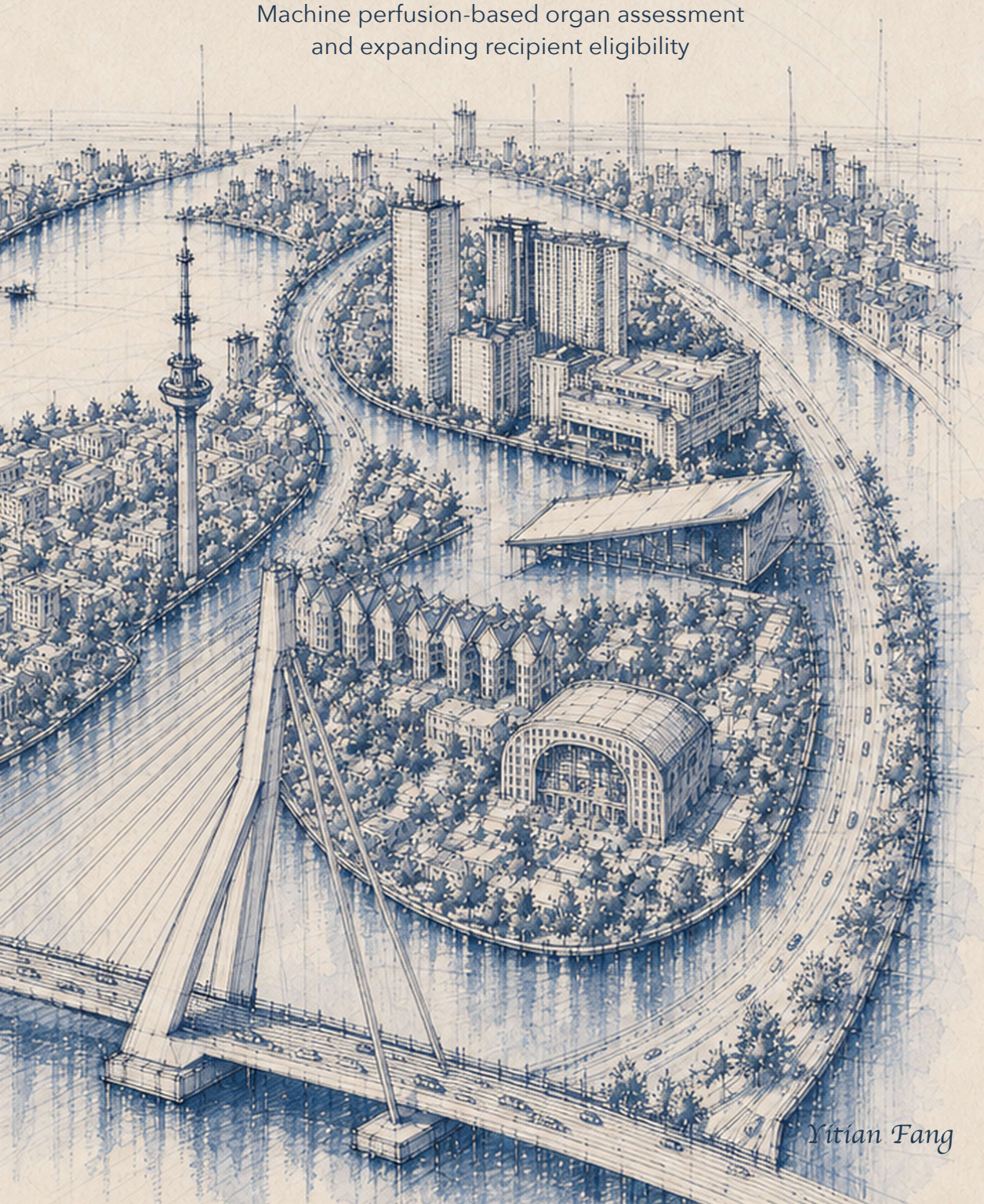
Optimizing Kidney Transplantation

Machine perfusion-based organ assessment
and expanding recipient eligibility



Yitian Fang

Propositions

to the thesis

Optimizing Kidney Transplantation

Machine perfusion-based organ assessment and expanding recipient eligibility

1. Normothermic machine perfusion should be regarded not only as a preservation technique, but as a dynamic assessment platform for donor organ quality. (this thesis)
2. Real-time imaging during machine perfusion may reduce reliance on static and subjective criteria in determining organ transplantability. (this thesis)
3. Marginal donor kidneys should not be discarded before their functional recovery potential has been assessed under near-physiological conditions. (this thesis)
4. Individualized assessment of comorbidities in recipients can help expand transplant eligibility beyond rigid contraindication-based decision-making. (this thesis)
5. Simultaneous liver-kidney transplantation should be considered for patients with severe renal dysfunction to justify the use of two scarce organs. (this thesis)
6. A good healthcare system should not be judged by the number of new technologies or publications, but by whether clinical innovation is appropriately indicated and responsibly implemented. (Daniels N, et al. BMJ. 2008)
7. The quality of healthcare should not depend on heroism, but on system reliability and effective teamwork. (National Academy of Medicine. 2013)
8. The aim of medical training is not to create medical "geniuses", but to ensure every doctor can practice independently and safely. (Haynes AB, et al. N Engl J Med. 2009)
9. Artificial intelligence in healthcare should serve patients and clinicians, not technological ambition. (WHO. 2021)
10. In scientific research, objectivity matters more than expectation. (Mlinarić A, et al. Biochem Med. 2017)
11. Football may start a scientific career, and turtle may sustain it.

Yitian Fang

August 2026

Optimizing Kidney Transplantation

Machine perfusion-based organ assessment and expanding recipient eligibility

Yitian Fang










Printing of this thesis was financially supported by Erasmus University Rotterdam, Department of Surgery, China Scholarship Council, Nederlandse Transplantatie Vereniging, XVIVO B.V., Chiesi Pharmaceuticals B.V., Medical Delta, and Chipsoft B.V.

Cover design: Yitian Fang by Codex
Layout: Yitian Fang
Printing: ProefschriftMaken
ISBN: 978-94-6534-626-7

© Copyright by Yitian Fang 2026. All rights reserved. No part of this thesis may be reproduced, stored in a retrieval system, or transmitted in any form or by any means, without prior permission of the author.

Optimizing Kidney Transplantation

Machine perfusion-based organ assessment and expanding recipient eligibility

Optimalisatie van niertransplantatie

Machineperfusie gebaseerde beoordeling van organen, en uitbreiding van ontvangercriteria

Thesis

to obtain the degree of Doctor from
Erasmus University Rotterdam
by command of the
rector magnificus

Prof.dr.ir. A.J. Schuit

and in accordance with the decision of the Doctorate Board.
The public defence shall be held on

Tuesday 10 November 2026
at 15:30 hrs
by

Yitian Fang
born in Suzhou, People's Republic of China.

Erasmus University Rotterdam



Doctoral Committee

Promotor:	Dr.ing. R.W.F. de Bruin
Co-promotor:	Dr. R.C. Minnee
Assessment committee:	Prof.dr. D.A. Hesselink
	Prof.dr. F.J.H. Gijsen
	Prof.dr. C.C. Baan

CONTENT

Chapter 1	General introduction	9
Part I Organ Quality Assessment During Machine Perfusion		
Chapter 2	Real-time laser speckle contrast imaging measurement during normothermic machine perfusion in pretransplant kidney assessment *Lasers in Surgery and Medicine, 2023*	29
Chapter 3	Pre-transplant kidney quality evaluation using photoacoustic imaging during normothermic machine perfusion *Photoacoustics, 2024*	49
Chapter 4	Enhancing kidney quality assessment: Power Doppler during normothermic machine perfusion *Artificial Organs, 2025*	73
Chapter 5	Physiological arterial pressure improves renal performance during normothermic machine perfusion in a porcine kidney DCD model *Heliyon, 2025*	93
Part II Clinical Practice in Kidney Transplantation		
Chapter 6	Bariatric surgery before and after kidney transplant: a propensity score-matched analysis *Surgery for Obesity and Related Diseases, 2023*	111
Chapter 7	Safety and efficacy of kidney transplantation in patients with aortoiliac stenosis: a retrospective cohort study *International Journal of Surgery, 2024*	131

Chapter 8	Simultaneous liver-kidney transplantation versus liver transplantation in end-stage liver disease patients with kidney dysfunction *European Surgical Research, 2025*	151
Chapter 9	Simultaneous liver-kidney versus liver transplantation categorized by pretransplant eGFR: Impact of the 2017 OPTN policy *Transplantation, 2026*	169
Chapter 10	Treatment of renal artery aneurysm by ex situ repair and autotransplantation: a nationwide cohort study. *European Surgical Research, 2024*	193
Chapter 11	Machine learning-driven assessment of early graft function in living donor kidney transplantation using intraoperative laser speckle contrast imaging *Submitted*	205
Chapter 12	General discussion and future perspectives	233
Appendices	Summary	248
	Samenvatting	252
	List of publications	257
	Acknowledgments	260
	PhD portfolio	268
	About the author	270

Chapter 1

General introduction

Introduction

Chronic kidney disease (CKD) is a significant global health challenge, affecting an estimated 700 million people worldwide. In 2017, the prevalence of CKD was estimated at 9.1%, contributing to approximately 1.2 million deaths.[1] Currently, CKD is the third fastest-growing cause of death globally and the only chronic disease exhibiting a continuous rise in age-adjusted mortality.[2]

The increasing burden of CKD is driven by population growth, aging, and the rising prevalence of hypertension, diabetes, and cardiovascular disease.[3] CKD is classified into 5 stages based on glomerular filtration rate (GFR), as shown in **Table 1**.[4] Once CKD progresses to stage 5, also known as end-stage renal disease (ESRD), either renal replacement therapy (peritoneal dialysis and hemodialysis) or kidney transplantation becomes necessary.

Table 1. CKD stages according to GFR

CKD stage	GFR (mL/min/1.73 m^2)	Terms
1	≥ 90	Normal or high
2	60-89	Mildly decreased[a]
3a	45-59	Mildly to moderately decreased
3b	30-44	Moderately to severely decreased
4	15-29	Severely decreased
5	< 15	Kidney failure

CKD, chronic kidney disease; GFR, glomerular filtration rate.
a. Relative to the young adult level. In the absence of evidence of kidney damage, neither G1 nor G2 fulfills the criteria for CKD.

Historical Perspective on Kidney Transplantation

The first successful kidney transplantation was performed in 1954 by Dr. Joseph Murray in Boston. This pioneering procedure involved genetically identical twins, thereby avoiding immune reaction.[5] In 1962, Murray led the first successful deceased donor kidney transplantation between genetically unrelated individuals, utilizing azathioprine for immunosuppression.[6] This landmark case marked the beginning of pharmacologically mediated transplant success.

With continuous advancements in surgical techniques and immunosuppressive therapy, kidney transplantation has become the preferred treatment for ESRD, offering lower mortality rates, reduced cardiovascular risk and improved quality of life compared to dialysis.[7-9] According to the 2024 United States Renal Data System (USRDS) Annual Data Report, the 5-year survival rates for patients who initiated dialysis for ESRD in 2018 were 40-50%, whereas the 5-year survival rates for kidney transplant recipients were 70-90%.[10]

Kidney Donor Classification

Kidney transplantation can be performed using organs from either living or deceased donors. Deceased donors are further categorized based on different criteria for determining death.

Donation after brain death (DBD): the donor is confirmed dead based on neurological criteria and cardiorespiratory support is maintained until organ procurement. Donation after circulatory death (DCD): the donor is confirmed death based on cardiorespiratory criteria before organ procurement.

Deceased donors are also classified as standard criteria donor (SCD) and extended criteria donor (ECD). ECD is defined as donors aged above 60 years without comorbidities or aged above 50 years with at least two risk factors among high blood pressure, death due to cerebrovascular accident, and serum creatinine level > 1.5 mg/dL. This classification reflects organ quality, with ECD kidneys exhibiting a 70% higher risk of graft failure and lower patient survival than SCD kidneys.[11, 12]

Global Shortage of Donor Kidneys

Despite advances in transplantation, there remains a severe imbalance between organ supply and demand. In the United States, the median waiting time for a deceased donor kidney transplant in 2023 was over 4 years.[13] According to the Organ Procurement and Transplantation Network (OPTN)/Scientific Registry of Transplant Recipients (SRTR) data, 141,886 adult candidates were on the kidney transplant waiting list in 2023, while only 27,351 kidney transplants were performed (**Figure 1**).[14] As a consequence of this organ

shortage, many candidates die while awaiting and others are removed from the waiting list because of becoming too sick to receive a transplant.

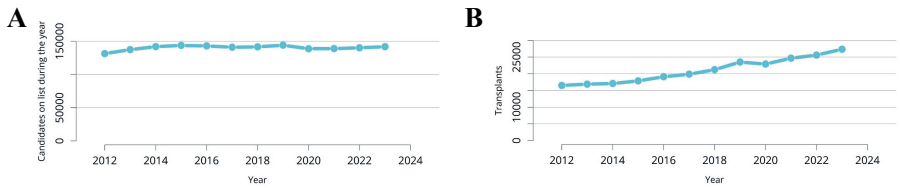


Figure 1. Total number of (A) adult candidates on the kidney transplant waiting list, and (B) adult kidney transplants.[14]

Extending the Use of Marginal Donor Kidneys

One possible solution to address the kidney shortage is increasing the use of marginal donor kidneys, which is being adopted by many countries. As shown in **Figure 2**, the recent rise in total adult kidney transplants is primarily attributed to the increased use of deceased donor kidneys, particularly from DCD donors and older donors (> 50 years).

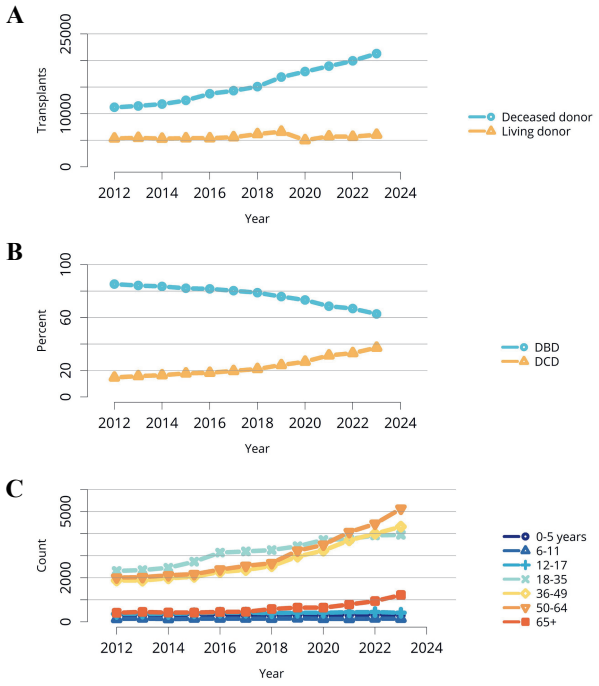


Figure 2. (A) Adult kidney transplants by donor type; (B) Distribution of deceased donors whose kidneys were recovered for transplant by donor type; (C) Deceased kidney donor count by age.[14]
DBD, donation after brain death; DCD, donation after circulatory death.

However, the use of marginal donor organs raises concerns regarding their functional and clinical outcomes. Aubert et al.[15] reported a significantly higher risk of graft loss in recipients of ECD kidneys compared to SCD kidneys. Similarly, a meta-analysis by Querard et al.[16] demonstrated superior patient and graft survival in recipients of SCD kidneys compared to SCD kidneys. Additionally, Van Ittersum et al.[17] found higher rates of death-censored graft failure and lower patient survival in recipients of ECD kidneys versus those who received SCD or living donor kidneys. These findings highlight the trade-off between increasing organ availability and ensuring acceptable post-transplant outcomes.

Candidate Selection for Kidney Transplantation

According to the Kidney Disease: Improving Global Outcomes (KDIGO) Clinical Practice Guidelines, all patients with CKD stages 4 and 5 (GFR < 30 ml/min/1.73 m^2) who are expected to progress to ESRD should be evaluated for kidney transplantation.[18] However, placement on the transplant waiting list is limited by individual comorbidities and prognosis. Several risk factors and comorbidities, such as include obesity, peripheral arterial disease, and liver disease, that influence an individual's suitability for transplantation are discussed in more detail below.[18]

Obesity

Obesity (BMI > 30 kg/m^2) presents technical challenges during implantation and is associated with an increased risk of post-transplant complications, making transplant eligibility in patients with obesity controversial.

Registry data indicate that kidney transplantation provides a significant survival advantage for this population compared to dialysis.[19, 20] However, patients with a BMI ≥ 40 kg/m^2 are less likely to experience survival benefit.[19] Several single-center studies suggest that transplant recipients with moderate to severe obesity have a higher incidence of wound infection, delayed graft function and post-transplant weight gain, although patient and graft survival rates remain unchanged.[21, 22] A paired study involving 28 pairs of obese and non-obese recipients who received kidneys from the same deceased donor found that obesity was associated with decreased 5-year graft survival.[23] In contrast, in a study where cardiovascular disease was rigorously screened prior to transplantation, five-year patient

and graft survival rates did not differ between obese and non-obese recipients, although wound complications were more frequent.[24] A large cohort study of 27,377 patients from the United Network for Organ Sharing (UNOS) database found that a BMI > 35 kg/m^2 was independently associated with an increased risk of delayed graft function, prolonged hospitalization, acute rejection and decreased overall graft survival.[25] Consequently, KDIGO guidelines recommend that patients with class II or class III obesity (BMI ≥ 35 kg/m^2) should be considered for weight loss interventions including dietary modification and bariatric surgery before kidney transplantation.

Peripheral Arterial Disease

Peripheral arterial disease (PAD) is highly prevalent among ESRD patients due to high rates of hypertension, diabetes mellitus, tobacco abuse, and disturbances in calcium-phosphorus metabolism. Population-based studies indicate that approximately 24% of dialysis-dependent patients have evidence of PAD based on non-invasive examination.[26] Among these patients, 24% present with clinical evidence (e.g., claudication, rest pain, or necrotic ulceration), 35% have an abnormal ankle-brachial index, and 46% have healthcare claims related to PAD.[18]

Advanced aortoiliac disease is considered a relative contraindication to kidney transplantation due to the technical challenges of vascular anastomosis, increased graft loss, and limited life expectancy.[27-32] However, studies suggest that despite these concerns, kidney transplantation remains beneficial for patients with PAD. Compared to dialysis, transplantation was associated with a 50% reduction in 5-year mortality.

Liver Disease

Since the implementation of the model of end-stage liver disease (MELD) system in 2002, the number of Simultaneous liver-kidney transplantation (SLKT) has increased by over 300%.[33] However, the decision to proceed with SLKT in patients with concurrent liver disease and CKD is complex, and practice is highly different worldwide. Despite the increasing demand for organ transplantation, the limited supply of donor organs remains a significant challenge for both single-organ and multi-organ transplant candidates.

Moreover, recent studies suggest that SLKT does not fully mitigate the influence of pretransplant CKD on post-liver transplant survival.[34]

In Europe, there is no standardized SLKT allocation policy. Within the Eurotransplant network, the Approved Combined Organ (ACO) designation applies to candidates requiring multi-organ transplants (e.g., lung-liver or lung-pancreas transplants), but does not apply to SLKT candidates. Instead, SLKT eligibility is primarily determined by MELD-based criteria, and varies across different countries and transplant centers.[35]

Organ Preservation

A donor organ of reliable quality is critical for successful transplantation. Organ preservation serves as the "supply line for organ transplantation", enabling time for organ allocation and transport, and recipient preparation. There are several organ preservation methods, including static cold storage (SCS), hypothermic machine perfusion (HMP), and normothermic machine perfusion (NMP).

Static Cold Storage

SCS remains the standard method for organ preservation in many countries due to its simplicity and effectiveness. The process involves flushing the kidney to remove donor blood, cooling it with a preservation solution at 0-4°C, and storing it on ice until transplantation (**Figure 3A**). SCS reduces the metabolic rate to approximately 5% of normal, thereby slowing tissue degradation. However, because this occurs in an anoxic environment, anerobic metabolism persists, leading to potential cellular damage.

A number of limitations are associated with SCS, including tissue damage induced by prolonged hypothermic preservation, difficulty in assessing donor organ viability, inevitable ischemia-reperfusion injury (IRI), and limited opportunity for organ repair.[36] These limitations are particularly concerning when preserving DCD and ECD kidneys, as prolonged cold storage is associated with a higher risk of graft failure.[37]

Hypothermic Machine Perfusion

HMP is increasingly being applied as an alternative to SCS, particularly for grafts obtained from nonoptimal donors. HMP involves flushing the kidney to remove blood before connecting it to a perfusion device that continuously circulates a cold preservation solution through the renal vasculature (**Figure 3B**). In the Netherlands, HMP has become the standard of care for preserving deceased donor kidneys.[38] Other European countries and the United States have also adopted HMP in clinical settings to investigate its efficacy.[39-42] Several studies have reported that HMP reduces the incidence of delayed graft function more effectively than SCS.[43-46] In clinical practice, although the benefits of HMP for preserving deceased donor kidneys remains unclear, multiple trials have demonstrated a small but significant advantage of HMP over SCS in short-term graft survival.[40, 43, 45-47]

Despite reduced metabolic needs, there is residual ongoing metabolism during hypothermic preservation. Therefore, hypoxia persists in both SCS and HMP as the preservation solution is not actively oxygenated. Recently, the addition of oxygen delivered during HMP offers potential in reducing ischemia reperfusion injury and improving early graft function during transplantation.[48, 49]

Normothermic Machine Perfusion

More recently, NMP has emerged as an alternative preservation technique. NMP utilizes pulsatile or centrifugal pump systems combined with membrane oxygenator to perfuse kidneys with warmed, oxygenated red cell-based solution (**Figure 3C**).[50] Unlike SCS and HMP, NMP maintains the kidney in a near-physiological state, allowing ex vivo restoration of organ function before transplantation.[51]

Currently, NMP remains in the exploratory phase. In preclinical studies, NMP has proven to be feasible for up to 24 or 48 hours in discarded human kidneys.[52, 53] This prolonged perfusion period provides opportunities for targeted therapeutic interventions to optimize organ viability.[54, 55] In clinical applications, Rijkse et al.[56] and Hosgood et al.[57] have demonstrated the safety of 1- to 2-hour NMP in deceased donor kidneys before transplantation, although the short-duration NMP did not significantly reduce the incidence of delayed graft function. Additionally, the increasing interest in NMP for kidney

preservation is also focused on its use as a device to assess the viability or quality of the kidney. Based on the macroscopic appearance, renal blood flow and urine production during NMP, studies indicate that initially declined kidneys were successfully transplanted.[58, 59]

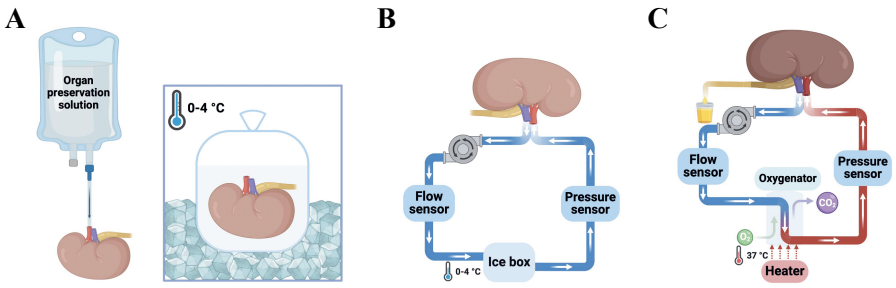


Figure 3. Schematics of (A) static cold storage (SCS), (B) hypothermic machine perfusion (HMP), and (C) normothermic machine perfusion (NMP).

Donor and Graft Quality Assessment

Suitability of a donor kidney for transplantation is influenced by several factors including donor age, renal function, medical history and histopathological findings. In addition to these clinical parameters, machine perfusion provides a diagnostic window to assess organ quality before transplantation.

Perfusion parameters such as renal blood flow and intrarenal resistance can serve as real-time indicators of kidney viability. Functional biomarkers, including creatinine clearance, fractional excretion of sodium, urine production, and cellular biomarkers, including neutrophil gelatinase lipocalin, aspartate aminotransferase, liver fatty acid binding protein and inflammatory cytokines (IL-6, IL-8, IL-18) could be helpful in determining the renal injury severity and predicting early graft outcomes.[58-61] Recently reported biomarkers, such as extracellular vesicles, microRNAs, and nanoparticles derived from blood or urine, have been investigated as potential indicators of microcirculatory function during NMP.[62, 63] However, no single perfusion parameter or biomarker is currently sensitive enough to fully predict organ quality and graft outcomes.

Perfusion Imaging Techniques

As perfusion enables delivering oxygen and nutrients to organs while removing waste products such as creatinine and other metabolites, it provides important diagnostic information on organ viability and functionality. Given the relatively high rate of graft failure in marginal donor kidneys, reliable imaging techniques are crucial for assessing organ quality, and microcirculation status, particularly during NMP before transplantation.

Laser Speckle Contrast Imaging

Laser speckle contrast imaging (LSCI) is an optical imaging technique that visualizes blood flow by analyzing the blurring effect of laser speckle patterns.[64] It operates by illuminating a scattering surface with coherent light and capturing the resulting speckle patterns using a photodetector, such as a complementary metal-oxide semiconductor (CMOS) camera (**Figure 4**). In biomedical use, the coherent light is typically the near-infrared light to ensure higher penetration depth. When scattering particles (e.g., red blood cell) move, the speckle pattern fluctuates, causing intensity variations that correlate with blood flow dynamics. Areas with greater movement appear more blurred over time.

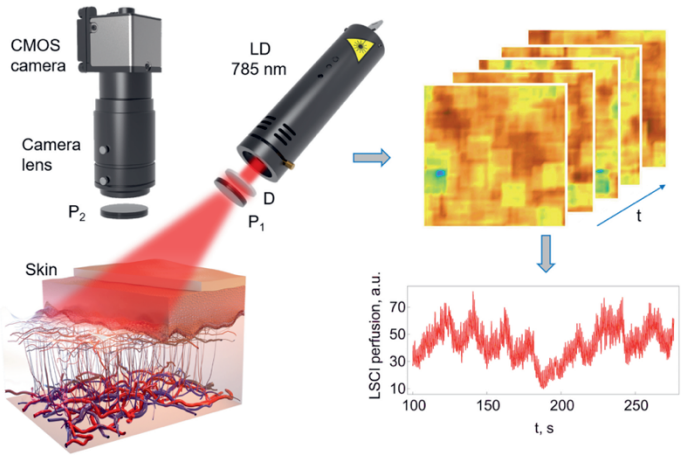


Figure 4. Schematics of the laser speckle contrast imaging (LSCI) setup and LSCI pattern plotted using the results averaged over the whole image.[65] CMOS, complementary metal-oxide semiconductor; D, diffuser; LD, laser diode; P1 and P2, linear polarizers.

The first biomedical application of LSCI was reported by Fercher and Biers in retinal blood flow measurement.[66] LSCI is now widely used in both preclinical and clinical settings to

assess vascular structure and microcirculation in burn wounds, cerebral blood flow, skin microvasculature, and other solid organs (**Figure 5**).[67, 68]

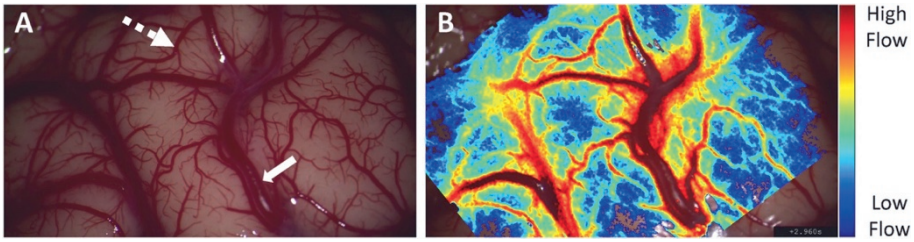


Figure 5. Example of the cortical flow assessment with laser speckle contrast imaging (LSCI). (A) Surgical microscope white light image of the surgical field of view; (B) Corresponding LSCI overlay image showing its ability to assess flow in large arteries (solid arrow) and small pial arteries (dotted arrow).[67]

Photoacoustic Imaging

Photoacoustic (PA) imaging is a hybrid imaging modality that uses short-pulsed electromagnetic radiation as an excitation source and detects the resulting ultrasound waves generated by photon absorption and thermoelastic expansion (**Figure 6**).[69]

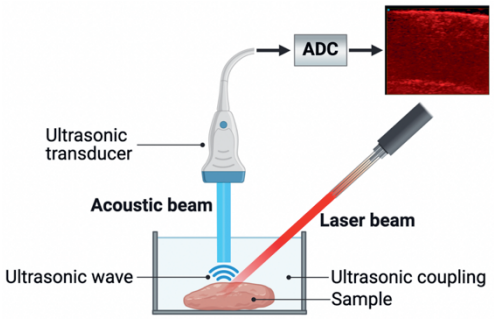


Figure 6. Schematics of the photoacoustic imaging setup.

The particular strength of PA imaging is that ultrasound waves undergo significantly less scattering and attenuation in biological tissues compared to light. Therefore, PA imaging achieves deeper tissue penetration and higher spatial resolution than traditional optical imaging methods.[70] Due to its non-ionizing nature, real-time imaging capability, and cost-effective integration with ultrasound systems, PA imaging is valuable for dynamic physiological monitoring and therapeutic outcome assessment.

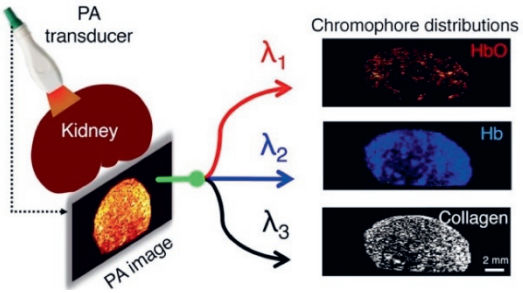


Figure 7. Example of photoacoustic (PA) images acquired at multiple wavelengths (λ) and individual distributions of oxygenated hemoglobin (HbO), deoxygenated hemoglobin (Hb), and collagen using spectral unmixing.

Additionally, PA imaging offers the ability to identify specific tissue components by delivering radiation at multiple wavelengths. Because different biological molecules have unique optical absorption spectra, PA imaging can distinguish and quantify different molecules such as oxygenated hemoglobin, deoxygenated hemoglobin, and collagen. This capability allows for analysis of blood oxygenation and tissue composition (**Figure 7**).[71]

Power Doppler

Doppler imaging is a widely used ultrasound-based technique that measures blood flow velocity by detecting shifts in the frequency of reflected sound waves. It is commonly applied in diagnosing vascular disease such as blood clots, arterial stenosis, reduced circulation, and heart valve abnormalities. Doppler imaging can be performed in spectral mode which measures the concentration of moving red blood cells, and color-flow mode which visualizes blood flow velocity.

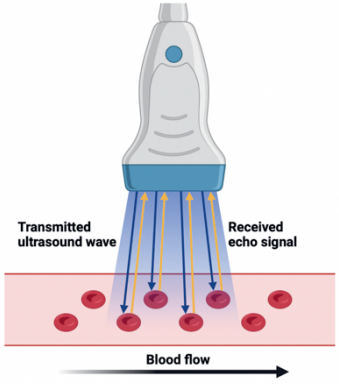


Figure 8. Schematics of Power Doppler imaging. The ultrasound probe sends ultrasound waves (blue arrows) that are reflected (orange arrows) after contact with moving red blood cells. The reflected signals change in frequency based on the motion of the cells.

Among these, Power Doppler (PD) is particularly advantageous for transplantation assessment. Compared to color-flow mode, PD detects blood flow intensity, making it more sensitive to low-flow perfusion. Additionally, PD is independent of Doppler angle, reducing operator dependency and improving measurement reliability. It is also less affected by aliasing artifacts, providing clearer visualization of microvascular flow (**Figure 8**).

Aim and Outline of This Thesis

This thesis investigates kidney quality assessment using NMP from an experimental perspective, and explores the safety and eligibility criteria of kidney transplant recipients from a clinical perspective. The aim of this thesis is to develop diverse and objective methods for donor kidney assessment, extend eligibility criteria for kidney transplant recipients, and optimize kidney allocation policies to improve transplantation outcomes.

Part I focuses on pre-clinical research using a kidney NMP model. This part explores the value of novel imaging techniques in kidney quality assessment, the impact of arterial perfusion pressure on kidney function, and the effectiveness of an objective scoring system for determining kidney transplantability.

Chapter 2 builds on the master thesis of van Ooijen.[72] This chapter investigates the value of LSCI in visualizing renal cortical perfusion and compares dual-side LSCI measurements with single aspect measurements to assess their added value.

Chapter 3 and **4** introduce a combined NMP and PA setup integrated with an ultrasound system. These chapters respectively assess the utility of PA imaging in measuring renal cortical oxygenation, and PD imaging in measuring blood flow intensity.

Chapter 5 investigates the impact of sub-physiological, physiological, and high-physiological arterial perfusion pressures on kidney function and injury during NMP. This chapter determines the optimal perfusion pressure for salvaging marginal kidneys deemed functionally insufficient under subphysiological perfusion conditions.

Part II focuses on clinical research investigating the safety and feasibility of kidney transplantation in patients with controversial comorbidities. This part pushes the boundaries of transplant eligibility criteria to increase the number of recipients who can benefit from kidney transplantation.

Chapter 6 examines the eligibility of ESRD patients with obesity for kidney transplantation. This chapter assesses short- and long-term outcomes in patients who

underwent both kidney transplantation and bariatric surgery to determine the optimal timing of bariatric surgery for this population.

Chapter 7 evaluates the safety and feasibility of kidney transplantation in ESRD patients with aortoiliac stenosis. This chapter analyzes clinical outcomes based on stenosis severity to support clinical decision-making in this population.

Chapter 8 and **9** investigates the efficacy of SLKT for patients with concurrent liver failure and kidney dysfunction. These chapters compare transplant outcomes between SLKT patients and liver transplant alone patients to refine SLKT eligibility criteria using Dutch Organ Transplantation Registration and OPTN/UNOS data, respectively.

Chapter 10 examines the feasibility of kidney autotransplantation in patients with renal artery aneurysm. This chapter presents a nationwide cohort on ex situ renal artery aneurysm repairs with autotransplantation to demonstrate its potential in preserving residual renal function and avoid retransplantation.

Chapter 11 introduces a novel approach that integrates intraoperative LSCI with machine learning to predict early graft function in living donor kidney transplantation. This chapter investigates the additional value of convolutional neural network-derived perfusion features in early risk stratification compared with clinical assessment alone.

Chapter 12 provides a general discussion of this thesis. This chapter synthesizes the key findings across experimental and clinical studies and highlight strategies for extending transplant eligibility, enhancing kidney quality assessment and envision future perspectives such as organ recondition through NMP and centralized organ hubs to optimize transplant outcomes.

Reference

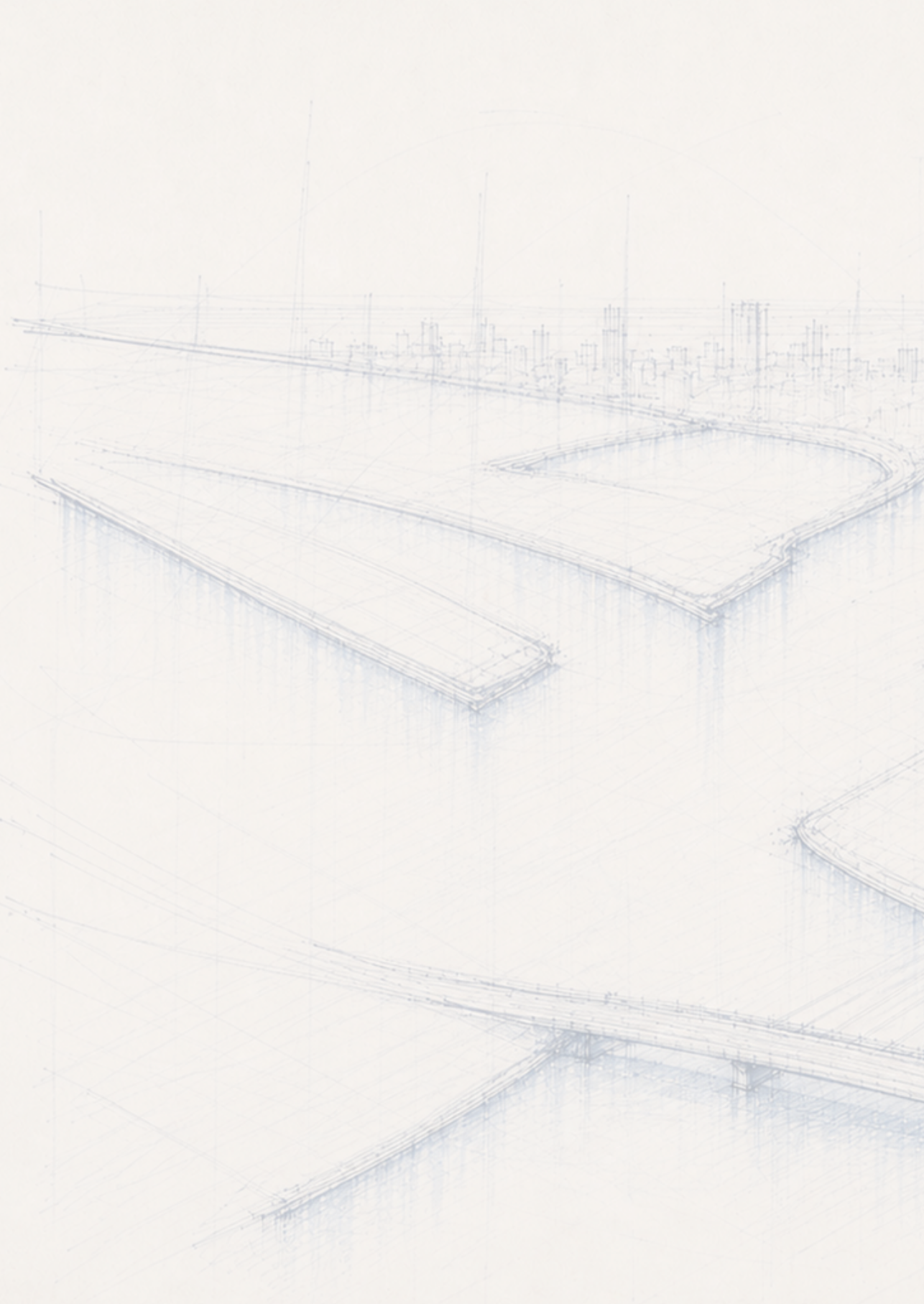
1. Collaboration GBDCKD. Global, regional, and national burden of chronic kidney disease, 1990-2017: a systematic analysis for the Global Burden of Disease Study 2017. Lancet. 2020;395(10225):709-33.
2. Francis A, Harhay MN, Ong ACM, Tummalapalli SL, Ortiz A, Fogo AB, et al. Chronic kidney disease and the global public health agenda: an international consensus. Nat Rev Nephrol. 2024;20(7):473-85.
3. Couser WG, Remuzzi G, Mendis S, Tonelli M. The contribution of chronic kidney disease to the global burden of major noncommunicable diseases. Kidney Int. 2011;80(12):1258-70.
4. Kidney Disease: Improving Global Outcomes CKDWG. KDIGO 2024 Clinical Practice Guideline for the Evaluation and Management of Chronic Kidney Disease. Kidney Int. 2024;105(4S):S117-S314.
5. Guild WR, Harrison JH, Merrill JP, Murray J. Successful homotransplantation of the kidney in an identical twin. Trans Am Clin Climatol Assoc. 1955;67:167-73.
6. Murray JE, Merrill JP, Harrison JH, Wilson RE, Dammin GJ. Prolonged survival of human-kidney homografts by immunosuppressive drug therapy. N Engl J Med. 1963;268:1315-23.
7. Tonelli M, Wiebe N, Knoll G, Bello A, Browne S, Jadhav D, et al. Systematic review: kidney transplantation compared with dialysis in clinically relevant outcomes. Am J Transplant. 2011;11(10):2093-109.
8. Boenink R, Astley ME, Huijben JA, Stel VS, Kerschbaum J, Ots-Rosenberg M, et al. The ERA Registry Annual Report 2019: summary and age comparisons. Clin Kidney J. 2022;15(3):452-72.
9. Hussien H, Apetrii M, Covic A. Health-related quality of life in patients with chronic kidney disease. Expert Rev Pharmacoecon Outcomes Res. 2021;21(1):43-54.
10. United States Renal Data System. 2024 USRDS Annual Data Report: Epidemiology of kidney disease in the United States. National Institutes of Health, National Institute of Diabetes and Digestive and Kidney Diseases, Bethesda, MD, 2024.
11. Metzger RA, Delmonico FL, Feng S, Port FK, Wynn JJ, Merion RM. Expanded criteria donors for kidney transplantation. Am J Transplant. 2003;3 Suppl 4:114-25.
12. Querard AH, Foucher Y, Combescure C, Dantan E, Larmet D, Lorent M, et al. Comparison of survival outcomes between Expanded Criteria Donor and Standard Criteria Donor kidney transplant recipients: a systematic review and meta-analysis. Transplant International. 2016;29(4):403-15.
13. Stewart D, Mupfudze T, Klassen D. Does anybody really know what (the kidney median waiting) time is? Am J Transplant. 2023;23(2):223-31.
14. Lentine KL, Smith JM, Lyden GR, Miller JM, Booker SE, Dolan TG, et al. OPTN/SRTR 2023 Annual Data Report: Kidney. Am J Transplant. 2025;25(2S1):S22-S137.
15. Aubert O, Kamar N, Vernerey D, Viglietti D, Martinez F, Duong-Van-Huyen JP, et al. Long term outcomes of transplantation using kidneys from expanded criteria donors: prospective, population based cohort study. BMJ. 2015;351:h3557.
16. Querard AH, Foucher Y, Combescure C, Dantan E, Larmet D, Lorent M, et al. Comparison of survival outcomes between Expanded Criteria Donor and Standard Criteria Donor kidney transplant recipients: a systematic review and meta-analysis. Transpl Int. 2016;29(4):403-15.
17. van Ittersum FJ, Hemke AC, Dekker FW, Hilbrands LB, Christiaans MH, Roodnat JI, et al. Increased risk of graft failure and mortality in Dutch recipients receiving an expanded criteria donor kidney transplant. Transpl Int. 2017;30(1):14-28.
18. Chadban SJ, Ahn C, Axelrod DA, Foster BJ, Kasiske BL, Kher V, et al. KDIGO Clinical Practice Guideline on the Evaluation and Management of Candidates for Kidney Transplantation. Transplantation. 2020;104(4S1 Suppl 1):S11-S103.
19. Gill JS, Lan J, Dong J, Rose C, Hendren E, Johnston O, et al. The survival benefit of kidney transplantation in obese patients. Am J Transplant. 2013;13(8):2083-90.
20. Krishnan N, Higgins R, Short A, Zehnder D, Pitcher D, Hudson A, et al. Kidney Transplantation Significantly Improves Patient and Graft Survival Irrespective of BMI: A Cohort Study. American Journal of Transplantation. 2015;15(9):2378-86.
21. Howard RJ, Thai VB, Patton PR, Hemming AW, Reed AI, Van der Werf WJ, et al. Obese kidney transplant recipients have good outcomes. Transplant P. 2001;33(7-8):3420-1.
22. Lynch RJ, Ranney DN, Shijie C, Lee DS, Samala N, Englesbe MJ. Obesity, surgical site infection, and outcome following renal transplantation. Ann Surg. 2009;250(6):1014-20.
23. Yamamoto S, Hanley E, Hahn AB, Isenberg A, Singh TP, Cohen D, et al. The impact of obesity in renal transplantation: an analysis of paired cadaver kidneys. Clin Transplant. 2002;16(4):252-6.
24. Johnson DW, Isbel NM, Brown AM, Kay TD, Franzen K, Hawley CM, et al. The effect of obesity on renal transplant outcomes. Transplantation. 2002;74(5):675-81.
25. Gore JL, Pham PT, Danovitch GM, Wilkinson AH, Rosenthal JT, Lipshutz GS, et al. Obesity and outcome following renal transplantation. Am J Transplant. 2006;6(2):357-63.

26. Jones DW, Dansey K, Hamdan AD. Lower Extremity Revascularization in End-Stage Renal Disease. Vasc Endovascular Surg. 2016;50(8):582-5.
27. Tozzi M, Franchin M, Soldini G, Ietto G, Chiappa C, Molteni B, et al. Treatment of aortoiliac occlusive or dilatative disease concomitant with kidney transplantation: how and when? Int J Surg. 2013;11 Suppl 1:S115-9.
28. Ozcelik A, Treckmann J, Paul A, Witzke O, Sotiropoulos G, Nadalin S, et al. Results of kidney transplantation with simultaneous implantation of vascular graft. Transplant Proc. 2007;39(2):509-10.
29. Tsivian M, Neri F, Nardo B, Bertelli R, Cavallari G, Fuga G, et al. Aortoiliac surgery concomitant with kidney transplantation: a single center experience. Clin Transplant. 2009;23(2):164-7.
30. Liew YP, Bartholomew JR, Demirjian S, Michaels J, Schreiber MJ, Jr. Combined effect of chronic kidney disease and peripheral arterial disease on all-cause mortality in a high-risk population. Clin J Am Soc Nephrol. 2008;3(4):1084-9.
31. Rajagopalan S, Dellegrottaglie S, Furniss AL, Gillespie BW, Satayathum S, Lameire N, et al. Peripheral arterial disease in patients with end-stage renal disease: observations from the Dialysis Outcomes and Practice Patterns Study (DOPPS). Circulation. 2006;114(18):1914-22.
32. Brar A, Jindal RM, Elster EA, Tedla F, John D, Sumrani N, et al. Effect of peripheral vascular disease on kidney allograft outcomes: a study of U.S. Renal data system. Transplantation. 2013;95(6):810-5.
33. Eason JD, Gonwa TA, Davis CL, Sung RS, Gerber D, Bloom RD. Proceedings of Consensus Conference on Simultaneous Liver Kidney Transplantation (SLK). Am J Transplant. 2008;8(11):2243-51.
34. Cullaro G, Verna EC, Lee BP, Lai JC. Chronic Kidney Disease in Liver Transplant Candidates: A Rising Burden Impacting Post-Liver Transplant Outcomes. Liver Transpl. 2020;26(4):498-506.
35. Eurotransplant Liver Allocation System. In: Eurotransplant, editor. 2022.
36. Chouchani ET, Pell VR, Gaude E, Aksentijevic D, Sundier SY, Robb EL, et al. Ischaemic accumulation of succinate controls reperfusion injury through mitochondrial ROS. Nature. 2014;515(7527):431-+.
37. Summers DM, Johnson RJ, Hudson A, Collett D, Watson CJ, Bradley JA. Effect of donor age and cold storage time on outcome in recipients of kidneys donated after circulatory death in the UK: a cohort study. Lancet. 2013;381(9868):727-34.
38. Brat A, de Vries KM, van Heurn EWE, Huurman VAL, de Jongh W, Leuvenink HGD, et al. Hypothermic Machine Perfusion as a National Standard Preservation Method for Deceased Donor Kidneys. Transplantation. 2022;106(5):1043-50.
39. Watson CJ, Wells AC, Roberts RJ, Akoh JA, Friend PJ, Akyol M, et al. Cold machine perfusion versus static cold storage of kidneys donated after cardiac death: a UK multicenter randomized controlled trial. Am J Transplant. 2010;10(9):1991-9.
40. Treckmann J, Moers C, Smits JM, Gallinat A, Maathuis MH, van Kasterop-Kutz M, et al. Machine perfusion versus cold storage for preservation of kidneys from expanded criteria donors after brain death. Transpl Int. 2011;24(6):548-54.
41. Summers DM, Ahmad N, Randle LV, O'Sullivan AM, Johnson RJ, Collett D, et al. Cold Pulsatile Machine Perfusion Versus Static Cold Storage for Kidneys Donated After Circulatory Death: A Multicenter Randomized Controlled Trial. Transplantation. 2020;104(5):1019-25.
42. Cannon RM, Brock GN, Garrison RN, Smith JW, Marvin MR, Franklin GA. To pump or not to pump: a comparison of machine perfusion vs cold storage for deceased donor kidney transplantation. J Am Coll Surg. 2013;216(4):625-33; discussion 33-4.
43. Moers C, Pirenne J, Paul A, Ploeg RJ, Machine Preservation Trial Study G. Machine perfusion or cold storage in deceased-donor kidney transplantation. N Engl J Med. 2012;366(8):770-1.
44. Tedesco-Silva HJ, Mello Offerni JC, Ayres Carneiro V, Ivani de Paula M, Neto ED, Brambate Carvalhinho Lemos F, et al. Randomized Trial of Machine Perfusion Versus Cold Storage in Recipients of Deceased Donor Kidney Transplants With High Incidence of Delayed Graft Function. Transplant Direct. 2017;3(5):e155.
45. Wang W, Xie D, Hu X, Yin H, Liu H, Zhang X. Effect of Hypothermic Machine Perfusion on the Preservation of Kidneys Donated After Cardiac Death: A Single-Center, Randomized, Controlled Trial. Artif Organs. 2017;41(8):753-8.
46. Zhong Z, Lan J, Ye S, Liu Z, Fan L, Zhang Y, et al. Outcome Improvement for Hypothermic Machine Perfusion Versus Cold Storage for Kidneys From Cardiac Death Donors. Artif Organs. 2017;41(7):647-53.
47. Jochmans I, Moers C, Smits JM, Leuvenink HG, Treckmann J, Paul A, et al. Machine perfusion versus cold storage for the preservation of kidneys donated after cardiac death: a multicenter, randomized, controlled trial. Ann Surg. 2010;252(5):756-64.
48. Ravaioli M, De Pace V, Angeletti A, Comai G, Vasuri F, Baldassarre M, et al. Hypothermic Oxygenated New Machine Perfusion System in Liver and Kidney Transplantation of Extended Criteria Donors:First Italian Clinical Trial. Sci Rep. 2020;10(1):6063.

49. Meister FA, Czigany Z, Rietzler K, Miller H, Reichelt S, Liu WJ, et al. Decrease of renal resistance during hypothermic oxygenated machine perfusion is associated with early allograft function in extended criteria donation kidney transplantation. Sci Rep-Uk. 2020;10(1).
50. Hosgood SA, Nicholson ML. First in man renal transplantation after ex vivo normothermic perfusion. Transplantation. 2011;92(7):735-8.
51. Bagul A, Hosgood SA, Kaushik M, Kay MD, Waller HL, Nicholson ML. Experimental renal preservation by normothermic resuscitation perfusion with autologous blood. Br J Surg. 2008;95(1):111-8.
52. Weissenbacher A, Lo Faro L, Boubriak O, Soares MF, Roberts IS, Hunter JP, et al. Twenty-four-hour normothermic perfusion of discarded human kidneys with urine recirculation. Am J Transplant. 2019;19(1):178-92.
53. Messner F, Soleiman A, Ofner D, Neuwirt H, Schneeberger S, Weissenbacher A. 48 h Normothermic Machine Perfusion With Urine Recirculation for Discarded Human Kidney Grafts. Transpl Int. 2023;36:11804.
54. Thompson ER, Bates L, Ibrahim IK, Sewpaul A, Stenberg B, McNeill A, et al. Novel delivery of cellular therapy to reduce ischemia reperfusion injury in kidney transplantation. Am J Transplant. 2021;21(4):1402-14.
55. Thompson ER, Sewpaul A, Figuereido R, Bates L, Tingle SJ, Ferdinand JR, et al. MicroRNA antagonist therapy during normothermic machine perfusion of donor kidneys. Am J Transplant. 2022;22(4):1088-100.
56. Rijkse E, de Jonge J, Kimenai H, Hoogduijn MJ, de Bruin RWF, van den Hoogen MWF, et al. Safety and feasibility of 2 h of normothermic machine perfusion of donor kidneys in the Eurotransplant Senior Program. BJS Open. 2021;5(1).
57. Hosgood SA, Callaghan CJ, Wilson CH, Smith L, Mullings J, Mehew J, et al. Normothermic machine perfusion versus static cold storage in donation after circulatory death kidney transplantation: a randomized controlled trial. Nat Med. 2023;29(6):1511-9.
58. Hosgood SA, Barlow AD, Hunter JP, Nicholson ML. Ex vivo normothermic perfusion for quality assessment of marginal donor kidney transplants. Br J Surg. 2015;102(11):1433-40.
59. Hosgood SA, Thompson E, Moore T, Wilson CH, Nicholson ML. Normothermic machine perfusion for the assessment and transplantation of declined human kidneys from donation after circulatory death donors. Br J Surg. 2018;105(4):388-94.
60. Kaths JM, Hamar M, Echeverri J, Linares I, Urbanellis P, Cen JY, et al. Normothermic ex vivo kidney perfusion for graft quality assessment prior to transplantation. Am J Transplant. 2018;18(3):580-9.
61. Hosgood SA, Brown RJ, Nicholson ML. Advances in Kidney Preservation Techniques and Their Application in Clinical Practice. Transplantation. 2021;105(11):E202-E14.
62. Woud WW, Merino A, Hoogduijn MJ, Boer K, van den Hoogen MWF, Baan CC, et al. Nanoparticle Release by Extended Criteria Donor Kidneys During Normothermic Machine Perfusion. Transplantation. 2019;103(5):e110-e1.
63. Rigalli JP, Barros ER, Sommers V, Bindels RJM, Hoenderop JGJ. Novel Aspects of Extracellular Vesicles in the Regulation of Renal Physiological and Pathophysiological Processes. Front Cell Dev Biol. 2020;8:244.
64. Senarathna J, Rege A, Li N, Thakor NV. Laser Speckle Contrast Imaging: theory, instrumentation and applications. IEEE Rev Biomed Eng. 2013;6:99-110.
65. Mizeva I, Potapova E, Dremin V, Kozlov I, Dunaev A. Spatial heterogeneity of cutaneous blood flow respiratory-related oscillations quantified via laser speckle contrast imaging. PLoS One. 2021;16(5):e0252296.
66. Fercher AF, Briers JD. Flow Visualization by Means of Single-Exposure Speckle Photography. Opt Commun. 1981;37(5):326-30.
67. Dimanche A, Goldberg J, Miller DR, Bervini D, Raabe A, Dunn AK. Laser speckle contrast imaging versus microvascular Doppler sonography in aneurysm surgery: A prospective study. World Neurosurg X. 2024;23:100377.
68. Dijkstra A, Guven G, van Baar ME, Trommel N, Hofland HWC, Kuijper TM, et al. Laser speckle contrast imaging, an alternative to laser doppler imaging in clinical practice of burn wound care derivation of a color code. Burns. 2023;49(8):1907-15.
69. Beard P. Biomedical photoacoustic imaging. Interface Focus. 2011;1(4):602-31.
70. Manohar S, Razansky D. Photoacoustics: a historical review. Adv Opt Photonics. 2016;8(4):586-617.
71. Hysi E, He X, Fadhel MN, Zhang T, Krizova A, Ordon M, et al. Photoacoustic imaging of kidney fibrosis for assessing pretransplant organ quality. JCI Insight. 2020;5(10).
72. van Ooijen LS. Three-dimensional visualization of the renal microcirculation using laser speckle contrast imaging [Master thesis]: TU Delft; 2022.

Part I

Organ Quality Assessment During Machine Perfusion



Chapter 2

Real-time laser speckle contrast imaging measurement during normothermic machine perfusion in pre-transplant kidney assessment

Yitian Fang, Lisanne van Ooijen, Gisela Ambagtsheer, Anton V. Nikolaev, Marian C. Clahsen-van Groningen, Jenny Dankelman, Ron W.F. de Bruin, Robert C. Minnee

Lasers in Surgery and Medicine, 2023

Abstract

Objectives Normothermic machine perfusion (NMP) provides a platform for pre-transplant kidney quality assessment that is essential for the use of marginal donor kidneys. Laser speckle contrast imaging (LSCI) presents distinct advantages as a real-time and non-contact imaging technique for measuring microcirculation. In this study, we aimed to assess the value of LSCI in visualizing renal cortical perfusion and investigate the additional value of dual-side LSCI measurements compared to single aspect measurement during NMP.

Methods Porcine kidneys were obtained from a slaughterhouse and then underwent NMP. LSCI was used to measure one-sided cortical perfusion in the first 100 minutes of NMP. Thereafter, the inferior renal artery branch was occluded to induce partial ischemia and LSCI measurements on both ventral and dorsal sides were performed.

Results LSCI fluxes correlated linearly with the renal blood flow (R^2=0.90, p<0.001). After renal artery branch occlusion, absence of renal cortical perfusion could be visualized and semi-quantified by LSCI. The overall ischemic area percentage of the ventral and dorsal sides was comparable (median [IQR], 38 [24-43]% versus 29 [17-46]%, p=0.43), but heterogenous patterns between the two aspects were observed. There was a significant difference in oxygen consumption (mean ± SD, 2.57 ± 0.63 versus 1.83 ± 0.49 mLO_2/min/100g, p<0.001), urine output (median [IQR], 1.3 [1.1-1.7] versus 0.8 [0.6-1.3] mL/min, p<0.05), LDH (mean ± SD, 768 ± 370 versus 905 ± 401 U/L, p<0.05) and AST (mean ± SD, 352 ± 285 versus 462 ± 383 U/L, p<0.01) before and after renal artery occlusion, while no significant difference was found in creatinine clearance, fractional excretion of sodium, total sodium reabsorption and histological damage.

Conclusions LSCI fluxes correlated linearly with renal blood flow during NMP. Renal cortical microcirculation and absent perfusion can be visualized and semi-quantified by LSCI. It provides a relative understanding of perfusion levels, allowing for a qualitative comparison between regions in the kidney. Dual-side LSCI measurements are of added value compared to single aspect measurement and renal function markers.

Introduction

Kidney transplantation is the optimal treatment for patients with end stage renal disease (ESRD).[1] However, due to the shortage of organs, expanded criteria donor (ECD) and donation after circulatory death (DCD) kidneys are increasingly being used to enlarge the donor pool.[2, 3] Unfortunately, a significant proportion of ECD and DCD kidneys are associated with impaired function and graft failure.[2, 4] To improve clinical outcomes after transplantation, normothermic machine perfusion (NMP) has emerged as a viable platform for graft quality assessment by simulating the body's environment, which is essential for the use of these marginal donor kidneys.[5] Using imaging techniques during NMP is a potentially relevant, but poorly explored field to assess graft quality. Laser speckle contrast imaging (LSCI), as a real-time, non-contact, full-field imaging technique with a large field of view, has gained interest as an imaging technique for evaluating microvascular circulation of various tissues, such as retina, cerebrum, skin and liver.[6-10] Despite extensive research on LSCI, few studies have explored its potential as kidney quality assessment tool. The only study that has used LSCI to measure the kidney during NMP, conducted by Heeman et al.[11], showed that one-sided measurement can assess cortical microcirculation and detect perfusion deficits. However, it is unknown whether there is heterogeneity of microcirculation between the ventral and dorsal aspects. Therefore, in this study, we aimed to investigate the value of LSCI in the assessment of renal cortical perfusion and determine the potential added value of measuring perfusion across the entire kidney surface. Additionally, we explored the added value of LSCI compared to standard clinical flow and functional parameters during NMP.

Materials and Methods

Animal Model

Porcine kidneys (n=10) from the slaughterhouse were used. Kidneys were obtained from female landrace pigs weighing 100~120kg at a local slaughterhouse. These kidneys were procured to mimic the DCD donor procedure.[12] At the same time, two liters of blood from the same pig were collected in a bucket containing 25000 IU of heparin (LEO Pharma A/S, Ballerup, Denmark). After cannulating the renal artery with a 5-mm straight cannula (Organ Recovery Systems, Itasca, USA), kidneys were flushed with 4°C Ringer's lactate (Baxter

BV, Utrecht, the Netherlands). Next, the kidneys were placed inside the LifePort Kidney Transporter 1.0 (Organ Recovery Systems, Itasca, USA) and perfused at 30 mmHg with 4°C Belzer UW machine perfusion solution (Belzer MPS, Bridge to Life Ltd., London, UK) until NMP. The estimated time from kidney procurement to NMP ranged from 24 to 36 hours. As we used the standard organ preservation method in the Netherlands, no significant impact was anticipated on our research outcomes. Warm ischemia time (WIT) was calculated from the end of blood collection until the beginning of cold solution flushing. As the kidneys were from pigs slaughtered for meat consumption, no approval from the animal ethics committee was required.

Study Design

The study consists of two distinct parts: reperfusion measurement and dual-side measurements. Prior to NMP, LSCI was used to obtain baseline fluxes of the kidneys without perfusion. The kidneys were then subjected to NMP, and LSCI measurement was performed on ventral side only at 10-minute intervals for 100 minutes. The kidneys were continuously perfused until the renal blood flow stabilized, followed by dual-side measurements. To achieve this, the ventral side measurement was performed while the kidney was placed in the reservoir with the ventral side facing upwards. Subsequently, the dorsal side measurement was performed after manually turning over the kidney. After measuring both sides, the inferior branch of the renal artery was occluded by vascular clamps or ligation to induce renal infarction. The dual-side measurements were then repeated one time, when the hemodynamics regained stability.

Normothermic Machine Perfusion

After the cold preservation period, kidneys were flushed with 200mL cold Ringer's lactate (Baxter, Utrecht, The Netherlands) prior to ex vivo NMP. The NMP system consists of a custom-made organ chamber, a centrifugal pump head (BPX-80 Bio-Pump™ Plus, Medtronic, Minneapolis, MN, USA) equipped with pump drive (BVP-BP, Harvard Apparatus, Germany), an oxygenator with heat exchanger (Hilite 1000, Medos, Germany) and a thermocirculator (E100, Lauda, Germany). The flow probe (73-4755, Harvard Apparatus, Germany) was positioned in-line and the pressure transducer (APT300, Harvard Apparatus, Germany) was directly connected to the renal artery cannula (Organ Recovery

Systems, Itasca, USA). The set-up was controlled by a commercially available electronic controller (PLUGSYS Servo Controller for Perfusion, Harvard Apparatus, Germany) which enables both flow and pressure-directed perfusion. The kidneys were perfused with autologous leukocyte depleted (leukocyte filter BioR 02 plus BS PF, Fresenius Kabi, Zeist, the Netherlands) blood-based solution (**Table S1**) at 37°C with a controlled pressure of 70mmHg.[12] During NMP, carbogen (95% O_2 and 5% CO_2) was supplied via the oxygenator at a flow rate of 500mL/min. Each kidney was weighed both before and after NMP.

LSCI Measurement

A commercially available LSCI system with a laser wavelength of 785 nm (MoorO_2Flo; Moor Instruments Ltd., Axminster, UK) was placed above the kidney (**Figure 1**). The exposure time was 20 milliseconds and spatial resolution was 3.9 microns per pixel. The working distance between the camera and the kidney was 20 cm to ensure the kidney was in the field of view. To perform LSCI, an opaque cover was placed over the setup to block all ambient light. To test the definition of LSCI, the images of four kidneys were processed in low resolution mode (116×150 pixels), and the remaining 6 kidneys were in high resolution mode (576×748 pixels). The processing algorithm was the same in each case and the only difference is the pixel resolution of the resulting images. Image frames were recorded at the rate of 20 Hz. Each measurement lasted for 10 seconds and 201 frames were recorded in total. The whole kidney was chosen as the region of interest (ROI) for further analyses. The measure mode is spatial with a kernel size of 5×5 pixels to calculate the speckle contrast K using the equation:

$$K = \frac{\sigma}{\langle I \rangle}, \tag{1}$$

where σ is the standard deviation of the intensity I, and $\langle I \rangle$ is the mean intensity.

In this mode, the basic formula for LSCI measurement of renal perfusion (Flux) is:

$$Flux \propto \left(\frac{\langle I \rangle}{\sigma}\right)^2, \tag{2}$$

and measured in perfusion unit (PU).

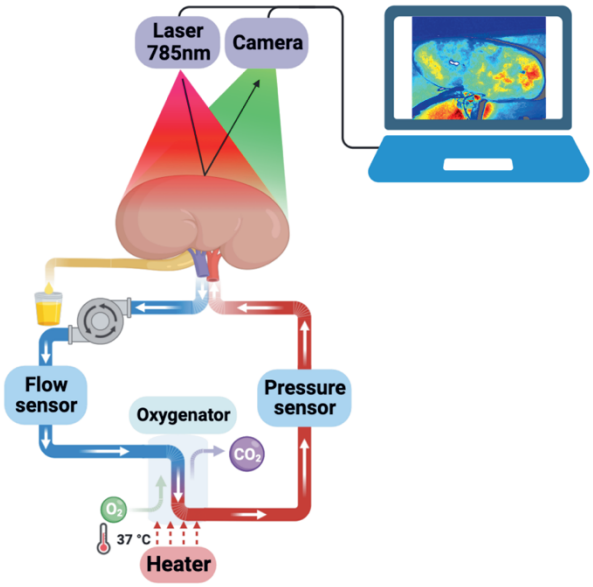


Figure 1. Schematic overview of the combined normothermic machine perfusion (NMP) and laser speckle contrast imaging (LSCI) setup.

Renal Function and Injury Assessment

Renal blood flow was recorded every 10 minutes. The percentage of blood flow decline was calculated using the formula $\frac{V_{before}-V_{after}}{V_{before}} \times 100\%$, where V_{before} is the blood flow before clamping the renal artery, and V_{after} is the blood flow after clamping the renal artery. The ratio of ischemic area was calculated using the formula $\frac{N_{all}-N_{ischemia}}{N_{all}} \times 100\%$, where N_{all} represents the number of pixels of the whole ROI, and $N_{ischemia}$ represents the number of pixels within the ischemic area. Perfusate samples from renal artery and vein, as well as urine samples, were taken before and after renal artery occlusion. Blood gas analyses enabled the calculation of oxygen consumption (VO_2). Perfusate and urine concentrations of lactate dehydrogenase (LDH), aspartate aminotransferase (AST), creatinine and sodium were determined in the hospital biochemistry laboratory using routine clinical assays. The concentrations of creatinine and sodium enabled the calculation of creatinine clearance (CrCl), fractional excretion of sodium (FENa) and total sodium reabsorption (TNa), of which the equations are presented in **Table S2**.[12, 13]

Cortical tissues from both non-ischemic and ischemic areas were collected after NMP and fixed in 4% buffered paraformaldehyde for 48h. The tissue samples were then embedded in paraffin and cut into 4 μm sections. Using periodic acid-Schiff (PAS) staining, renal tubular necrosis was evaluated and scored on a semiquantitative scale of 0 to 3 (0-no changes, 1-mild, 2-moderate, 3-severe changes) by an experienced renal pathologist blinded to the study. The tubular injury score was based on the degree of brush border loss, tubular dilatation, epithelial vacuolation, thinning and sloughing, and luminal debris/casts.

Statistical Analysis

Continuous variables were tested for normality using Shapiro-Wilk test and reported as mean ± standard deviation (SD) if normally distributed or median with interquartile range (IQR) in the case of non-normal distribution. To compare the LSCI flux, renal function and tubular injury before and after arterial clamping, continuous variables were compared using the paired t-test or Wilcoxon signed-rank test depending on the normality. The raw LSCI data were processed using MATLAB (MathWorks, Inc., Natick, USA). Statistical analyses were performed using SPSS version 26 (SPSS Inc., Chicago, USA). The graphs were plotted using GraphPad Prism 9.3.1 (GraphPad Software Inc., San Diego, CA). A p-value ≤ 0.05 was considered statistically significant.

Results

All kidneys were included in the analyses. The WIT of the kidneys was 38.4 ± 8.5min. The weight of the kidneys was 283 ± 45g before NMP and 318 ± 53g after NMP.

Reperfusion Measurement

The representative LSCI patterns from low resolution and high resolution modes were shown in **Figure 2**, and the flux measurements for each kidney at representative time points were displayed in **Table S3**.

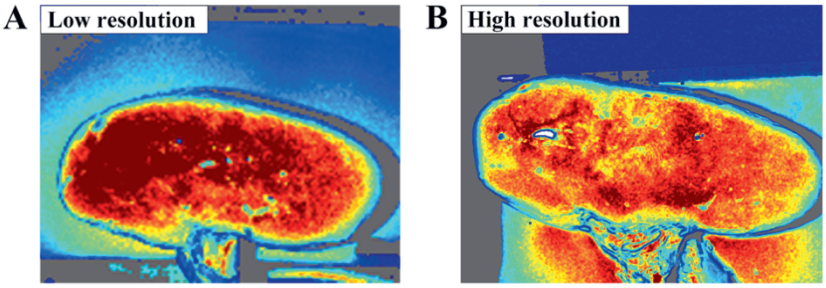


Figure 2. Representative LSCI patterns of the kidneys from (A) low resolution mode and (B) high resolution mode during NMP.

During the first 100 minutes of NMP, an increase of renal cortical perfusion could be clearly visualized through LSCI (**Figure 3A**). The mean value of each measurement was used to explore the relevance between the renal blood flow and LSCI flux. With the increase of blood flow, LSCI fluxes also increased correspondingly, from the baseline of 63 ± 44 PU to 797 ± 271 PU (**Figure 3B**). The LSCI flux correlated linearly with the renal blood flow (R^2=0.90, p<0.001, **Figure 3C**).

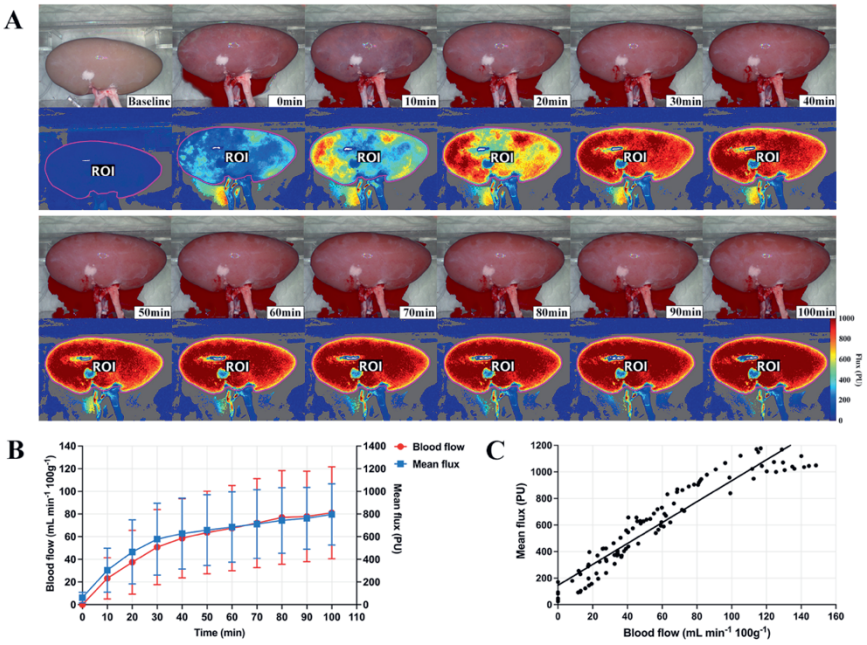


Figure 3. (A) Macroscopic appearances (above) and the corresponding LSCI patterns (below) of one kidney during the first 100min of NMP. (B) Renal blood flow and the LSCI flux during the first 100min of NMP. (C) Linear regression analysis on LSCI flux versus renal blood flow during the first 100min of NMP (R^2=0.90, p<0.001). ROI, region of interest.

Dual-side LSCI Measurement

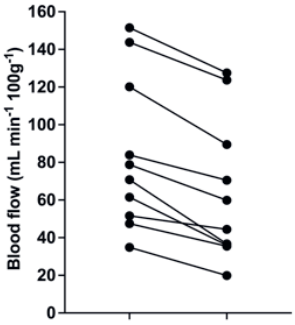


Figure 4. Renal blood flow changes before (left) and after artery branch occlusion (right).

All kidneys were adequately perfused without macroscopic ischemic lesions based on a visual inspection of homogeneously pink outer surface. The LSCI fluxes were 885 ± 234 PU on the ventral side and 931 ± 295 PU on the dorsal side. As shown in **Figure 4**, a decline of blood flow was observed in all kidneys by 14% to 48% after clamping the renal artery branch.

Part of the previously well-perfused region was replaced by ischemic lesions and the infarct border was clearly identified by LSCI. In eight out of ten kidneys, ischemic lesions could be seen on both sides after the artery branch occlusion (**Figure 5A**), with a percentage of the surface ranging from 23% to 49% on the ventral side and 16% to 58% on the dorsal side. However, in the remaining two kidneys, an ischemic lesion could be observed on only one side, with 46% of the ventral side and 58% of the dorsal side affected (**Figure 5B**), respectively.

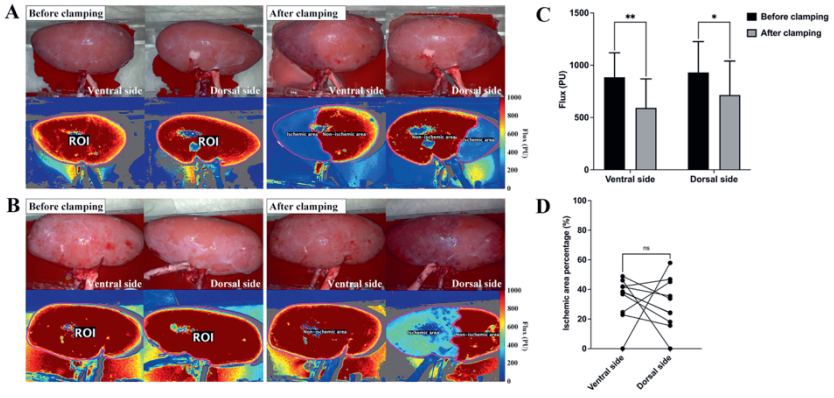


Figure 5. Representative macroscopic appearances and LSCI patterns of renal cortical perfusion in two different situations after the renal artery branch occlusion during NMP: (A) Ischemic lesions could be seen on both ventral and dorsal sides after artery branch occlusion, with ischemia in 39% and 24% of the whole area, respectively; (B) Ischemic lesions could be observed on only one side after artery branch occlusion, inducing ischemia in 58% of the dorsal area. (C) LSCI flux of the kidneys on the ventral and dorsal sides before and after the renal artery branch occlusion during NMP. (D) Ischemic area percentage of all kidneys on the ventral and dorsal sides. ROI, region of interest. Wilcoxon matched-pairs signed rank. $^{*}p<0.05$, $^{**}p<0.01$, $^{***}p<0.001$.

Compared to the LSCI measurement before clamping, the fluxes on both sides were significantly decreased after artery branch occlusion (ventral side: median [IQR], 912 [657-1082] versus 484 [420-740] PU, Wilcoxon matched-pairs signed rank, $p<0.01$; dorsal side: median [IQR], 943 [741-1212] versus 600 [408-1057] PU, Wilcoxon matched-pairs signed rank, $p<0.01$, **Figure 5C**). The ischemic area ratio between the ventral and dorsal sides was comparable (median [IQR], 38 [24-43]% versus 29 [17-46]%, Wilcoxon matched-pairs signed rank, $p=0.43$, **Figure 5D**). The comparison of histograms before and after artery occlusion provided insight into the changes in renal cortical perfusion (**Figure S1**).

Renal Function

As a surrogate marker for the glomerular filtration rate, CrCl tended to decrease after renal artery occlusion (median [IQR], 0.94 [0.68-1.11] versus 0.61 [0.35-0.94] mL/min/100g, Wilcoxon matched-pairs signed rank, $p=0.06$), but the difference was not statistically significant (**Figure 6A**). To evaluate tubular transport function, FENa was calculated. Kidneys showed comparable FENa before and after occlusion during NMP (median [IQR], 60.2 [27.0-83.4]% versus 51.9 [22.8-77.9]%, Wilcoxon matched-pairs signed rank, $p=0.32$, **Figure 6B**). Although VO_2 significantly decreased after clamping the artery (2.57 ± 0.63 versus 1.83 ± 0.49 mLO_2/min/100g, paired t-test, $p<0.001$, **Figure 6C**), the capability of reabsorbing the sodium was similar before and after occlusion (median [IQR], 47.75 [10.86-126.47] versus 37.21 [11.76-106.06] mmol/min/100g, Wilcoxon matched-pairs signed rank, $p=0.63$, **Figure 6D**). Before occlusion, kidneys showed a significantly higher urine output than after occlusion (median [IQR], 1.3 [1.1-1.7] versus 0.80 [0.6-1.3] mL/min, Wilcoxon matched-pairs signed rank, $p<0.05$, **Figure 6E**).

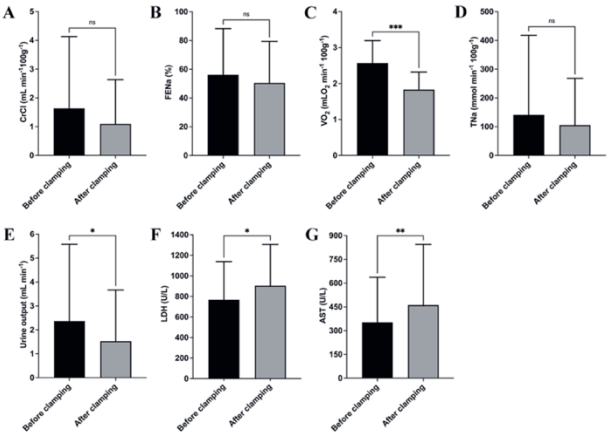


Figure 6. Renal function and injury makers before and after inferior renal artery branch occlusion during NMP. (A) creatinine clearance (CrCl, mL/min/100g); (B) fractional excretion of sodium (FENa, %); (C) oxygen consumption (VO_2, mLO_2/min/100g); (D) total sodium reabsorption (TNa, mmol/min/100g); (E) urine output (mL/min); (F) lactate dehydrogenase (LDH, U/L) and (G) aspartate aminotransferase (AST, U/L). Data presented as mean ± SD. (A), (B), (D), (E), Wilcoxon matched-pairs signed rank, and (C), (F), (G), paired t-test. $^{*}p<0.05$, $^{**}p<0.01$, $^{***}p<0.001$.

Renal Injury Measurement

To evaluate renal injury, LDH and AST concentrations in perfusate were measured. LDH concentrations became significantly higher after occlusion (768 ± 370 versus 905 ± 401 U/L, paired t-test, $p<0.05$, **Figure 6F**). Similarly, AST concentrations were also higher after occlusion (352 ± 285 versus 462 ± 383 U/L, paired t-test, $p<0.01$, **Figure 6G**). Moreover, PAS-stained renal sections were scored on a scale from 1 to 3 based on acute tubular necrosis (ATN). In both non-ischemic and ischemic tissue, biopsies showed moderate ATN with proximal tubule dilation and absence of brush border (**Figure 7A**), with no difference between the groups (2.45 ± 0.50 versus 2.50 ± 0.47, paired t-test, $p=0.34$, **Figure 7B**).

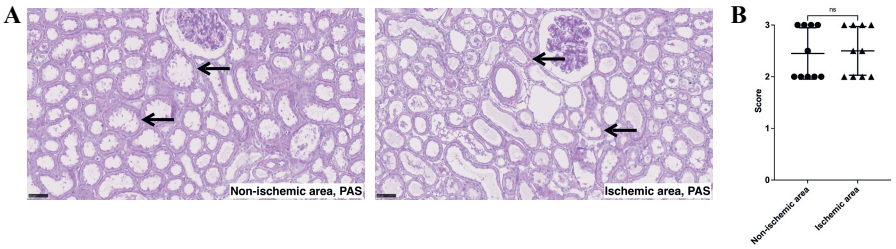


Figure 7. (A) Histomorphology of both non-ischemic and ischemic areas showed moderate severity of acute tubular injury, tubular dilation and proximal tubule brush border loss. (B) Tissues were assessed based on acute tubular necrosis using paired t-test (ranging from mild to severe: 1-3). Black arrows indicate dilated proximal tubules with brush border loss. PAS, periodic.

Discussion

In this study, we conducted LSCI measurements in human-sized porcine kidneys during NMP. The reperfusion experiment demonstrated a strong linear correlation between LSCI fluxes and renal blood flow. Furthermore, by conducting dual-side measurements, we were able to visualize and semi-quantify the renal cortical microcirculation and perfusion decline using LSCI. Dual-side LSCI measurements provided more comprehensive information than single-sided measurement.

LSCI relies on the blurring effect of the speckle phenomenon, which occurs when a scattering object is illuminated by coherent laser light. The interference pattern formed by the backscattered light creates a speckle pattern.[14-16] In LSCI, this blurring effect is used to visualize blood flow by tracking the motion of red blood cells. However, LSCI only provides relative measurements of blood flow rather than absolute values.[15, 17] A larger value of perfusion units corresponds to more perfusion, which means more movement of red blood cells. Despite similar macroscopic appearances, LSCI revealed heterogeneities in microcirculation across individual kidneys and over time. Our study found that the LSCI flux correlated linearly with the renal blood flow when the distance between the kidney and camera was fixed, which is consistent with findings by Heeman et al.[11] With approximately 85% nephrons as cortical nephrons, most of the ultrafiltration and electrolyte reabsorption occur in the renal cortex.[18] Therefore renal cortical perfusion likely provides more information on kidney viability and function than general blood flow.

During the dual-side measurements, we occluded the inferior renal artery branch to induce renal infarction, simulating arterial stenosis and thrombosis. Compared to the macroscopic appearance, LSCI enabled a more sensitive identification and semi-quantification of the ischemic lesion. Although no statistical difference was found in the ischemic areas between the ventral and dorsal sides, none of the kidneys displayed the same patterns of infarction on both aspects, and two kidneys showed renal infarction on one aspect only. This indicates the heterogeneities in vascular anatomy and intrarenal blood distribution between the ventral and dorsal sides. Considering the more complex variation in renal artery anatomy, this heterogeneity of segmental blood supply in human kidneys could be even greater.[19] As a rapid and non-invasive imaging technique, dual-side LSCI measurements provide more

information on cortical perfusion and deficiency than single aspect measurement without extending the time of organ exposure.

Currently, Doppler ultrasound is used as the standard of care to examine renal blood flow. It requires physical contact between the probe and the object being measured, which increases risk of contamination. In the preclinical phase, Schutter et al.[20] used magnetic resonance imaging (MRI) to visualize the perfusate distribution in renal cortex and medulla during NMP. However, the use of MRI during NMP requires a large volume of blood-based perfusate and complicated procedures, which limits its practicality. Compared to ultrasound and MRI, LSCI provides a simple, valuable alternative for real-time cortical perfusion assessment. Additionally, it is promising to apply LSCI to intraoperative diagnosis of anastomotic stenosis which typically occurs shortly after kidney reperfusion during transplantation and may lead to graft impairment and failure.[21, 22]

As the LSCI patterns in both low resolution and high resolution modes can effectively detect microcirculation changes, the choice of resolution mode depends on specific research objectives and the desired level of details. Low resolution mode offers faster image processing, which can be advantageous when analyzing a large number of images. However, the main drawback of low resolution mode is the reduction in image details, leading to the loss of nuances in the speckle patterns. High resolution mode captures more crucial details, allowing for more precise analysis of microcirculation. The higher pixel density in high resolution images leads to sharper and more visually informative images, helping researchers and clinicians identify subtle microcirculatory changes. However, processing high resolution images requires more computational resources and time.

Besides LSCI measurements, renal function and injury were also measured. Urine output dropped significantly after clamping the renal artery branch, as did the oxygen consumption. However, no significant difference was found in CrCl, FENa and TNa. Renal injury markers, LDH and AST were significantly elevated after renal artery occlusion in the perfusate. However, histology showed no significant differences between the ischemic and non-ischemic areas. The reason for this may be that the ischemia time was not long enough to induce renal injury that can be identified histologically. It is currently unclear whether occluding a branch of the renal artery would trigger a compensatory increase in blood flow

in the remaining sections of the kidney. However, relying solely on renal function and injury markers may lead to the oversight of regional perfusion deficiencies.

Our study has several limitations to be addressed. Firstly, the use of slaughterhouse kidneys might result in higher interindividual variability in kidney viability and extent of renal injury, which could have interfered with our outcome measurements. Secondly, although LSCI is a powerful technique for recording blood perfusion, the physics of the scattering process is complex and unable to measure absolute flow, making it difficult to statistically compare perfusion between individuals. Thirdly, the measurement depth of LSCI is limited to 0.9mm, which restricts its ability to measure deeper areas of the kidney.[23] Lastly, further studies using a transplant model should be conducted to validate our findings.

Conclusion

LSCI is a promising real-time imaging technique for assessing renal cortical perfusion during NMP. Our results indicate that LSCI fluxes have a strong linear correlation with renal blood flow, and LSCI can be used to visualize and semi-quantify renal cortical microcirculation and perfusion deficiency. Moreover, dual-side LSCI measurements provides complementary information compared to single aspect measurements, which is not reflected by standard renal function and morphology assessment. Therefore, we recommend dual-side LSCI measurements as an additional kidney perfusion assessment tool during NMP, which is crucial for evaluating organ viability and improving clinical outcomes after transplantation.

Reference

1. Tonelli M, Wiebe N, Knoll G, Bello A, Browne S, Jadhav D, et al. Systematic review: kidney transplantation compared with dialysis in clinically relevant outcomes. Am J Transplant. 2011;11(10):2093-109.
2. Port FK, Bragg-Gresham JL, Metzger RA, Dykstra DM, Gillespie BW, Young EW, et al. Donor characteristics associated with reduced graft survival: an approach to expanding the pool of kidney donors. Transplantation. 2002;74(9):1281-6.
3. Lomero M, Gardiner D, Coll E, Haase-Kromwijk B, Procaccio F, Immer F, et al. Donation after circulatory death today: an updated overview of the European landscape. Transpl Int. 2020;33(1):76-88.
4. Hamed MO, Chen Y, Pasea L, Watson CJ, Torpey N, Bradley JA, et al. Early graft loss after kidney transplantation: risk factors and consequences. Am J Transplant. 2015;15(6):1632-43.
5. Hosgood SA, Thompson E, Moore T, Wilson CH, Nicholson ML. Normothermic machine perfusion for the assessment and transplantation of declined human kidneys from donation after circulatory death donors. Br J Surg. 2018;105(4):388-94.
6. Feng X, Yu Y, Zou D, Jin Z, Zhou C, Liu G, et al. Functional imaging of human retina using integrated multispectral and laser speckle contrast imaging. J Biophotonics. 2022;15(2):e202100285.
7. Miller DR, Ashour R, Sullender CT, Dunn AK. Continuous blood flow visualization with laser speckle contrast imaging during neurovascular surgery. Neurophotonics. 2022;9(2):021908.
8. Schwartz KS, Theis EN, Bunting K, McCaughey RA, Lang JA. Laser speckle contrast imaging and laser Doppler flowmetry reproducibly assess reflex cutaneous vasoconstriction. Microvasc Res. 2022;142:104363.
9. Sturesson C, Milstein DM, Post IC, Maas AM, van Gulik TM. Laser speckle contrast imaging for assessment of liver microcirculation. Microvasc Res. 2013;87:34-40.
10. Eriksson S, Nilsson J, Lindell G, Sturesson C. Laser speckle contrast imaging for intraoperative assessment of liver microcirculation: a clinical pilot study. Med Devices (Auckl). 2014;7:257-61.
11. Heeman W, Maassen H, Calon J, van Goor H, Leuvenink H, van Dam GM, et al. Real-time visualization of renal microperfusion using laser speckle contrast imaging. J Biomed Opt. 2021;26(5).
12. Venema LH, van Leeuwen LL, Posma RA, van Goor H, Ploeg RJ, Hannaert P, et al. Impact of Red Blood Cells on Function and Metabolism of Porcine Deceased Donor Kidneys During Normothermic Machine Perfusion. Transplantation. 2022;106(6):1170-9.
13. Ogurlu B, Pamplona CC, Van Tricht IM, Hamelink TL, Lantinga VA, Leuvenink HGD, et al. Prolonged Controlled Oxygenated Rewarming Improves Immediate Tubular Function and Energetic Recovery of Porcine Kidneys During Normothermic Machine Perfusion. Transplantation. 2022.
14. Boas DA, Dunn AK. Laser speckle contrast imaging in biomedical optics. J Biomed Opt. 2010;15(1):011109.
15. Briers D, Duncan DD, Hirst E, Kirkpatrick SJ, Larsson M, Steenbergen W, et al. Laser speckle contrast imaging: theoretical and practical limitations. J Biomed Opt. 2013;18(6):066018.
16. Heeman W, Steenbergen W, van Dam G, Boerma EC. Clinical applications of laser speckle contrast imaging: a review. J Biomed Opt. 2019;24(8):1-11.
17. Zheng C, Lau LW, Cha J. Dual-display laparoscopic laser speckle contrast imaging for real-time surgical assistance. Biomed Opt Express. 2018;9(12):5962-81.
18. Gopalan C, Kirk E. Chapter 7 - Renal physiology. In: Gopalan C, Kirk E, editors. Biology of Cardiovascular and Metabolic Diseases: Academic Press; 2022. p. 123-40.
19. Aristotle S, Sundarapandian, Felicia C. Anatomical study of variations in the blood supply of kidneys. J Clin Diagn Res. 2013;7(8):1555-7.
20. Schutter R, Lantinga VA, Hamelink TL, Pool MBF, van Varsseveld OC, Potze JH, et al. Magnetic resonance imaging assessment of renal flow distribution patterns during ex vivo normothermic machine perfusion in porcine and human kidneys. Transpl Int. 2021;34(9):1643-55.
21. Bakir N, Sluiter WJ, Ploeg RJ, van Son WJ, Tegzess AM. Primary renal graft thrombosis. Nephrol Dial Transplant. 1996;11(1):140-7.
22. Hurst FP, Abbott KC, Neff RT, Elster EA, Falta EM, Lentine KL, et al. Incidence, predictors and outcomes of transplant renal artery stenosis after kidney transplantation: analysis of USRDS. Am J Nephrol. 2009;30(5):459-67.
23. Davis MA, Kazmi SM, Dunn AK. Imaging depth and multiple scattering in laser speckle contrast imaging. J Biomed Opt. 2014;19(8):086001.

Supplementary

Table S1. Components of the normothermic machine perfusion perfusate

Priming	Volume (mL)
Ringer's lactate (Baxter, Utrecht, The Netherlands)	300
Autologous leukocyte-depleted blood	500
Additives	
8.4% sodium bicarbonate (B. Braun Melsungen AG, Germany)	10
5% glucose (Baxter, Utrecht, The Netherlands)	10
Verapamil (Sigma-Aldrich, Zwijndrecht, the Netherlands)	1
Dexamethasone (Centrafarm, Etten-Leur, The Netherlands)	0.3
90mg creatinine (Sigma-Aldrich, Zwijndrecht, the Netherlands)	-
Infusion 20mL/h	
Aminoplasmal (B. Braun Melsungen AG, Germany)	45
8.4% sodium bicarbonate (B. Braun Melsungen AG, Germany)	1.5
100 U/mL insulin (NovoRapid®, Bagsværd, Denmark)	0.5

Table S2. Equations for calculating renal function

Parameter	Equation	Abbreviations
Creatinine clearance (CrCl, mL $min^{-1}100g^{-1}$)	$\left(\frac{\frac{U_{Cr} * U}{P_{Cr}}}{g}\right) * 100$	U_{Cr}, urine creatinine concentration (mmol/L) U, urine output rate (mL/min) P_{Cr}, perfusate creatinine concentration (mmol/L) g, kidney weight (gram)
Fractional excretion of sodium (FENa, %)	$\left(\frac{U_{Na} * P_{Cr}}{P_{Na} * U_{Cr}}\right) * 100$	U_{Na}, urine sodium concentration (mmol/L) P_{Na}, perfusate sodium concentration (mmol/L) P_{Cr}, perfusate creatinine concentration (mmol/L) U_{Cr}, urine creatinine concentration (mmol/L)
Oxygen consumption (VO_2, mLO_2 $min^{-1}100g^{-1}$)	$\left(\frac{(Hb * 2.4794 + p_aO_2 * K) - (0.024794 * Hb * S_vO_2 + p_vO_2 * K)}{g}\right) * Q$	Hb, hemoglobin concentration (mmol/L) pO_2, partial oxygen pressure (kPa) K, solubility constant of oxygen in water at 37°C that equals 0.0225 (mLO_2 per kPa) SO_2, saturation (%) Q, renal blood flow (dL/min) g, kidney weight (gram)
Total sodium reabsorption (TNa, mmol $min^{-1}100g^{-1}$)	$\left(\frac{(CrCl * P_{Na}) - (U_{Na} * U)}{g}\right) * 100$	P_{Na}, perfusate sodium concentration (mmol/L) U_{Na}, urine sodium concentration (mmol/L) U, urine output rate (mL/min) g, kidney weight (gram)

Table S3. LSCI fluxes for each kidney at representative time points

	Baseline	10 min	20 min	30 min	40 min	50 min	60 min	70 min	80 min	90 min	100 min
Kidney 1	27±14	145±39	236±75	369±116	540±161	589±172	596±178	621±193	670±214	684±219	763±257
Kidney 2	39±15	93±32	96±40	123±53	157±62	196±69	240±74	307±83	360±87	403±91	438±97
Kidney 3	25±13	105±52	198±97	329±148	372±142	378±137	386±136	388±131	385±131	395±146	406±150
Kidney 4	84±38	180±64	255±91	302±105	323±105	375±115	421±130	460±133	565±165	620±173	707±204
Kidney 5	63±22	397±115	657±195	903±339	957±351	1023±353	1046±369	1074±387	1072±389	1040±395	1120±408
Kidney 6	47±73	715±231	839±280	949±239	1004±227	1003±232	1013±235	1024±239	1036±239	1046±240	1050±246
Kidney 7	93±49	230±177	288±172	371±175	424±180	463±190	504±201	546±205	576±213	612±213	628±215
Kidney 8	172±89	341±147	560±151	628±159	630±157	628±153	640±156	646±156	687±172	719±184	731±188
Kidney 9	44±12	423±152	869±269	979±295	1019±308	1067±319	1122±337	1150±351	1168±355	1171±364	1178±369
Kidney 10	38±12	421±159	656±198	832±203	849±211	863±214	891±227	905±224	921±231	934±234	946±247

Data are presented as mean ± standard deviation, in perfusion units (PU).

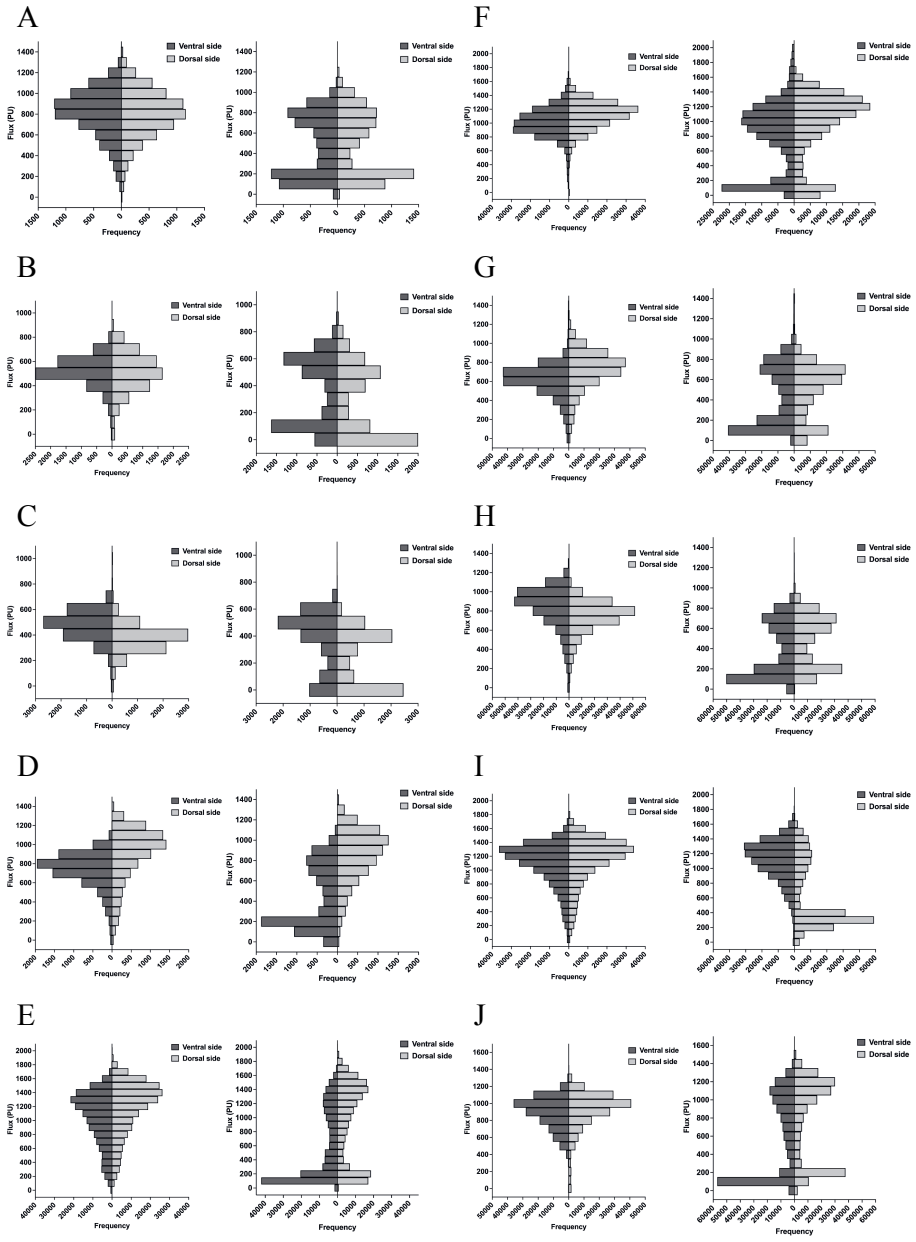
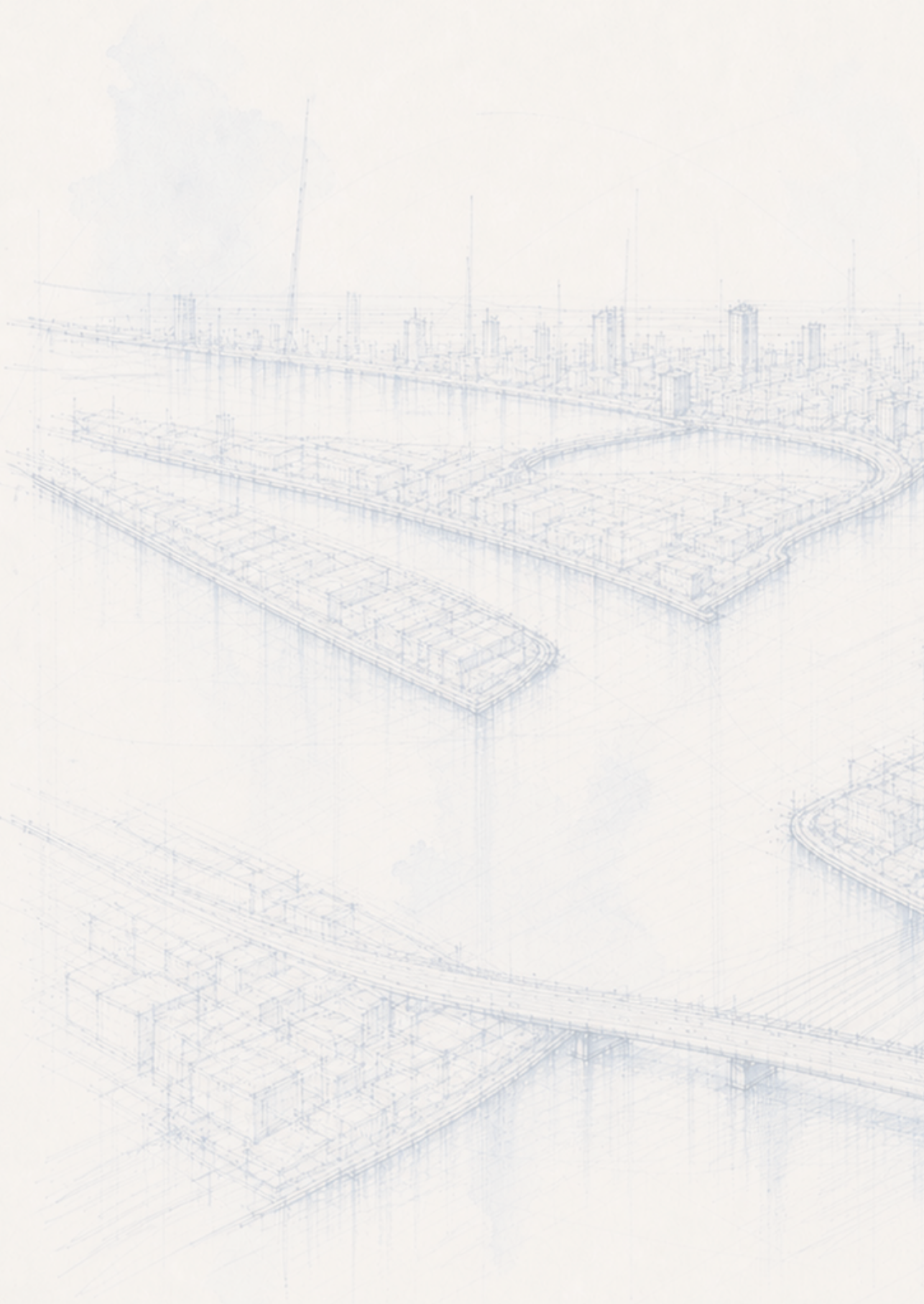


Figure S1. Frequency distribution of LSCI flux with different intensities for each kidney (A-J) before (left) and after renal artery occlusion (right) in the dual-side measurements.



Chapter 3

Pre-transplant kidney quality evaluation using photoacoustic imaging during normothermic machine perfusion

Anton V. Nikolaev*, Yitian Fang*, Jeroen Essers, Kranthi M. Panth, Gisela Ambagtsheer, Marian C. Clahsen-van Groningen, Robert C. Minnee, Gijs van Soest, Ron W.F. de Bruin

* Authors contributed equally to this study.

Photoacoustics, 2024

The work presented in this chapter was supported by the "HOST" project funded by the Dutch Research Council (NWO, project number 20719), and contributes to the Medical Delta scientific research program "Medical Delta MIMIC: Medische instrumenten maken: van idee naar kliniek".

Abstract

Due to the shortage of kidneys donated for transplantation, surgeons are forced to use the organs with an elevated risk of poor function or even failure. Although the existing methods for pre-transplant quality evaluation have been validated over decades in population cohort studies across the world, new methods are needed as long as delayed graft function or failure in a kidney transplant occurs. In this study, we explored the potential of utilizing photoacoustic (PA) imaging during normothermic machine perfusion (NMP) as a means of evaluating kidney quality. We closely monitored twenty-two porcine kidneys using 3D PA imaging during a two-hour NMP session. Based on biochemical analyses of perfusate and produced urine, the kidneys were categorized into "nonfunctional" and "functional" groups. Our primary focus was to quantify oxygenation (sO_2) within the kidney cortical layer of depths 2 mm, 4 mm, and 6 mm using two-wavelength PA imaging. Next, receiver operating characteristic (ROC) analysis was performed to determine an optimal cortical layer depth and time point for the quantification of sO_2 to discriminate between functional and non-functional organs. Finally, for each depth, we assessed the correlation between sO_2 and creatinine clearance (CrCl), oxygen consumption (VO_2), and renal blood flow (RBF).

We found that hypoxia of the renal cortex is associated with poor renal function. In addition, the determination of sO_2 within the 2 mm depth of the renal cortex after 30 min of NMP effectively distinguishes between functional and non-functional kidneys. The non-functional kidneys can be detected with the sensitivity and specificity of 80% and 85% respectively, using the cut-off point of $sO_2 < 39\%$. Oxygenation significantly correlates with RBF and VO_2 in all kidneys. In functional kidneys, sO_2 correlated with CrCl, which is not the case for non-functional kidneys.

We conclude that the presented technique has a high potential for supporting organ selection for kidney transplantation.

Introduction

Kidney transplantation is considered an optimal treatment for end-stage renal disease (ESRD).[1] Due to the lack of available kidney donations, patients have to wait up to 10 years for a suitable organ depending on geographical location. Consequently, many patients die on the waiting list.[2-8]

Donations from living donors or otherwise healthy donations after brain death (DBD) are preferable for transplantation. Nevertheless, to increase the donor pool, the use of kidneys from expanded criteria donors (ECD), i.e., older individuals including those with circulatory conditions, and donation after circulatory death (DCD) donors have become more prevalent.[9, 10] The use of ECD and DCD kidneys is associated with an elevated risk of impaired graft function and even failure in a kidney transplant.[9, 11] Besides, the quality of a donated kidney is affected by multiple parameters which include donor characteristics, organ procurement, preservation, transplantation, and post-transplant management.[12, 13] Therefore, successfully expanding the donor pool with ECD and DCD donors requires a rigorous and objective assessment of kidney function to mitigate severe risks.

Currently, pre-transplant kidney quality assessment predominantly relies on donor characteristics, kidney macroscopic appearance, and renal biopsies. However, these approaches have several limitations. Evaluations based on donor characteristics and macroscopic appearance are subjective and vary among different transplant centers and even individual clinicians. The Kidney Donor Profile Index (KDPI) is an internationally accepted metric that relies on the donor's characteristics.[13, 14] However, the number of medical centers that have integrated KDPI into their practice is limited. Renal biopsy can provide valuable insights into the histological features of kidney transplants but carries associated risks due to its invasive nature. Besides, histological examination is subject to sampling variability as it provides highly localized information. Biopsies overestimate organ damage and thus do not reliably predict the performance of the transplant.[14-16] Finally, the histological assessment is not a real-time measure and the kidney has to be preserved until the outcome is known, which is undesirable.[17]

Alternatively, medical imaging can provide valuable functional and morphological information about the kidney.[18] Ultrasound (US) is a first-choice modality because of its

usability, safety, and relatively low price, but is limited by aberration in obese patients. Doppler US methods can be used to characterize flow and perfusion in the transplanted organ.[19] X-ray computed tomography (CT) can provide high-resolution imaging and also enables CT angiography at low cost, but comes with the downside of ionizing radiation exposure.[20] Magnetic resonance imaging (MRI) is not preferred because of limited access and relatively high cost.[21] More experimental approaches include fluorescence angiography with indocyanine green (ICG) dye to measure the perfusion of a kidney cortex up to 1 cm depth.[22, 23] Photoacoustic (PA) imaging has been applied to detect fibrosis in ex-vivo mouse and pig kidneys.[24] Our work further explores an application of PA for pre-transplant functional kidney quality evaluation and aims to investigate the clinical value of a combination of PA and normothermic machine perfusion (NMP).

Photoacoustic imaging is a non-invasive and non-ionizing modality, which can provide real-time imaging data with molecular specificity relying on spectroscopic contrast. Photoacoustics capitalizes on the acoustic wave that is emitted by chromophores (i.e., light-absorbing molecules) after being exposed to a short light pulse. Unlike optical imaging modalities, PA can image up to a depth of a few centimeters, making it suitable for imaging renal cortex. The unique absorption spectrum of each chromophore enables its quantification within the sample.[25, 26]

We hypothesize that, since PA imaging can provide real-time and objective information about the molecular composition of the kidney, it can potentially improve the quality assessment in terms of speed and accuracy of pre-transplant kidney quality evaluation.

Normothermic machine perfusion is an experimental technique that aims to retain or improve and assess kidney function where the organ is supplied with perfusate enriched with nutrients and oxygen carriers at body temperature to mimic the physiological environment of a human body.[17, 27] Also, NMP can be utilized as a platform for testing kidney viability, such as assessed by oxygen consumption, which we exploit in our study.[28] The macroscopic appearance, renal blood flow (RBF), and urine output are the most intuitive indicators to assess kidney quality, but they vary greatly based on the different perfusate components and kidney size.[29, 30] More specifically, biomarkers such as glomerular filtration rate and oxygen consumption can be measured by perfusate and urine

samples. These biomarkers reflect renal function and viability. However, the analysis requires time-consuming laboratory procedures, and waste products of metabolism such as creatinine need to be added to the perfusate to analyze the filtration rate.

Several studies have explored the applications of medical imaging of kidneys during NMP for pre-transplant kidney assessment. Markgraf et. al. applied hyperspectral optical imaging on the cortical area of a kidney during NMP, which allows the quantification of oxygen saturation or water content on the organ's surface.[31, 32] Alternatively, Schuller et al. used MRI to assess the renal flow distribution of a kidney during NMP.[33] Finally, Fang et. al demonstrated that laser speckle contrast imaging (LSCI) can visualize cortical perfusion which correlates with oxygen consumption and urine production.[34]

The goal of our work is to investigate the value of PA imaging during NMP as a tool for kidney quality evaluation before transplantation which is also the novelty of the presented study. We investigate whether sO_2 measured with PA is associated with organ quality. We also investigate how oxygenation correlates with organ quality assessed by biochemical metrics, such as creatinine clearance (CrCl), oxygen consumption (VO_2), and by functional metrics such as renal blood flow (RBF).

Materials and Methods

Experimental Setup Design

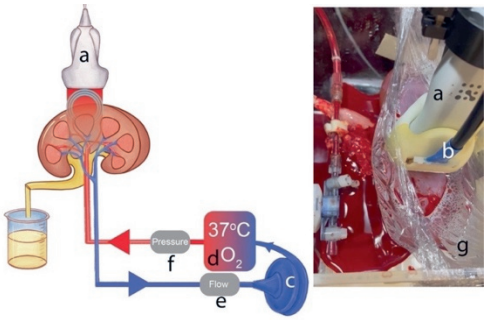


Figure 1. The experimental PA NMP setup. (a) US transducer equipped with (b) laser fiber bundles. (c) Centrifugal pump head. (d) Oxygenator with a heat exchanger. (e) Flow sensor. (f) Pressure sensor. (g) Interface film filled with water.

The schematic of the experimental setup is depicted in **Figure 1**. The setup is comprised of a custom-made NMP setup and a Vevo3100 LAZRX system (Fujifilm VisualSonics, Toronto, Canada) equipped with an MX201 ultrasound (US) linear transducer array (VisualSonics, Toronto, Canada) operating at 15 MHz central frequency. The transducer is attached to a linear translational stage enabling 3D image acquisition.

The NMP system consists of a centrifugal pump head (BPX-80 BioPump™ Plus, Medtronic, Minneapolis, MN, USA) equipped with a pump drive (BVP-BP, Harvard Apparatus, Germany), an oxygenator with a heat exchanger (Hilite 1000, Medos, Germany), and a thermocirculator (E100, Lauda, Germany). A flow probe (73-4755, Harvard Apparatus, Germany) is connected in-line with the kidney, and a pressure sensor (APT300, Harvard Apparatus, Germany) is directly connected to the renal artery cannula (Organ Recovery Systems, Itasca, USA). The setup is controlled by a commercially available electronic controller (PLUGSYS Servo Controller for Perfusion, Harvard Apparatus, Germany) which enables both flow and pressure-directed perfusions. The choice of the design was motivated by the reusability of the materials as opposed to commercially available systems.

Kidney Preparation and Sample Collection

Twenty-two porcine kidneys from female landrace pigs were obtained from a local slaughterhouse. The kidneys were explanted by a designated butcher following a standardized slaughter procedure. Once the kidneys were explanted, back-table preparation was performed by 2 of the authors. Since the organs were obtained from pigs intended for meat consumption, no approval from the animal ethics committee was required.

Directly after the animal slaughter, two liters of blood were collected in a bucket containing 25000 IU of heparine (LEO Pharma A/S, Ballerup, Denmark), and filtered by leukocyte filter (BioR 02 plus, Fresenius Kabi, Zeist, the Netherlands). After cannulating the renal arteries with a 5 mm straight cannula (Organ Recovery Systems, Itasca, USA), the kidneys were flushed with 500 mL Ringer's lactate (Baxter BV, Utrecht, the Netherlands) at a temperature of 4°C. Warm ischemia time (WIT) was calculated from the blood collection until cold flushing. Next, the kidneys were loaded into LifePort (Organ Recovery Systems, Itasca, USA) devices for transportation and cold preservation until NMP. In the LifePort, the kidney was perfused with 4°C Belzer UW machine perfusion solution (Belzer MPS, Bridge to Life Ltd., London, UK), at 30 mmHg of pressure.

In this study, cardiac arrest occurred in pigs and kidneys experienced a period of warm ischemia due to the slaughter procedure. This scenario mimics the DCD condition as DCD donors also experience cardiac arrest before organ donation in clinical practice.[35] Fourteen

kidneys underwent 30 min WIT, and the remaining 8 kidneys underwent prolonged WIT of 75 min. A kidney from a healthy, young pig subjected to 75 min WIT was proven to be a model for DCD kidney with substantial renal injury which is actively used in research including the Netherlands.[36, 37]

After removing the kidneys from the LifePort, they were flushed with 100 mL Ringer's lactate at 4°C to remove the remaining UW solution. They were subsequently perfused with autologous blood-based solution (**Table S1**) at 37°C with a controlled pressure of 70 mmHg. Carbogen (95% O_2 and 5% CO_2) was supplied via the oxygenator at flow rate of 500 mL/min.

During NMP, each kidney was positioned inside a custom-made chamber. To facilitate acoustic coupling and prevent direct contact between the kidney and the transducer, transparent polyethylene film was used to cover the kidney. The transducer was positioned above the kidney and the space between the transducer and the film was filled with water for acoustic coupling. There was no water leakage through the film into the chamber during the measurements.

Before and after NMP, renal cortical biopsies were collected for histological examination. The collected blood was used as perfusate. Renal blood flow was recorded every 10 min. The perfusate samples from renal artery and vein as well as urine samples were collected at 30 min, 60 min, and 120 min of NMP for further laboratory analysis. Urine production was recorded at the same time points. The PA data was acquired approximately every 20 min

Renal Function Assessment

Arterial and venous blood gas analyses from the perfusate samples were performed to calculate VO_2 :

$$VO_2 = \left(\frac{C_aO_2 - C_vO_2}{m}\right) \times Q \quad (1)$$

where C_aO_2 and C_vO_2 are arterial and venous oxygenation contents (mLO_2/L), m is kidney mass (gram), and Q is RBF (dL/min).[35]

The perfusate and urine concentrations of creatinine were measured using routine clinical assays to calculate CrCl:

$$CrCl = \left(\frac{C_{Cr\ in\ Urine} \times Q_{urine}}{C_{Cr\ in\ Perfusate}} / m\right) \times 100 \quad (2)$$

where C Cr in Urine is creatinine concentration in urine (mmol/L), Q Urine is urine output rate (mL/min), C Cr in Perfusate is creatinine concentration in perfusate (mmol/L).[35]

Pathological Assessment

Renal biopsies were fixed in 4% buffered paraformaldehyde for 48 h and then transferred to 70% ethanol until embedded in paraffin. The embedded tissues were cut into 4 µm slices and stained with periodic acid-Schiff (PAS). Acute tubular necrosis (ATN) was evaluated and scored on a semi-quantitative scale of 0 to 3 (0 - no changes, 1 - mild, 2 - moderate, 3 - severe changes) by a renal pathologist blinded to the study. The score was based on the degree of brush border loss, tubular dilatation, epithelial vacuolation, thinning, sloughing, and luminal debris/casts.[38, 39]

Kidney Classification

We used the values of VO_2 and CrCl to divide the kidneys into Group 1 and Group 2. Group 1 was referred to as "non-functional" kidneys, whilst Group 2 comprised "functional" kidneys. The criteria for defining these groups were based on the studies that utilized a comparable NMP setup and perfusate. Specifically, non-functional kidneys were defined as exhibiting CrCl ≤ 1 mL/min/100g and VO_2 ≤ 2.6 mL/min/100g at 120 min of NMP, whilst functional kidneys were defined by CrCl > 1 mL/min/100 g and VO_2 > 2.6 mL/min/100g.[40, 41]

In practice, a kidney transplant showing inferior function is associated with low urine production, low RBF, and high intrarenal resistance (IRR = arterial pressure/RBF).[42, 43] Therefore, the separation was validated by comparing total urine production, RBF, and IRR between the groups at the end of NMP. The significance of the difference between the groups was calculated with the Wilcoxon test.

Image Data Acquisition and Data Analysis

During each measurement, we acquired 3D PA and US B-mode image data by mechanically translating the US transducer above each kidney over a 45.5 mm distance with a step size of 0.5 mm, resulting in 91 acquired imaging frames (20 mm width and 30 mm depth). Each 2D PA image dataset was acquired at two wavelengths, 750 nm and 850 nm with persistence set as low, at each translational step. This pair of wavelengths is used in 'Oxy Hemo' mode embedded in the Vevo 3100 LAZR-X system, but also in the LED-based PA Cyberdyne Acoustic X system (Cyberdine Inc., Tsukuba, Japan). Therefore, the use of those wavelengths can simplify the clinical translation of the proposed technique. Interleaved acquisition was employed to collect the PA and Bmode 2D image data. Although we ensured the kidney was stable during the measurement, small accident motions were observed in B-mode images during the acquisition procedure. Those motions were neglected due to its low amplitude and persistence set.

The beamformed PA data at both wavelengths was exported from the Vevo3100 LAZR-X system for further processing. The data was utilized to calculate the relative concentrations of oxygenated and nonoxygenated hemoglobin C_{HbO2} and C_{Hb}:

$$\begin{bmatrix} C_{Hb} \\ C_{HbO2} \end{bmatrix} = \begin{bmatrix} \mu_{Hb}(750nm) & \mu_{HbO2}(750nm) \\ \mu_{Hb}(850nm) & \mu_{HbO2}(850nm) \end{bmatrix}^{-1} \begin{bmatrix} p(750nm) \\ p(850nm) \end{bmatrix} \quad (3)$$

where p is an acquired PA pressure, μ HbO2 and μ Hb are absorption spectra of oxygenated and non-oxygenated hemoglobin.

The acquired PA data was utilized to calculate the oxygenation sO_2 (%):

$$sO_2 = \frac{C_{HbO2}}{C_{HbO2}+C_{Hb}} \times 100\% \quad (4)$$

Fluence compensation was not applied to the PA data because it requires prior knowledge of the optical properties of the light propagation media. Even if those properties can be estimated for the optically heterogeneous renal cortex, the cellular changes induced in the kidneys by warm ischemia can alter those parameters and result in inaccurate compensation.[44, 45] The time gain compensation (TGC) was manually adjusted to enhance

the PA signal within the PA image and saved in a preset. We applied this preset to measure all kidneys.

Statistical Analysis

For the analysis, we calculated sO_2 for each slice within the renal cortical layer of depths 2, 4, and 6 mm, respectively. The cortex surface was segmented from the B-mode US data. To determine the optimal settings for measurement of sO2 , we compared the sO_2 values at 30 min, 60 min, and 110 min of NMP. The exact sO_2 values for the time points were obtained by linear interpolation of the initially acquired data. The significance of the difference in sO_2 between Group 1 and Group 2 was calculated using the Wilcoxon test. We also applied the Kruskal-Wallis test to statistically compare the sO_2 values at different depths at each time point. Finally, we performed receiver operating characteristic (ROC) analysis to determine an optimal depth and time point for measurement.

We examined the correlation between sO_2 and the RBF, CrCl, and VO_2 over time in Group 1 and Group 2 using the Spearman linear correlation test. We represented RBF, urine production, and sO_2 data in box plots (median, lower, and upper quartiles, whiskers indicate the maximum and minimum data point unless the data point is an outlier).[46] All image and data processing was performed in Matlab 2023a (The MathWorks, Natick, MA, USA).

Results

Kidney Group Division

According to the criteria defined in Section 2.4, the kidneys were divided into two groups: Group 1 (non-functional, n = 15) and Group 2 (functional, n = 7). There were significant differences in the tolerance to warm ischemia among different individual kidneys. Eight kidneys with 30 min WIT and 7 kidneys with 75 min WIT were included in Group 1, while Group 2 consisted of the remaining kidneys with 30 min WIT and one kidney with 75 min WIT. The RBF, IRR metrics, and total urine production at the end of NMP for both groups are shown in **Figure 2**. The statistically significant difference between the groups in RBF and urine production justifies the rationale behind the group division.

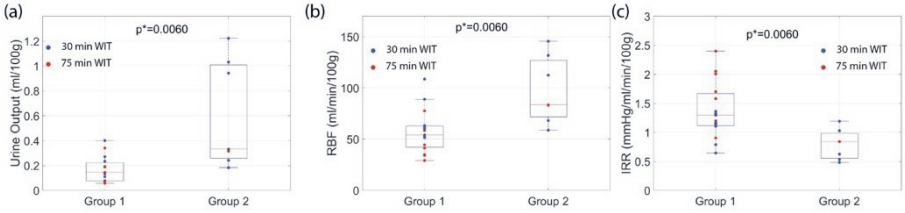


Figure 2. (a) Total urine production measured in Group 1 and Group 2 at 120 min of NMP; (b) RBF measured in Group 1 and Group 2 at 120 min of NMP; (c) IRR measured in Group 1 and Group 2 at 120 min of NMP. The Blue and Red dots represent kidneys subjected to 30 min and 75 min WIT respectively.

Oxygenation Measurement

The sO_2 maps over time in kidneys from Group 1 and Group 2 are presented in **Figure 3**, where an increase of sO_2 in the kidney of Group 2 over time can be observed. The mean sO_2 values in the cortical layers of 2 mm, 4 mm, and 6 mm over time are shown in **Figure 4**. Overall, the kidneys from Group 2 express higher sO_2 over time. The area under the curve (AUC) measured in Group 1 is significantly lower than that in Group 2. The significance is the highest for sO_2 measured in the renal cortex of 2 mm depth.

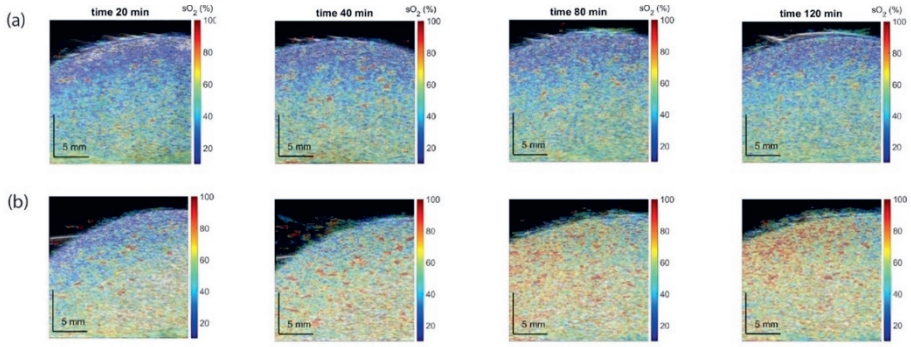


Figure 3. Oxygenation sO_2 map measured at 20 min, 40 min, 80 min, and 120 min of NMP for a kidney from (a) Group 1 and (b) Group 2. The mentioned time points are approximate since the measurement at exact time points was impossible due to practical reasons.

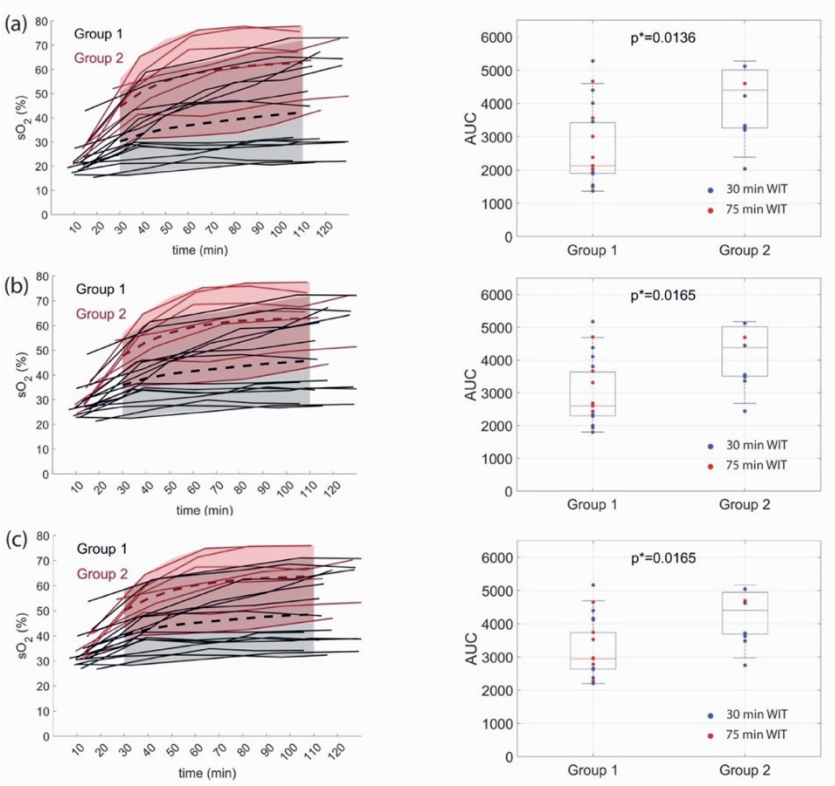


Figure 4. Oxygenation over time (left) and AUC per kidney for the organs (right) from Group 1 (black) and Group 2 (red) measured within the renal cortical layer of depths (a) 2 mm, (b) 4 mm, and (c) 6 mm. The dashed black and red lines depict the mean sO_2 levels for kidneys from Group 1 and Group 2 respectively. The gray and light red areas depict 90% confidence interval for kidneys from Group 1 and Group 2 respectively. The Blue and Red dots represent kidneys subjected to 30 min and 75 min WIT respectively.

The results presented in **Figure 4** suggest that the most significant difference in sO_2 between Group 1 and Group 2 can be reached by measuring within 2 mm of cortical depth, and the contrast diminishes with increasing layer depth. The Kruskal-Wallis test did not reveal a statistically significant difference between sO_2 measured at the same time points but at different depths, except in Group 1 at 30 min of NMP ($p = 0.01$). The ROC analysis shown in **Figure 5** confirms this result: the largest AUC = 0.85 was calculated from ROCs derived from sO_2 measurements measured in 2 mm and 4 mm layer thickness after 30 min of NMP.

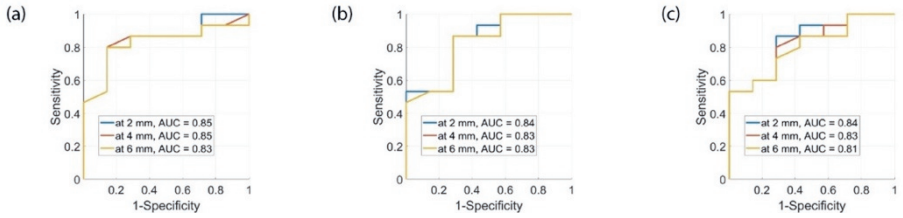


Figure 5. ROC curves for sO_2 as a classifier between the kidneys from Group 1 and Group 2 at (a) 30 min, (b) 60 min, and (c) 110 min after NMP start measured within the renal cortical layer of depths 2 mm, 4 mm, and 6 mm.

By measuring sO_2 within 2 mm cortical depth after 30 min of NMP, the kidneys from Group 2 can be discriminated by thresholding the sO_2 value below 39% resulting in sensitivity and specificity of 80% and 86% respectively. By measuring sO_2 within 2 mm cortical depth after 60 min of NMP, the kidneys from Group 2 can be discriminated by thresholding the sO_2 value below 54% resulting in sensitivity and specificity of 71% and 86% respectively (**Figure 5** and **Figure 6**).

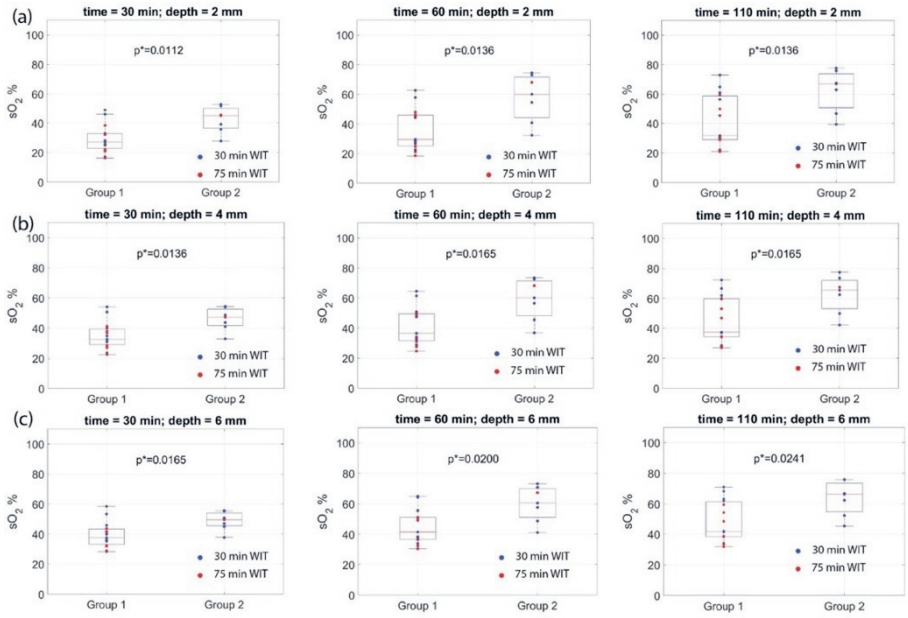


Figure 6. Oxygenation measured within the renal cortical layer of (a) 2 mm, (b) 4 mm, (c) 6 mm depth at time points 30 min, 60 min, and 110 min from the start of NMP. Red and Blue markers depict the kidney samples subject to 75 min and 30 min WIT respectively.

The correlation plot between sO_2 measured at 2 mm depth and CrCl, VO_2, and RFB are depicted in **Figure 7**. In Group 1, sO_2 correlates with RBF, and VO_2, whilst it does not correlate with CrCl. In Group 2, sO_2 correlates positively with CrCl, RBF, and VO_2.

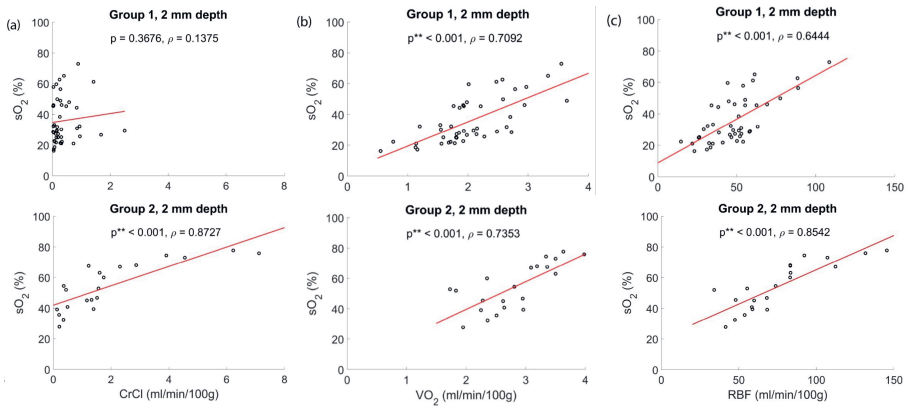


Figure 7. Correlation between sO_2 and (a) CrCl, (b) VO_2, and (c) RBF measured at 2 mm depth in Group1 and Group2. The analysis utilized the data acquired at all-time points.

Visual and Pathological Inspection

Visual assessment of the kidneys before NMP did not reveal any substantial differences in organ appearance. Additionally, during the perfusion, the kidneys had a similar pink appearance. The representative histological images of biopsies are shown in **Figure 8**, and the full overview of the histology grades is provided in **Table S2**. After NMP, 5 kidneys from Groups 1 and 2 kidneys from Group 2 received grade 3, revealing severe ATN, whilst the rest of the kidneys received grade 2, revealing moderate ATN.

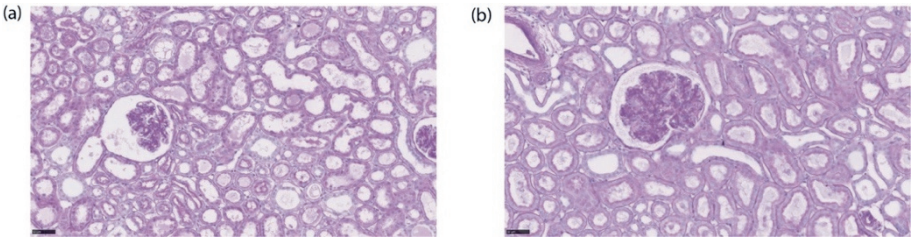


Figure 8. Representative histological images of biopsies taken from kidneys from (a) Group 1 (grade 3) and (b) Group 2 (grade 2) after 120 min of NMP. Moderate severity of acute tubular injury, tubular dilation, and tubule brush loss can be observed in both cases.

For the kidneys with grade 2, the pathological examination revealed partial loss of brush border in tubular epithelial cells, slight enlargement of Bowman's space in glomeruli, moderate tubular dilation, interstitial edema, and the presence of tubular casts in renal tubules. These changes indicate moderate acute ischemic injury. Kidneys with grade 3 exhibited more pronounced alterations, including more significant brush border loss, marked enlargement of Bowman's space, and higher prevalence of cast formation, indicating severe acute ischemic injury.

Discussion

In this study, we explored the value of PA imaging for kidney evaluation before transplantation. Specifically, we investigated sO_2 within the renal cortex during NMP as a quality metric to indicate the suitability of kidneys for transplantation.

The novelty of our work is that we performed PA imaging while the organ was connected to NMP. This technique can help a transplant surgeon to make a better decision about the translatability of a donated kidney. The main contribution of this work is that we demonstrated, through ex-vivo experiments, the association between hypoxia in the renal cortex and low levels of CrCl and VO_2. We hypothesize that the relatively low level of cortical sO_2 observed during NMP is associated with inferior function. This hypothesis is further supported by the findings of low urine production, low RBF, and high IRR in these kidneys.

Hypoxia is a consequence of warm ischemia, where proximal tubular cells swell, resulting in increased IRR and decreased flow through the renal cortex.[47] Consequently, prolonged warm ischemia disrupts the oxygen supply, leading to significant hypoxia which can be detected by PA imaging. There is an overlap in sO_2 values between Group 1 and Group 2 despite the statistically significant difference between the groups at all time points. Low sO_2 in a renal cortex indicates a high risk of inferior renal function and transplant failure, while high sO_2 does not necessarily guarantee proper renal function and needs to be interpreted cautiously together with other functional markers.

Our results suggest that the best time point to measure sO_2 is after 30 min of NMP within 2 mm of the renal cortical depth. This can be explained by the fact that in the first 30 min of

NMP, substantial shifts occur in various indicators of renal function and viability due to the abrupt transition from hypothermic to normothermic preservation. The sensitivity of these indicators to even minor differences in measurement time introduces variability, diminishing the robustness of the results. Therefore, we suggest that the optimal time point for measurement is after 30 min when the hemodynamics becomes relatively stable. This rationale aligns with the clinical practice of performing one hour or longer NMP to evaluate kidney transplantability.[48] The discrimination was poorest by measuring sO_2 within a deeper cortical layer. Measurements at greater depths can be influenced by low signal-to-noise ratio and fluence coloring, which can affect the accuracy of the sO_2 measurement.[49]

The pathology results demonstrated that renal injury becomes more prominent during NMP which is also confirmed by the literature.[50] Unlike the histological and biochemical analysis, PA can provide information about the kidney viability already after 30 min of NMP which is more practical than waiting for the laboratory results and prevents deterioration of kidney quality during prolonged NMP.

The experimental results demonstrate the correlation between sO_2 and viability parameters such as RBF, VO_2, and CrCl of the kidneys in Group 2. This finding indicates sO_2 measured by PA imaging reflects the inner physiology of a kidney. The level of CrCl in Group 2 does not correlate with sO_2. This further supports our conclusion that sO_2 can discriminate between non-functioning and functioning transplants.

The correlation of sO_2 with RBF, along with the significant difference in RBF between Group 1 and Group 2 after 2 h of NMP, suggests a direct relation between those two metrics. Despite the correlation between the metrics, there are two principal differences: Firstly, unlike RBF, the sO_2 metric provides information about the oxygenation of the kidney cortex. Meanwhile, RBF depends on the size of vasculature which is not linearly related to cortical perfusion. Secondly, unlike RBF, PA can locally quantify sO_2 and it allows to identify regions of occluded vasculature which is supported by our previous analysis of laser speckle dynamics in kidneys during NMP.[34]

The proposed approach can be compared with alternative recently proposed optical-based imaging modalities: LSCI, fluorescence angiography, and hyperspectral imaging. In contrast with the abovementioned modalities, PA can quantify sO_2 at up to a few

centimeters' depth whilst the optical imaging modalities are limited by a few millimeters. Besides, unlike PA, fluorescent angiography only measures perfusion within the cortical area without quantification of oxygen saturation.

Notwithstanding, provided that the cortical perfusion corresponds to the sO_2 level and the measurement is made only at 2 mm depth, we assume that those modalities can be equally used for the kidney quality assessment.

The macroscopic appearance of all kidneys during NMP was normal without showing perfusion insufficiency. Evaluation of the macroscopic appearance is a subjective method for evaluation of perfusion in the superficial layer of the cortex as we also demonstrated.[34] The difference in blood volume reaching the cortical area in the kidneys from Group 1 and Group 2 is insufficient to make the discrimination only with the naked eye. Besides, low-oxygenated and highly oxygenated blood are also hard to distinguish.

Similarly, the histological examination of biopsies did not reveal significant differences between the two groups, despite some kidneys from Group 1 being graded as 3 after NMP. Two potential factors may contribute to this grading discrepancy. Firstly, individuals vary in their tolerance to warm ischemia, and this divergence in response could account for unexpected pathology grading. Secondly, renal biopsies are prone to sampling variability. Given that biopsy reflects only a small portion of the kidney, it may not comprehensively depict the overall condition, leading to discrepancies in pathology grading.

Currently, renal biopsy is still the gold standard for accurate pretransplant quality assessment. However, it is important to note that besides its limitation of being unable to characterize the entire kidney and its invasive nature, renal biopsy may not be as sensitive as PA imaging since it cannot assess renal function, and has been documented to overestimate kidney damage.[16] Therefore, while renal biopsy continues to hold value in certain aspects, PA imaging provides a more refined approach to assess renal function during NMP.

Our study has several limitations to be addressed. Firstly, the use of slaughterhouse kidneys might result in higher interindividual variability in kidney viability and extent of renal injury, which could have interfered with our outcome measurements. Secondly, while

porcine kidneys are commonly utilized in preclinical machine perfusion experiments, their anatomical and physiological characteristics differ from human kidneys. It is important to exercise caution when extrapolating our findings to clinical scenarios. Moreover, due to the sources of porcine kidneys, we were unable to perform transplantation and determine the definitive outcomes of transplant function. Further research should focus on applying PA imaging techniques to experimental kidneys intended for transplantation to validate our findings.

Conclusion

It is feasible to apply photoacoustic imaging on kidney viability assessment during normothermic machine perfusion. Low cortical oxygenation can identify kidneys with a high risk of inferior function and transplant failure. The presented technique has a high potential for clinical use since it can support organ selection in a transplantation setting.

Reference

1. Tonelli M, Wiebe N, Knoll G, Bello A, Browne S, Jadhav D, et al. Systematic review: kidney transplantation compared with dialysis in clinically relevant outcomes. Am J Transplant. 2011;11(10):2093-109.
2. Organ Procurement & Transplantation Network [Internet]. Available from: https://optn.transplant.hrsa.gov/.
3. Summary statistics on organ transplants, wait-lists and donors [Internet]. Canadian Institute for Health Information. Available from: https://www.cihi.ca/.
4. Nederlandse Transplantatie Stichting [Internet]. Available from: https://www.transplantatiestichting.nl/.
5. Eurotransplant: statistics report library [Internet]. Available from: https://www.eurotransplant.org/statistics/.
6. N.H.S. Blood and Trasnplant, AnnualActivity Report [Internet]. Available from: https://www.odt.nhs.uk/.
7. Scandiatransplant [Internet]. Available from: http://www.scandiatransplant.org/.
8. Lee S, Yoo KD, An JN, Oh YK, Lim CS, Kim YS, et al. Factors affecting mortality during the waiting time for kidney transplantation: A nationwide population-based cohort study using the Korean Network for Organ Sharing (KONOS) database. PLoS One. 2019;14(4):e0212748.
9. Port FK, Bragg-Gresham JL, Metzger RA, Dykstra DM, Gillespie BW, Young EW, et al. Donor characteristics associated with reduced graft survival: an approach to expanding the pool of kidney donors. Transplantation. 2002;74(9):1281-6.
10. Lomero M, Gardiner D, Coll E, Haase-Kromwijk B, Procaccio F, Immer F, et al. Donation after circulatory death today: an updated overview of the European landscape. Transpl Int. 2020;33(1):76-88.
11. Hamed MO, Chen Y, Pasea L, Watson CJ, Torpey N, Bradley JA, et al. Early graft loss after kidney transplantation: risk factors and consequences. Am J Transplant. 2015;15(6):1632-43.
12. Legendre C, Canaud G, Martinez F. Factors influencing long-term outcome after kidney transplantation. Transpl Int. 2014;27(1):19-27.
13. Foley ME, Vinson AJ, Skinner TAA, Kiberd BA, Tennankore KK. The Impact of Combined Warm and Cold Ischemia Time on Post-transplant Outcomes. Can J Kidney Health Dis. 2023;10:20543581231178960.
14. Girolami I, Gambaro G, Ghimenton C, Beccari S, Calio A, Brunelli M, et al. Pre-implantation kidney biopsy: value of the expertise in determining histological score and comparison with the whole organ on a series of discarded kidneys. J Nephrol. 2020;33(1):167-76.
15. von Moos S, Akalin E, Mas V, Mueller TF. Assessment of Organ Quality in Kidney Transplantation by Molecular Analysis and Why It May Not Have Been Achieved, Yet. Front Immunol. 2020;11:833.
16. Aubert O, Reese PP, Audry B, Bouatou Y, Raynaud M, Viglietti D, et al. Disparities in Acceptance of Deceased Donor Kidneys Between the United States and France and Estimated Effects of Increased US Acceptance. JAMA Intern Med. 2019;179(10):1365-74.
17. Hosgood SA, Callaghan CJ, Wilson CH, Smith L, Mullings J, Mehew J, et al. Normothermic machine perfusion versus static cold storage in donation after circulatory death kidney transplantation: a randomized controlled trial. Nat Med. 2023;29(6):1511-9.
18. Sjekavica I, Novosel L, Rupcic M, Smiljanic R, Mursic M, Duspara V, et al. Radiological Imaging in Renal Transplantation. Acta Clin Croat. 2018;57(4):694-712.
19. Viazzi F, Leoncini G, Derchi LE, Pontremoli R. Ultrasound Doppler renal resistive index: a useful tool for the management of the hypertensive patient. J Hypertens. 2014;32(1):149-53.
20. Vernuccio F, Gondalia R, Churchill S, Bashir MR, Marin D. CT evaluation of the renal donor and recipient. Abdom Radiol (NY). 2018;43(10):2574-88.
21. Hohenwalter MD, Skowlund CJ, Erickson SJ, Hariharan S, Rilling WS, Crain MR, et al. Renal transplant evaluation with MR angiography and MR imaging. Radiographics. 2001;21(6):1505-17.
22. Gerken ALH, Nowak K, Meyer A, Weiss C, Kruger B, Nawroth N, et al. Quantitative Assessment of Intraoperative Laser Fluorescence Angiography With Indocyanine Green Predicts Early Graft Function After Kidney Transplantation. Ann Surg. 2022;276(2):391-7.
23. Rother U, Gerken ALH, Karampinis I, Klumpp M, Regus S, Meyer A, et al. Dosing of indocyanine green for intraoperative laser fluorescence angiography in kidney transplantation. Microcirculation. 2017;24(8).
24. Hysi E, He X, Fadhel MN, Zhang T, Krizova A, Ordon M, et al. Photoacoustic imaging of kidney fibrosis for assessing pretransplant organ quality. JCI Insight. 2020;5(10).
25. Zhou Y, Yao J, Wang LV. Tutorial on photoacoustic tomography. J Biomed Opt. 2016;21(6):61007.
26. Riksen JJM, Nikolaev AV, van Soest G. Photoacoustic imaging on its way toward clinical utility: a tutorial review focusing on practical application in medicine. J Biomed Opt. 2023;28(12):121205.
27. Mazilescu LI, Urbanellis P, Kim SJ, Goto T, Noguchi Y, Konvalinka A, et al. Normothermic Ex Vivo Kidney Perfusion for Human Kidney Transplantation: First North American Results. Transplantation. 2022;106(9):1852-9.

28. Hamelink TL, Ogurlu B, De Beule J, Lantinga VA, Pool MBF, Venema LH, et al. Renal Normothermic Machine Perfusion: The Road Toward Clinical Implementation of a Promising Pretransplant Organ Assessment Tool. Transplantation. 2022;106(2):268-79.
29. Hosgood SA, Brown RJ, Nicholson ML. Advances in Kidney Preservation Techniques and Their Application in Clinical Practice. Transplantation. 2021;105(11):E202-E14.
30. Pool MBF, Hamelink TL, van Goor H, van den Heuvel MC, Leuvenink HGD, Moers C. Prolonged ex-vivo normothermic kidney perfusion: The impact of perfusate composition. PLoS One. 2021;16(5):e0251595.
31. Markgraf W, Feistel P, Thiele C, Malberg H. Algorithms for mapping kidney tissue oxygenation during normothermic machine perfusion using hyperspectral imaging. Biomed Tech (Berl). 2018;63(5):557-66.
32. Markgraf W, Lilienthal J, Feistel P, Thiele C, Malberg H. Algorithm for Mapping Kidney Tissue Water Content during Normothermic Machine Perfusion Using Hyperspectral Imaging. Algorithms. 2020;13(11).
33. Schutter R, Lantinga VA, Hamelink TL, Pool MBF, van Varsseveld OC, Potze JH, et al. Magnetic resonance imaging assessment of renal flow distribution patterns during ex vivo normothermic machine perfusion in porcine and human kidneys. Transpl Int. 2021;34(9):1643-55.
34. Fang Y, van Ooijen L, Ambagtsheer G, Nikolaev AV, Clahsen-van Groningen MC, Dankelman J, et al. Real-time laser speckle contrast imaging measurement during normothermic machine perfusion in pretransplant kidney assessment. Lasers Surg Med. 2023;55(8):784-93.
35. Venema LH, van Leeuwen LL, Posma RA, van Goor H, Ploeg RJ, Hannaert P, et al. Impact of Red Blood Cells on Function and Metabolism of Porcine Deceased Donor Kidneys During Normothermic Machine Perfusion. Transplantation. 2022;106(6):1170-9.
36. Lohmann S, Eijken M, Moldrup U, Moller BK, Hunter J, Moers C, et al. A Pilot Study of Postoperative Animal Welfare as a Guidance Tool in the Development of a Kidney Autotransplantation Model With Extended Warm Ischemia. Transplantation Direct. 2019;5(11).
37. Lignell S, Lohmann S, Rozenberg KM, Leuvenink HGD, Pool MBF, Lewis KR, et al. Improved Normothermic Machine Perfusion After Short Oxygenated Hypothermic Machine Perfusion of Ischemically Injured Porcine Kidneys. Transplant Direct. 2021;7(2):e653.
38. Abdulkader RC, Liborio AB, Malheiros DM. Histological features of acute tubular necrosis in native kidneys and long-term renal function. Ren Fail. 2008;30(7):667-73.
39. Urbanellis P, Kollmann D, Linares I, Ganesh S, Oquendo F, Mazilescu L, et al. Significant Dysfunction of Kidney Grafts Exposed to Prolonged Warm Ischemia Is Minimized Through Normothermic Ex Vivo Kidney Perfusion. Transplantation Direct. 2020;6(8).
40. Markgraf W, Malberg H. Preoperative Function Assessment of Ex Vivo Kidneys with Supervised Machine Learning Based on Blood and Urine Markers Measured during Normothermic Machine Perfusion. Biomedicines. 2022;10(12).
41. Ogurlu B, Pamplona CC, Van Tricht IM, Hamelink TL, Lantinga VA, Leuvenink HGD, et al. Prolonged Controlled Oxygenated Rewarming Improves Immediate Tubular Function and Energetic Recovery of Porcine Kidneys During Normothermic Machine Perfusion. Transplantation. 2023;107(3):639-47.
42. Nicholson ML, Hosgood SA. Renal transplantation after ex vivo normothermic perfusion: the first clinical study. Am J Transplant. 2013;13(5):1246-52.
43. Jochmans I, Moers C, Smits JM, Leuvenink HG, Treckmann J, Paul A, et al. The prognostic value of renal resistance during hypothermic machine perfusion of deceased donor kidneys. Am J Transplant. 2011;11(10):2214-20.
44. Ban S, Min E, Baek S, Kwon HM, Popescu G, Jung W. Optical properties of acute kidney injury measured by quantitative phase imaging. Biomed Opt Express. 2018;9(3):921-32.
45. Li WJ, Wu CF, Fang YH, Li JX, Huang Z. Evaluation of optical attenuation coefficient of living kidney using OCT. Proc Spie. 2019;11078.
46. Mcgill R, Tukey JW, Larsen WA. Variations of Box Plots. Am Stat. 1978;32(1):12-6.
47. Yin M, Currin RT, Peng XX, Mekeel HE, Schoonhoven R, Lemasters JJ. Different patterns of renal cell killing after warm and cold ischemia. Ren Fail. 2002;24(2):147-63.
48. Hosgood SA, Thompson E, Moore T, Wilson CH, Nicholson ML. Normothermic machine perfusion for the assessment and transplantation of declined human kidneys from donation after circulatory death donors. Br J Surg. 2018;105(4):388-94.
49. Hochuli R, An L, Beard PC, Cox BT. Estimating blood oxygenation from photoacoustic images: can a simple linear spectroscopic inversion ever work? Journal of Biomedical Optics. 2019;24(12).
50. Huijink TM, van 't Hof CJ, van Furth LA, de Haan NA, Maassen H, Venema LH, et al. Loss of Endothelial Glycocalyx During Normothermic Machine Perfusion of Porcine Kidneys Irrespective of Pressure and Hematocrit. Transplant Direct. 2023;9(8):e1507.

Supplementary

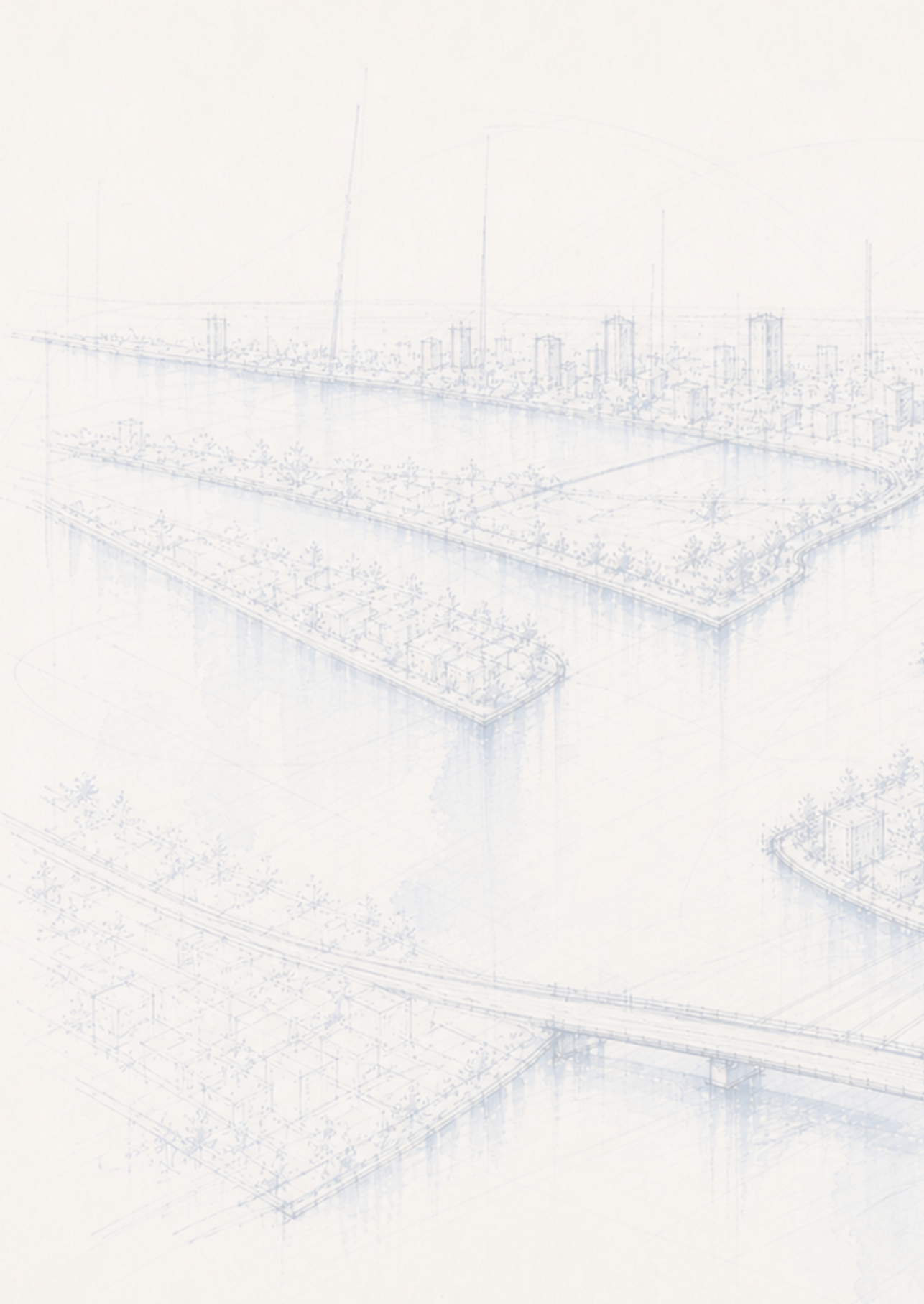
Table S1. Components of the normothermic machine perfusion perfusate

Priming	**Volume (mL)**
Ringer's lactate (Baxter)	300
Autologous leukocyte-depleted blood	500
Additives	
200 g/L albumin (Prothya Biosolutions)	20
8.4% sodium bicarbonate (B. Braun)	10
5% glucose (Baxter)	10
Verapamil (Sigma-Aldrich)	1
Dexamethasone (Centrafarm)	0.3
90mg creatinine (Sigma-Aldrich)	-
Infusion 20mL/h	
Aminoplasmal (B. Braun)	45
8.4% sodium bicarbonate (B. Braun)	1.5
100 U/mL insulin (NovoRapid®)	0.5

Table S2. Histopathological grading for each kidney with correspondent sO_2

Sample	Group	WIT (min)	Mean sO_2 (%)			Histology grade	
			30 min	60 min	110 min	Before NMP	After NMP
1	1	30	20	26	29	2	2
2	1	75	17	21	20	2	2
3	1	75	18	28	28	2	2
4	1	30	19	27	31	2	3
5	1	30	27	45	56	2	2
6	1	30	15	22	22	2	3
7	1	75	16	18	21	3	3
8	1	75	21	47	59	2	2
9	1	30	43	57	65	2	2
10	1	75	21	46	45	2	2
11	1	30	19	44	61	2	2
12	1	30	30	62	72	2	3
13	1	75	19	45	49	2	2
14	1	30	23	29	30	2	2
15	1	75	21	24	30	2	3
16	2	30	20	40	46	2	3
17	2	30	21	73	77	2	2
18	2	30	28	74	75	2	2
19	2	30	30	54	63	2	2
20	2	75	27	68	67	2	2
21	2	30	52	60	67	2	2
22	2	30	17	32	39	2	3

NMP, normothermic machine perfusion; sO_2, oxygenation; WIT, warm ischemia time.



Chapter 4

Enhancing kidney quality assessment: Power Doppler during normothermic machine perfusion

Yitian Fang*, Anton V. Nikolaev*, Jeroen Essers, Gisela Ambagtsheer, Marian C. Clahsen-van Groningen, Robert C. Minnee, Ron W.F. de Bruin, Gijs van Soest

* Authors contributed equally to this study.

Artificial Organs, 2025

The work presented in this chapter was supported by the "HOST" project funded by the Dutch Research Council (NWO, project number 20719), and contributes to the Medical Delta scientific research program "Medical Delta MIMIC: Medische instrumenten maken: van idee naar kliniek".

Abstract

Objectives Marginal donor kidneys are increasingly used for transplantation to overcome organ shortage. This study aims to investigate the additional value of Power Doppler (PD) imaging in kidney quality assessment during normothermic machine perfusion (NMP).

Methods Porcine kidneys (n=22) retrieved from a local slaughterhouse underwent 2 hours of NMP. Based on creatinine clearance (CrCl) and oxygen consumption (VO_2) at 120 minutes, kidneys were classified into Group 1 (n=7, CrCl >1 ml/min/100g and VO_2 >2.6 ml/min/100g) and Group 2 (n=15, CrCl ≤1 ml/min/100g and/or VO_2 ≤2.6 ml/min/100g). PD imaging was performed at 30, 60, and 120 minutes, and PD metrics, including vascularization index (VI), flow index (FI), and vascularization flow index (VFI) were calculated. Renal blood flow (RBF), CrCl, and VO_2 were measured at the same time points during NMP. The metrics were compared utilizing correlation analysis.

Results FI and VFI moderately correlated with CrCl ($r=0.537$, $p<0.0001$; $r=0.536$, $p<0.0001$, respectively), while VI strongly correlated with VO_2 ($r=0.839$, $p<0.0001$). At 120 minutes, PD metrics demonstrated the highest diagnostic accuracy for distinguishing between the two groups, with an area under the curve (AUC) of 0.943 for VI, 0.924 for FI, and 0.943 for VFI. Cutoff values of 17% for VI, 50 a.u. for FI, and 9 a.u. for VFI provided 100% specificity and 73% sensitivity in identifying kidneys in Group 2, with an overall diagnostic accuracy of 82%. Baseline kidney biopsies showed moderate acute tubular necrosis in both groups with no significant differences.

Conclusions PD metrics strongly correlate with renal viability and effectively differentiate kidneys with higher and lower functionality during NMP. PD imaging can be a valuable alternative to RBF during NMP for kidney quality assessment.

Introduction

Kidney transplantation is considered the optimal treatment for end-stage renal disease.[1] Due to persistent organ shortage, kidneys from donation after circulatory death (DCD) or expanded criteria donors (ECD) are increasingly used for transplantation. Unfortunately, such kidneys are associated with a high risk of graft failure due to the suboptimal conditions of the donors such as old age, uncertain medical history, long ischemia time or pre-donation acute kidney injury.[2, 3] To reduce the risk of graft failure, organ quality has to be carefully assessed before transplantation, mainly based on procurement biopsies despite its invasive nature.[4]

Normothermic machine perfusion (NMP) has emerged as an experimental preservation technique which aims to restore and assess kidney function by supplying the organ with perfusate enriched with nutrients and oxygen at 35-37°C to simulate the physiological environment of the human body.[5, 6] This innovative platform allows for the evaluation of renal functional capacities and injury through various parameters, including renal blood flow (RBF), intrarenal resistance (IRR), urine output, creatinine clearance (CrCl), oxygen consumption (VO_2) and optical imaging during NMP.[7, 8]

Markgraf et al. utilized hyperspectral optical imaging (HSI) to measure renal cortex oxygen saturation and water content as indicators of tissue damage.[9, 10] Schuller et al. used magnetic resonance imaging (MRI) to assess renal blood distribution during NMP.[11, 12] Our previous research demonstrated the value of laser speckle contrast imaging (LSCI) and photoacoustic (PA) imaging to visualize renal cortical microcirculation and assess kidney quality.[13, 14]

Alternatively, renal perfusion can be assessed using Ultrasound (US) Power Doppler (PD). Based on the Doppler effect, PD measures the amplitude of the Doppler signal and visualizes blood flow patterns.[15, 16] PD imaging has been widely used in various clinical scenarios to assess blood flow, vascular structures and hemodynamic abnormalities.[17-20] In kidney transplant patients, PD is mainly used to detect vascular complications, early acute rejection and renal dysfunction.[21-23]

Despite its use in post-transplant practice, no study has reported PD imaging in assessing organ quality during pre-transplant NMP. Recognizing this gap, our study aims to

investigate the additional value of PD imaging in kidney quality assessment during NMP and its correlation with function and viability markers.

Materials and Methods

Study Design

Twenty-two kidneys from 6-month-old female Landrace pigs were harvested from a local slaughterhouse. The animals were exsanguinated before slaughtering which simulates DCD conditions. Next, kidneys were transported to the laboratory and underwent 2 hours of NMP for quality assessment.

During NMP, traditional functional parameters, including CrCl and VO_2, and PD data were acquired at 30, 60, and 120 minutes of NMP. Kidneys were classified into two groups based on the CrCl and VO_2 values at 120 minutes. Specifically, Group 1 included kidneys with CrCl>1 ml/min/100g and VO_2>2.6 ml/min/100g, while Group 2 included kidneys with CrCl≤1 ml/min/100g and/or VO_2≤2.6 ml/min/100g. These thresholds were established based on previous studies utilizing similar NMP protocols and perfusate compositions. Although the kidneys were not transplanted, those with relatively low CrCl and VO_2 during NMP may be associated with poor post-transplant function.[24, 25]

Since the kidneys were obtained from pigs intended for meat consumption, no approval from the animal ethics committee was required.

Kidney Preparation

Back-table procedures have been described elsewhere.[13] Briefly, two liters of blood were collected in a heparinized bucket and filtered by leukocyte filter (BioR 02 plus, Fresenius Kabi, the Netherlands) during exsanguination. The kidneys were then explanted by a designated butcher following a standardized procedure. Once the kidneys were explanted, the renal artery was cannulated and flushed with 500 mL 4°C Ringer's lactate (Baxter BV, Utrecht, the Netherlands). During transportation to the laboratory, kidneys were preserved using hypothermic machine perfusion (LifePort®, Organ Recovery Systems, USA) until NMP. Warm ischemia time (WIT) was calculated from the blood collection until cold

flushing. Cold ischemia time (CIT) was defined as the hypothermic machine perfusion period.

Before NMP, the kidneys were flushed with 100 mL 4°C Ringer's lactate to remove the cold preservation solution. Subsequently, kidneys underwent 2 hours of NMP with autologous blood-based solution (**Table S1**) at 37°C with a controlled pressure of 70 mmHg. Carbogen (95% O_2 and 5% CO_2) was supplied via the oxygenator at flow rate of 0.5 L/min.

Experimental Setup

The schematic of the perfusion and measurement setup is depicted in **Figure 1**.

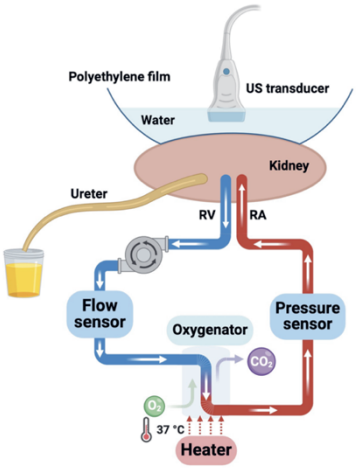


Figure 1. Schematic of the normothermic machine perfusion (NMP) and ultrasound (US) setup. RA, renal artery; RV, renal vein.

The NMP system consists of a centrifugal pump head (BPX-80 Bio-Pump™ Plus, Medtronic, Minneapolis, USA) equipped with a pump drive (BVP-BP, Harvard Apparatus, Germany), an oxygenator with a heat exchanger (Hilite 1000, Medos, Germany), and a thermocirculator (E100, Lauda, Germany). A flow probe (73-4755, Harvard Apparatus, Germany) is connected in-line with the kidney and a pressure sensor (APT300, Harvard Apparatus, Germany) is directly connected to the 5mm straight cannula (Organ Recovery Systems, USA). The set-up is controlled by a commercially available electronic controller (PLUGSYS Servo Controller for Perfusion, Harvard Apparatus, Germany) which enables both flow and pressure-directed perfusions.

The PD system, a Vevo3100 ultrasound (Fujifilm VisualSonics, Canada) system, is equipped with an MX201 US linear transducer array (VisualSonics, Canada) operating at 15 MHz central frequency. During the PD acquisition, the transducer was attached to a linear translational stage enabling 3D image acquisition. To provide the acoustic coupling, we covered the kidney with a polyethylene film filled with water as coupling media.

Renal Function, Viability, and Injury Measurement

RBF was monitored by the flow sensor continuously throughout NMP. The perfusate samples from the renal artery and vein were collected at 30, 60, and 120 minutes of NMP for blood gas analysis (epoc® Blood Analysis System, Siemens Healthineers, Canada). The urine output was recorded and collected at the same time points for further measurement.

CrCl, defined as the volume of perfusate plasma that is cleared of creatinine per unit time, is used as a renal function marker. VO_2, defined as the amount of oxygen consumed per unit time, is used as a renal viability marker.[26]

Baseline kidney biopsies were taken before NMP and fixed in 4% buffered paraformaldehyde. The tissue samples were then embedded in paraffin and cut into 5 μm sections. Using periodic acid-Schiff (PAS) staining, acute tubular necrosis (ATN) was evaluated and scored on a semiquantitative scale of 0 to 3 (0-no changes, 1-mild, 2-moderate, 3-severe changes) by an experienced renal pathologist blinded to the study. ATN score was based on the degree of brush border loss, tubular dilatation, epithelial vacuolation, thinning and sloughing, and luminal debris/casts.

Power Doppler Measurement

PD data were acquired from the lateral aspect of the renal cortex at 30, 60, and 120 minutes of NMP. To achieve this, the kidney was positioned laterally, and the US transducer was positioned directly above the kidney. The transducer was automatically translated over a range of 45 mm by 0.5 mm step. The settings for the PD measurements are reported in **Table S2**, which were chosen manually to optimize the visualization of the renal cortical vasculature during NMP.

PD data were used to calculate vascularization index (VI), flow index (FI), and vascularization flow index (VFI). VI was defined as the ratio of colored pixels to all pixels within the region of interest (ROI), indicating the number of blood-filled vessels. FI was defined as the mean PD signal intensity from all colored pixels, indicating the blood volume at the time of measurement. VFI is the combination of vascularization and blood volume, mathematically multiplying VI by FI.[27] The equations are shown as below:

$$VI\ (\%) = \frac{\#\ colored\ pixels}{\#\ total\ pixels} \times 100\%, \quad (1)$$

$$FI(a.u.) = \frac{\sum_{i=1}^{\#\ colored\ pixels} w(i)}{\#colored\ pixels}, \quad (2)$$

$$VFI(a.u.) = VI \times FI, \quad (3)$$

where $w(i)$ is a value of the i^{th} colored pixel which represents intensity of the PD signal. The pixel value represents power of the Doppler signal and normalized based of the settings and scaled between 0 and 255. The ROI is defined as the renal cortical layer at a depth of 5 mm from the kidney surface, as the majority of functional nephrons are located within this cortical layer. For further data analysis we calculated the mean value of each metric within the acquired volume.

Statistical Analysis

We reported continuous variables using median and interquartile range (IQR). Renal function, viability and PD metrics at each time point were compared between groups using the Mann-Whitney U test. The correlations between PD metrics and functional parameters, as well as between RBF and functional parameters were investigated using the Spearman's linear correlation test. Receiver operating characteristic (ROC) curves were used to determine the cutoff values for distinguishing between the two groups. Due to the organ scarcity, it is recommended to accept all potentially viable kidneys.[28, 29] Therefore, cutoff values were defined to maximize specificity for identifying Group 2 kidneys. We adopted a significance level of 95%. We used Matlab 2023a (The MathWorks, Natick, MA, USA) and GraphPad Prism 9.3.1 (GraphPad Software Inc., San Diego, CA) for data processing, statistical analysis and data presentation.

Results

All kidneys underwent 2 hours of NMP without macroscopic abnormalities. Based on the pre-set criteria, 7 kidneys were classified into Group 1 and 15 kidneys into Group 2. The average WITs were 35 minutes for Group 1 and 50 minutes for Group 2, and CITs were 5.6 hours and 6.4 hours, respectively.

Renal Function and Viability Assessment

RBF demonstrated significant variations between the two groups. Specifically, at 30, 60 and 120 minutes, RBF was 54 (45-58), 83 (66-88), and 83 (76-128) ml/min/100g in Group 1, and 39 (29-50), 49 (42-55), and 55 (43-65) ml/min/100g in Group 2 (p=0.078, p=0.005, and p=0.003, respectively, **Figure 2A**). CrCl showed significant difference from 30 minutes [0.43 (0.20-1.25) vs 0.17 (0.06-0.28) ml/min/100g, p=0.039] until 120 minutes [1.61 (1.46-4.27) vs 0.33 (0.17-0.79) ml/min/100g, p<0.001, **Figure 2B**]. VO_2 diverged significantly by 60 minutes of NMP, with Group 1 displaying higher VO_2 of 2.63 (2.34-3.03) mlO_2/min/100g compared to 1.82 (1.69-2.19) mlO_2/min/100g in Group 2 (p=0.004, **Figure 2C**). Urine output was also higher in Group 1, particularly at 120 minutes [43 (28-85) vs 8 (6-18) ml/h, p=0.002, **Figure 2D**].

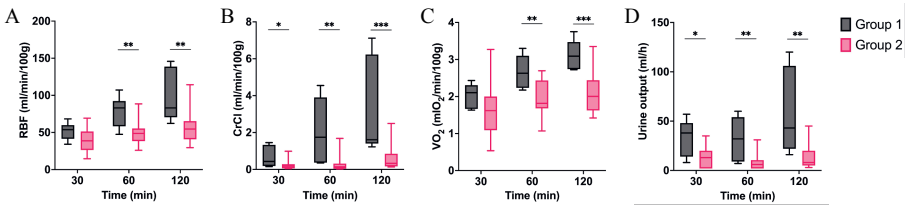


Figure 2. Function and viability parameters measured during NMP. (A) Renal blood flow (RBF); (B) Creatinine clearance (CrCl); (C) Oxygen consumption (VO_2); (D) Urine output. *p≤0.05, **p≤0.01, ***p≤0.001.

Power Doppler Metrics Assessment

Representative PD imaging frames from both groups are shown in **Figure 3**. PD images distinctly discriminate the difference in renal cortical perfusion between the groups during NMP. In Group 1, PD images showed a progressive increase in signal intensity and vascularization over time, suggesting effective restoration of perfusion. In contrast, Group 2 demonstrated less improvement in perfusion recovery, as indicated by lower signal intensity and vascularization percentages.

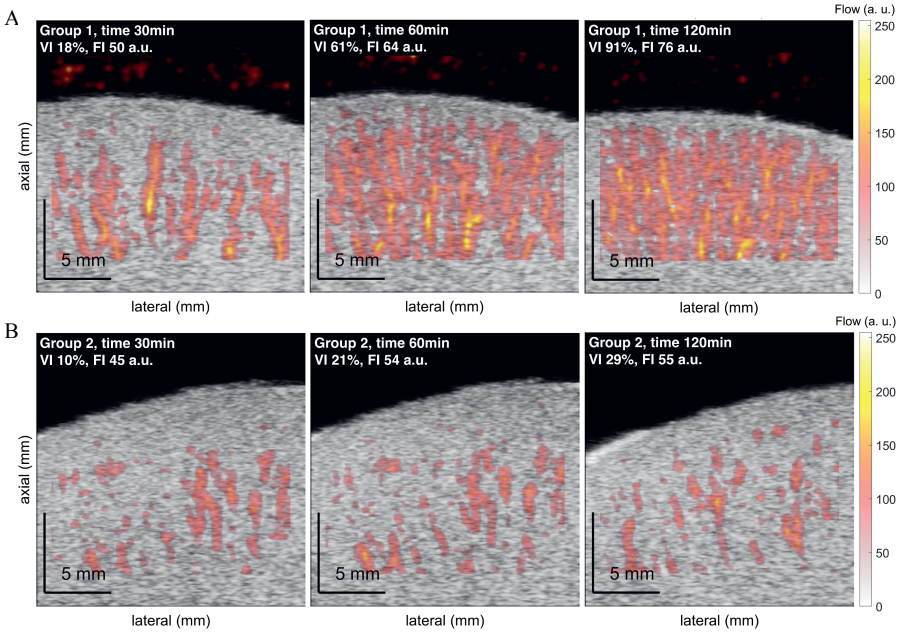


Figure 3. Representative Power Doppler (PD) imaging frames of renal cortex in (A) Group 1 and (B) Group 2 at 30, 60, and 120 minutes of NMP. FI, flow index; VI, vascularization index.

The values of VI, FI, and VFI are depicted in **Figure 4**. VI differed significantly between the two groups at 30 minutes of NMP [9 (7-17)% vs 2 (1-8)%, p=0.026, **Figure 4A**]. FI also differed between the two groups. Group 1 showed a significantly higher FI at 30 minutes, indicating more robust perfusion compared to Group 2 [46 (44-51) vs 36 (33-44) a.u., p=0.032, **Figure 4B**]. VFI showed similar trends, with Group 1 exhibiting a significantly higher VFI at 30 minutes [5 (4-10) vs 1 (0-4) a.u., p=0.026, **Figure 4C**].

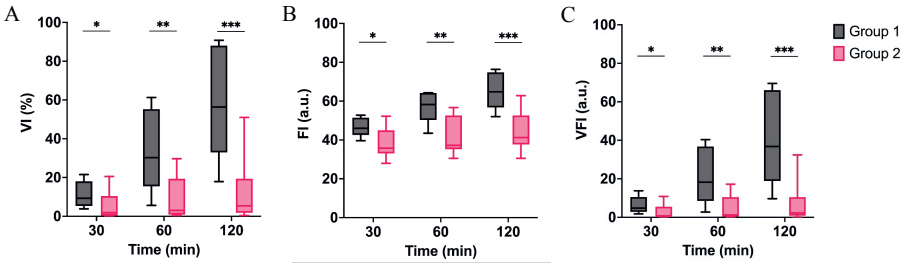


Figure 4. Quantitative PD metrics showing significant differences between Group 1 and Group 2 at 30 minutes of NMP. (A) Vascularization index (VI); (B) Flow index (FI); (C) Vascularization flow index (VFI). *p≤0.05, **p≤0.01, ***p≤0.001.

Correlation between RBF and Functional Metrics

We investigated the correlation between renal perfusion velocities and functional parameters as depicted in **Figure 5**. Both RBF and PD metrics demonstrated significant positive correlations with CrCl and VO2. Specifically, while the correlation between RBF and CrCl was low positive (r=0.423, p<0.001), PD metrics demonstrated moderate correlations with CrCl (VI, r=0.528, p<0.0001; FI, r=0.537, p<0.0001; VFI, r=0.536, p<0.0001). Notably, both RBF and PD metrics showed strong positive correlations with VO_2, while VI exhibited the highest correlation coefficient (r=0.839, p<0.0001).

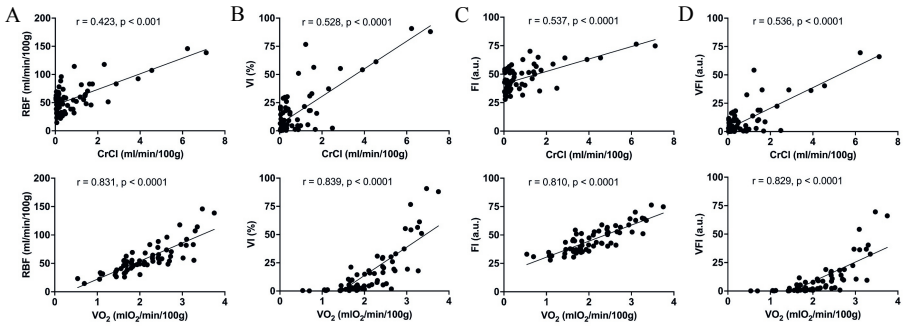


Figure 5. Correlation between (A) RBF, (B) VI, (C) FI, (D) VFI and CrCl (left) and VO_2 (right). Black scatters represent all kidneys at all measured time points.

Cutoff Values for Intergroup Differentiation

The ROC curve analyses of PD metrics and RBF at 30, 60, and 120 minutes of NMP are shown in **Figure S1**, **S2** and **Table S3**, **S4**. Among these time points, PD metrics at 120 minutes showed the most robust cutoff values for distinguishing between the two groups, with an area under the curve (AUC) of 0.943 for VI, 0.924 for FI, and 0.943 for VFI. Similarly, RBF at 120 minutes had the highest AUC of 0.886 (p=0.004).

To minimize the risk of rejecting kidneys associated with favorable post-transplant outcomes, we determined cutoff values that achieved 100% specificity for identifying Group 2 kidneys. Cutoff value of 60 ml/min/100g for RBF shows 67% sensitivity, a negative predictive value (NPV) of 58% and overall accuracy of 77%, while cutoff values of 17% for VI, 50 a.u. for FI, and 9 a.u. for VFI demonstrated 73% sensitivity, NPVs of 64% and improved diagnostic accuracy of 82%.

Renal Injury Assessment

Representative histological images of kidney biopsies are depicted in **Figure 6**. In both groups, the tubules exhibited loss of brush border, debris, and lumen dilation, suggesting moderate ATN prior to NMP. No significant difference of the semiquantitative scale was observed between the groups.

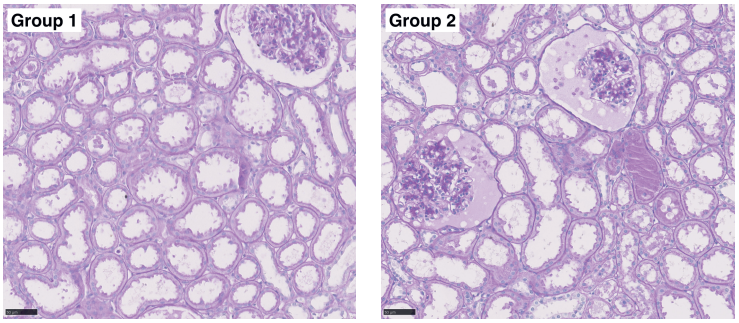


Figure 6. Representative periodic-acid-Schiff (PAS) staining of Group 1 (left) and Group 2 (right) prior to NMP. 40 × magnification.

Discussion

This study used a porcine kidney NMP model to investigate the value of PD imaging in assessing kidney quality. We observed significant differences in PD metrics between kidneys exhibiting high and low renal function during NMP. Our findings revealed a moderate positive correlation between PD metrics and renal function, and a strong positive correlation between PD metrics and renal viability. Compared to RBF, PD imaging may provide earlier detection of kidneys with poor post-transplant outcomes in this porcine model.

PD imaging has unique advantages in ease of use, real-time monitoring, and relatively low cost, as it can be performed with standard ultrasound equipment without high operational costs and contrast agents. Additionally, PD imaging can be performed using a portable ultrasound system which costs under €1,000. Since NMP is gradually being introduced into clinical practice in academic medical centers,[30, 31] it is feasible to apply PD imaging for pre-transplant kidney quality assessment in clinical settings.

In functional kidneys, PD imaging displays a diffused, homogeneous blush color across the entire renal cortex. In contrast, non-functional kidneys significantly lower VI, FI, and VFI,

indicating fewer blood-filled vessels and reduced blood volume in the renal cortex. It can be explained by the prolonged WIT and high sensitivity to ischemic injury that result in high intrarenal resistance and inferior blood flow during machine perfusion.[32-34]

Compared to RBF as routine monitoring during NMP, PD metrics differentiated kidneys in the two groups earlier. This discrepancy reflects the heterogeneity of the perfusion in the entire kidney (RBF) versus renal cortical perfusion status (PD), which is in line with the study by Schutter et al.[11] which reported heterogeneous corticomedullar ratios in kidneys with consistent RBF during NMP.

Post-transplant PD imaging assessments can be affected by extrarenal variables rather than inherent renal injury. Renal cortical blood perfusion is easily affected by blood pressure, renal capillary wedge pressure, and vascular compliance, which reflects systemic hemodynamics.[35] In contrast, pre-transplant assessment with standardized perfusion setups can reduce bias from extrarenal variables. We investigated the correlation between PD metrics and function and viability markers. VI, FI, and VFI showed a better correlation with CrCl than RBF. This can be explained by the fact that the majority of functional nephrons are located in the renal cortex. However, due to the complex mechanisms of kidney function, predicting renal function solely based on PD imaging is not ideal. These metrics need to be combined with other characteristics, biomarkers and biophysical properties to accurately evaluate function. In terms of renal viability, both RBF and PD metrics showed a strong correlation with VO_2, with VI displaying the highest correlation coefficient, indicating that PD metrics are reliable markers of renal metabolic activity.

Our results showed that, with appropriate cutoff values, both PD metrics and RBF can achieve 100% specificity in identifying kidneys with low renal function and viability during NMP, with PD showing higher overall accuracy. Based on this, kidneys classified as having low function and viability (Group 2) are recommended to be discarded. We also applied the ex vivo normothermic perfusion (EVNP) score, based on macroscopic appearance, RBF, and urine output on the kidneys. Group 1 kidneys scored 1 (n=4) or 2 (n=3), while Group 2 kidneys scored 2 (n=8) or 3 (n=7) (Table S5).[8] Kidneys with an EVNP score of 2 present in both groups suggests an ambiguous threshold for transplant suitability. This overlap may also be attributed to the subjectivity of macroscopic assessment and inherent differences between porcine and human kidney perfusion.

We analyzed the correlation between PD metrics and EVNP scores. As shown in **Figure S3**, kidneys with EVNP score 1, 2, and 3 exhibited distinct VI, FI, and VFI values, with the most significant differences observed at 120 minutes of NMP. At this timepoint, kidneys with an EVNP score of 1 demonstrated significantly higher PD metrics than those with an EVNP score of 3. This trend suggests that PD imaging may offer predictive value consistent with this clinically validated scoring system.

However, it is important to note that predictive accuracy based on PD metrics may vary depending on classification criteria, and relying solely on a single factor carries a risk of false-negative predictions. Incorporating PD imaging into the current scoring system might enhance its accuracy and improve transplant decision-making.[8]

Interestingly, histological results revealed no significant differences between the groups. One explanation could be that the functional differences do not correlate with histological changes. In addition, due to sampling error: the local evaluation of the renal parenchyma may not represent the overall condition of the kidney.[36]

The present study has several limitations to be addressed. Firstly, while renal function and viability measured during NMP can reflect kidney quality, the absence of a reperfusion model with allogenic whole blood or a transplant model makes it unable to determine the actual differences in post-transplant kidney function between the two groups. Secondly, the use of slaughterhouse animals introduces great interindividual variability in kidney viability and injury due to the less controlled procedure, which could have influenced our outcome measurements. Thirdly, while porcine kidneys are commonly utilized in preclinical machine perfusion experiments, their anatomical and physiological characteristics differ from human kidneys. It is important to exercise caution when extrapolating our findings to clinical scenarios. Further research should focus on applying PD imaging to experimental kidneys intended for transplantation to validate our findings.

Conclusion

This study demonstrated the potential of PD imaging in pre-transplant kidney quality assessment using a porcine kidney NMP model. The PD metrics strongly correlate with renal viability and can potentially identify kidneys with poor post-transplant outcomes. PD imaging can be a valuable alternative to RBF during NMP. The explorative translation into clinical practice might help to optimize the utilization of marginal kidneys.

Reference

1. Tonelli M, Wiebe N, Knoll G, Bello A, Browne S, Jadhav D, et al. Systematic review: kidney transplantation compared with dialysis in clinically relevant outcomes. Am J Transplant. 2011;11(10):2093-109.
2. Port FK, Bragg-Gresham JL, Metzger RA, Dykstra DM, Gillespie BW, Young EW, et al. Donor characteristics associated with reduced graft survival: an approach to expanding the pool of kidney donors. Transplantation. 2002;74(9):1281-6.
3. Rao PS, Ojo A. The alphabet soup of kidney transplantation: SCD, DCD, ECD--fundamentals for the practicing nephrologist. Clin J Am Soc Nephrol. 2009;4(11):1827-31.
4. von Moos S, Akalin E, Mas V, Mueller TF. Assessment of Organ Quality in Kidney Transplantation by Molecular Analysis and Why It May Not Have Been Achieved, Yet. Front Immunol. 2020;11:833.
5. Mazilescu LI, Urbanellis P, Kim SJ, Goto T, Noguchi Y, Konvalinka A, et al. Normothermic Ex Vivo Kidney Perfusion for Human Kidney Transplantation: First North American Results. Transplantation. 2022;106(9):1852-9.
6. Hosgood SA, Callaghan CJ, Wilson CH, Smith L, Mullings J, Mehew J, et al. Normothermic machine perfusion versus static cold storage in donation after circulatory death kidney transplantation: a randomized controlled trial. Nature Medicine. 2023;29(6):1511-9.
7. Hamelink TL, Ogurlu B, De Beule J, Lantinga VA, Pool MBF, Venema LH, et al. Renal Normothermic Machine Perfusion: The Road Toward Clinical Implementation of a Promising Pretransplant Organ Assessment Tool. Transplantation. 2022;106(2):268-79.
8. Hosgood SA, Barlow AD, Hunter JP, Nicholson ML. Ex vivo normothermic perfusion for quality assessment of marginal donor kidney transplants. Br J Surg. 2015;102(11):1433-40.
9. Markgraf W, Feistel P, Thiele C, Malberg H. Algorithms for mapping kidney tissue oxygenation during normothermic machine perfusion using hyperspectral imaging. Biomed Tech (Berl). 2018;63(5):557-66.
10. Markgraf W, Lilienthal J, Feistel P, Thiele C, Malberg H. Algorithm for Mapping Kidney Tissue Water Content during Normothermic Machine Perfusion Using Hyperspectral Imaging. Algorithms. 2020;13(11):289.
11. Schutter R, Lantinga VA, Hamelink TL, Pool MBF, van Varsseveld OC, Potze JH, et al. Magnetic resonance imaging assessment of renal flow distribution patterns during ex vivo normothermic machine perfusion in porcine and human kidneys. Transpl Int. 2021;34(9):1643-55.
12. Hamelink TL, Ogurlu B, Pamplona CC, Castelein J, Bennedsgaard SS, Qi H, et al. Magnetic resonance imaging as a noninvasive adjunct to conventional assessment of functional differences between kidneys in vivo and during ex vivo normothermic machine perfusion. Am J Transplant. 2024.
13. Fang YT, van Ooijen L, Ambagtsheer G, Nikolaev AV, Clahsen-van Groningen MCCV, Dankelman J, et al. Real-time laser speckle contrast imaging measurement during normothermic machine perfusion in pretransplant kidney assessment. Laser Surg Med. 2023;55(8):784-93.
14. Nikolaev AV, Fang Y, Essers J, Panth KM, Ambagtsheer G, Clahsen-van Groningen MC, et al. Pre-transplant kidney quality evaluation using photoacoustic imaging during normothermic machine perfusion. Photoacoustics. 2024;36:100596.
15. Martinoli C, Pretolesi F, Crespi G, Bianchi S, Gandolfo N, Valle M, et al. Power Doppler sonography: clinical applications. European Journal of Radiology. 1998;27:S133-S40.
16. Szabo TL. Chapter 11 - Doppler Modes. In: Szabo TL, editor. Diagnostic Ultrasound Imaging: Inside Out (Second Edition). Boston: Academic Press; 2014. p. 431-500.
17. Aziz MU, Eisenbrey JR, Deganello A, Zahid M, Sharbidre K, Sidhu P, et al. Microvascular Flow Imaging: A State-of-the-Art Review of Clinical Use and Promise. Radiology. 2022;305(2):250-64.
18. Smith E, Azzopardi C, Thaker S, Botchu R, Gupta H. Power Doppler in musculoskeletal ultrasound: uses, pitfalls and principles to overcome its shortcomings. J Ultrasound. 2021;24(2):151-6.
19. Bhasin S, Cheung PP. The Role of Power Doppler Ultrasonography as Disease Activity Marker in Rheumatoid Arthritis. Dis Markers. 2015;2015.
20. Yamasato K, Zalud I. Three dimensional power Doppler of the placenta and its clinical applications. J Perinat Med. 2017;45(6):693-700.
21. Franke D. The diagnostic value of Doppler ultrasonography after pediatric kidney transplantation. Pediatr Nephrol. 2022;37(7):1511-22.
22. Shebel HM, Akl A, Dawood A, El-Diasty TA, Shokeir AA, Ghoneim MA. Power Doppler Sonography in Early Renal Transplantation: Does It Differentiate Acute Graft Rejection from Acute Tubular Necrosis? Saudi J Kidney Dis T. 2014;25(4):733-40.
23. Datta R, Sandhu M, Saxena AK, Sud K, Minz M, Suri S. Role of duplex Doppler and power Doppler sonography in transplanted kidneys with acute renal parenchymal dysfunction. Australas Radiol. 2005;49(1):15-20.

24. Ogurlu B, Pamplona CC, Van Tricht IM, Hamelink TL, Lantinga VA, Leuvenink HGD, et al. Prolonged Controlled Oxygenated Rewarming Improves Immediate Tubular Function and Energetic Recovery of Porcine Kidneys During Normothermic Machine Perfusion. Transplantation. 2023;107(3):639-47.
25. Markgraf W, Malberg H. Preoperative Function Assessment of Ex Vivo Kidneys with Supervised Machine Learning Based on Blood and Urine Markers Measured during Normothermic Machine Perfusion. Biomedicines. 2022;10(12).
26. Venema LH, van Leeuwen LL, Posma RA, van Goor H, Ploeg RJ, Hannaert P, et al. Impact of Red Blood Cells on Function and Metabolism of Porcine Deceased Donor Kidneys During Normothermic Machine Perfusion. Transplantation. 2022;106(6):1170-9.
27. Odibo AO, Goetzinger KR, Huster KM, Christiansen JK, Odibo L, Tuuli MG. Placental volume and vascular flow assessed by 3D power Doppler and adverse pregnancy outcomes. Placenta. 2011;32(3):230-4.
28. Hobeika MJ, Miller CM, Pruett TL, Gifford KA, Locke JE, Cameron AM, et al. PROviding Better ACcess To ORgans: A comprehensive overview of organ-access initiatives from the ASTS PROACTOR Task Force. Am J Transplant. 2017;17(10):2546-58.
29. Cooper M, Formica R, Friedewald J, Hirose R, O'Connor K, Mohan S, et al. Report of National Kidney Foundation Consensus Conference to Decrease Kidney Discards. Clin Transplant. 2019;33(1):e13419.
30. Hosgood SA, Callaghan CJ, Wilson CH, Smith L, Mullings J, Mehew J, et al. Normothermic machine perfusion versus static cold storage in donation after circulatory death kidney transplantation: a randomized controlled trial. Nat Med. 2023;29(6):1511-9.
31. Rijkse E, de Jonge J, Kimenai H, Hoogduijn MJ, de Bruin RWF, van den Hoogen MWF, et al. Safety and feasibility of 2 h of normothermic machine perfusion of donor kidneys in the Eurotransplant Senior Program. BJS Open. 2021;5(1).
32. Birk AV, Liu S, Soong Y, Mills W, Singh P, Warren JD, et al. The mitochondrial-targeted compound SS-31 re-energizes ischemic mitochondria by interacting with cardiolipin. J Am Soc Nephrol. 2013;24(8):1250-61.
33. Kaasik A, Safiulina D, Zharkovsky A, Veksler V. Regulation of mitochondrial matrix volume. Am J Physiol Cell Physiol. 2007;292(1):C157-63.
34. Liu S, Soong Y, Seshan SV, Szeto HH. Novel cardiolipin therapeutic protects endothelial mitochondria during renal ischemia and mitigates microvascular rarefaction, inflammation, and fibrosis. Am J Physiol Renal Physiol. 2014;306(9):F970-80.
35. O'Neill WC. Renal resistive index: a case of mistaken identity. Hypertension. 2014;64(5):915-7.
36. Dhaun N, Bellamy CO, Cattran DC, Kluth DC. Utility of renal biopsy in the clinical management of renal disease. Kidney Int. 2014;85(5):1039-48.

Supplementary

Table S1. Components of the normothermic machine perfusion perfusate

Priming	**Volume (mL)**
Ringer's lactate (Baxter, the Netherlands)	300
Autologous leukocyte-depleted blood	500
Additives	
8.4% sodium bicarbonate (B. Braun, Germany)	10
5% glucose (Baxter, the Netherlands)	10
Verapamil (Sigma-Aldrich, the Netherlands)	1
Dexamethasone (Centrafarm, the Netherlands)	0.3
90mg creatinine (Sigma-Aldrich, the Netherlands)	-
Infusion 20mL/h	
Aminoplasmal (B. Braun, Germany)	45
8.4% sodium bicarbonate (B. Braun, Germany)	1.5
100 U/mL insulin (NovoRapid®, Denmark)	0.5

Table S2. Settings used for PD data acquisition

PRF (kHz)	Frequency (MHz)	Gate	Wall filter	Sensitivity	Dynamic range (dB)
2	12.5	4	High	5	30

Table S3. ROC curve analysis of PD metrics

Time	PD metrics	AUC	95% CI	p value
30 min	VI (%)	0.800	0.616-0.984	0.026
	FI (a.u.)	0.791	0.603-0.978	0.032
	VFI (a.u.)	0.800	0.616-0.984	0.026
60 min	VI (%)	0.867	0.710-1.000	0.007
	FI (a.u.)	0.886	0.742-1.000	0.004
	VFI (a.u.)	0.867	0.710-1.000	0.007
120 min	VI (%)	0.943	0.848-1.000	0.001
	FI (a.u.)	0.924	0.814-1.000	0.002
	VFI (a.u.)	0.943	0.848-1.000	0.001

AUC, area under the curve; 95% CI, 95% confidence interval; FI, flow index; PD, Power Doppler; VFI, vascularization flow index; VI, vascularization index.

Table S4. ROC curve analysis of RBF

Time	AUC	95% CI	p value
30 min	0.748	0.535-0.960	0.067
60 min	0.867	0.692-1.000	0.007
120 min	0.886	0.747-1.000	0.004

AUC, area under the curve; 95% CI, 95% confidence interval; RBF, renal blood flow.

Table S5. Ex vivo normothermic perfusion assessment score of the kidneys

Group	Kidney	Macroscopic assessment[a]	Renal blood flow (ml/min/100g)[b]	Total urine output (ml)[c]	EVNP score[d]
Group 1	K3	Grade I	74	15	2
Group 1	K4	Grade I	83	70	1
Group 1	K7	Grade I	58	23	2
Group 1	K13	Grade I	83	111	1
Group 1	K19	Grade I	107	108	1
Group 1	K20	Grade I	92	97	1
Group 1	K21	Grade I	50	26	2
Group 2	K1	Grade I	54	15	2
Group 2	K2	Grade I	49	26	3
Group 2	K5	Grade I	89	8	2
Group 2	K6	Grade I	63	7	2
Group 2	K8	Grade I	58	29	2
Group 2	K9	Grade I	46	39	3
Group 2	K10	Grade I	37	30	3
Group 2	K11	Grade I	50	4	2
Group 2	K12	Grade I	34	5	3
Group 2	K14	Grade I	45	66	2
Group 2	K15	Grade I	48	7	3
Group 2	K16	Grade I	26	18	3
Group 2	K17	Grade I	53	21	2
Group 2	K18	Grade I	55	11	2
Group 2	K22	Grade I	38	35	3

a. Grade I: excellent perfusion (global pink appearance, score 1); grade II: moderate perfusion (patchy appearance, score 2); grade III: poor perfusion (global mottled and purple/black appearance, score 3).
b. Threshold ≥ 50: score 0; threshold < 50: score 1.
c. Threshold ≥ 43: score 0; threshold < 43: score 1.
d. Ex vivo normothermic perfusion (EVKP) score is the sum of macroscopic assessment, renal blood flow and total urine output scores.

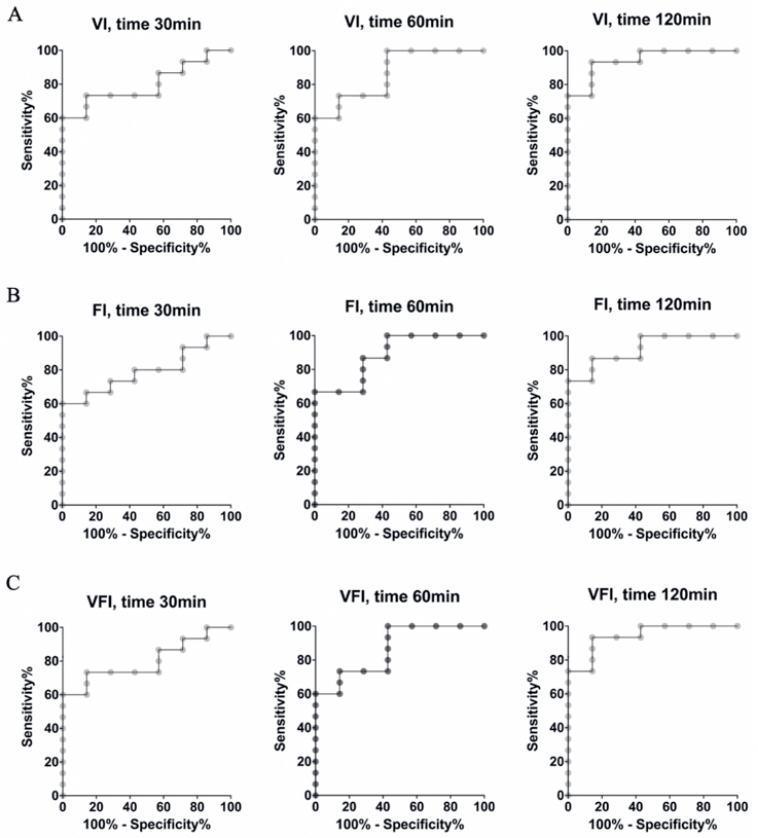


Figure S1. ROC curves of (A) vascularization index (VI), (B) flow index (FI), and (C) vascularization flow index (VFI) to differentiate between the functional and non-functional kidneys at 30, 60, 120 minutes NMP.

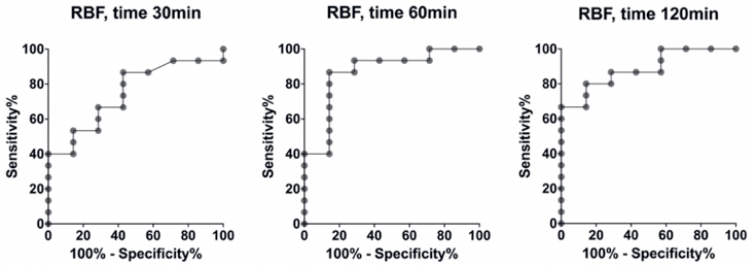


Figure S2. ROC curves of renal blood flow (RBF) to differentiate between the functional and non-functional kidneys at 30, 60 and 120 minutes NMP.

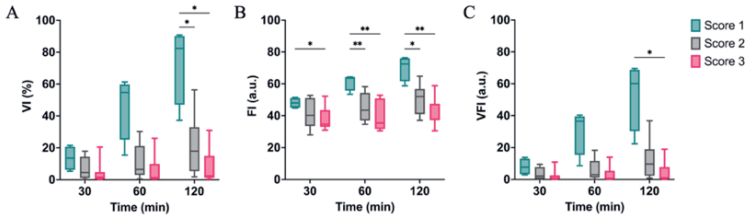
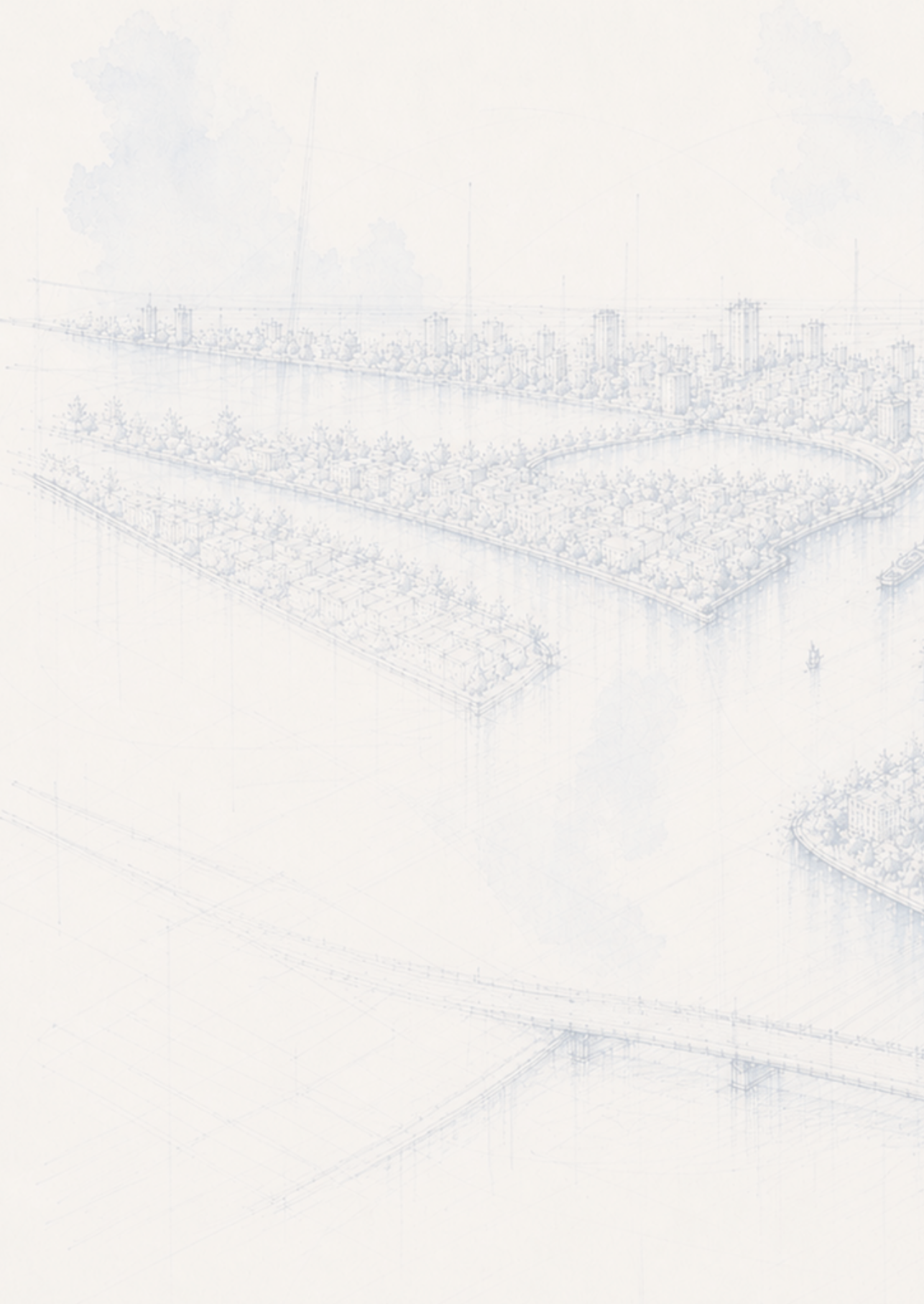


Figure S3. Power Doppler metrics (A) VI, (B) FI, and (C) VFI of the kidneys classified by ex vivo normothermic perfusion (EVNP) score during NMP. *p≤0.05, **p≤0.01, ***p≤0.001.



Chapter 5

Physiological arterial pressure improves renal performance during normothermic machine perfusion in a porcine kidney DCD model

Yitian Fang, Gisela Ambagtsheer, Lin Xia, Marian C. Clahsen-van Groningen, Robert C. Minnee, Ron W.F. de Bruin

Heliyon, 2025

Abstract

Background Normothermic machine perfusion (NMP) provides a platform for kidney quality assessment. Donation after circulatory death (DCD) donor kidneys are associated with great ischemic injury and high intrarenal resistance (IRR). This experimental study aims to investigate the impact of different perfusion pressures on marginal kidney function and injury during NMP.

Methods Twenty-seven slaughterhouse porcine kidneys were retrieved and subjected to 60 minutes of warm ischemia time to mimic DCD condition. These kidneys were randomized into 75 mmHg (subphysiological, n=9), 95 mmHg (physiological, n=9), and 115 mmHg NMP (high physiological, n=9). Renal function and injury were assessed during NMP.

Results Three groups showed comparable IRR, with the 115 mmHg group exhibiting the highest blood flow. The 95 mmHg group [0.48 (0.36-1.15) ml/min/100g] and 115 mmHg group [0.93 (0.45-1.41) ml/min/100g] showed significantly higher creatinine clearance compared to the 75 mmHg group [0.16 (0.08-0.37) ml/min/100g] during the first hour of NMP (p=0.049, p=0.009, respectively). The 115 mmHg group exhibited significantly higher oxygen consumption compared to the 75 mmHg group at 30 minutes of NMP [1.37 (1.05-1.92) versus 0.72 (0.61-0.82) mlO_2/min/100g, p=0.009]. Perfusate neutrophil gelatinase-associated lipocalin (NGAL) levels were consistently lowest in the 95 mmHg group and highest in the 75 mmHg group. Aspartate aminotransferase (AST) levels of the 115 mmHg group were significantly higher than the 75 mmHg group.

Conclusions For kidneys with high IRR, both 95 mmHg and 115 mmHg perfusion pressures enable an early improvement in renal hemodynamics and function compared to 75 mmHg during NMP, while a high physiological perfusion can cause additional injury.

Introduction

Selecting eligible organs from marginal donors, such as those from donation after circulatory death (DCD) donors, poses a challenge in the field of kidney transplantation.[1, 2] Normothermic machine perfusion (NMP) has emerged as a promising platform for kidney quality assessment before transplantation by recreating a physiological environment conducive to organ restoration and energy substrate replenishment.

DCD donor kidneys are strongly associated with substantial ischemic injury and increased risk of graft failure due to prolonged non-heart-beating periods. Warm ischemia, characteristic of DCD donation, results in rapid depletion of intracellular adenosine triphosphate (ATP), thereby disrupting ATP-dependent cellular processes. This disruption includes the inhibition of Na^+-K^+-ATPase activity, leading to intracellular sodium accumulation and subsequent cell swelling, particularly within the renal medulla.[3, 4] This intracellular swelling increases the osmotic gradient, driving water into the mitochondrial matrix and causing matrix swelling.[5] Consequently, DCD donor kidneys frequently exhibit high intrarenal resistance (IRR) and inferior renal function during NMP.

Increasing arterial perfusion pressure has been proven an effective strategy to improve renal perfusion and function during NMP.[6, 7] However, the appropriate pressure to ensure sufficient blood flow without causing additional vascular injury for such kidneys remains unclear.

Previous studies have mostly perfused kidneys at mean arterial pressures ranging from 50-85 mmHg, both in experimental and clinical settings.[8-11] Such subphysiological pressures may not be optimally tailored to address the compromised intravascular condition of marginal kidneys. Research has shown that kidneys perfused at 95 mmHg demonstrated superior renal function without additional endothelial damage compared to those perfused at 75 mmHg.[7] However, this study did not explore the impact of such physiological pressure on marginal kidneys and its subsequent effect on tubular injury, where the ischemic damage primarily occurs.

This study aims to fill this gap by investigating the impact of subphysiological, physiological, and high physiological arterial perfusion pressures on renal function and injury in a porcine kidney DCD model characterized by high IRR.

Materials and Methods

Study Design

Twenty-seven porcine kidneys were procured from juvenile female landrace pigs (weighing ~100 kg) in a local slaughterhouse. We chose this organ source due to its comparable dimensions to human kidneys and ease of obtainment.[12] These kidneys were randomized into three groups with varying perfusion pressures: subphysiological (75 mmHg, n=9), physiological (95 mmHg, n=9), and high physiological (115 mmHg, n=9). To simulate the conditions of DCD donor kidneys, each kidney was subjected to 60 minutes of warm ischemia time (WIT) to induce comparable ischemic injury and high IRR. Subsequently, all kidneys underwent NMP for 2 hours, during which renal function and injury were assessed at designated time points. The 2-hour NMP duration was chosen based on current clinical NMP practices, where one to two hours of perfusion are commonly used.[10, 13]

This study was conducted in compliance with the European Communities Council Directive 2010/63/EU and the 3R principle. By utilizing kidneys from pigs slaughtered for meat production, we reduced the need for additional animal sacrifice for research purposes. Since the kidneys were obtained from pigs slaughtered for meat consumption, no approval from the Medical Ethics Committee was required.

Organ Retrieval

After the pig was stunned, two liters of autologous blood were collected in a bucket containing 25000 IU of heparin (LEO Pharma A/S, Ballerup, Denmark). Following kidney retrieval, each organ was subjected to 60 minutes WIT, arterially cannulated, and flushed with 500ml cold Ringer's lactate (Baxter BV, Utrecht, the Netherlands). Kidneys were then transported to the laboratory using hypothermic machine perfusion (LifePort®, Organ Recovery Systems, Itasca, USA) with 1L of University of Wisconsin Belzer machine perfusion solution (Belzer MPS®) at a pressure of 30 mmHg until NMP. The duration from

kidney retrieval to NMP ranged from 2 to 7 hours. Throughout this period, the kidneys remained under hypothermic machine perfusion. As a standard preservation method in the Netherlands for deceased donor kidneys, its impact on renal function and injury is expected to be minimal.[14] The collected blood was processed to deplete leukocytes using a leukocyte reduction filter (BioR-plus, Fresenius Kabi AG, Homburg, Germany) and stored at 4°C for further use.

Normothermic Machine Perfusion

All kidneys were perfused in the laboratory using the NMP setup commercially available from Harvard Apparatus®, Germany, as previously described.[15] In brief, kidneys were perfused with an oxygenated, red blood cell-based solution at 37°C in a pressure-controlled mode, achieving the settled pressure by adjusting the centrifugal pump speed. The detailed components of the perfusate is provided in **Table S1**. The urine output was recorded every 30 minutes and added back to the perfusate after measurement. This recirculation was done to maintain electrolyte balance and ensure a constant circulating volume within the perfusion system. Creatinine was added in the perfusate to evaluate renal clearance.

Renal Function and Injury Assessment

Throughout NMP, renal blood flow (RBF) was continuously monitored and urine output was measured every 30 minutes. Perfusate and urine samples were collected at 30-minute intervals for further analysis. Oxygen consumption (VO_2) and perfusate lactate levels were determined through blood gas analyses. Creatinine clearance (CrCl), fractional excretion of sodium (FENa) and total sodium reabsorption (TNa) were calculated using established equations.[16, 17]

To assess tubular injury under different perfusion pressures, neutrophil gelatinase-associated lipocalin (NGAL) was quantified in the perfusate as an early biomarker of tubular injury using a pig NGAL ELISA kit (BioPorto Diagnostics A/S, Hellerup, Denmark). Perfusate samples were also analyzed at the clinical biochemistry lab (Triallab, Erasmus Medical Center) to determine lactate dehydrogenase (LDH) and aspartate aminotransferase (AST) levels.

Histopathology Assessment

Renal cortex biopsies were taken from each kidney before and after NMP, fixed in 4% buffered paraformaldehyde, and embedded in paraffin before being sectioned into 5µm slices. Using periodic acid-Schiff (PAS) staining, acute tubular necrosis (ATN) and acute glomerular ischemia were graded on a scale of 0 to 3 (0-none, 1-mild, 2-moderate, 3-severe injury) by an expert renal pathologist blinded to the study. ATN severity was determined based on brush border loss, tubular dilatation, tubular cell necrosis, vacuolation, and interstitial edema at the cortical-medullary junction. Acute glomerular ischemia was assessed by Bowman's space enlargement and glomerular capillary collapse.

Statistical Analysis

Continuous variables are presented as mean ± standard deviation (SD) or median with interquartile range (IQR). Two-way ANOVA was used to compare the functional and viability markers between groups. Fixed effects were time, group factor, and the interaction of the group factor with time, while individual kidneys were considered as random effects. A Geisser–Greenhouse correction and a restricted maximum likelihood approach were used. Statistical analysis was performed using GraphPad Prism 9.3.1 (GraphPad Software Inc., San Diego, CA).

Results

The median cold ischemia time was 5.9 (3.3-6.1), 3.8 (2.8-6.3), 4.4 (3.0-6.0) hours, and the median weight was 262 (254-298), 261 (232-273), 264 (252-284) grams in the 75 mmHg, 95 mmHg, and 115 mmHg groups, respectively ($p=0.755$ and $p=0.951$, respectively). All kidneys underwent NMP for 2 hours without macroscopic abnormalities.

Hemodynamics

RBF exhibited a sharp increase over time in all groups during NMP (p<0.001). In the first 30 minutes, RBF in the 75 mmHg group was significantly lower compared to the 95 mmHg and 115 mmHg groups (p=0.029 and p=0.006, respectively). This difference between the 75 mmHg and 95 mmHg groups diminished with perfusion ongoing (p=0.08), but RBF remained significantly higher in the 115 mmHg group compared to the 75 mmHg group (p=0.010). At the end of perfusion, the mean RBF was 272 ± 57, 300 ± 68, and 389 ± 85 ml/min for the 75 mmHg, 95 mmHg, and 115 mmHg groups, respectively (**Figure 1A**).

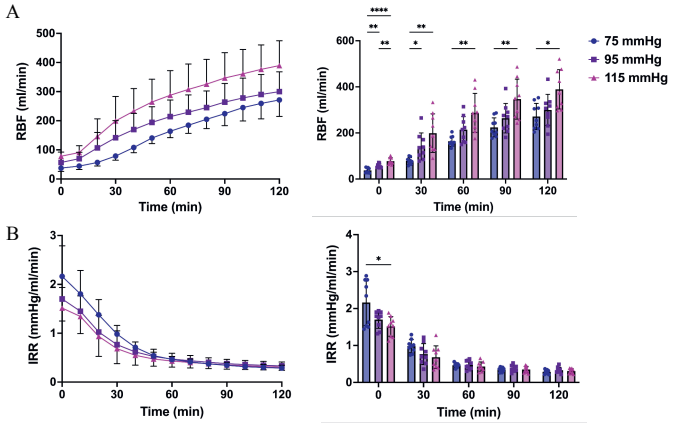


Figure 1. (A) Renal blood flow (RBF), and (B) intrarenal resistance (IRR) during normothermic machine perfusion. Data presented as median ± SD. *p<0.05, **p<0.01, ***p<0.001, ****p<0.0001.

IRR decreased significantly in all three groups over time (p<0.001). Higher perfusion pressures were associated with lower IRR during the first hour of NMP. During the second hour, intergroup differences diminished, with IRR maintaining around 0.31 mmHg/ml/min in all groups (p=0.387, **Figure 1B**).

Renal Function

There was a statistically significant difference in CrCl when comparing the 75 mmHg group to the 95 mmHg and 115 mmHg groups during the first hour of NMP [median (IQR), 75 mmHg 0.16 (0.08-0.37) versus 95 mmHg 0.48 (0.36-1.15) ml/min/100g, p=0.049; 75 mmHg 0.16 (0.08-0.37) versus 115 mmHg 0.93 (0.45-1.41) ml/min/100g, p=0.009]. This trend persisted during the second hour, although it lost its significance, with median CrCl

of 0.21 (0.18-0.44), 0.48 (0.36-1.15), 0.66 (0.39-1.70) ml/min/100g at the end of NMP (**Figure 2A**). FENa decreased significantly over time in all three groups (p<0.001). There was no significant difference between the groups at the end of NMP [75 mmHg 25.7 (21.5-58.1)%, 95 mmHg 51.6 (30.2-61.3)%, 115 mmHg 42.1 (34.1-79.3)%, p=0.529, **Figure 2B**]. VO_2 increased over time in all three groups (p<0.001). At 30 minutes of NMP, the 115 mmHg group exhibited significantly higher VO_2 compared to the 75 mmHg group [75 mmHg 0.72 (0.61-0.82) versus 115 mmHg 1.37 (1.05-1.92) mlO_2/min/100g, p=0.009]. However, VO_2 in the 75 mmHg group increased rapidly, reaching a comparable level with the other two groups by the end of NMP [75 mmHg 2.08 (1.82-2.30), 95 mmHg 2.10 (1.82-2.43), 115 mmHg 2.32 (1.91-2.39) mlO_2/min/100g, p=0.544, **Figure 2C**].

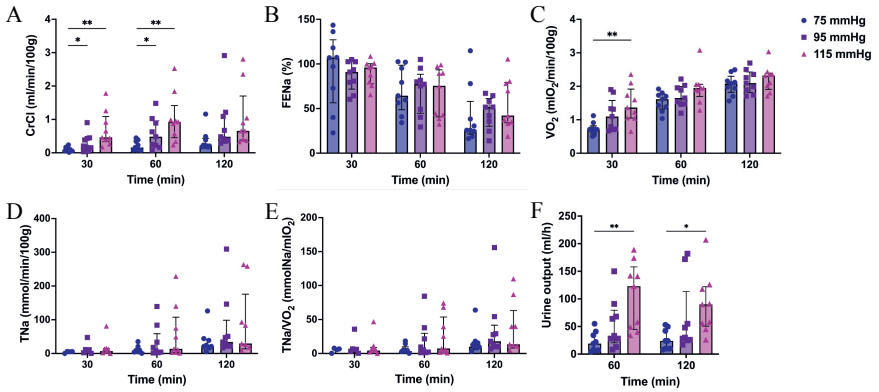


Figure 2. Renal function assessment during NMP. (A) creatinine clearance (CrCl, ml/min/100g); (B) fractional excretion of sodium (FENa, %); (C) oxygen consumption (VO_2, mlO_2/min/100g); (D) total sodium reabsorption (TNa, mmol/min/100g); (E) oxygen utilization efficiency (TNa/VO_2, $mmolNa/mlO_2$); (F) urine output. Data are presented as median with interquartile range. $^{*}p<0.05$, $^{**}p<0.01$, $^{***}p<0.001$.

Furthermore, higher perfusion pressure contributed to higher TNa, although not statistically significant between the three groups [75 mmHg 21.09 (11.29-41.47), 95 mmHg 34.03 (21.74-98.51), 115 mmHg 29.62 (13.67-175.81) mmol/min/100g, p=0.376, **Figure 2D**]. Similarly, oxygen utilization followed the same trend as TNa, with no significant difference between groups at the end of NMP [75 mmHg 9.95 (5.54-16.82), 95 mmHg 17.96 (9.99-41.70), 115 mmHg 13.52 (7.87-63.30) $mmolNa/mlO_2$, p=0.352, **Figure 2E**]. Both kidneys in the 95 mmHg and 115 mmHg groups produced more urine than those in the 75 mmHg group, although this was statistically significant only between the 75 mmHg and 115 mmHg

groups during the two-hour NMP [75 mmHg 24 (10-46) versus 95 mmHg 30 (26-114) ml/h, p=0.200; 75 mmHg 24 (10-46) versus 115 mmHg 90 (51-122) ml/h, p=0.015, **Figure 2F**].

Renal Injury

Baseline NGAL levels were comparable in the three groups [75 mmHg 659.7 (531.2-894.4), 95 mmHg 682.3 (451.0-961.8), 115 mmHg 584.7 (374.7-706.9) µg/ml, p=0.558]. In both the 75 mmHg and 115 mmHg groups, NGAL levels exhibited a trend of initial increase followed by a decrease, while in the 95 mmHg group, NGAL levels decreased continuously, with median values of 403.3 (329.5-637.0), 212.8 (162.5-521.3), and 286.8 (112.4-515.7) µg/ml at the end of NMP. At 30 minutes of NMP, NGAL levels were significantly lower in the 95 mmHg group compared to the 75 mmHg group [549.8 (372.3-689.0) vs. 721.6 (529.3-1094.5) µg/ml, p=0.041, **Figure 3A**]. Baseline perfusate lactate levels were similar in the three groups [75 mmHg 15.0 (14.5-15.5), 95 mmHg 15.0 (14.5-16.0), 115 mmHg 15.0 (14.9-16.5) mmol/L, p=0.496], which slightly increased to 15.2 (10.7-17.0) mmol/L in the 75 mmHg group while decreasing to 11.7 (10.0-12.8) mmol/L in the 95 mmHg group and 11.5 (7.0-16.2) mmol/L in the 115 mmHg group at the end of NMP (**Figure 3B**).

Both LDH and AST exhibited an increasing trend over time in all three groups. LDH levels were slightly higher in the 115 mmHg group compared to the other two groups [75 mmHg 423 (369-533), 95 mmHg 489 (416-569), 115 mmHg 555 (484-685) U/L, p=0.075, **Figure 3C**]. AST levels were slightly lower in the 75 mmHg group compared to the 95 mmHg [78 (63-117) versus 97 (85-148) U/L, p=0.494], but significantly lower when compared to the 115 mmHg group throughout NMP (p=0.002, **Figure 3D**).

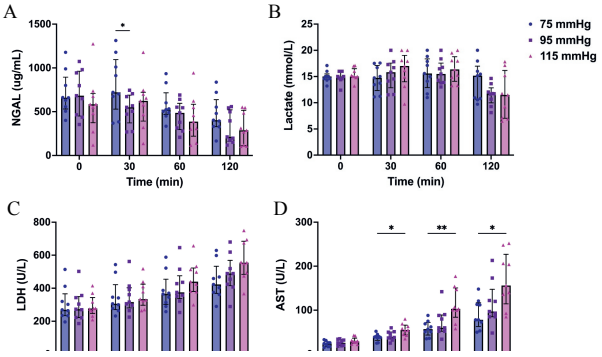


Figure 3. Renal injury assessment during NMP. (A) Neutrophil gelatinase-associated lipocalin (NGAL, ug/ml); (B) perfusate lactate (mmol/L); (C) lactate dehydrogenase (LDH, U/L) and (D) aspartate aminotransferase (AST, U/L). Data are presented as median with interquartile range. $^{*}p<0.05$, $^{**}p<0.01$.

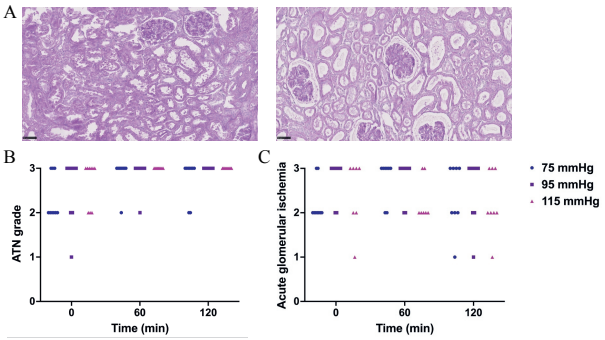


Figure 4. (A) Representative morphological images showing moderate acute tubular necrosis (ATN) and mild acute glomerular ischemia (left), and severe ATN and severe acute glomerular ischemia (right), respectively (PAS staining, 40× magnification); (B) histological grades of ATN; (C) histological grades of acute glomerular ischemia.

Representative images of ATN and acute glomerular ischemia at moderate and severe levels are depicted in **Figure 4A**. In all groups, most kidneys exhibited moderate to severe ATN. Throughout NMP, kidneys remained unchanged or slightly worsened in ATN, with no significant differences observed between the groups (p=0.115, **Figure 4B**). Similarly, most kidneys displayed moderate to severe acute glomerular ischemia, which remained unchanged or mildly worsened during NMP. No significant intergroup differences were observed (p=0.903, **Figure 4C**).

Discussion

In this study, we investigated the impact of different perfusion pressures (subphysiological, physiological, and high physiological) on the renal function and injury using a porcine kidney DCD model during NMP. Our findings indicate that compared to the commonly used perfusion pressure of 75 mmHg, a physiological perfusion pressure of 95 mmHg led to improved renal function without causing additional renal injury. However, NMP under a high physiological pressure (115 mmHg) led to additional injury despite achieving superior renal function. Increasing perfusion pressure to the physiological level could potentially salvage kidneys considered functionally insufficient under subphysiological perfusion pressures during NMP.

NMP represents a promising approach for assessing organ quality by providing oxygenated blood-based perfusate at normothermic temperatures, allowing kidneys to restore metabolism and exhibit functionality. By monitoring functional parameters during perfusion, it becomes feasible to identify marginal kidneys that are suitable for transplantation, thereby increasing the utilization of donor organs. For example, Hosgood et al. reported that 5 out of 10 initially declined kidneys were successfully transplanted

based on renal blood flow and urine production during NMP at a perfusion pressure of 70 mmHg.[18] However, it could be argued that a more physiological perfusion pressure might enhance the functionality of the remaining kidneys, thereby meeting the transplantation criteria. Therefore, demonstrating a kidney's physiological function during NMP is crucial for optimizing organ selection and transplantation outcomes.

In clinical practice, increasing the mean arterial pressure (MAP) is commonly applied to achieve satisfactory reperfusion during kidney transplantation.[19-21] Under physiological conditions, renal artery pressure is naturally higher than normal blood pressure due to gravity. However, in most clinical studies, a subphysiological pressure of 75 mmHg has been chosen as the perfusion pressure for two reasons.[10, 13] Firstly, the optimal perfusion pressure is still under exploration, and using a relatively low pressure serves as a cautious approach to preserve vascular integrity.[22] Secondly, it has been demonstrated to be safe to perfuse the kidneys at 75 mmHg, although most favorable outcome data come from kidneys initially considered eligible for transplantation, which typically exhibit low IRR and mild injury. Therefore, existing literature suggests the feasibility for NMP at 75 mmHg in "good" kidneys. However, for "poor" kidneys, it remains uncertain whether this perfusion pressure is optimal or if NMP under such pressure can facilitate the kidney to present optimal functionality.

In research settings, high perfusion pressures have been explored in a few preclinical studies. For example, NMP has successfully been performed on discarded kidneys for 24-48 hours at 70-100 mmHg (MAP 90 mmHg).[9, 23] Similarly, Pool et al.[24] used porcine kidneys undergoing NMP for 7 hours at a pressure of 110/70 mmHg (MAP 97 mmHg).

Our results demonstrated a trend towards better functionality and viability of kidneys perfused at higher perfusion pressures, particularly significant during the first 30 minutes of NMP. Consistent with previous literature, we observed higher RBF and lower IRR attributed associated with higher arterial perfusion pressure in the early stage of NMP.[6, 7, 25] During this phase, the kidneys experienced a dramatic transition from cold storage to normothermic perfusion, resulting in a rapid shift in metabolic demand. Higher arterial perfusion pressure ensured that sufficient effective blood volume reached the renal cortex, supporting ATP-dependent metabolic activity, as reflected by higher VO_2. Additionally,

renal functionality, indicated by CrCl, increased correspondingly with the elevated metabolic levels.

Interestingly, the significant differences in hemodynamics and renal functionality during the early stage of NMP diminished as perfusion progressed. The observed "catch-up" effect in the 75 mmHg group during the second hour of NMP, characterized by a rapid increase in RBF and VO_2, suggests that kidneys perfused under subphysiological pressure exhibited autoregulatory mechanisms to optimize blood flow distribution. However, this “catch-up” effect is limited, as evidenced by relatively lower urine output and renal function at the end of NMP. To alleviate initial ischemia injury, applying enough perfusion pressure to provide sufficient blood volume is critical in the beginning of NMP.

We further assessed renal injury during NMP. NGAL release represents an intrinsic response of proximal tubule cells to ischemic injury.[26] The short half-life (10 minutes) makes it a sensitive and early marker of acute kidney injury.[27] All groups exhibited a decrease in perfusate NGAL compared to baseline levels, which is in contrast to previous studies demonstrating a significant increase in NGAL levels during prolonged NMP.[23, 28] This discrepancy indicates that short-term NMP under physiological or high physiological pressures may not induce additional tubular injury. Moreover, kidneys perfused at 95 mmHg exhibited significantly lower NGAL levels at 30 minutes of NMP in comparison with the 75 mmHg group, suggesting a potential protective effect of physiological pressure NMP against ischemic injury in the initial stage. This finding complements previous research demonstrating that 95 mmHg NMP does not induce additional endothelial or glycocalyx injury compared to 75 mmHg NMP.[7, 25]

The alterations in perfusate lactate levels further support this point. Specifically, the lactate level in the 75 mmHg group was higher than its baseline level and the other two groups by the end of NMP. This finding is in accordance with previous literature indicating that higher perfusate lactate levels are correlated with lower blood flow and higher NGAL levels, making it a surrogate biomarker for the donor kidney function.[29] Lactate levels are influenced by both glycolysis and gluconeogenesis in the kidney.[30-32] The lactate accumulation in the 75 mmHg group may be attributed to limited blood flow and oxygen

supply, which leads to low oxygen tension in the inner medulla, resulting in impaired lactate metabolism and anaerobic glycolysis.[33]

The general injury biomarkers LDH and AST exhibited an upward trend during the perfusion process, indicating a general kidney injury increasement. This finding was confirmed by the histological results, which revealed signs of acute tubular necrosis and collapse of glomerular capillaries. Similar trends have been reported in other studies.[9, 24, 25] With the current perfusion techniques, ischemia-reperfusion injury may be inevitable during NMP. Interestingly, kidneys in the 75 mmHg and 95 mmHg groups exhibited comparable renal injury in terms of AST and LDH, while higher injury levels were observed in the 115 mmHg group. Considering 115 mmHg as a value of high physiological pressure, it may lead to renal cellular injury, resulting in the leakage of intracellular LDH and AST.[34] However, it is important to note that AST can also be released from damaged red blood cells. At higher flow rates and pump speeds, the mechanical stress may exacerbate red blood cell damage, resulting in increased AST release in the 115 mmHg group.

Our study has several limitations to be addressed. Firstly, although pig kidneys are recognized to have similar anatomical and metabolic characteristics to human kidneys, the use of a slaughterhouse porcine kidney model may not perfectly replicate the complexities of human renal physiology and pathology.[35] Secondly, our study primarily focused on markers of renal tubular injury. Additional injury markers, such as reactive oxygen species and endothelial cell injury markers such as CD31 and CD34, could provide a more comprehensive understanding of kidney injury during NMP. Thirdly, as a preliminary study, it is not sufficient to drive changes in clinical practice. Further research with longer perfusion duration and transplantation is needed to validate these findings.

Conclusion

For kidneys with high IRR, both 95 mmHg and 115 mmHg arterial perfusion pressures enable an early improvement in renal hemodynamics and function during NMP. However, a high physiological perfusion pressure can lead to additional injury, suggesting a delicate balance between renal function and injury in marginal kidneys.

Reference

1. Audard V, Matignon M, Dahan K, Lang P, Grimbert P. Renal transplantation from extended criteria cadaveric donors: problems and perspectives overview. Transpl Int. 2008;21(1):11-7.
2. Stallone G, Infante B, Gesualdo L. Older donors and older recipients in kidney transplantation. J Nephrol. 2010;23 Suppl 15:S98-103.
3. Birk AV, Liu S, Soong Y, Mills W, Singh P, Warren JD, et al. The mitochondrial-targeted compound SS-31 re-energizes ischemic mitochondria by interacting with cardiolipin. J Am Soc Nephrol. 2013;24(8):1250-61.
4. Liu S, Soong Y, Seshan SV, Szeto HH. Novel cardiolipin therapeutic protects endothelial mitochondria during renal ischemia and mitigates microvascular rarefaction, inflammation, and fibrosis. Am J Physiol Renal Physiol. 2014;306(9):F970-80.
5. Kaasik A, Safiulina D, Zharkovsky A, Veksler V. Regulation of mitochondrial matrix volume. Am J Physiol Cell Physiol. 2007;292(1):C157-63.
6. Patel M, Hosgood S, Nicholson ML. The effects of arterial pressure during normothermic kidney perfusion. J Surg Res. 2014;191(2):463-8.
7. Hosgood S, Harper S, Kay M, Bagul A, Waller H, Nicholson ML. Effects of arterial pressure in an experimental isolated haemoperfused porcine kidney preservation system. Br J Surg. 2006;93(7):879-84.
8. Vallant N, Wolfhagen N, Sandhu B, Hamaoui K, Cook T, Pusey C, et al. A Comparison of Pulsatile Hypothermic and Normothermic Ex Vivo Machine Perfusion in a Porcine Kidney Model. Transplantation. 2021;105(8):1760-70.
9. Messner F, Soleiman A, Ofner D, Neuwirt H, Schneeberger S, Weissenbacher A. 48 h Normothermic Machine Perfusion With Urine Recirculation for Discarded Human Kidney Grafts. Transpl Int. 2023;36:11804.
10. Hosgood SA, Callaghan CJ, Wilson CH, Smith L, Mullings J, Mehew J, et al. Normothermic machine perfusion versus static cold storage in donation after circulatory death kidney transplantation: a randomized controlled trial. Nat Med. 2023;29(6):1511-9.
11. Nikolaev AV, Fang Y, Essers J, Panth KM, Ambagtsheer G, Clahsen-van Groningen MC, et al. Pre-transplant kidney quality evaluation using photoacoustic imaging during normothermic machine perfusion. Photoacoustics. 2024;36:100596.
12. Cluzel GL, Ryan PM, Herisson FM, Caplice NM. High-fidelity porcine models of metabolic syndrome: a contemporary synthesis. Am J Physiol Endocrinol Metab. 2022;322(4):E366-E81.
13. Rijkse E, de Jonge J, Kimenai H, Hoogduijn MJ, de Bruin RWF, van den Hoogen MWF, et al. Safety and feasibility of 2 h of normothermic machine perfusion of donor kidneys in the Eurotransplant Senior Program. BJS Open. 2021;5(1).
14. Brat A, de Vries KM, van Heurn EWE, Huurman VAL, de Jongh W, Leuvenink HGD, et al. Hypothermic Machine Perfusion as a National Standard Preservation Method for Deceased Donor Kidneys. Transplantation. 2022;106(5):1043-50.
15. Fang YT, van Ooijen L, Ambagtsheer G, Nikolaev AV, Clahsen-van Groningen MCCV, Dankelman J, et al. Real-time laser speckle contrast imaging measurement during normothermic machine perfusion in pretransplant kidney assessment. Laser Surg Med. 2023;55(8):784-93.
16. Venema LH, van Leeuwen LL, Posma RA, van Goor H, Ploeg RJ, Hannaert P, et al. Impact of Red Blood Cells on Function and Metabolism of Porcine Deceased Donor Kidneys During Normothermic Machine Perfusion. Transplantation. 2022;106(6):1170-9.
17. Ogurlu B, Pamplona CC, Van Tricht IM, Hamelink TL, Lantinga VA, Leuvenink HGD, et al. Prolonged Controlled Oxygenated Rewarming Improves Immediate Tubular Function and Energetic Recovery of Porcine Kidneys During Normothermic Machine Perfusion. Transplantation. 2023;107(3):639-47.
18. Hosgood SA, Thompson E, Moore T, Wilson CH, Nicholson ML. Normothermic machine perfusion for the assessment and transplantation of declined human kidneys from donation after circulatory death donors. Br J Surg. 2018;105(4):388-94.
19. Campos L, Parada B, Furriel F, Castelo D, Moreira P, Mota A. Do intraoperative hemodynamic factors of the recipient influence renal graft function? Transplant Proc. 2012;44(6):1800-3.
20. Kaufmann KB, Baar W, Silbach K, Knorlein J, Janigen B, Kalbhenn J, et al. Modifiable Risk Factors for Delayed Graft Function After Deceased Donor Kidney Transplantation. Prog Transplant. 2019;29(3):269-74.
21. Kinoshita K, Yamanaga S, Kaba A, Tanaka K, Ogata M, Fujii M, et al. Optimizing Intraoperative Blood Pressure to Improve Outcomes in Living Donor Renal Transplantation. Transplant Proc. 2020;52(6):1687-94.
22. Feihl F, Liaudet L, Waeber B. The macrocirculation and microcirculation of hypertension. Curr Hypertens Rep. 2009;11(3):182-9.

23. Weissenbacher A, Lo Faro L, Boubriak O, Soares MF, Roberts IS, Hunter JP, et al. Twenty-four-hour normothermic perfusion of discarded human kidneys with urine recirculation. Am J Transplant. 2019;19(1):178-92.
24. Pool MBF, Hamelink TL, van Goor H, van den Heuvel MC, Leuvenink HGD, Moers C. Prolonged ex-vivo normothermic kidney perfusion: The impact of perfusate composition. PLoS One. 2021;16(5):e0251595.
25. Huijink TM, van 't Hof CJ, van Furth LA, de Haan NA, Maassen H, Venema LH, et al. Loss of Endothelial Glycocalyx During Normothermic Machine Perfusion of Porcine Kidneys Irrespective of Pressure and Hematocrit. Transplant Direct. 2023;9(8):e1507.
26. Mishra J, Ma Q, Prada A, Mitsnefes M, Zahedi K, Yang J, et al. Identification of neutrophil gelatinase-associated lipocalin as a novel early urinary biomarker for ischemic renal injury. J Am Soc Nephrol. 2003;14(10):2534-43.
27. Sen S, Godwin ZR, Palmieri T, Greenhalgh D, Steele AN, Tran NK. Whole blood neutrophil gelatinase-associated lipocalin predicts acute kidney injury in burn patients. J Surg Res. 2015;196(2):382-7.
28. Lohmann S, Pool MBF, Rozenberg KM, Keller AK, Moers C, Moldrup U, et al. Mesenchymal stromal cell treatment of donor kidneys during ex vivo normothermic machine perfusion: A porcine renal autotransplantation study. Am J Transplant. 2021;21(7):2348-59.
29. Weissenbacher A, Stone JP, Lo Faro ML, Hunter JP, Ploeg RJ, Coussios CC, et al. Hemodynamics and Metabolic Parameters in Normothermic Kidney Preservation Are Linked With Donor Factors, Perfusate Cells, and Cytokines. Front Med (Lausanne). 2021;8:801098.
30. Meyer C, Stumvoll M, Dostou J, Welle S, Haymond M, Gerich J. Renal substrate exchange and gluconeogenesis in normal postabsorptive humans. Am J Physiol Endocrinol Metab. 2002;282(2):E428-34.
31. Bellomo R. Bench-to-bedside review: lactate and the kidney. Crit Care. 2002;6(4):322-6.
32. Mather A, Pollock C. Glucose handling by the kidney. Kidney Int Suppl. 2011(120):S1-6.
33. Chen Y, Fry BC, Layton AT. Modeling glucose metabolism and lactate production in the kidney. Math Biosci. 2017;289:116-29.
34. Meng L, Yu W, Wang T, Zhang L, Heerdt PM, Gelb AW. Blood Pressure Targets in Perioperative Care. Hypertension. 2018;72(4):806-17.
35. Nath J, Guy A, Smith TB, Cobbold M, Inston NG, Hodson J, et al. Metabolomic perfusate analysis during kidney machine perfusion: the pig provides an appropriate model for human studies. PLoS One. 2014;9(12):e114818.

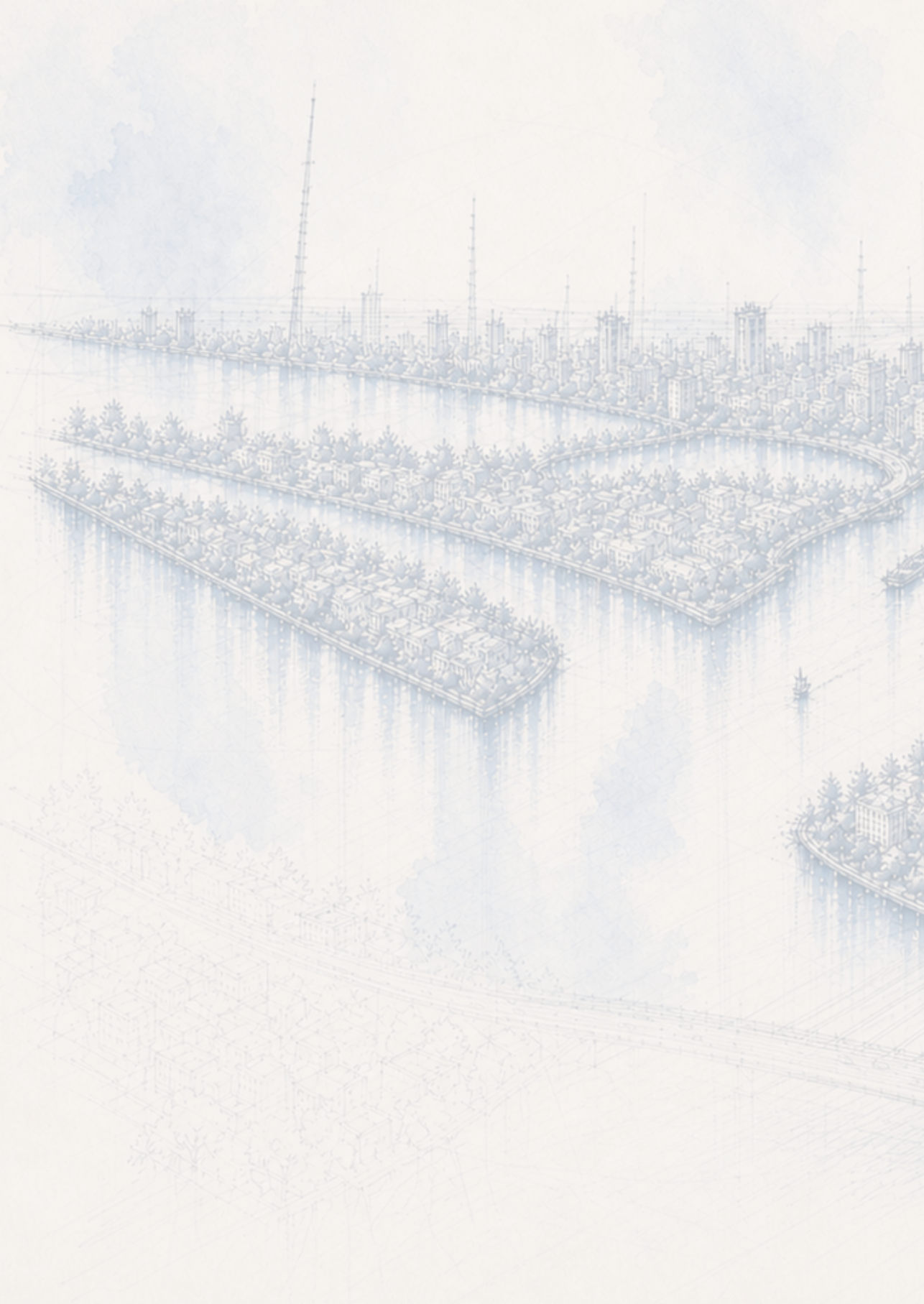
Supplementary

Table S1. Components of the normothermic machine perfusion perfusate

Priming	**Dosage**
Ringer's lactate (Baxter, The Netherlands)	300 mL
Autologous leukocyte-depleted blood	500 mL
Additives	
Albumin (Prothya Biosolutions, the Netherlands)	20 g
8.4% sodium bicarbonate (B. Braun, Germany)	10 mL
5% glucose (Baxter, The Netherlands)	10 mL
Verapamil (Centrafarm, the Netherlands)	2.5 mg
Dexamethasone (Centrafarm, The Netherlands)	6 mg
Creatinine (Sigma-Aldrich, the Netherlands)	90 mg
Infusion	
Aminoplasmal (B. Braun, Germany)	5 mL/h
Verapamil (Centrafarm, the Netherlands)	0.25 mg/h

Part II

Clinical Practice in Kidney Transplantation



Chapter 6

Bariatric surgery before and after kidney transplant: a propensity score-matched analysis

Yitian Fang, Loubna Outmani, Anoek A.E. de Joode, Hendrikus J.A.N. Kimenai, Joke I. Roodnat, Judith W.H. ’t Hart, Ulas L. Biter, René A. Klaassen, Ron W.F. de Bruin, Jan N.M. IJzermans, Robert A. Pol, Robert C. Minnee

Surgery for Obesity and Related Diseases, 2023

Abstract

Background Obesity is becoming more prevalent in end-stage renal disease population. Bariatric surgery (BS) is increasingly considered in as an approach to become eligible for kidney transplantation (KT) or reduce obesity-related morbidities.

Objectives To assess short- and long-term outcome of patients who underwent both BS and KT and to determine the optimal timing of BS.

Methods Patients who underwent both KT and BS between January 2000 and December 2020 were included and stratified according to the sequence of the two operations. The primary outcomes were patient and graft survival. Secondary outcomes were postoperative complications and efficacy of weight loss.

Results Twenty-two patients were included in the KT first group and 34 in the BS first group. Death-uncensored graft survival in the KT first group was significantly higher than the BS first group (90.9% vs. 71.4%, P=0.009), without significant difference in patient survival and death-censored graft survival (100% vs. 90.5%, P=0.082; and 90.9% vs. 81.0%, P=0.058). There was no significant difference in one-year total weight loss (1y TWL: median [IQR], 36.0 [28.0-42.0] vs. 29.6 [21.5-40.6] kg, P=0.424), one-year percentage of excess weight loss (1y %EWL: median [IQR], 74.9 [54.1-99.0] vs. 57.9 [47.5-79.4], P=0.155), and the incidence of postoperative complications (36.4% vs. 50.0%, P=0.316) between the KT first and BS first groups.

Conclusions Both pre- and post-transplant BS are effective and safe. Different conditions of each transplant candidate should be considered in detail. For patients with high risk of transplantation due to obesity, BS should be considered prior to KT.

Introduction

Obesity, defined as a body mass index (BMI) ≥ 30kg/m^2 is becoming more prevalent in patients with end-stage renal disease (ESRD).[1] Patients with obesity are predisposed to diabetic nephropathy, hypertensive nephrosclerosis and focal and segmental glomerulosclerosis, which accelerates the progression of chronic kidney failure.[2, 3] Moreover, although obesity is not an absolute contra-indication for kidney transplantation (KT), patients with obesity have reduced access to receive KT[4] since it is associated with a higher incidence of posttransplant complications, such as surgical site infection, new onset of diabetes after transplantation and delayed graft function (DGF).[5, 6]

Recent evidence suggests that bariatric surgery (BS) plays an effective role in achieving long-term weight loss and reducing obesity-related complications in kidney transplant patients.[7] To the kidney transplant recipients, BS improved renal function, graft survival and decreased obesity-related comorbidities such as diabetes mellitus and hypertension.[8, 9] To the kidney transplant candidates, BS has been proven to be effective in weight loss and improving eligibility for KT.[10-12] Meanwhile, the question on what is the optimal timing of BS in the kidney transplant population has not been answered unequivocally. A systematic review which enrolled 15 clinical studies with a total of 119 patients who underwent BS either before or after transplant showed that it was the safest to perform BS after transplant.[8] However, a certain group of patients also benefited from pre-transplant BS, as complication rates were acceptable and BS improved eligibility for kidney transplant.

To our knowledge, there has been no clinical trial to directly compare the outcomes of patients who underwent both operations in different order. The aim of this study is to assess short- and long-term outcomes of ESRD patients who underwent both BS and KT, trying to determine the optimal timing of BS for ESRD patients with obesity.

Materials and Methods

Study Design

In this retrospective cohort study, all patients ≥18 years who have undergone both KT and BS between January 2000 and January 2020 were screened using the transplant database of

Erasmus Medical Center (EMC) and University Medical Center Groningen (UMCG). All the individuals accepting BS prior to KT were to lose weight to be eligible for transplant. These patients were stratified into two groups according to the sequence of the two operations, group 1: patients who underwent KT before BS (KT first group), group 2: patients who underwent BS before KT (BS first group). A standardized immunosuppressive protocol was applied after transplantation. All patients had induction therapy with basiliximab (20mg) on postoperative day (POD) 0 and 4, tacrolimus (0.1mg per kg per day to maintain trough levels of 7-10ng/mL), mycophenolate mofetil (500mg twice daily) and prednisolone (20mg daily). ABO incompatible, cross-match positive, or high panel reactive antibody patients were treated according to local protocol. All patients were followed up until death or June 2021. All clinical data was obtained from the electronic patient dossier of EMC and UMCG. Patient demographics, co-morbidities, surgical details, postoperative complications and follow-up results were recorded. This study was approved by the Ethics Committee of the Erasmus Medical Center Rotterdam (MEC-2018-1699) and conducted in accordance with the provisions of the declaration of Helsinki.

Kidney transplantation related outcome

Patient and graft survival, duration of hospital stay and postoperative complications were analyzed. Patient survival was defined as the time from transplantation to death or the last follow-up. Uncensored graft survival was defined as the time from transplantation to graft failure or death or the last follow-up with a functioning graft. Death-censored graft survival was defined as the time from transplantation to graft failure or the last follow-up with a functioning graft, with censoring death with a functioning graft. Postoperative complications were recorded up to 90 days after transplantation except for the incidence of incisional hernia and rejection, which was recorded throughout the follow-up after transplantation. Allograft rejection was based on renal graft biopsy-proven diagnosis (Category 2, 3 and 4 according to Banff classification). DGF was defined as the need for dialysis in the first posttransplant week or failure of creatinine to decrease in the first 24 hours. Primary nonfunction (PNF) was defined as the absence of graft function immediately after transplantation and dialysis for 3 months post-transplant. Graft failure was defined as the need for retransplant or long-term dialysis.

Bariatric Surgery Related Outcome

Efficacy of BS and postoperative complications were analyzed. Pre- and postoperative BMI, one-year total weight loss (TWL), and one-year percentage of excess weight loss (%EWL) were calculated to determine the efficacy. As a BMI of 25 was the upper limit of normal body weight, excess weight was defined as the extra weight over the BMI of 25.[13, 14] %EWL was calculated using the formula: $\frac{postoperative\ weight - preoperative\ weight}{preoperative\ excess\ weight} \times 100$. Postoperative complications were registered up to 90 days and classified according to the Clavien-Dindo classification.[15]

Statistical Analysis

Baseline characteristics and both outcomes of KT and BS were compared between the two groups. Continuous variables were reported as mean ± standard deviation (SD) if normally distributed or median with interquartile range (IQR) if data was skewed using Kolmogorov-Smirnov test. Categorical variables were described as numbers and percentages. Continuous variables were compared using student's t-test or Mann–Whitney U test. Categorical variables were compared using χ^2 test or Fisher's exact test. Kaplan-Meier curves and log-rank test were used to compare patient and graft survival. Since the age at transplantation was statistically inconsistent between the two groups, the propensity score matching (PSM) was used to avoid the age-related bias when analyzing transplant related outcomes. The nearest neighbor-matching algorithm with a maximum caliper of 0.25 was used to match patients in KT first group with comparable patients in BS first group according to the age at transplantation. Statistical analyses and Kaplan-Meier curves were performed using Stata/SE 16.0. The bar graph was plotted using GraphPad Prism 9.3.1. A p-value of < 0.05 was considered statistically significant.

Results

Baseline Characteristics

A total of 56 patients were eligible for the study, with 22 patients (77.3% female) in the KT first and 34 patients (67.6% female) in the BS first group. Baseline characteristics of these patients are shown in Table 1. The age at transplantation in the KT first group was

significantly lower than the BS first group (42.7 ± 8.6 vs. 52.5 ± 10.0 years, P<0.001). 14 (63.6%) and 23 (67.6%) patients were dialysis dependent before transplantation in the KT first and BS first groups respectively with a similar dialysis vintage (median [interquartile range (IQR)], 27 [19.5-44.5] vs. 27 [20-43] months; P=0.822). A significantly higher proportion of patients in the KT first group received a retransplant compared to the BS first group (36.4% vs. 2.9%, P=0.002). No significant difference was found in the causes of ESRD, smoking history, donor sources and co-morbidities between the two groups. After PSM, 21 patients were included in the matched BS first group. There was no significant difference in age at transplantation (42.7 ± 8.6 vs. 48.3 ± 9.9 years, P<0.054) and the other baseline characteristics between the two groups (**Table 1**).

Kidney Transplantation Outcome

The KT related complications are shown in **Table 2**. While not reaching statistical significance, the KT first group had a shorter duration of hospital stay compared to the matched BS first group (median [IQR], 10.5 [10.0-17.5] vs. 13.0 [10.0-15.0] days; P=0.788). The incidence of urological, vascular, incisional and cardio-cerebrovascular complications was similar between the matched BS first group and KT first group (RR, 1.29; 95%CI, 0.85-1.97; P=0.232; and RR, 0.84; 95%CI, 0.26-2.70; P=1.000; and RR, 1.31; 95%CI, 0.41-4.22; P=0.721; and RR, 2.10; 95%CI, 0.21-21.42; P=0.607, respectively). Within 30 days after transplantation, DGF occurred in 3 (13.6%) and 4 (19.0%) patients in the KT first and the matched BS first groups. PNF occurred in 1 (4.8%) patient in the matched BS first group.

Mean follow-up after KT was 9.4 years in the KT first group, and 4.4 years in the BS first group. During follow-up, 5 (22.7%) and 8 (38.1%) patients in the KT first and matched BS first groups were diagnosed with biopsy-proven rejection (RR, 1.68; 95%CI, 0.65-4.31; P=0.273). Two (9.1%) grafts were lost in the KT first group due to chronic rejection, at 66.0 and 98.1 months after transplantation respectively. Four (19.0%) grafts were lost in the BS first group due to chronic rejection (n=2), PNF (n=1) and oxalate nephropathy (n=1), at 31.7, 68.6, 0.3 and 55.1 months after transplantation. All four were included after PSM. Four patients died in the BS first group with functioning grafts due to esophageal cancer (n=1), pneumosepsis (n=1), Covid-19 infection (n=1) and drug intoxication (n=1)

respectively, and 2 cases were included in the matched BS first group. In the baseline groups, there was a significant difference in patient and graft survival (100% vs. 88.2%, P=0.041, **Figure 1A**; and 90.9% vs. 76.5%, P=0.009, **Figure 1B**), but not in death-censored graft survival (90.9% vs. 88.2%, P=0.130, **Figure 1C**). Whereas after PSM, graft survival was still significantly higher in the KT first group than in the matched BS first group (90.9% vs. 71.4%, P=0.009, **Figure 1E**), no statistical difference was found in patient survival and death-censored graft survival between the two groups (100% vs. 90.5%, P=0.082, **Figure 1D**; and 90.9% vs. 81.0%, P=0.058, **Figure 1F**).

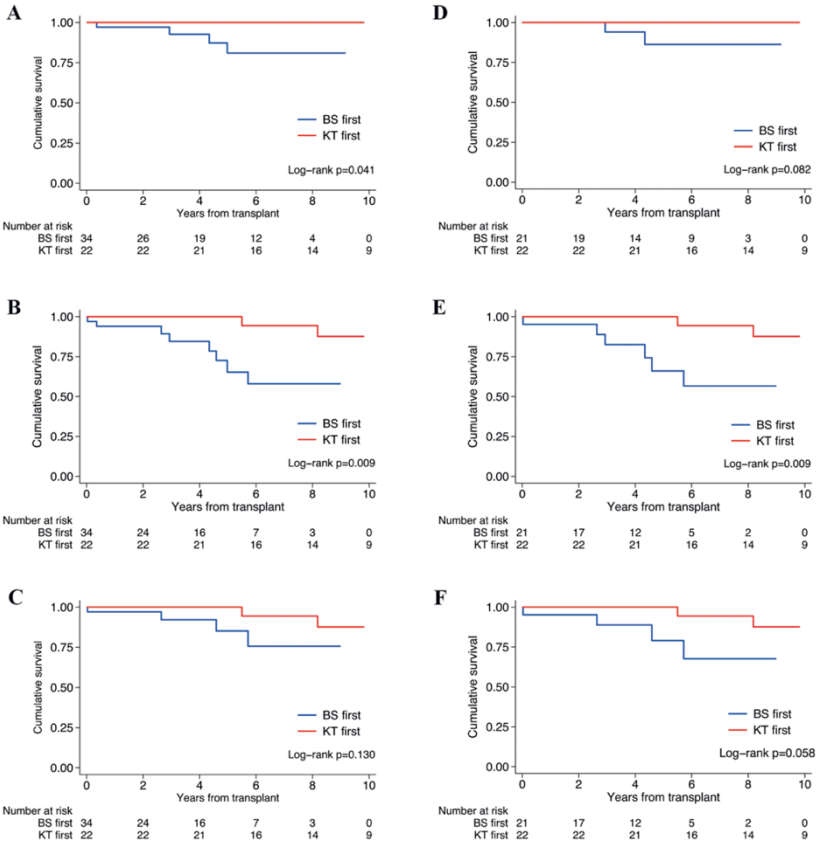


Figure 1. Before propensity score matching (PSM): A. Patient survival, B. Graft survival, C. Death-censored graft survival. After PSM: D. Patient survival, E. Graft survival, F. Death-censored graft survival. Kaplan-Meier method was used to assess patient and graft survival from the time of transplantation. P-values according to log-rank test. The blue curve represents the group who underwent kidney transplantation after bariatric surgery, and the red curve represents the group who underwent kidney transplantation prior to bariatric surgery.

Bariatric Surgery Outcome

The BS related outcomes are shown in **Table 3**. In the KT first group, BS included sleeve gastrectomy (n=17) and Roux-en-Y gastric bypass (n=5). In the BS first group, they were sleeve gastrectomy (n=16), Roux-en-Y gastric bypass (n=16) and gastric banding (n=2). The age at BS was similar between the two groups (48.3 ± 9.4 vs. 48.3 ± 10.9 years, P=0.998). The preoperative BMI was not different between the KT first and BS first group (median [IQR], 39.7 [37.9-44.0] vs. 42.0 [40.0-45.8] kg/m^2, P=0.090). The median interval between KT and BS was 5.5 years (IQR 2.4-6.4) in the KT first group and 2.7 years (IQR 1.5-6.7) in the BS first group. Mean follow-up after BS was 3.8 years in the KT first group, and 8.7 years in the BS first group. After one year's follow-up the BMI of both groups was within the range of obesity but showed comparable reduction (30.1 ± 6.5 vs. 32.0 ± 4.1, P=0.215). There was no significant difference in one-year TWL and %EWL between the KT first and BS first groups (1y TWL: median [IQR], 36.0 [28.0-42.0] vs. 29.6 [21.5-40.6] kg, P=0.424; 1y %EWL: median [IQR], 74.9 [54.1-99.0] vs. 57.9 [47.5-79.4], P=0.155).

Figure 2 illustrates the different types of BS performed between 2000 and 2020. Operations that were done in the early 2000s mainly included gastric bypass and adjustable gastric banding, while sleeve gastrectomy was not commonly used until 2009-2012. Over the last decade the sleeve has become the most common procedure.

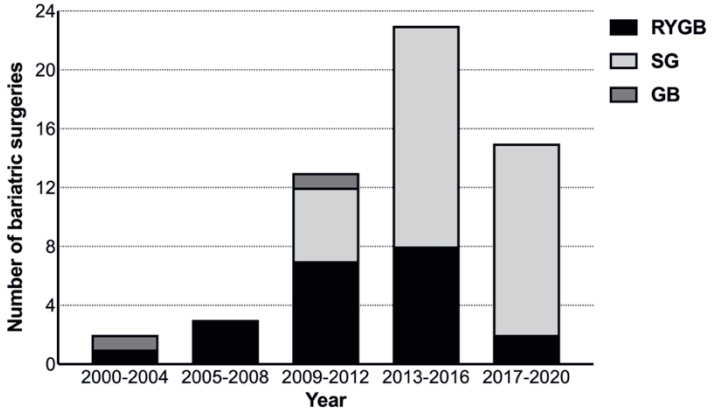


Figure 2. Number of bariatric surgeries undertaken in different periods.
GB, gastric banding; RYGB, Roux-en-Y gastric bypass; SG, sleeve gastrectomy.

Postoperative complications were classified according to the Clavien-Dindo classification (**Table 4**). Only grade I to III complications were found in both groups and there was no significant difference in the incidence of each grade and total complications (KT first vs. BS first, grade I: 18.2% vs. 8.8%, P=0.415; grade II: 13.6% vs. 14.7%, P=1.000; grade IIIa: 0% vs. 2.9%, P=1.000; grade IIIb: 4.5% vs. 23.5%, P=0.074; total: 36.4% vs. 50.0%, P=0.316).

Table 3. Clinical outcomes at and after bariatric surgery

	KT first (n=22)	BS first (n=34)	P-value
Age at BS (years), mean ± SD	48.3 ± 9.4	48.3 ± 10.9	0.998
Pre-BS BMI (kg/m^2), median (IQR)	39.7 (37.9-44.0)	42.0 (40.0-45.8)	0.090
Type of BS, n (%)			0.063
SG	17 (77.3)	16 (47.1)	
RYGB	5 (22.7)	16 (47.1)	
GB	0 (0)	2 (5.8)	
Time between KT and BS (years), median (IQR)	5.5 (2.4-6.4)	2.7 (1.5-6.7)	0.123
BMI at one year after BS (kg/m^2), mean (SD)	30.1 ± 6.5	32.0 ± 4.1	0.215
One-year TWL (kg), median (IQR)	36.0 (28.0-42.0)	29.6 (21.5-40.6)	0.424
One-year %EWL, median (IQR)	74.9 (54.1-99.0)	57.9 (47.5-79.4)	0.155
SG	74.9 (54.1-107.4)	52.5 (40.0-73.4)	
RYGB	67.1 (32.5-93.5)	63.7 (54.0-89.1)	
GB	-	46.0 (37.2-54.8)	

BS, bariatric surgery; BMI, body mass index; GB, gastric banding; IQR, interquartile range; KT, kidney transplantation; RYGB, Roux-en-Y gastric bypass; SG, sleeve gastrectomy; TWL, total weight loss; %EWL, the percentage of excess weight loss.

Table 4. Postoperative complications after bariatric surgery according to the Clavien-Dindo classification

Complications	KT first (n=22)	BS first (n=34)	p-value
Grade I, n (%)	4 (18.2)	3 (8.8)	0.415
Persistent vomiting requiring antiemetics	1	0	
Transient elevation of serum creatinine	3	0	
Dyspnea requiring oxygen therapy	0	1	
Dumpling syndrome	0	1	
Postoperative atrial fibrillation	0	1	
Grade II, n (%)	3 (13.6)	5 (14.7)	1.000
Anastomotic bleeding requiring hemostatics	0	1	
Urinary tract infection requiring antibiotics	1	1	
Splenic lesion requiring blood transfusions	0	1	
Infected abdominal hematoma requiring antibiotics	2	1	
Postoperative anemia requiring blood transfusions	0	1	
Grade IIIa, n (%)	0 (0)	1 (2.9)	1.000
Abscess caused by port infection requiring drainage	0	1	
Grade IIIb, n (%)	1 (4.5)	8 (23.5)	0.074
Anastomotic stenosis requiring surgical reconstruction	0	2	
Anastomotic bleeding requiring surgical hemostasis	0	2	
Anastomotic leak requiring surgical repair	0	1	
Gastric perforation requiring surgical repair	0	1	
Internal herniation treated by surgery	1	1	
Small intestine damage repairing surgical repair	0	1	
Grade IVa, n (%)	0 (0)	0 (0)	-
Grade IVb, n (%)	0 (0)	0 (0)	-
Grade V, n (%)	0 (0)	0 (0)	-
Total, n (%)	8 (36.4)	17 (50.0)	0.316

Discussion

In this retrospective cohort study, we compared baseline characteristics, postoperative complications, and outcomes between patients with either a KT first or BS first approach. Our analysis showed that death-uncensored graft survival in the KT first group was significantly higher than the BS first group, but there was no significant difference in patient survival, death-censored graft survival or post-transplant complications. Both pre- and post-transplant BS achieved remarkable weight loss and the incidence of postoperative complications is acceptable.

Ideally, BS should be initiated as early as possible. A randomized clinical trial by Cohen et al. showed that BS is associated with remission of albuminuria and improvement of renal function in patients with early-stage chronic kidney disease, which may help patients eventually avoid KT.[16] However, when it comes to patients with ESRD, another study showed that BS only improved transplant candidacy and stable weight loss, but not renal function[17]. Moreover, pre-transplant BS may have prolonged time on dialysis to establish sufficient weight loss and recover from long-term complications, which remains an independent predictor of mortality after KT.[18] When transplant is technically feasible despite being overweight, patients with an expected long waiting time because of blood type O or B, might decide to have BS first. However, because kidney donors are so scarce, the opportunity to receive a donor kidney may often postpone the consideration of BS. In our study, patients with severe obesity (BMI $\geq$ 40 kg/m^2) were more likely to have BS before transplant, which caused higher baseline BMI in the BS first group.

During the long-term follow-up, four patients in the BS first group died. On this basis, we directly compared the outcomes of patients who underwent BS before and after KT. Our results demonstrated that the difference in mortality was not statistically significant, but death-uncensored graft survival was significantly higher in the cohort with post-transplant BS. In the recently published study comparing pre- and post-transplant BS with matched controls respectively, Cohen et al. found that mortality was significantly lower in the patients with post-transplant BS, but not the pre-transplant BS.[19] Although the findings of the two studies are different, both show that patients undergoing BS after KT benefit more.

Roux-en-Y gastric bypass, as one of the bariatric surgeries, aims to induce decreased absorption of nutrients in the small intestine. This raises the concern of malabsorption of immunosuppressive agents in transplant recipients. A pilot study by Rogers et al. showed that transplant recipients with gastric bypass surgery required higher dosage of immunosuppressive agents to maintain similar concentrations compared to non-bypass patients.[20] The study by Yemini et al. observed that tacrolimus blood concentrations declined slightly but remained within therapeutic range without serious rejection among transplanted patients who underwent laparoscopic Roux-en-Y gastric bypass.[21] However, it is not advisable to increase the tacrolimus dose solely based on bodyweight. Our previous experience found that such practices resulted in overexposure in more than half of overweight patients.[22] In this data, graft rejection occurred in 7 (33.3%) patients receiving Roux-en-Y gastric bypass and 8 (32.0%) patients receiving other types of BS (RR 1.04, 95% CI 0.45-2.39, P=0.923). Although not significantly different, more research into the pharmacokinetics of immunosuppressive agents among transplant recipients with obesity is needed.

Another potential complication of BS is the formation of calcium oxalate stones in the kidneys. Obesity itself can increase the risk of kidney stone formation.[23] Furthermore, Roux-en-Y gastric bypass is associated with oxalate nephropathy and graft loss.[24, 25] In a systematic review evaluating the risk of hyperoxaluria in patient who underwent BS, it was concluded that Roux-en-Y gastric bypass was associated with increased urine oxalate and these patients had a significantly higher risk of stone formation.[26] In our study, oxalate deposits were found in four patients, all of whom had undergone Roux-en-Y gastric bypass. One of them lost the graft due to oxalate nephropathy. For this reason, sleeve gastrectomy may be a preferred choice compared to Roux-en-Y gastric bypass. Dietary interventions such as a low oxalate and salt diet show promising results in decreasing oxaluria and calcium oxalate relative supersaturation indexes.[27] Our colleagues first proposed that a systematic low-oxalic acid diet with supplementation of calcium, cholestyramine and sodium bicarbonate and intensifying dialysis effectively prevented oxalate nephropathy in a cohort of patients with enteric hyperoxaluria.[28] It may be beneficial for the transplant candidates and recipients who have undergone Roux-en-Y gastric bypass to adhere to such a low-oxalic acid diet.

Due to the introduction of minimally invasive and robotic surgery, it is currently possible to perform robot-assisted kidney transplantation (RAKT). By RAKT, the graft is placed in the abdominal cavity through a Pfannenstiel incision, and vascular and ureteral anastomoses are then performed robotically. Although the Pfannenstiel incision seems the same length as the open surgery, RAKT has its own advantages in specific populations. For patients with centripetal obesity, it provides more flexible operation space in the pelvic region while the operative area of iliac fossa is difficult to expose due to abdominal fat accumulation using open surgical approach. With the help of RAKT, patients who were previously declined may have the opportunity of transplant. Spaggiari et al. were the first to publish their randomized trial in which 11 patients underwent simultaneous robotic-assisted kidney transplantation and sleeve gastrectomy.[29] Compared to patients with class II (BMI 35-39.9kg/m^2) and class III obesity (BMI ≥ 40kg/m^2) who received RAKT alone, estimated blood loss, readmission rates, incidence of surgical complications and graft survival at one-year follow-up were comparable. Also, renal graft function was similar, indicating that performing kidney transplantation and sleeve gastrectomy simultaneously does not have a negative effect on graft function. As long-term data is not yet available, it is premature to conclude that simultaneous KT and BS should become the gold standard in ESRD patients.

Our study is limited by several factors. Firstly, the present study is a retrospective cohort analysis, of which a potential selection bias is unavoidable. To minimize this bias, we combined the data of two high volume transplant centers, which resulted in one of the largest cohorts of ESRD patients who underwent both BS and KT. However, the baseline BMI of patients in the BS first group was still higher and they may have a potentially higher risk of postoperative complications. Secondly, in this population of ESRD patients with obesity, some died after BS while awaiting KT. Unfortunately, these data were not collected prospectively. Thirdly, as the study involves patients over a 21-year period, the safety and public acceptance of BS have been tremendously improved. This dynamic change should be also taken into consideration when evaluating the robustness of the results.

Conclusions

In conclusion, both pre- and post-transplant BS are effective and safe approaches to lose weight among ESRD patients. The optimal timing of BS should be individualized, the severity of obesity, expected waiting time and willingness of patients should all be considered. For patients with high risk of transplantation due to obesity, BS should be given priority over KT. Otherwise, post-transplant BS is feasible when unexpected organs are urgently allocated. With the major advances in robotic surgery, simultaneous KT and BS may become an additional option in the future. Anyway, careful attention should be warranted in both preoperative evaluation and postoperative management and more studies are needed to elucidate the optimal treatment for this group of patients.

Reference

1. Diwan TS, Cuffy MC, Linares-Cervantes I, Govil A. Impact of obesity on dialysis and transplant and its management. Semin Dial. 2020;33(3):279-85.
2. Hall JE, Jones DW, Kuo JJ, da Silva A, Tallam LS, Liu J. Impact of the obesity epidemic on hypertension and renal disease. Curr Hypertens Rep. 2003;5(5):386-92.
3. Griffin KA, Kramer H, Bidani AK. Adverse renal consequences of obesity. Am J Physiol Renal Physiol. 2008;294(4):F685-96.
4. Lassalle M, Fezeu LK, Couchoud C, Hannedouche T, Massy ZA, Czernichow S. Obesity and access to kidney transplantation in patients starting dialysis: A prospective cohort study. PLoS One. 2017;12(5):e0176616.
5. Lafranca JA, JN IJ, Betjes MG, Dor FJ. Body mass index and outcome in renal transplant recipients: a systematic review and meta-analysis. BMC Med. 2015;13:111.
6. Aalten J, Christiaans MH, de Fijter H, Hene R, van der Heijde JH, Roodnat J, et al. The influence of obesity on short- and long-term graft and patient survival after renal transplantation. Transpl Int. 2006;19(11):901-7.
7. Kim Y, Bailey AJ, Morris MC, Kassam AF, Shah SA, Diwan TS. Kidney transplantation after sleeve gastrectomy in the morbidly obese candidate: results of a 2-year experience. Surg Obes Relat Dis. 2020;16(1):10-4.
8. Dziodzio T, Biebl M, Öllinger R, Pratschke J, Denecke C. The Role of Bariatric Surgery in Abdominal Organ Transplantation-the Next Big Challenge? Obes Surg. 2017;27(10):2696-706.
9. Schindel H, Winkler J, Yemini R, Carmeli I, Nesher E, Keidar A. Survival benefit in bariatric surgery kidney recipients may be mediated through effects on kidney graft function and improvement of co-morbidities: A case-control study. Surg Obes Relat Dis. 2019;15(4):621-7.
10. Gazzetta PG, Bissolati M, Saibene A, Ghidini CGA, Guarneri G, Giannone F, et al. Bariatric Surgery to Target Obesity in the Renal Transplant Population: Preliminary Experience in a Single Center. Transplant Proc. 2017;49(4):646-9.
11. Yemini R, Nesher E, Carmeli I, Winkler J, Rahamimov R, Mor E, et al. Bariatric Surgery Is Efficacious and Improves Access to Transplantation for Morbidly Obese Renal Transplant Candidates. Obes Surg. 2019;29(8):2373-80.
12. Freeman CM, Woodle ES, Shi J, Alexander JW, Leggett PL, Shah SA, et al. Addressing morbid obesity as a barrier to renal transplantation with laparoscopic sleeve gastrectomy. Am J Transplant. 2015;15(5):1360-8.
13. Oria HE, Carrasquilla C, Cunningham P, Hess DS, Johnell P, Kligman MD, et al. Guidelines for weight calculations and follow-up in bariatric surgery. Surg Obes Relat Dis. 2005;1(1):67-8.
14. Deitel M, Greenstein RJ. Recommendations for reporting weight loss. Obes Surg. 2003;13(2):159-60.
15. Husain F, Jeong IH, Spight D, Wolfe B, Mattar SG. Risk factors for early postoperative complications after bariatric surgery. Ann Surg Treat Res. 2018;95(2):100-10.
16. Cohen RV, Pereira TV, Aboud CM, Petry TBZ, Lopes Correa JL, Schiavon CA, et al. Effect of Gastric Bypass vs Best Medical Treatment on Early-Stage Chronic Kidney Disease in Patients With Type 2 Diabetes and Obesity: A Randomized Clinical Trial. JAMA Surg. 2020;155(8):e200420.
17. Kassam AF, Mirza A, Kim Y, Hanseman D, Woodle ES, Quillin RC, 3rd, et al. Long-term outcomes in patients with obesity and renal disease after sleeve gastrectomy. Am J Transplant. 2020;20(2):422-9.
18. Helantera I, Salmela K, Kyllonen L, Koskinen P, Gronhagen-Riska C, Finne P. Pretransplant dialysis duration and risk of death after kidney transplantation in the current era. Transplantation. 2014;98(4):458-64.
19. Cohen JB, Lim MA, Tewksbury CM, Torres-Landa S, Trofe-Clark J, Abt PL, et al. Bariatric surgery before and after kidney transplantation: long-term weight loss and allograft outcomes. Surg Obes Relat Dis. 2019;15(6):935-41.
20. Rogers CC, Alloway RR, Alexander JW, Cardi M, Trofe J, Vinks AA. Pharmacokinetics of mycophenolic acid, tacrolimus and sirolimus after gastric bypass surgery in end-stage renal disease and transplant patients: a pilot study. Clin Transplant. 2008;22(3):281-91.
21. Yemini R, Nesher E, Winkler J, Carmeli I, Azran C, Ben David M, et al. Bariatric surgery in solid organ transplant patients: Long-term follow-up results of outcome, safety, and effect on immunosuppression. Am J Transplant. 2018;18(11):2772-80.
22. Andrews LM, de Winter BCM, Tang JT, Shuker N, Bouamar R, van Schaik RHN, et al. Overweight Kidney Transplant Recipients Are at Risk of Being Overdosed Following Standard Bodyweight-Based Tacrolimus Starting Dose. Transplantation Direct. 2017;3(2).
23. Taylor EN, Stampfer MJ, Curhan GC. Obesity, weight gain, and the risk of kidney stones. JAMA. 2005;293(4):455-62.

24. Choudhury RA, Hoeltzel G, Prins K, Chow E, Moore HB, Lawson PJ, et al. Sleeve Gastrectomy Compared with Gastric Bypass for Morbidly Obese Patients with End Stage Renal Disease: a Decision Analysis. J Gastrointest Surg. 2020;24(4):756-63.
25. Khorgami Z, Shoar S, Andalib A, Aminian A, Brethauer SA, Schauer PR. Trends in utilization of bariatric surgery, 2010-2014: sleeve gastrectomy dominates. Surg Obes Relat Dis. 2017;13(5):774-8.
26. Upala S, Jaruvongvanich V, Sanguankeo A. Risk of nephrolithiasis, hyperoxaluria, and calcium oxalate supersaturation increased after Roux-en-Y gastric bypass surgery: a systematic review and meta-analysis. Surg Obes Relat Dis. 2016;12(8):1513-21.
27. Escribano J, Balaguer A, Roqué i Figuls M, Feliu A, Ferre N. Dietary interventions for preventing complications in idiopathic hypercalciuria. Cochrane Database Syst Rev. 2014(2):CD006022.
28. Roodnat JI, de Mik-van Egmond AME, Visser WJ, Berger SP, van der Meijden WAG, Knauf F, et al. A Successful Approach to Kidney Transplantation in Patients With Enteric (Secondary) Hyperoxaluria. Transplant Direct. 2017;3(12):e331.
29. Spaggiari M, Di Cocco P, Tulla K, Kaylan KB, Masrur MA, Hassan C, et al. Simultaneous robotic kidney transplantation and bariatric surgery for morbidly obese patients with end-stage renal failure. Am J Transplant. 2021;21(4):1525-34.

Table 1. Clinical characteristics at the time of transplantation

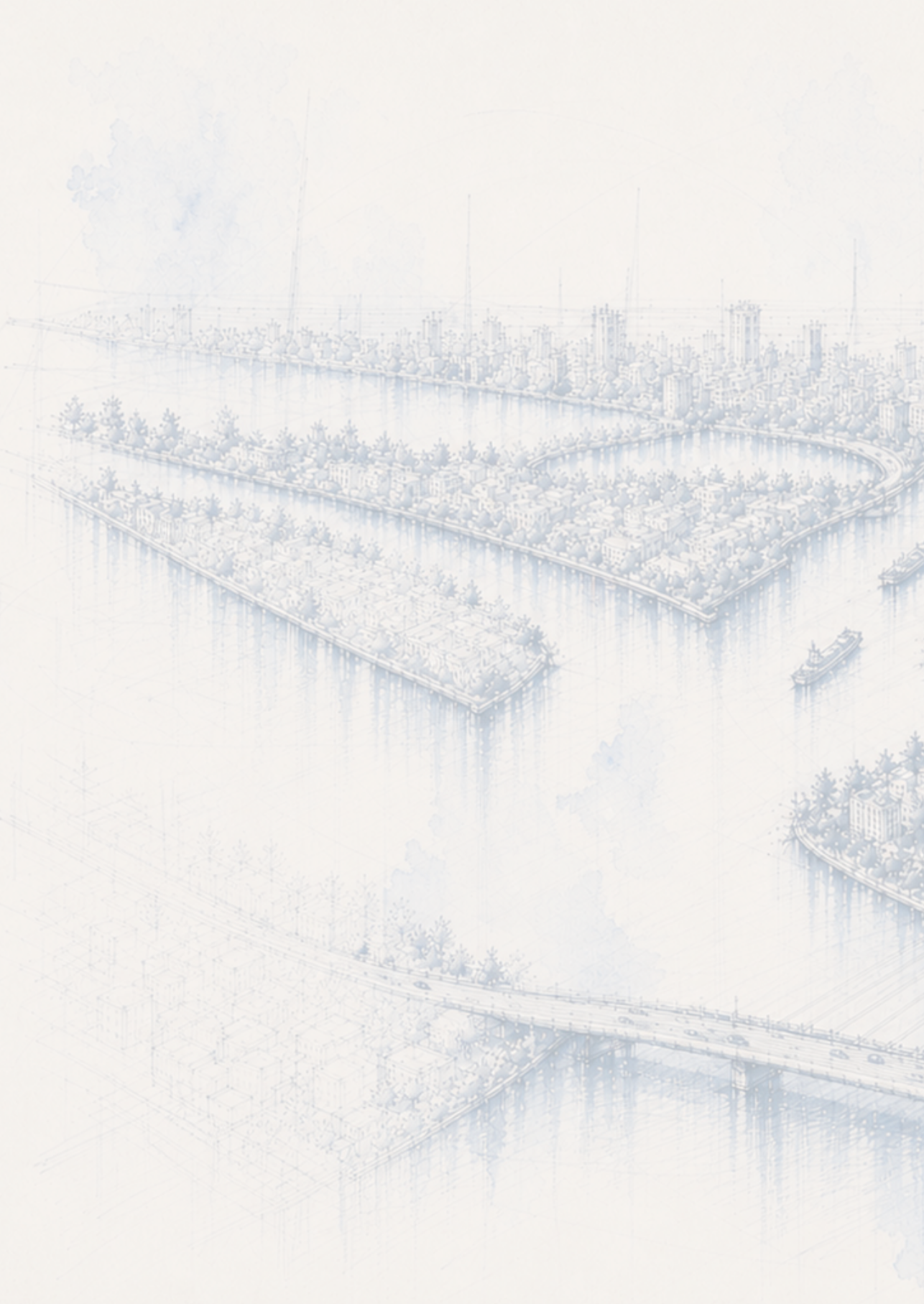
	Before matching			After matching		
	KT first (n=22)	BS first (n=34)	P-value	KT first (n=22)	BS first (n=21)	P-value
Age at KT (years), mean ± SD	42.7 ± 8.6	52.5 ± 10.0	< 0.001	42.7 ± 8.6	48.3 ± 9.9	0.054
Male, n (%)	5 (22.7)	11 (32.4)	0.436	5 (22.7)	6 (28.6)	0.661
BMI at KT (kg/m^2), mean ± SD	35.8 ± 4.0	32.1 ± 4.4	0.002	35.8 ± 4.0	31.8 ± 4.5	0.003
Cause of ESRD, n (%)			0.234			0.213
Diabetes mellitus	8 (36.4)	17 (50.0)		8 (36.4)	13 (62.0)	
Primary hypertension	2 (9.1)	5 (14.7)		2 (9.1)	0 (0)	
Glomerulonephritis	4 (18.2)	7 (20.6)		4 (18.2)	4 (19.0)	
Congenital nephropathy	5 (22.7)	5 (14.7)		5 (22.7)	4 (19.0)	
Others	3 (13.6)	0 (0)		3 (13.6)	0 (0)	
Smoking history, n (%)	9 (40.9)	9 (26.5)	0.259	9 (40.9)	3 (14.3)	0.052
Dialysis, n (%)	14 (63.6)	23 (67.6)	0.757	14 (63.6)	16 (76.2)	0.370
Duration (months), median (IQR)	27 (19.5-44.5)	27 (20-43)	0.988	27 (19.5-44.5)	29.5 (18.5-53.5)	0.822
Donor source, n (%)			0.289			0.168
Living-related donor	16 (72.7)	20 (58.8)		16 (72.7)	11 (52.4)	
Deceased donor	6 (27.3)	14 (41.2)		6 (27.3)	10 (47.6)	
Transplantation, n (%)			0.002			0.021
First transplant	14 (63.6)	33 (97.1)		14 (63.6)	20 (95.2)	
Retransplant	8 (36.4)	1 (2.9)		8 (36.4)	1 (4.8)	
Co-morbidities, n (%)						
Diabetes mellitus	8 (36.4)	21 (61.8)	0.063	8 (36.4)	13 (61.9)	0.094
Hypertension	13 (59.1)	23 (67.6)	0.514	13 (59.1)	13 (61.9)	0.850
Cardiac disease	9 (40.9)	17 (50.0)	0.505	9 (40.9)	7 (33.3)	0.607
Cerebrovascular disease	0 (0)	1 (2.9)	1.000	0 (0)	1 (4.8)	0.488
Peripheral vascular disease	6 (27.3)	4 (11.8)	0.167	6 (27.3)	2 (9.5)	0.240
Respiratory disease	3 (13.6)	6 (17.6)	1.000	3 (13.6)	3 (14.3)	1.000
Malignancy	0 (0)	2 (5.9)	0.514	0 (0)	1 (4.8)	0.488

BMI, body mass index; BS, bariatric surgery; ESRD, end-stage renal disease; IQR, interquartile range; KT, kidney transplantation.

Table 2. Postoperative complications after transplantation

	Before matching				After matching			
	KT first (n=22)	BS first (n=34)	RR (95% CI)	P-value	KT first (n=22)	BS first (n=21)	RR (95% CI)	P-value
Hospital stay (days), median (IQR)	10.5 (10.0-17.5)	12.5 (8.8-17.0)	-	0.619	10.5 (10.0-17.5)	13.0 (10.0-15.0)	-	0.788
Urological complications, n (%)	13 (59.1)	24 (70.6)	1.20 (0.79-1.80)	0.375	13 (59.1)	16 (76.2)	1.29 (0.85-1.97)	0.232
UTI	7 (31.8)	13 (38.2)	1.20 (0.57-2.53)	0.625	7 (31.8)	8 (38.1)	1.20 (0.53-2.72)	0.666
Urinary leakage	2 (9.1)	4 (11.8)	1.29 (0.26-6.48)	1.000	2 (9.1)	2 (9.5)	1.05 (0.16-6.77)	1.000
Hydronephrosis	1 (4.5)	2 (5.9)	1.29 (0.13-13.43)	1.000	1 (4.5)	2 (9.5)	2.10 (0.21-21.42)	0.607
Ureteric stricture	3 (13.6)	3 (8.8)	0.65 (0.14-2.92)	0.670	3 (13.6)	2 (9.5)	0.70 (0.13-3.77)	1.000
Hematuria	0 (0)	2 (5.9)	-	0.514	0 (0)	2 (9.5)	-	0.233
Vascular complications, n (%)	5 (22.7)	5 (14.7)	0.65 (0.21-1.98)	0.491	5 (22.7)	4 (19.0)	0.84 (0.26-2.70)	1.000
Renal artery thrombosis	3 (13.6)	1 (2.9)	0.22 (0.02-1.94)	0.289	3 (13.6)	0 (0)	-	0.233
Perigraft bleeding	1 (4.5)	2 (5.9)	1.29 (0.13-13.43)	1.000	1 (4.5)	2 (9.5)	2.10 (0.21-21.42)	0.607
Lymphocele	1 (4.5)	2 (5.9)	1.29 (0.13-13.43)	1.000	1 (4.5)	2 (9.5)	2.10 (0.21-21.42)	0.607
Incisional complications, n (%)	4 (18.2)	13 (38.2)	2.10 (0.79-5.63)	0.111	4 (18.2)	5 (23.8)	1.31 (0.41-4.22)	0.721
Incisional hernia	2 (9.1)	6 (17.6)	1.94 (0.43-8.77)	0.460	2 (9.1)	2 (9.5)	1.05 (0.16-6.77)	1.000
Surgical wound dehiscence	0 (0)	5 (14.7)	-	0.145	0 (0)	3 (14.3)	-	0.108
Surgical site infection	1 (4.5)	2 (5.9)	1.29 (0.13-13.43)	1.000	1 (4.5)	0 (0)	-	1.000
Abdominal wall infection	1 (4.5)	0 (0)	-	0.393	1 (4.5)	0 (0)	-	1.000
Cardiovascular complications, n (%)	1 (4.5)	3 (8.8)	1.94 (0.22-17.50)	1.000	1 (4.5)	2 (9.5)	2.10 (0.21-21.42)	0.607
Angina pectoris	0 (0)	1 (2.9)	-	0.393	0 (0)	0 (0)	-	-
Atrial fibrillation	0 (0)	2 (5.9)	-	1.000	0 (0)	2 (9.5)	-	0.233
Transient ischemic attack	1 (4.5)	0 (0)	-	0.514	1 (4.5)	0 (0)	-	1.000
Others, n (%)	10 (45.5)	18 (52.9)	1.17 (0.67-2.03)	0.584	10 (45.5)	13 (61.9)	1.36 (0.77-2.40)	0.280
Rejection	5 (22.7)	10 (29.4)	1.29 (0.51-3.28)	0.581	5 (22.7)	8 (38.1)	1.68 (0.65-4.31)	0.273
DGF	3 (13.6)	4 (11.8)	0.86 (0.21-3.49)	1.000	3 (13.6)	4 (19.0)	1.40 (0.35-5.51)	0.698
PNF	0 (0)	1 (2.9)	-	1.000	0 (0)	1 (4.8)	-	0.488
NODAT	1 (4.5)	2 (5.9)	1.29 (0.13-13.43)	1.000	1 (4.5)	0 (0)	-	1.000
Anemia	1 (4.5)	1 (2.9)	0.65 (0.04-9.82)	1.000	1 (4.5)	0 (0)	-	1.000

BS, bariatric surgery; DGF, delayed graft function; KT, kidney transplantation; NODAT, new onset diabetes mellitus after transplantation; PNF, primary nonfunction; UTI, urinary tract infection.

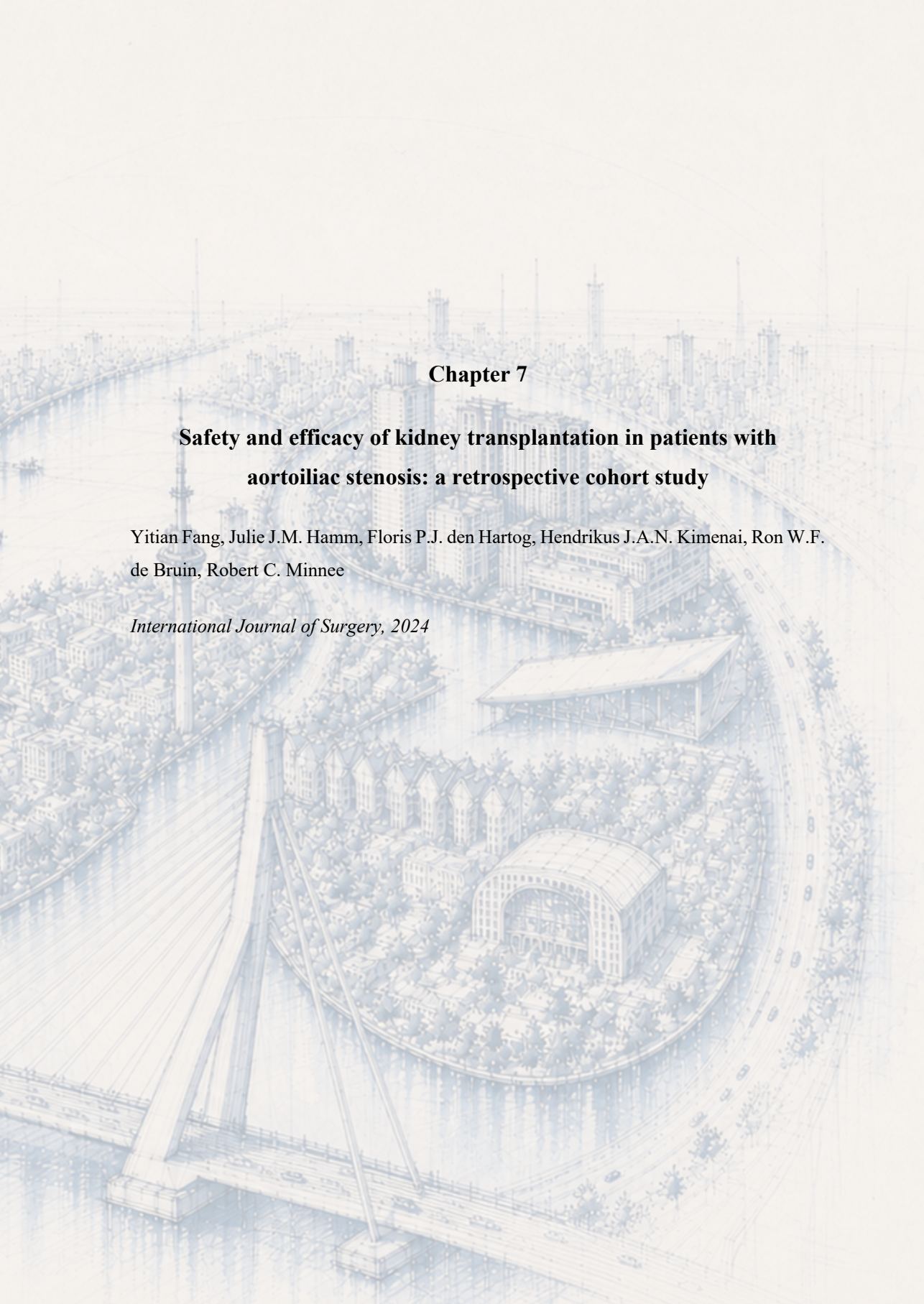


Chapter 7

Safety and efficacy of kidney transplantation in patients with aortoiliac stenosis: a retrospective cohort study

Yitian Fang, Julie J.M. Hamm, Floris P.J. den Hartog, Hendrikus J.A.N. Kimenai, Ron W.F. de Bruin, Robert C. Minnee

International Journal of Surgery, 2024



Abstract

Background The impact of aortoiliac occlusive disease on kidney transplantation remains unclear. This study aims to investigate the clinical outcomes of kidney transplant patients with aortoiliac atherosclerotic stenosis.

Methods Retrospective data from our transplant center were used to identify patients undergoing kidney transplantation between January 2010 and December 2020. Aortoiliac atherosclerotic stenosis was screened and stratified by the Trans-Atlantic Inter-Society Consensus (TASC) II classification. The primary outcome was patient survival. Secondary outcomes were 90-day mortality, death-censored graft survival, graft function and arterial complications. Propensity score matching was used to match all patients in the stenosis group with patients without stenosis sharing similar characteristics.

Results The analysis included 655 patients, 524 without stenosis, and 131 with aortoiliac stenosis (95 with TASC A/B stenosis, 36 with TASC C/D stenosis). Recipient age (median [IQR], 66 [60-70] vs. 66 [59-71] years; $p = 0.47$), gender (male: 87 [66%] vs. 355 [68%], $p = 0.85$), and comorbidities were comparable between the stenosis and no-stenosis groups. Forty-six (35%) patients with stenosis were symptomatic. Patient survival was significantly lower in the stenosis group compared to the no-stenosis group (TASC A/B: 30.6% vs. no-stenosis: 44.1%, $p = 0.013$; TASC C/D: 11.4% vs. no-stenosis: 44.1%, $p < 0.001$). The incidence rates of artery dissection, lower extremity ischemia and acute thrombosis were significantly higher in the stenosis group ($p < 0.001$). However, death-censored graft survival (TASC A/B: 73.6% vs. no-stenosis: 72.9%, $p = 0.62$; TASC C/D: 58.1% vs. no-stenosis: 72.9%, $p = 0.16$) and graft function were comparable between the groups.

Conclusions Aortoiliac atherosclerotic stenosis significantly impacts patient survival but not graft survival. Our analyses suggest that patients with TASC A/B stenosis have prolonged survival and enhanced quality of life through kidney transplantation. However, for patients with TASC C/D stenosis, kidney transplantation improves quality of life without bringing survival benefits.

Introduction

Kidney transplantation is the optimal treatment for end-stage renal disease (ESRD).[1] Unfortunately, not all ESRD patients are eligible for kidney transplantation. Aortoiliac atherosclerotic stenosis, a common type of peripheral artery occlusive disease in ESRD patients, is considered as relative contra-indication for kidney transplantation.[2] Previous studies suggest that ESRD patients are prone to atherogenesis and aortoiliac atherosclerotic stenosis, likely due to uremia-associated inflammation, high-density lipoprotein (HDL) dysfunction, and uremic vasculopathy.[3] Increased numbers of specific proinflammatory subsets of T cells and monocytes contribute to the destabilization of atherosclerotic plaques.[4, 5] HDL from ESRD patients is rendered a damaging particle that promotes endothelial dysfunction, vasoconstriction, and inflammatory activation.[6] Additionally, the hypertrophy, proliferation, and calcification of vascular smooth muscle cells have been reported to play a pivotal role in uremic vasculopathy.[7] Kidney transplantation in this population has raised several concerns, including the complexity of the vascular anastomosis and inferior life expectancy.[8-11] Consequently, it is still debated whether patients with aortoiliac atherosclerotic stenosis would benefit from kidney transplantation.

Aortoiliac stenosis can be classified according to the Trans-Atlantic Inter-Society Consensus (TASC) II classification.[12] TASC A and B stenosis refer to mild or moderate narrowing of the aorto-iliac artery, while TASC C and D stenosis are severe stenosis or occlusion which can extend into the femoral artery. For TASC A and B stenosis, endovascular or endoluminal interventions are recommended, whereas TASC C and D stenosis requires surgical management as the first approach.[13, 14] Several studies have reported inferior survival outcomes in kidney transplant patients with TASC C/D stenosis.[15, 16] However, these studies exclusively involved patients who underwent contrast enhanced imaging. Although contrast enhanced imaging provides a more detailed visualization of the stenosis compared to vascular ultrasound, the contrast agents used can be nephrotoxic. Therefore, it is not a standard pre-transplant screening procedure, leading to a selection bias in the research subjects. Moreover, the baseline characteristics of patients with and without stenosis in the studies were not comparable, undermining the robustness of their research conclusions.

This study aimed to investigate the clinical outcomes of kidney transplantation in patients with aortoiliac atherosclerotic stenosis. The patient survival, graft survival, graft function and complications were systematically compared. We enrolled low-risk patients and used propensity score matching (PSM) to minimize selection bias and confounding factors.

Methods

Study Design and Data Collection

We conducted a retrospective, single-center, observational study using our transplant database. This study was approved by the Medical Ethics Committee and registered on ClinicalTrials.gov (NCT06020534). This work has been reported in line with the STROCSS criteria.[17]

We identified all patients undergoing kidney transplantation in our center between January 2010 and December 2020. The exclusion criteria were age < 18 years when transplanted, combined organ transplantation, or no follow-up data. These patients were categorized into no-stenosis group and stenosis group, based on the presence of aortoiliac stenosis. To minimize potential confounding factors between two groups, we used PSM to match patients in the stenosis group with individuals from the no-stenosis group who shared similar characteristics.

As a standard pre-transplant assessment, all patients underwent artery duplex sonography examination of aortoiliac vessels, which has proven to be reliable for the detection of aortoiliac stenosis.[18] When stenosis was detected, contrast-enhanced CT or MRI of the aortoiliac segment was used to obtain anatomical information and assess the severity. Aortoiliac stenosis was defined as lumen narrowing > 50% in the aortoiliac artery. Patients were regularly followed up by our nephrologists, with all relevant data recorded in the electronic patient record system. The follow-up duration extended until the patient's death or January 2023. During this time frame, we compared the clinical outcomes such as patient survival, graft function and arterial complications between the groups.

Outcome Measurements

The primary outcome was patient survival. The secondary outcomes were 90-day mortality, death-censored graft survival, graft function and arterial complications. To estimate renal function, the estimated glomerular filtration rate (eGFR) was calculated using the Chronic Kidney Disease Epidemiology Collaboration (CKD-EPI) equation at 1, 3, and 6 months and each post-transplant year.[19] Follow-up assessment was performed using follow-up index (FUI).[20]

Patient survival and 90-day mortality were calculated from the date of transplantation until the end points. Death-censored graft survival was defined as the time from transplant to graft failure, with censoring for death with a functioning graft. All arterial complications relevant to kidney transplantation were reported. FUI was calculated as the ratio between the actual investigation period and the potential follow-up period. A FUI value closer to 1 indicates a smaller risk of selection bias.[20]

Statistical Analysis

Continuous variables were presented as medians with interquartile ranges (IQRs). Categorical variables were presented as frequencies and percentages. PSM was performed in a nearest neighbor-matching approach with a maximum caliper of 0.1 in a 1:4 ratio.[21] The matching parameters included age, dialysis mode, retransplant, donor type, comorbidities and smoking status. The Mann-Whitney-U test was used to compare continuous variables, and the chi-squared test was used to compare categorical variables. Kaplan-Meier curves and log-rank test were used to compare patient and graft survival. P-values of pairwise multiple comparisons were adjusted with the Benjamini-Hochberg procedure. The relative risk of aortoiliac stenosis on patient mortality and graft failure was assessed using Cox-regression model. A two-sided $p < 0.05$ was considered statistically significant. All analyses were conducted using R version 4.2.2.

Results

Study Cohort

We initially identified 2,127 patients who had undergone kidney transplantation in our center between January 2010 and December 2020. Thirty-six patients were excluded due to age under 18 years at transplant (n = 9), combined organ transplantation (n = 15), or no follow-up data (n = 12). Among the remaining patients, 131 patients were diagnosed with pretransplant stenosis, and 1960 patients without stenosis. These patients were enrolled in PSM, yielding a final cohort of 131 patients in the stenosis group and 524 matched patients in the no-stenosis group. In the stenosis group, 96 patients were classified with TASC A/B stenosis, and 35 with TASC C/D stenosis according to the TASC II classification (**Figure 1**).

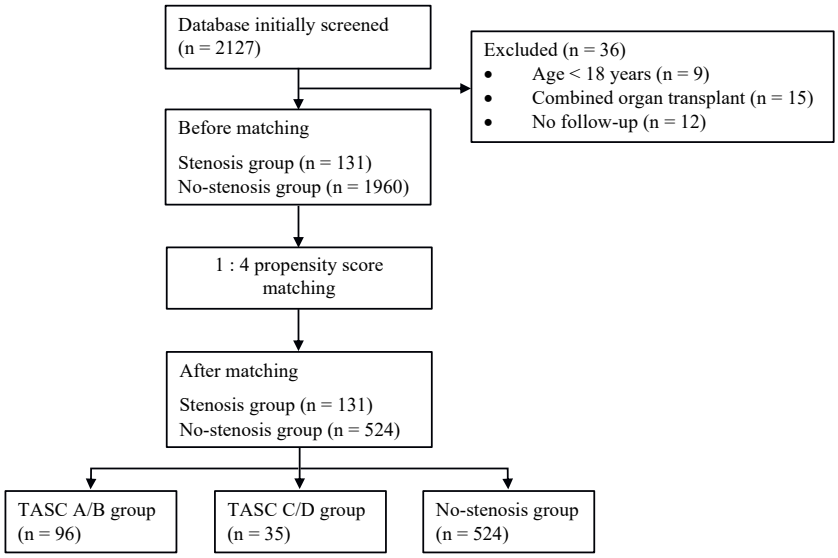


Figure 1. Flow diagram of study screening, recruitment and enrollment. TASC, Trans-Atlantic Inter-Society Consensus.

Baseline Characteristics

Before PSM, patients in the stenosis group were significantly older at transplantation than patients in the no-stenosis group (median [IQR], 66 [60-70] vs. 58 [47-66] years; $p < 0.001$). The proportion of male gender was similar between the two groups (87 [66%] vs. 1214 [62%], $p = 0.35$). More patients in the stenosis group underwent dialysis compared to the

patients in the no-stenosis group (102 [78%] vs. 1294 [66%], $p = 0.021$). The duration of dialysis was comparable. There was a significantly higher incidence of diabetes mellitus (72 [55%] vs. 540 [28%], $p < 0.001$), cardio-cerebrovascular disease (68 [52%] vs. 466 [24%], $p < 0.001$) and smoking (93 [71%] vs. 870 [44%], $p < 0.001$) in the stenosis group.

After PSM, recipient age (median [IQR], 66 [60-70] vs. 66 [59-71] years; $p = 0.47$), gender (male: 87 [66%] vs. 355 [68%], $p = 0.85$), diabetes mellitus (72 [55%] vs. 284 [54%], $p = 0.95$), hypertension (92 [70%] vs. 366 [70%], $p = 0.99$), cardio-cerebrovascular disease (68 [52%] vs. 251 [48%], $p = 0.47$) and other demographics were comparable between the stenosis and no-stenosis groups. There was no statistical difference in the distribution of ESRD causes (vascular: 37 [28%] vs. 160 [31%]; diabetes mellitus: 46 [35%] vs. 152 [29%]; glomerulonephritis: 23 [18%] vs. 76 [15%]; polycystic kidney: 7 [5%] vs. 48 [9%]; interstitial disease: 5 [4%] vs. 21 [4%]; others/unknown: 13 [10%] vs. 66 [13%]; $p = 0.57$) between the two groups (**Table 1**).

The median follow-up was 4.8 years (IQR, 3.0-7.2), corresponding to a mean FUI of 0.98 ± 0.10 relative to the predefined end date. No patients had been lost to follow-up within 30 days after kidney transplantation, and 279 deaths (42.6%) were known to have occurred after a median follow-up of 4.1 years (IQR, 1.9-6.2; FUI = 1). Twenty-four patients were "potential survivors" with an FUI < 1.

Pretransplant Symptoms and Interventions

Among the patients with aortoiliac atherosclerotic stenosis, 46 patients (35%) presented symptoms, including claudication, lower limb pain and limb gangrene (28 with TASC A/B stenosis, and 18 with TASC C/D stenosis). For these patients, a comprehensive multidisciplinary meeting involving transplant surgeons, vascular surgeons, and nephrologists was organized to determine the pretransplant intervention. A conservative approach was adopted for 15 patients. Percutaneous transluminal angioplasty (PTA) and stent placement were performed in 24 patients. Femoral popliteal bypass surgery was performed in 7 patients. Peritransplant endarterectomy was performed in 3 patients. Ten patients ultimately required amputation. Additionally, 13 symptomatic patients and 30 asymptomatic patients suffered from coronary occlusive disease.

Table 1. Baseline characteristics before and after propensity score matching

	Before matching			After matching		
	No stenosis (n = 1960)	Stenosis (n = 131)	*p* value	No stenosis (n = 524)	Stenosis (n = 131)	*p* value
Age (years)	58 (47-66)	66 (60-70)	< 0.001	66 (59-71)	66 (60-70)	0.47
Male sex	1214 (62)	87 (66)	0.35	355 (68)	87 (66)	0.85
BMI (kg/m^2)	26 (23-30)	28 (24-32)	0.092	28 (24-31)	28 (24-32)	0.71
Cause of ESRD	511 (26)	37 (28)	< 0.001	160 (31)	37 (28)	0.57
Vascular	303 (16)	46 (35)		152 (29)	46 (35)	
Diabetes mellitus	487 (25)	23 (18)		76 (15)	23 (18)	
Glomerulonephritis	242 (12)	7 (5)		48 (9)	7 (5)	
Polycystic kidney	86 (4)	5 (4)		21 (4)	5 (4)	
Interstitial disease	331 (17)	13 (10)		67 (13)	13 (10)	
Others/unknown						
Type of dialysis			0.021			0.98
pre-emptive	666 (34)	29 (22)		120 (23)	29 (22)	
Hemodialysis	860 (44)	74 (57)		297 (57)	74 (57)	
Peritoneal dialysis	278 (14)	17 (13)		69 (13)	17 (13)	
Combined modality	156 (8)	11 (8)		38 (7)	11 (8)	
Dialysis (months)	22 (12-38)	23 (15-38)	0.27	22 (11-36)	23 (15-38)	0.20
Retransplant	329 (17)	21 (16)	0.92	87 (17)	21 (16)	0.98
Donor type			0.090			0.85
Living donor	1209 (62)	70 (53)		290 (55)	70 (53)	
DBD	310 (16)	21 (16)		87 (17)	21 (16)	
DCD	441 (23)	40 (31)		147 (28)	40 (31)	
Comorbidities						
Diabetes mellitus	540 (28)	72 (55)	< 0.001	284 (54)	72 (55)	0.95
Hypertension	1239 (63)	92 (70)	0.13	366 (70)	92 (70)	0.99
CCVD	466 (24)	68 (52)	< 0.001	251 (48)	68 (52)	0.47
Smoking status			< 0.001			0.99
Never smoker	1090 (56)	38 (29)		150 (29)	38 (29)	
Former smoker	570 (29)	65 (50)		261 (50)	65 (50)	
Current smoker	300 (15)	28 (21)		113 (22)	28 (21)	

Data are presented as n (%), or median (interquartile range). BMI, body mass index; CCVD, cardio-cerebrovascular disease; DBD, donation after brain death; DCD, donation after circulatory death; ESRD, end-stage renal disease.

Patient Survival

The differences in survival rates are shown in **Figure 2A**. Compared to the no-stenosis group, a significantly higher 90-day mortality was observed in patients with aortoiliac stenosis (no stenosis vs. TASC A/B stenosis: 1.9% vs. 7.3%, $p = 0.009$; no stenosis vs. TASC C/D stenosis: 1.9% vs. 8.6%, $p = 0.016$). Among patients who died within 90 post-transplant days in the stenosis group (7 in TASC A/B group, and 3 in TASC C/D group), the primary causes of death were cardiovascular events (n = 4), sepsis (n = 4), and respiratory failure (n = 2).

By the end of the follow-up, there were 202 deaths (39%) in the no-stenosis group, 48 (50%) in the TASC A/B group, and 29 (83%) in the TASC C/D group. Kaplan Meier survival analysis revealed a significant difference in overall survival between the no-stenosis group and TASC A/B group ($p = 0.013$), as well as the no-stenosis group and TASC C/D group ($p < 0.001$). The survival rates at 1, 3, 5, and 10 years in TASC A/B group (84.4%, 72.5%, 59.1% and 30.6%, respectively) and TASC C/D group (82.9%, 65.6%, 41.7% and 11.4%, respectively) were significantly worse than those in the no-stenosis group (94.8%, 86.1%, 73.4% and 44.1%, respectively). Cox-regression analysis showed an increased risk of patient mortality associated with both TASC A/B stenosis (HR 1.49, 95% CI 1.09-2.04, $p = 0.013$) and TASC C/D stenosis (HR 2.66, 95% CI 1.80-3.93, $p < 0.001$; **Table 2**).

Table 2. Hazard ratios of aortoiliac stenosis for patient mortality and graft failure

	Patient mortality			Death-censored graft failure		
	HR	95% CI	*P* value	HR	95% CI	*P* value
TASC A/B stenosis	1.49	1.09-2.04	0.013	1.15	0.67-1.96	0.622
TASC C/D stenosis	2.66	1.80-3.93	< 0.001	1.94	0.98-3.87	0.059

CI, confidence interval; HR, hazard ratio; TASC, Trans-Atlantic Inter-Society Consensus.

Graft Survival

In total, 106 cases of graft failure occurred, with 81 (15%) in the no-stenosis group, 16 (17%) in the TASC A/B group and 9 (26%) in the TASC C/D group. The death-censored graft survival rates were similar between the no-stenosis group and TASC A/B group ($p = 0.620$). At 1, 3, 5, and 10 years, the death-censored graft survival rates were 93.5%, 90.0%,

85.8% and 72.9%, respectively for the no-stenosis group, and 91.5%, 90.3%, 84.5% and 73.6%, respectively for the TASC A/B group. Patients in the TASC C/D group had inferior graft survival rates at 1, 3, 5, and 10 years (87.9%, 79.5%, 74.5% and 58.1%, respectively) compared to those in the no-stenosis group, but the difference was not significant (p = 0.160) (**Figure 2B**). The survival curves align with the Cox-regression analysis, showing that both TASC A/B stenosis and TASC C/D stenosis are not risk factors for graft failure (TASC A/B: HR 1.15, 95% CI 0.67-1.96, p = 0.622; TASC C/D: HR 1.94, 95% CI 0.98-3.87, p = 0.059; **Table 2**).

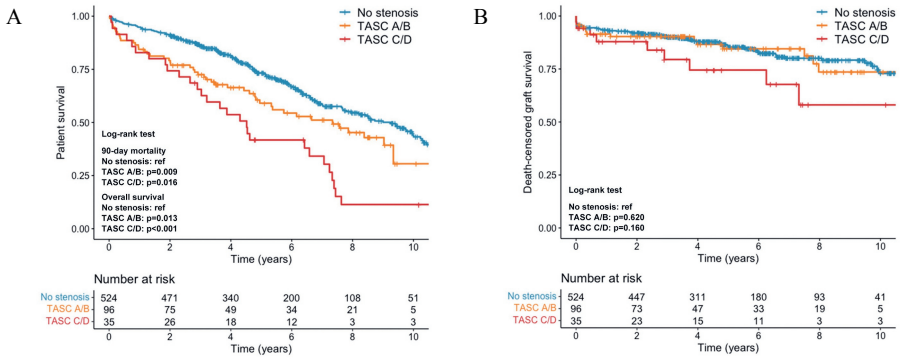


Figure 2. Kaplan-Meier curves comparing (A) patient survival and (B) death-censored graft survival in transplant patients stratified by TASC classification. P-values of pairwise multiple comparisons were adjusted with the Benjamini-Hochberg procedure. TASC, Trans-Atlantic Inter-Society Consensus.

Graft Function

The spaghetti plots of eGFR stratified by TASC classification are shown in **Figure 3**. Patients in the no-stenosis group displayed stable graft function during the long-term follow-up, whereas a fluctuation and decline were observed in both TASC A/B and TASC C/D groups. However, there was no significant difference in eGFR among patients in the TASC A/B and TASC C/D groups compared to those in the no-stenosis group each posttransplant year (**Table S1**, **S2**).

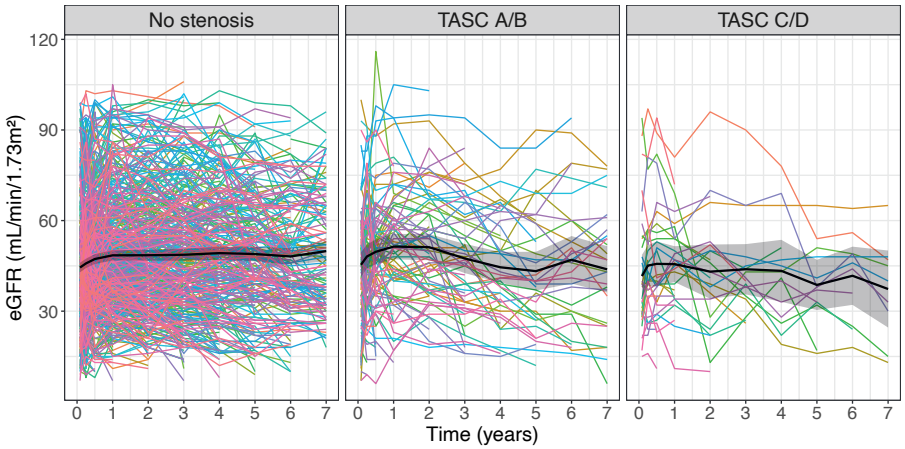


Figure 3. Spaghetti plots of renal function stratified by aorto-iliac stenosis classification. eGFR, estimated graft filtration rate; TASC, Trans-Atlantic Inter-Society Consensus.

Arterial Complications and Management

In the TASC A/B group, arterial complications occurred in 4 patients (4%). Three patients had intraoperative external iliac artery dissection and underwent arterial reconstruction, with good recovery of renal function. Another patient had acute lower extremity ischemia caused by intraoperative clamping of the external iliac artery, and symptoms improved after stenting and angioplasty. In the TASC C/D group, 3 patients (9%) encountered arterial complications. One patient had acute arterial thrombosis, and underwent heparin anticoagulation and thrombectomy, successfully restoring graft function. Another patient had artery kinking, and renal perfusion improved after reanastomosis. Unfortunately, one patient had artery prosthesis rupture, followed by failed reanastomosis and transplantectomy. In the matched no-stenosis group, 6 patients (1%) experienced arterial complications, including artery kinking, artery dissection, arterial thrombosis, anastomotic bleeding, and anastomotic stenosis. Five of these patients preserved graft function after reanastomosis or reoperation, while one patient required transplantectomy. The incidence of arterial complications was significantly higher among patients with aorto-iliac stenosis ($p < 0.001$).

Subgroup Analysis Based on Graft Placement

Subgroup survival analyses based on graft placement are presented in **Figure 4**. In the TASC A/B group, 48 patients underwent ipsilateral graft placement, while the other 48 received contralateral graft placement. Patients undergoing ipsilateral graft placement showed 1-, 3-, and 5-year survival rates of 79.2%, 64.2% and 54.0%, respectively, which was significantly lower than the no-stenosis group (p = 0.003). In contrast, for those undergoing contralateral graft placement, the corresponding rates were 89.6%, 81.0% and 64.3%, demonstrating no significant difference compared to the no-stenosis group (p = 0.66). In the TASC C/D group, 28 patients received the grafts on the ipsilateral side, while 7 patients received grafts on the contralateral side. The 1-, 3-, and 5-year survival rates were 82.1%, 64.1% and 41.5% for ipsilateral graft placement, and 85.7%, 71.4% and 42.9% for contralateral graft placement, respectively. Both rates were significantly lower than the no-stenosis group ($p < 0.001$ and $p = 0.003$, **Figure 4A**).

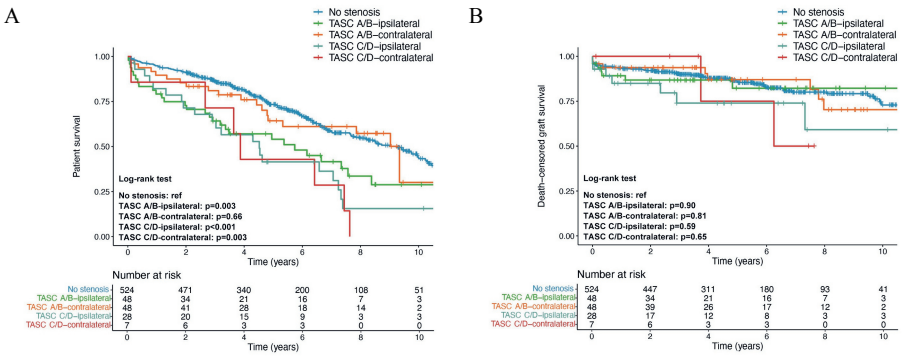


Figure 4. Kaplan-Meier curves comparing (A) patient survival and (B) death-censored graft survival in transplant recipients stratified by TASC classification and graft placement. P-values of pairwise multiple comparisons were adjusted with the Benjamini-Hochberg procedure. TASC, Trans-Atlantic Inter-Society Consensus.

For the death-censored graft survival, patients in the TASC A/B group who underwent ipsilateral graft placement displayed death-censored graft survival rates of 89.2%, 86.8% and 82.2% at 1, 3 and 5 years, and patients with contralateral graft placement displayed rates of 93.7%, 93.7% and 87.0%, respectively. In the TASC C/D group, patients who underwent ipsilateral graft placement displayed death-censored graft survival rates of 84.9%, 74.0%, and 74.0%, while those with contralateral graft placement displayed rates of

100%, 100%, and 75.0%, respectively. All subgroups achieved comparable graft survival as the no-stenosis group (**Figure 4B**).

Discussion

In this retrospective cohort study, we utilized a large transplant database to investigate the clinical outcomes of kidney transplantation in patients with aortoiliac atherosclerotic stenosis, assessing whether aortoiliac atherosclerotic stenosis should be a contra-indication for kidney transplantation. By providing these insights, we hope this study can support clinical decision-making for ESRD patients with aortoiliac stenosis.

The patients in the stenosis group exhibited older age, higher prevalence of diabetes mellitus, smoking and dialysis. These factors play a crucial role in the development of peripheral arterial disease, including aortoiliac atherosclerotic stenosis.[22-26] Based on the fact that cardiovascular events are the leading cause of early posttransplant mortality, our data indicates that aortoiliac stenosis augments vascular disease burden and further increases the risk of 90-day mortality.[27, 28] This finding is in line with the study by Babakry et al., which reported that patients with aortoiliac stenosis had significantly inferior cardiovascular event-free survival.[16]

Furthermore, we investigated the impact of aortoiliac atherosclerotic stenosis on long-term patient outcomes. Our data demonstrate that the 5-year survival rates of patients in TASC A/B group and TASC C/D group were 59.1% and 41.7%, respectively. In comparison to the survival data of ESRD patients subjected to dialysis, which remains approximately 40%, patients with TASC A/B stenosis can derive substantial survival benefits from kidney transplantation.[29, 30] Nevertheless, the survival benefits appear marginal for patients with TASC C/D stenosis, as the survival gap is not significant.

The eligibility of the ESRD patients with aortoiliac stenosis for transplantation remains controversial. Contra-indications on life expectancy are variable and may differ depending on the institutional and geographic contexts. According to the European Society for Organ Transplantation (ESOT), a life expectancy of less than two years is an absolute contra-indication for kidney transplantation.[31] However, the American Society of Transplantation (AST) recommends a minimum life expectancy of 5 years to be considered for kidney

transplantation.[32] The study by Rijkse et al. showed that it is safe to perform kidney transplantation in patients with TASC A/B stenosis, while patients with TASC C/D stenosis have a significantly higher mortality, making kidney transplantation inadvisable.[15] Our data reveals that patients with TASC A/B stenosis align with eligibility standards under both guidelines, evidenced by 2-year and 5-year survival rates of 79.1% and 59.1%, respectively. For patients with TASC C/D stenosis, the scenario becomes nuanced. This high-risk cohort appears to meet the ESOT criterion, with a 2-year survival rate of 74.3%, yet the AST guideline presents a potential mismatch, as the 5-year survival rate stands at 41.7%.

We also looked into the impact on long-term graft outcomes. Surprisingly, the presence of stenosis did not significantly impact death-censored graft survival. Similar cases were reported by Voiculescu et al. showing that in patients with proximal transplant renal artery stenosis, vascular problems could be managed without causing graft loss.[33] Additionally, as a valid surrogate of renal function, posttransplant eGFR revealed a comparable performance between patients with TASC A/B or C/D stenosis and those without stenosis. This finding underscores the resilience of grafts against aortoiliac stenosis, highlighting the possibility to achieve satisfactory graft survival and function across varying severities of stenosis, thereby bringing an enhanced quality of life to these patients.

In terms of graft placement, a considerably higher proportion of ipsilateral kidney implantation was observed in the TASC C/D group compared to the TASC A/B group, likely due to the higher incidence of bilateral stenosis in the TASC C/D group. Among patients who underwent ipsilateral kidney implantation, more patients with TASC A/B stenosis underwent endovascular intervention or no intervention, while those with TASC C/D stenosis were more likely to undergo surgical intervention, reflecting the varying treatment strategies depending on the severity of the stenosis. Both endovascular and surgical interventions have been demonstrated to be safe and effective in the treatment of arterial occlusive disease with kidney transplantation.[13, 14, 34, 35] Our data indicate that patients with TASC A/B stenosis who received contralateral graft placements showed significantly better long-term survival, while graft survival was comparable between different graft implantation sites. However, due to the limited subgroup size, more studies with larger populations are needed to validate this finding.

The basic principle of kidney transplantation is that the patient should derive overall benefit from transplantation compared to the alternative of dialysis. For patients with TASC A/B stenosis, kidney transplantation effectively prolongs survival and improves the quality of life. However, for those with TASC C/D stenosis, kidney transplantation distinctly improves their quality of life but cannot provide corresponding survival benefits. This paradox heralds in an additional layer of complexity in the decision-making process for kidney allocation. The intricate balance of potentially extending the life expectancy of an individual through kidney transplantation while weighing against potentially better long-term survival outcomes for other recipients introduces a formidable challenge that necessitates careful consideration.

Our study has some limitations to be addressed. Firstly, as a retrospective study, there is a guarantee for selection bias in patients with most severe aortoiliac stenosis, as these patients might be rejected for kidney transplantation and would not be included in the study. Secondly, the study's single-center design could introduce institutional-specific practices that may not be universally applicable. Variations in surgical techniques and postoperative management could influence outcomes and limit generalizability. Multi-center studies with larger group size are needed to reach safe conclusions. Lastly, details of stenosis proximal or distal to the transplanted kidney were unknown, which could impact graft survival and function.

Conclusion

Aortoiliac atherosclerotic stenosis significantly deteriorates patient survival, but not graft survival of kidney transplant patients. Nevertheless, patients with TASC A/B stenosis can experience prolonged survival and an enhanced quality of life through kidney transplantation, thus challenging the notion of aortoiliac stenosis as a contra-indication. In contrast, while kidney transplantation can substantially improve the quality of life for patients with TASC C/D stenosis, it might not bring corresponding survival benefits. The decision regarding kidney transplantation for these individuals necessitates careful consideration. Extensive pre-, peri-, and posttransplant cardiovascular risk management is required in this high-risk population.

Reference

1. Abecassis M, Bartlett ST, Collins AJ, Davis CL, Delmonico FL, Friedewald JJ, et al. Kidney transplantation as primary therapy for end-stage renal disease: a National Kidney Foundation/Kidney Disease Outcomes Quality Initiative (NKF/KDOQITM) conference. Clin J Am Soc Nephrol. 2008;3(2):471-80.
2. Chadban SJ, Ahn C, Axelrod DA, Foster BJ, Kasiske BL, Kher V, et al. Summary of the Kidney Disease: Improving Global Outcomes (KDIGO) Clinical Practice Guideline on the Evaluation and Management of Candidates for Kidney Transplantation. Transplantation. 2020;104(4):708-14.
3. Lin CS, Chen SJ, Sung CC, Lin CL, Lin SH, Cheng SM, et al. Hemodialysis Is Associated With Increased Peripheral Artery Occlusive Disease Risk Among Patients With End-Stage Renal Disease: A Nationwide Population-Based Cohort Study. Medicine (Baltimore). 2015;94(28):e1164.
4. Betjes MG. Immune cell dysfunction and inflammation in end-stage renal disease. Nat Rev Nephrol. 2013;9(5):255-65.
5. Betjes MG, Langerak AW, van der Spek A, de Wit EA, Litjens NH. Premature aging of circulating T cells in patients with end-stage renal disease. Kidney Int. 2011;80(2):208-17.
6. Speer T, Rohrer L, Blyszczuk P, Shroff R, Kuschnerus K, Krankel N, et al. Abnormal high-density lipoprotein induces endothelial dysfunction via activation of Toll-like receptor-2. Immunity. 2013;38(4):754-68.
7. Lin CY, Hsu SC, Lee HS, Lin SH, Tsai CS, Huang SM, et al. Enhanced expression of glucose transporter-1 in vascular smooth muscle cells via the Akt/tuberous sclerosis complex subunit 2 (TSC2)/mammalian target of rapamycin (mTOR)/ribosomal S6 protein kinase (S6K) pathway in experimental renal failure. J Vasc Surg. 2013;57(2):475-85.
8. Ozcelik A, Treckmann J, Paul A, Witzke O, Sotiropoulos G, Nadalin S, et al. Results of kidney transplantation with simultaneous implantation of vascular graft. Transplant Proc. 2007;39(2):509-10.
9. Tsivian M, Neri F, Nardo B, Bertelli R, Cavallari G, Fuga G, et al. Aortoiliac surgery concomitant with kidney transplantation: a single center experience. Clin Transplant. 2009;23(2):164-7.
10. Liew YP, Bartholomew JR, Demirjian S, Michaels J, Schreiber MJ, Jr. Combined effect of chronic kidney disease and peripheral arterial disease on all-cause mortality in a high-risk population. Clin J Am Soc Nephrol. 2008;3(4):1084-9.
11. Rajagopalan S, Dellegrottaglie S, Furniss AL, Gillespie BW, Satayathum S, Lameire N, et al. Peripheral arterial disease in patients with end-stage renal disease: observations from the Dialysis Outcomes and Practice Patterns Study (DOPPS). Circulation. 2006;114(18):1914-22.
12. Norgren L, Hiatt WR, Dormandy JA, Nehler MR, Harris KA, Fowkes FG, et al. Inter-Society Consensus for the Management of Peripheral Arterial Disease (TASC II). J Vasc Surg. 2007;45 Suppl S:S5-67.
13. Gallagher KA, Ravin RA, Schweitzer E, Stern T, Bartlett ST. Outcomes and timing of aortic surgery in renal transplant patients. Ann Vasc Surg. 2011;25(4):448-53.
14. Tozzi M, Franchin M, Soldini G, Ietto G, Chiappa C, Molteni B, et al. Treatment of aortoiliac occlusive or dilatative disease concomitant with kidney transplantation: how and when? Int J Surg. 2013;11 Suppl 1:S115-9.
15. Rijkse E, Kimenai H, Roodnat JI, Ten Raa S, Bijdevaate DC, van Dam JL, et al. Impact of Aortoiliac Stenosis on Graft and Patient Survival in Kidney Transplant Recipients Using the TASC II Classification. Transplantation. 2019;103(10):2164-72.
16. Babakry S, Rijkse E, Roodnat JI, Bijdevaate DC, JNM IJ, Minnee RC. Risk of post-transplant cardiovascular events in kidney transplant recipients with preexisting aortoiliac stenosis. Clin Transplant. 2022;36(1):e14515.
17. Mathew G, Agha R, Albrecht J, Goel P, Mukherjee I, Pai P, et al. STROCSS 2021: Strengthening the reporting of cohort, cross-sectional and case-control studies in surgery. Int J Surg. 2021;96:106165.
18. Voiculescu A, Hollenbeck M, Plum J, Hetzel GR, Modder U, Pfeiffer T, et al. Iliac artery stenosis proximal to a kidney transplant: clinical findings, duplex-sonographic criteria, treatment, and outcome. Transplantation. 2003;76(2):332-9.
19. Stevens LA, Schmid CH, Greene T, Zhang YL, Beck GJ, Froissart M, et al. Comparative performance of the CKD Epidemiology Collaboration (CKD-EPI) and the Modification of Diet in Renal Disease (MDRD) Study equations for estimating GFR levels above 60 mL/min/1.73 m2. Am J Kidney Dis. 2010;56(3):486-95.
20. von Allmen RS, Weiss S, Tevaearai HT, Kuemmerli C, Tinner C, Carrel TP, et al. Completeness of Follow-Up Determines Validity of Study Findings: Results of a Prospective Repeated Measures Cohort Study. PLoS One. 2015;10(10):e0140817.
21. Linden A, Samuels SJ. Using balance statistics to determine the optimal number of controls in matching studies. J Eval Clin Pract. 2013;19(5):968-75.

22. Selvin E, Erlinger TP. Prevalence of and risk factors for peripheral arterial disease in the United States: results from the National Health and Nutrition Examination Survey, 1999-2000. Circulation. 2004;110(6):738-43.
23. Joosten MM, Pai JK, Bertoia ML, Rimm EB, Spiegelman D, Mittleman MA, et al. Associations between conventional cardiovascular risk factors and risk of peripheral artery disease in men. JAMA. 2012;308(16):1660-7.
24. Ostchega Y, Paulose-Ram R, Dillon CF, Gu Q, Hughes JP. Prevalence of peripheral arterial disease and risk factors in persons aged 60 and older: data from the National Health and Nutrition Examination Survey 1999-2004. J Am Geriatr Soc. 2007;55(4):583-9.
25. Mikolajczyk-Stecyna J, Korcz A, Gabriel M, Pawlaczyk K, Oszkinis G, Slomski R. Risk factors in abdominal aortic aneurysm and in Polish population aortoiliac occlusive disease and differences between them [corrected]. Sci Rep. 2013;3:3528.
26. Clair DG, Beach JM. Strategies for managing aortoiliac occlusions: access, treatment and outcomes. Expert Rev Cardiovasc Ther. 2015;13(5):551-63.
27. Briggs JD. Causes of death after renal transplantation. Nephrol Dial Transplant. 2001;16(8):1545-9.
28. Awan AA, Niu J, Pan JS, Erickson KF, Mandayam S, Winkelmayer WC, et al. Trends in the Causes of Death among Kidney Transplant Recipients in the United States (1996-2014). Am J Nephrol. 2018;48(6):472-81.
29. Eknoyan G, Beck GJ, Cheung AK, Daugirdas JT, Greene T, Kusek JW, et al. Effect of dialysis dose and membrane flux in maintenance hemodialysis. N Engl J Med. 2002;347(25):2010-9.
30. Bourrier M, Ferguson TW, Embil JM, Rigatto C, Komenda P, Tangri N. Peripheral Artery Disease: Its Adverse Consequences With and Without CKD. Am J Kidney Dis. 2020;75(5):705-12.
31. Ebpg, European Renal A, European Society for Organ T. European Best Practice Guidelines for Renal Transplantation (part 1). Nephrol Dial Transplant. 2000;15 Suppl 7:1-85.
32. Steinman TI, Becker BN, Frost AE, Olthoff KM, Smart FW, Suki WN, et al. Guidelines for the referral and management of patients eligible for solid organ transplantation. Transplantation. 2001;71(9):1189-204.
33. Voiculescu A, Schmitz M, Hollenbeck M, Braasch S, Luther B, Sandmann W, et al. Management of arterial stenosis affecting kidney graft perfusion: a single-centre study in 53 patients. Am J Transplant. 2005;5(7):1731-8.
34. Cyrek AE, Flogel L, Pacha A, Kaths M, Treckmann J, Paul A, et al. Kidney transplantation following iliac revascularization in severe atherosclerosis: a comparative study. Langenbecks Arch Surg. 2023;408(1):105.
35. Matia I, Adamec M, Varga M, Janousek L, Lipar K, Viklicky O. Aortoiliac reconstruction with allograft and kidney transplantation as a one-stage procedure: long term results. Eur J Vasc Endovasc Surg. 2008;35(3):353-7.

Supplementary

Table S1. Comparison of graft function between matched no-stenosis and TASC A/B patients

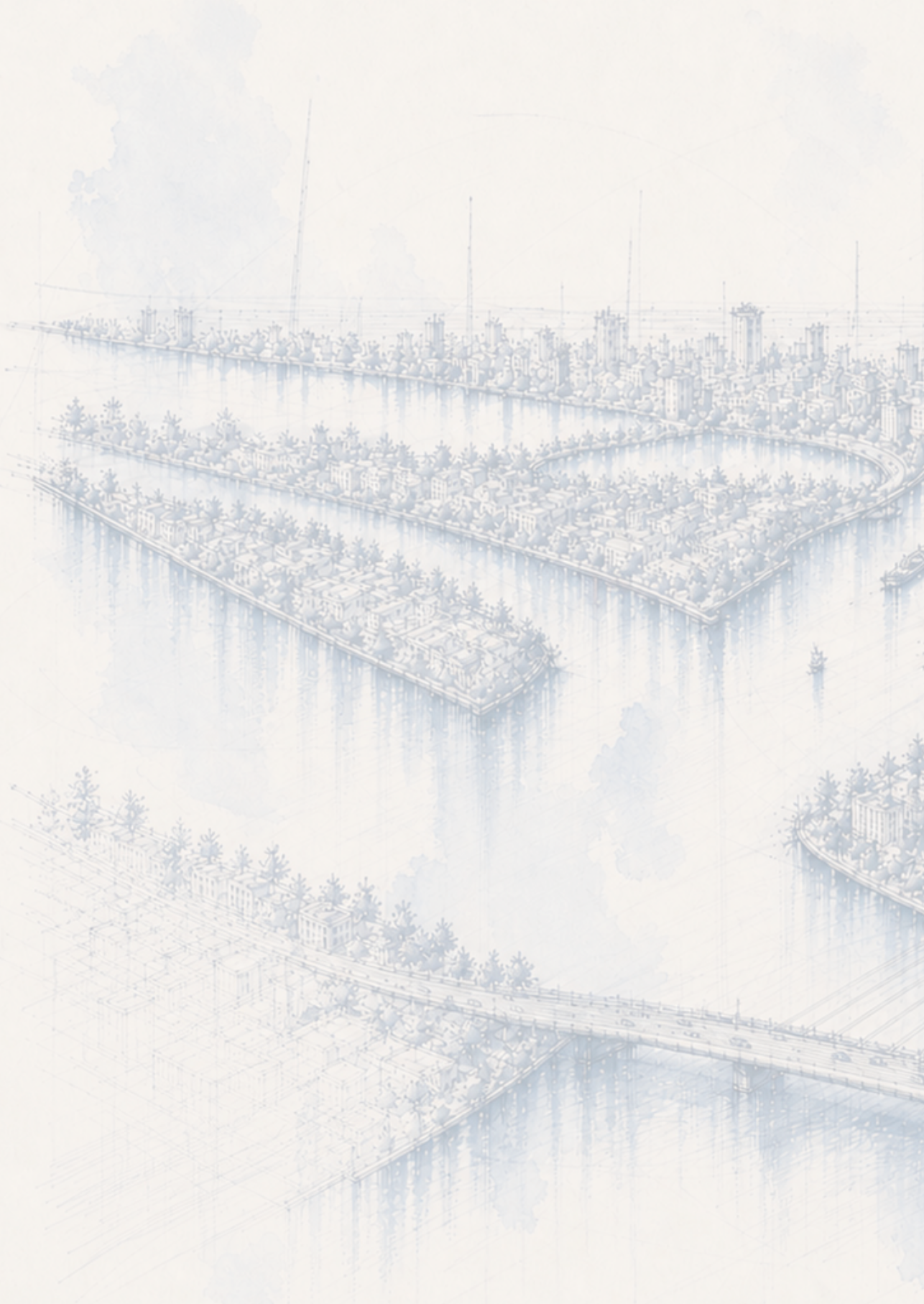
	eGFR (mL/min/1.73m^2)		*p* value
	No stenosis group	TASC A/B group	
1 month	43 (33-54)	47 (33-58)	0.35
3 months	44 (34-55)	48 (35-59)	0.46
6 months	44 (35-58)	47 (36-58)	0.26
1 year	46 (35-59)	49 (39-61)	0.23
2 years	46 (35-60)	49 (36-62)	0.22
3 years	47 (34-61)	46 (35-60)	0.77
4 years	48 (34-63)	44 (33-58)	0.38
5 years	48 (36-61)	43 (32-59)	0.10
6 years	47 (35-63)	46 (32-60)	0.70
7 years	47 (34-65)	47 (31-56)	0.33

Data are presented as median (interquartile range). eGFR, estimated glomerular filtration rate.

Table S2. Comparison of graft function between matched no-stenosis and TASC C/D patients

	eGFR (mL/min/1.73m^2)		*p* value
	No stenosis group	TASC C/D group	
1 month	43 (33-54)	38 (28-53)	0.24
3 months	44 (34-55)	40 (34-55)	0.57
6 months	44 (35-58)	39 (32-56)	0.44
1 year	46 (35-59)	46 (34-54)	0.62
2 years	46 (35-60)	42 (27-52)	0.22
3 years	47 (34-61)	40 (35-47)	0.56
4 years	48 (34-63)	42 (28-55)	0.38
5 years	48 (36-61)	38 (33-50)	0.10
6 years	47 (35-63)	46 (25-49)	0.70
7 years	47 (34-65)	40 (23-48)	0.30

Data are presented as median (interquartile range). eGFR, estimated glomerular filtration rate.



Chapter 8

Simultaneous liver-kidney transplantation versus liver transplantation in end-stage liver disease patients with kidney dysfunction

Sarah Bouari*, Yitian Fang*, Jacqueline van de Wetering, Vincent E. de Meijer, Robert A. Pol, Stefan P. Berger, Wojciech G. Polak, Hans Blokzijl, Aiko P.J. de Vries, Minneke J. Coenraad, Hwai-Ding Lam, Dorottya K. de Vries, Robert J. Porte, Caroline M. den Hoed, Jan N.M. IJzermans, Robert C. Minnee, TransplantLines Investigators

* Authors contributed equally

European Surgical Research, 2025

Abstract

Introduction The role of simultaneous liver-kidney transplantation (SLKT) in end-stage liver disease patients with varying kidney dysfunction remains unclear. This study aims to compare clinical outcomes of SLKT recipients with those undergoing liver transplant alone (LTA) with comparable kidney dysfunction.

Methods This retrospective cohort study included the SLKT cohort (n=52) from the Dutch Organ Transplantation Registration and the LTA cohort (n=829) from Erasmus Medical Center between 2000 and 2020. Patients were stratified by pretransplant renal function (CKD stages 3b-5) and pretransplant renal replacement therapy (RRT) status. Patient and graft survival, and renal function were compared across renal function strata.

Results Across CKD stages 3b and 4, there was no statistically significant difference in overall survival rates (p=0.59 and p=0.23, respectively). For patients with CKD stage 5 or RRT, patient survival rates at 1, 3, and 5 years posttransplant were significantly lower in the LTA group (60.3%, 51.7%, and 51.7%, respectively) compared to the SLKT group (90.0%, 90.0%, and 80.8%, p=0.048). Death-censored liver graft survival rates at 1, 3, and 5 years were also significantly lower in the LTA group (59.8%, 49.9%, and 49.9%) versus SLKT group (86.4%, 86.4%, and 77.0%, p=0.048). Cox proportional hazards model confirmed the association between SLKT and improved patient survival (HR 0.31, 95% CI: 0.10–0.98, p=0.046).

Conclusion For patients with CKD stage 5 or those on pretransplant RRT, SLKT was associated with better survival outcomes compared to LTA. Primary etiology of liver disease and severity of kidney dysfunction should be considered when determining SLKT eligibility. Due to the limited group size, these findings should be interpreted with caution and further validated.

Introduction

Simultaneous liver-kidney transplantation (SLKT) is indicated for patients with end-stage liver disease and concurrent kidney failure requiring renal replacement therapy.[1] However, its role in patients with moderate kidney dysfunction remains less well-defined. In such cases, kidney dysfunction may be reversible after liver transplantation, potentially eliminating the need for a subsequent kidney transplant.

The prevalence of pre-existing chronic kidney disease (CKD) among liver transplant candidates exceeds 20%.[2] This trend is driven by the increasing incidence of patients suffering from metabolic dysfunction-associated liver disease as an indicator for liver transplantation.[3, 4] Accordingly, the number of SLKT procedures has also risen, particularly in the United States.[5] A key factor in this increase has been the introduction of the Model for End-stage Liver Disease (MELD) score in 2002 for liver transplant priority assessment.[6] As the presence of kidney failure increases the MELD score, those with renal impairment may receive higher priority for liver transplantation, consequently increasing the number of SLKTs performed.

Despite the growing demand for organ transplantation, the supply of donor organs remains insufficient to meet the needs of waitlisted patients for both SLKT and single-organ transplants. Moreover, recent studies suggest that SLKT does not mitigate the influence of pretransplant CKD on post-liver transplant survival.[3] This concern prompted the United Network for Organ Sharing (UNOS) to implement a SLKT allocation policy in 2017 following the steady increase of SLKT in the US.[7-9] This policy establishes eligibility criteria for SLKT, and introduces a "safety net" to prioritize kidney allocation to liver transplant recipients with persistent renal failure.[10, 11]

In Europe, there is no standardized SLKT allocation policy. Within the Eurotransplant network, the Approved Combined Organ (ACO) designation applies to candidates requiring multi-organ transplants (e.g., lung-liver or liver-pancreas transplants), but does not apply to SLKT candidates. Instead, SLKT eligibility is primarily determined by MELD-based criteria, and varies across countries and transplant centers.[12]

Limited research has compared SLKT and liver transplantation alone (LTA) outcomes, with most studies conducted in the US and UK, leaving a gap in data on European transplant populations.[3, 13] To address this, we analyzed the Dutch transplant population, stratifying patients by pretransplant renal function. We then compared patient and liver graft outcomes in SLKT patients with those undergoing LTA with comparable kidney dysfunction.

Materials and Methods

This retrospective cohort study utilized data from the Dutch Organ Transplantation Registry (NOTR) database, a mandatory national audit which records all organ transplants performed in the Netherlands. Patients who underwent SLKT between 2000 and 2020 at the Erasmus Medical Center (EMC), University Medical Center Groningen (UMCG), and Leiden University Medical Center (LUMC) were screened. For comparison, patients who underwent LTA at EMC during the same period were also included. Pediatric patients, recipients who had previous transplant history, received additional solid organs beyond the liver and kidney, or underwent sequential kidney transplant after liver transplant were excluded from the study.

This study was conducted and reported in accordance with the Strengthening the Reporting of Observational Studies in Epidemiology (STROBE) guideline.[14] The study proposal was approved by the TransplantLines scientific committee (#2021-003)[15] and the Medical Ethics Committee of University Medical Center Groningen (METC#2014/077). The study adhered to the principles of the Declaration of Helsinki guidelines, and written informed consent was obtained from all participants.

According to the Kidney Disease: Improving Global Outcomes (KDIGO) guidelines, pretransplant renal replacement therapy (RRT) status, and estimated glomerular filtration rate (eGFR) at the time of transplant, patients were categorized into CKD stage 1 (eGFR ≥ 90 ml/min/1.73 m^2), stage 2 (eGFR 60–89 ml/min/1.73 m^2), stage 3a (eGFR 45–59 ml/min/1.73 m^2), stage 3b (eGFR 30–44 ml/min/1.73 m^2), stage 4 (eGFR 15–29 ml/min/1.73 m^2), and stage 5 or RRT groups (eGFR < 15 ml/min/1.73 m^2 or undergoing RRT).[16] As this study focuses on patients with moderate-to-severe kidney dysfunction, further analyses compared outcomes in patients with CKD stage 3b to 5 or RRT across LTA and SLKT groups.

Demographics and clinical data of the SLKT cohort were extracted from the NOTR database, and data of the LTA cohort were collected from the institutional transplant database. Collected variables included recipient age, sex, pretransplant renal function, donor type, indication for liver transplantation, indication for kidney transplantation, and laboratory MELD score.

The primary outcome of interest was patient survival. Secondary outcomes included death-censored liver/kidney graft survival, and posttransplant renal function. Death-censored liver/kidney graft survival was defined as the time interval between transplantation and graft failure, with censoring of patient deaths occurring while the graft was still functioning (death with functioning graft). Renal function was assessed using eGFR, calculated using the Chronic Kidney Disease Epidemiology Collaboration (CKD-EPI) equation both pretransplant and at 1, 3, and 5 years posttransplant.[17]

Immunosuppression Regimen

A standardized immunosuppressive regimen was applied at all three centers, with adjustments based on organ type and renal function. During the anhepatic phase, 500 mg of intravenous methylprednisolone was administered, followed by basiliximab (20 mg) on postoperative days 0 and 4 as induction therapy.

For LTA patients, maintenance immunosuppression consisted of prednisolone, tacrolimus, and mycophenolate mofetil (MMF). Tacrolimus was initiated on postoperative day 5-6 at 0.1 mg/kg/day, targeting trough levels of 6-10 μg/L for the first 6 months and 4-8 μg/L thereafter. Prednisolone was tapered from 20 mg on day 0 to 2.5 mg by 3 months, and discontinued after 4 months if stable graft function was achieved. MMF (1,000 mg twice daily) was continued during the early postoperative period and adjusted based on tolerance and hematologic parameters. In cases of renal dysfunction, tacrolimus monotherapy was converted to combination therapy with reduced tacrolimus exposure (3-5 μg/L) and MMF (1.5-3 mg/L) or mTOR inhibitor (2-3 μg/L).

For SLKT patients, the same induction regimen was used. Maintenance immunosuppression followed the standard kidney transplantation protocol. Tacrolimus was initiated on day 0 at 0.1 mg/kg/day, targeting trough levels of 8-12 μg/L during the first 4

weeks, 5-10 µg/L by weeks 5-12, and 5-8 µg/L after 3 months. Prednisolone was tapered from 50 mg on day 0 to 5 mg by 4 months, and discontinued after 5 months. MMF was administered at 1,000 mg twice daily, with dose adjustments to maintain trough levels of 1.5-3 mg/L. Cyclosporine was used as an alternative calcineurin inhibitor in selected cases of tacrolimus intolerance.

Statistical Analysis

Continuous variables were reported as medians with interquartile ranges (IQRs), and categorical variables were reported as numbers with percentages. The Kruskal-Wallis test was used to compare continuous variables between groups, and the chi-squared test was used for categorical variables. Kaplan-Meier curves and the log-rank test were used to compare patient and graft survival stratified by CKD stage for both LTA and SLKT groups. Cox proportional hazards models were used to determine the association between SLKT and survival outcomes (patient mortality and liver graft loss), adjusting for donor type, recipient age and recipient sex as covariates, and tested using Schoenfeld residuals. P-value < 0.05 was considered statistically significant. Data processing, statistical analysis and data visualization were conducted using R (version 4.2.2).

Results

This study included 52 patients who underwent SLKT between 2000 and 2020, as recorded in the NOTR database. During the same period, 829 eligible patients who underwent LTA at EMC were included. The median follow-up duration after transplantation was 5.2 years (IQR: 1.9-10.5).

Distribution of Pretransplant Renal Function

The distribution of pretransplant renal function among patients undergoing LTA and SLKT is summarized in **Table 1**. One LTA patient had missing pretransplant kidney function and was excluded from analyses. Among LTA patients, the majority were categorized within CKD stage 1 (457, 55.1%), followed by stage 2 (219, 26.4%), stage 3a (64, 7.7%), stage 3b (40, 4.8%) and stage 4 (32, 3.9%), with the fewest transplants performed in patients with stage 5 or RRT (16, 1.9%). In contrast, the majority of SLKT patients had advanced CKD,

with 30 (57.7%) classified as stage 5 or RRT, followed by stage 4 (13, 25.0%), stage 3a (4, 7.7%), stage 3b (4, 7.7%), and stage 2 (1, 1.9%).

Table 1. Distribution of pretransplant KDIGO stages in LTA and SLKT patients

CKD stage	eGFR, ml/min/1.73 m^2	LTA (n=829)[a]	SLKT (n=52)
Stage 1	≥ 90	457 (55.1)	-
Stage 2	60-89	219 (26.4)	1 (1.9)
Stage 3a	45-59	64 (7.7)	4 (7.7)
Stage 3b	30-44	40 (4.8)	4 (7.7)
Stage 4	15-29	32 (3.9)	13 (25.0)
Stage 5 or RRT	<15	16 (1.9)	30 (57.7)

Data are presented as number with percentage.
SLKT, simultaneous liver-kidney transplantation; eGFR, estimated glomerular filtration rate; LTA, liver transplantation alone; RRT, renal replacement therapy.
a. Pretransplant eGFR was missing in one patient.

For SLKT patients with relatively preserved pretransplant eGFR (CKD stages 2-3a), SLKT was performed due to specific clinical indications of irreversible or progressive renal disease. Specifically, the patient with CKD stage 2 had Caroli disease and concomitant polycystic kidney disease. Among the four patients with CKD stage 3a, one had polycystic liver and kidney disease, one had primary hyperoxaluria type 1 with oxalosis nephropathy, one had HCV cirrhosis with cyclosporine-induced nephropathy, and one had PSC with IgA nephropathy. For CKD stage 3b (n=4), the indications included PSC with immune-mediated kidney injury, Henoch-Schönlein purpura with IgA nephropathy, polycystic liver and kidney disease, and alcoholic cirrhosis with chronic kidney dysfunction.

Demographic and Clinical Characteristics

Demographic and clinical characteristics are summarized in **Table 2**. No significant differences were observed between LTA and SLKT recipients regarding age, sex, or donor type. However, the primary indication for liver transplantation varied significantly in patients with CKD stages 4 ($p=0.008$) and 5 or RRT ($p<0.001$). Among LTA recipients, acute liver failure was the most common indication for transplantation in both CKD stage 4 (46.9%) and stage 5 or RRT (68.8%). In contrast, among SLKT patients, polycystic disease was the predominant indication (38.5% in stage 4, and 56.7% in stage 5 or RRT), followed by metabolic disease (30.8% and 16.7%, respectively).

MELD scores were significantly higher in LTA recipients than in SLKT recipients across all subgroups. In patients with CKD stage 3b, median laboratory MELD scores were 23 (IQR: 18-32) for LTA versus 15 (IQR: 14-17) for SLKT (p = 0.048). Similarly, in stage 4, LTA recipients had a median MELD score of 37 (IQR: 26-40) compared to 21 (IQR: 17-25) in SLKT recipients (p=0.001), and in stage 5, MELD scores were 40 (IQR: 36-40) in LTA versus 21 (IQR: 21-22) in SLKT (p<0.001), suggesting that LTA recipients had more severe liver disease at the time of transplantation than SLKT recipients.

Patient and Graft Survival

Patient and death-censored liver graft survival stratified by CKD stages are shown in **Figure 1**. For patients with CKD stages 3b and 4, there was no statistically significant difference in overall patient survival rates (p=0.59 and p=0.23, respectively), although the 5-year patient survival rates of SLKT group were higher than that of LTA group (CKD stage 3b: 100% vs 77.1%; CKD stage 4: 90.9% vs 71.1%). Death-censored liver graft survival followed similar trends (p=0.23 and p=0.50, respectively).

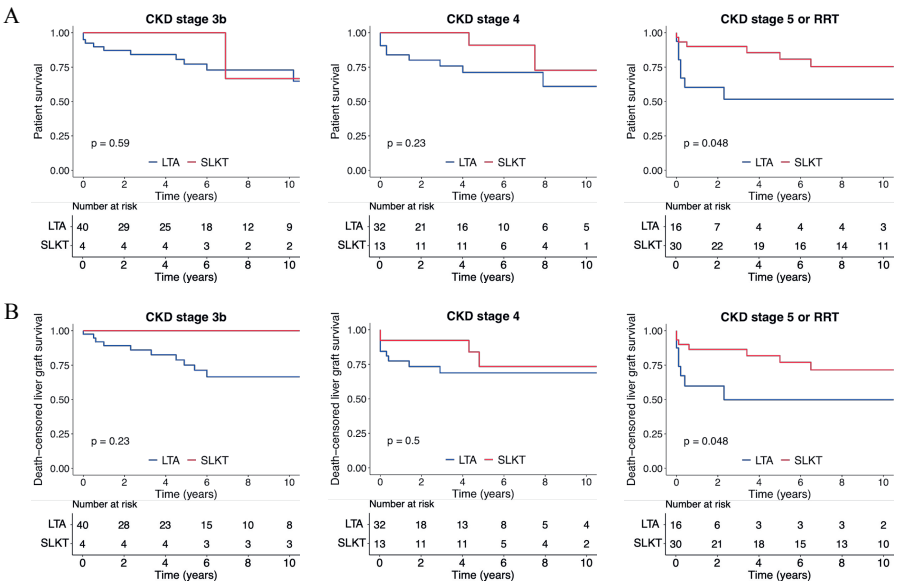


Figure 1. (A) Patient and (B) death-censored liver graft survival stratified by CKD stage 3b, 4, and 5 or renal replacement therapy (RRT).

However, in patients with CKD stage 5 or RRT, survival outcomes favored SLKT. Patient survival rates at 1, 3, and 5 years were 60.3%, 51.7%, and 51.7% in the LTA group compared to 90.0%, 90.0%, and 80.8% in the SLKT group, respectively (p=0.048). Similarly, death-censored liver graft survival rates at 1, 3, and 5 years were significantly lower in the LTA group (59.8%, 49.9%, and 49.9%) versus SLKT group (86.4%, 86.4%, and 77.0%, p=0.048). Among LTA patients, only one patient with CKD stage 5 subsequently underwent kidney transplantation from a living donor after 1.6 years after liver transplantation.

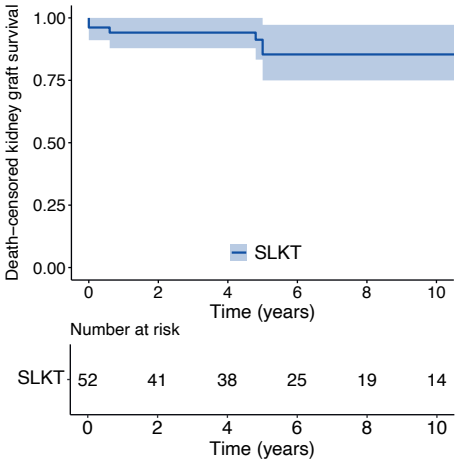


Figure 2. Death-censored kidney graft survival in simultaneous liver-kidney transplantation (SLKT).

For SLKT recipients, death-censored kidney graft survival at 1, 3, and 5 years were 94.1%, 94.1%, and 85.4%, respectively (**Figure 2**). Causes of graft failure in LTA and SLKT patients are summarized in **Table 3**.

Table 3. Cause of graft failure in LTA and SLKT patients stratified by pretransplant renal function

	Stage 3b		Stage 4		Stage 5 or RRT	
	LTA (n=40)	SLKT (n=4)	LTA (n=32)	SLKT (n=13)	LTA (n=16)	SLKT (n=30)
Cause of liver graft failure						
Death with functioning graft	3 (7.5)	-	2 (6.3)	-	1 (6.3)	3 (10.0)
Acute rejection	1 (2.5)	-	-	-	-	-
Chronic rejection	1 (2.5)	-	1 (3.1)	-	1 (6.3)	-
Primary nonfunction	1 (2.5)	-	2 (6.3)	1 (7.7)	2 (12.5)	1 (3.3)
Infection	1 (2.5)	-	3 (9.4)	-	2 (12.5)	1 (3.3)
Recurrent disease	1 (2.5)	-	-	-	-	1 (3.3)
Nonanastomotic biliary stricture	3 (7.5)	-	-	-	-	-
Hemorrhage	-	-	1 (3.1)	-	-	-
Thrombosis	-	-	1 (3.1)	1 (7.7)	-	2 (6.7)
De novo malignancy	-	-	1 (3.1)	-	-	1 (3.3)
Other	2 (5.0)	-	-	1 (7.7)	2 (12.5)	1 (3.3)
Cause of kidney graft failure						
Death with functioning graft		1 (25.0)		2 (15.4)		7 (23.3)
Primary nonfunction		-		-		1 (3.3)
Recurrent disease		-		-		1 (3.3)
Thrombosis		-		1 (7.7)		-
Other		-		1 (7.7)		3 (10.0)

LTA, liver transplantation alone; SLKT, simultaneous liver-kidney transplantation; RRT, renal replacement therapy.

Impact of SLKT on Survival

Cox proportional hazards model (**Table 4**) showed no significant survival benefit of SLKT over LTA for patients with CKD stage 3b (HR 0.57, 95% CI: 0.07-4.82, p=0.603) or stage 4 (HR 0.38, 95% CI: 0.08-1.79, p=0.220). Similarly, SLKT also showed no significant advantage in liver graft survival in CKD stages 3b and 4 cohorts (p=0.446 and p=0.490, respectively).

However, for patients with CKD stage 5 or RRT, SLKT was associated with significantly improved patient survival (HR 0.31, 95% CI: 0.10-0.98, p=0.046). While liver graft survival is better in SLKT recipients, this association did not reach statistical significance (HR 0.37, 95% CI 0.13-1.10, p=0.075).

Table 4. Cox proportional hazards models for the association of SLKT and survival outcomes

	Patient mortality		Liver graft loss	
	HR* (95% CI)	p-value	HR* (95% CI)	p-value
Stage 3b	0.57 (0.07-4.82)	0.603	0.44 (0.05-3.60)	0.446
Stage 4	0.38 (0.08-1.79)	0.220	0.62 (0.16-2.38)	0.490
Stage 5 or RRT	0.31 (0.10-0.98)	0.046	0.37 (0.13-1.10)	0.075

*Adjusted for donor type, recipient age, and sex.
RRT, renal replacement therapy; SLKT, simultaneous liver-kidney transplantation.

Table 5. Renal function at 1-, 3- and 5-year posttransplant, stratified by pretransplant renal function

	LTA	SLKT	p-value
Stage 3b			
1 year	55 (44-83)	59 (52-72)	0.706
3 years	55 (45-75)	53 (51-56)	0.977
5 years	55 (45-65)	59 (53-66)	0.776
Stage 4			
1 year	66 (49-80)	50 (41-65)	0.052
3 years	71 (48-84)	51 (42-62)	0.132
5 years	57 (49-79)	55 (48-58)	0.403
Stage 5 or RRT			
1 year	64 (56-75)	54 (39-61)	0.160
3 years	63 (63-66)	52 (47-75)	0.283
5 years	70 (64-72)	62 (51-81)	0.671

LTA, liver transplantation alone; RRT, renal replacement therapy; SLKT, simultaneous liver-kidney transplantation.

Renal Function after Transplantation

Posttransplant renal function at 1, 3, and 5 years is presented in **Table 5**. Median eGFR ranged from 55 to 77 ml/min/1.73 m^2 in LTA recipients, and ranged from 55 to 62 ml/min/1.73 m^2 in SLKT recipients, the difference was not statistically significant ($p>0.05$ for all comparisons).

Discussion

This study comparing SLKT and LTA outcomes demonstrates that for patients with CKD stage 5 or those on RRT, SLKT is associated with significantly better patient and liver graft survival. However, for patients with CKD stage 3b and 4, although SLKT achieves higher survival rates, the differences are not statistically significant.

Our previous systematic review and meta-analysis found that while SLKT patients exhibit similar patient survival, they experience improved liver graft survival compared to LTA patients with renal dysfunction.[18] However, limited data make it unclear which CKD stage benefits most from SLKT. Tinti et al.[13] stratified SLKT and LTA recipients based on pretransplant eGFR using the UK National transplant database and found that only patients on RRT benefited from SLKT. Moreover, Cullaro et al.[3] analyzed a CKD cohort with a mean eGFR of 52 (IQR 35-72) ml/min/1.73 m^2, and found that pretransplant CKD was associated with increased posttransplant mortality, an effect not mitigated by SLKT. Our findings further support that SLKT significantly improved patient and liver graft survival in patients with CKD stage 5 or RRT.

The UNOS currently recommends SLKT for CKD patients with an eGFR of ≤ 60 ml/min/1.73m^2 for more than 90 days, with the most recent GFR ≤ 30 mL/min/1.73m^2 or maintenance dialysis.[19] Critics argue that current criteria may be too lenient, leading to overutilization of donor kidneys for SLKT in patients who may not clinically benefit, reducing kidney availability for those waiting kidney transplant alone. On the other hand, proponents emphasize that SLKT provides safe long-term outcomes and is essential for patients with irreversible renal dysfunction.

In addition to renal function, the primary cause of kidney dysfunction should be considered when determining eligibility for SLKT. For example, in our cohort, the cause of kidney dysfunction varies significantly between SLKT and LTA recipients, with polycystic and metabolic diseases being more common in SLKT and acute liver failure in LTA. The observed improvement in posttransplant renal function among LTA patients suggests that kidney dysfunction associated with acute liver failure is often reversible. Supporting this, Northup et al.[20] reported that approximately 70% of patients with hepatorenal syndrome experienced spontaneous renal recovery following LTA, making routine SLKT unnecessary in this subgroup.

A possible solution is to incorporate kidney biopsy into pretransplant assessment to determine the reversibility of renal injury.[21, 22] Pichler et al.[23] demonstrated that performing pretransplant kidney biopsies in liver transplant candidates with kidney dysfunction of unknown etiology reduced unnecessary kidney allocation by 70% without negatively affecting patient survival or 1-year posttransplant eGFR. However, the risks of kidney biopsy in patients with coagulation disorders should be carefully considered.[24]

Given that patients requiring a kidney transplant are typically waitlisted for over three years, alternative strategies beyond SLKT should be considered.[25] One such strategy is kidney after liver transplantation (KALT), which is already performed in both the US and Europe.[26-28] Althuser et al.[27] found that after implementing “safety net” policies, the proportion of SLKT cases among total liver transplant recipients decreased from 10.2% to 9.0%, while the number of KALT procedures increased by 65% over 2.5 years. Cheng et al.[29] demonstrated that such policies improved organ utilization and liver transplant outcomes. Similarly, in the Eurotransplant region, patients who require dialysis after the other organ transplant between 90-360 days will receive bonus points for a delayed kidney transplant. Furthermore, delaying kidney transplantation allows for the possibility of using a living donor, further preserving the limited supply of deceased donor kidneys. In our cohort, the majority of LTA patients did not undergo subsequent kidney transplantation, likely due to recovery of renal dysfunction secondary to hepatorenal syndrome following liver transplantation. The poorer survival outcomes observed in the LTA group, particularly among CKD stage 5 patients, likely reflect severe baseline illness that excluded kidney

transplantation eligibility or resulted in death before transplantation. Additionally, some patients may require kidney transplantation beyond the follow-up period of our study.

This study has several limitations to be addressed. First, the group size of SLKT was small. To counteract this, we included all patients who underwent SLKT in the Netherlands over a 20-year period, using data from the national transplant registry to ensure completeness and accuracy. To strengthen the robustness of our analyses, we compared outcomes with a large, consecutive cohort of LTA recipients stratified by CKD stage. Nevertheless, subgroup analyses by primary liver disease were not feasible. For example, among patients with CKD stage 5 or RRT, acute liver failure was more common in the LTA group, whereas polycystic disease in the SLKT group. Patients undergoing transplantation for acute liver failure tend to have worse short-term outcomes compared to those undergoing elective procedures. Second, despite groups were matched by CKD stage, patients with more severe conditions or hepatorenal syndrome may have been preferentially allocated to LTA, introducing potential allocation bias that could affect the robustness of survival comparison. Larger-scale studies with more covariates are needed to address this limitation. Third, the duration of pretransplant CKD and dialysis, which are key determinants for SLKT eligibility according to current allocation policies, were not available, preventing a comprehensive assessment of their impact on outcomes.

In conclusion, for patients with CKD stage 3b and 4, LTA provides comparable patient and liver graft survival to SLKT. However, for patients with CKD stage 5 or RRT, SLKT was associated with significantly improved patient survival. Determining SLKT eligibility requires consideration of primary etiology of liver disease, renal dysfunction severity, and long-term organ allocation strategies. Given the limited group size, these findings should be interpreted with caution, and large-scale studies are needed to validate and inform policy development.

Reference

1. Singal AK, Ong S, Satapathy SK, Kamath PS, Wiesner RH. Simultaneous liver kidney transplantation. Transpl Int. 2019;32(4):343-52.
2. Teo VXY, Heng RRY, Tay PWL, Ng CH, Tan DJH, Ong Y, et al. A meta-analysis on the prevalence of chronic kidney disease in liver transplant candidates and its associated risk factors and outcomes. Transpl Int. 2021;34(12):2515-23.
3. Cullaro G, Verna EC, Lee BP, Lai JC. Chronic Kidney Disease in Liver Transplant Candidates: A Rising Burden Impacting Post-Liver Transplant Outcomes. Liver Transpl. 2020;26(4):498-506.
4. Goldberg DS, Vianna RM, Martin EF, Martin P, Arosemena Benitez LR, O'Brien CB, et al. Simultaneous Liver Kidney Transplant in Elderly Patients With Chronic Kidney Disease: Is There an Appropriate Upper Age Cutoff? Transplantation. 2020;104(12):2538-46.
5. Nadim M, Sung, RS., Davis, CL., Andreoni, KA. Simultaneous Liver-Kidney Transplantation Summit: Current State and Future Directions. American Journal of Transplantation. 2012.
6. Kamath PS, Wiesner RH, Malinchoc M, Kremers W, Therneau TM, Kosberg CL, et al. A model to predict survival in patients with end-stage liver disease. Hepatology. 2001;33(2):464-70.
7. Committee OUKT. Simultaneous Liver Kidney (SLK) Allocation Policy. 2015.
8. Nadim MK, Sung RS, Davis CL, Andreoni KA, Biggins SW, Danovitch GM, et al. Simultaneous liver-kidney transplantation summit: current state and future directions. Am J Transplant. 2012;12(11):2901-8.
9. Ekser B, Contreras AG, Andraus W, Taner T. Current status of combined liver-kidney transplantation. Int J Surg. 2020;82S:149-54.
10. Formica RN, Aeder M, Boyle G, Kucheryavaya A, Stewart D, Hirose R, et al. Simultaneous Liver-Kidney Allocation Policy: A Proposal to Optimize Appropriate Utilization of Scarce Resources. Am J Transplant. 2016;16(3):758-66.
11. Asch WS, Bia MJ. New Organ Allocation System for Combined Liver-Kidney Transplants and the Availability of Kidneys for Transplant to Patients with Stage 4-5 CKD. Clin J Am Soc Nephrol. 2017;12(5):848-52.
12. Eurotransplant Liver Allocation System. In: Eurotransplant, editor. 2022.
13. Tinti F, Mitterhofer AP, Umbro I, Nightingale P, Inston N, Ghallab M, et al. Combined liver-kidney transplantation versus liver transplant alone based on KDIGO stratification of estimated glomerular filtration rate: data from the United Kingdom Transplant registry - a retrospective cohort study. Transpl Int. 2019;32(9):918-32.
14. Cuschieri S. The STROBE guidelines. Saudi J Anaesth. 2019;13(Suppl 1):S31-S4.
15. Eisenga MF, Gomes-Neto AW, van Londen M, Ziengs AL, Douwes RM, Stam SP, et al. Rationale and design of TransplantLines: a prospective cohort study and biobank of solid organ transplant recipients. BMJ Open. 2018;8(12):e024502.
16. Stevens PE, Levin A, Kidney Disease: Improving Global Outcomes Chronic Kidney Disease Guideline Development Work Group M. Evaluation and management of chronic kidney disease: synopsis of the kidney disease: improving global outcomes 2012 clinical practice guideline. Ann Intern Med. 2013;158(11):825-30.
17. Levey AS, Stevens LA, Schmid CH, Zhang YL, Castro AF, 3rd, Feldman HI, et al. A new equation to estimate glomerular filtration rate. Ann Intern Med. 2009;150(9):604-12.
18. Bouari S, Rijkse E, Metselaar HJ, van den Hoogen MWF, JNM IJ, de Jonge J, et al. A comparison between combined liver kidney transplants to liver transplants alone: A systematic review and meta-analysis. Transplant Rev (Orlando). 2021;35(4):100633.
19. Samoylova ML, Wegermann K, Shaw BI, Kesseli SJ, Au S, Park C, et al. The Impact of the 2017 Kidney Allocation Policy Change on Simultaneous Liver-Kidney Utilization and Outcomes. Liver Transpl. 2021;27(8):1106-15.
20. Northup PG, Argo CK, Bakhru MR, Schmitt TM, Berg CL, Rosner MH. Pretransplant predictors of recovery of renal function after liver transplantation. Liver Transpl. 2010;16(4):440-6.
21. Tanriover B, Mejia A, Weinstein J, Foster SV, Ghalib R, Mubarak A, et al. Analysis of kidney function and biopsy results in liver failure patients with renal dysfunction: a new look to combined liver kidney allocation in the post-MELD era. Transplantation. 2008;86(11):1548-53.
22. Wadei HM, Heckman MG, Rawal B, Taner CB, Mai ML, Cortese C, et al. Renal outcomes of liver transplant recipients who had pretransplant kidney biopsy. Transplantation. 2014;98(12):1323-30.
23. Pichler RH, Huskey J, Kowalewska J, Moiz A, Perkins J, Davis CL, et al. Kidney Biopsies May Help Predict Renal Function After Liver Transplantation. Transplantation. 2016;100(10):2122-8.
24. Jouet P, Meyrier A, Mal F, Callard P, Guettier C, Stordeur D, et al. Transjugular renal biopsy in the treatment of patients with cirrhosis and renal abnormalities. Hepatology. 1996;24(5):1143-7.

25. Saran R, Li Y, Robinson B, Abbott KC, Agodoa LY, Ayanian J, et al. US Renal Data System 2015 Annual Data Report: Epidemiology of Kidney Disease in the United States. Am J Kidney Dis. 2016;67(3 Suppl 1):Svii, S1-305.
26. Cullaro G, Verna EC, Emond JC, Orandi BJ, Mohan S, Lai JC. Early Kidney Allograft Failure After Simultaneous Liver-kidney Transplantation: Evidence for Utilization of the Safety Net? Transplantation. 2021;105(4):816-23.
27. Altshuler PJ, Shah AP, Frank AM, Glorioso J, Dang H, Shaheen O, et al. Simultaneous liver kidney allocation policy and the Safety Net: an early examination of utilization and outcomes in the United States. Transpl Int. 2021;34(6):1052-64.
28. Bouari S, Polak WG, van de Wetering J, Metselaar HJ, JNM IJ, Minnee RC. Combined liver-kidney transplantation with delayed kidney implantation: A case report. Int J Surg Case Rep. 2023;106:108276.
29. Cheng XS, Kim WR, Tan JC, Chertow GM, Goldhaber-Fiebert J. Comparing Simultaneous Liver-Kidney Transplant Strategies: A Modified Cost-Effectiveness Analysis. Transplantation. 2018;102(5):e219-e28.

Table 2. Demographics and clinical characteristics of LTA and SLKT patients stratified by pretransplant renal function

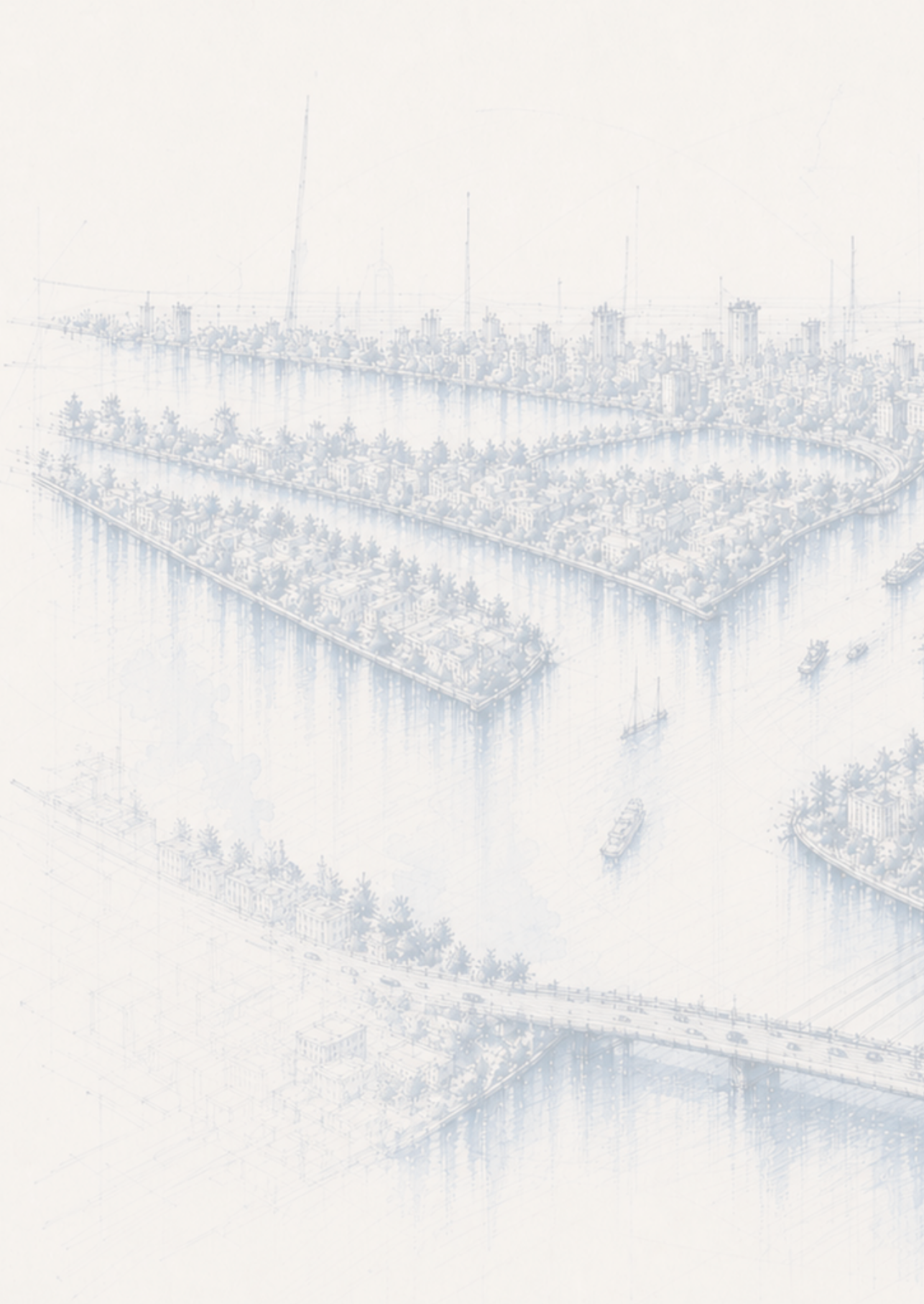
	Stage 3b			Stage 4			Stage 5 or RRT		
	LTA (n=40)	SLKT (n=4)	p-value	LTA (n=32)	SLKT (n=13)	p-value	LTA (n=16)	SLKT (n=30)	p-value
Age (years)	55 (43-62)	52 (45-60)	0.967	47 (35-58)	53 (43-58)	0.556	51 (38-56)	53 (46-60)	0.467
Sex (male)	22 (55.0)	2 (50.0)	0.848	15 (46.9)	7 (53.8)	0.672	7 (43.8)	9 (30.0)	0.351
Donor type			0.226			0.857			0.957
DBD	31 (77.5)	2 (50.0)		29 (89.6)	12 (92.3)		15 (93.7)	28 (93.3)	
DCD	9 (22.5)	2 (50.0)		3 (9.4)	1 (7.7)		1 (6.3)	2 (6.7)	
Indication for LT			0.734			0.008			<0.001
Acute liver failure	9 (22.5)	-		15 (46.9)	1 (7.7)		11 (68.8)	-	
Alcoholic cirrhosis	7 (17.5)	1 (25.0)		3 (9.4)	1 (7.7)		-	2 (6.7)	
Cancer	7 (17.5)	-		2 (6.3)	-		-	1 (3.3)	
PSC	6 (15.0)	1 (25.0)		3 (9.4)	1 (7.7)		-	1 (3.3)	
HBV cirrhosis	-	-		-	-		-	1 (3.3)	
HCV cirrhosis	1 (2.5)	-		3 (9.4)	-		-	1 (3.3)	
Autoimmune cirrhosis	1 (2.5)	-		-	-		1 (6.3)	-	
PBC	1 (2.5)	-		1 (3.1)	-		-	-	
NASH	1 (2.5)	-		1 (3.1)	-		-	-	
Metabolic disease	1 (2.5)	-		3 (9.4)	4 (30.8)		-	5 (16.7)	
Polycystic disease	1 (2.5)	1 (25.0)		-	5 (38.5)		1 (6.3)	17 (56.7)	
Others	5 (12.5)	1 (25.0)		1 (3.1)	1 (7.7)		3 (18.8)	2 (6.7)	
MELD score	23 (18-32)	15 (14-17)	0.048	37 (26-40)	21 (17-25)	0.001	40 (36-40)	21 (21-22)	<0.001
Indication for KT			-			-			-
Polycystic disease		1 (25.0)			5 (38.5)			16 (53.3)	
Metabolic disease		-			1 (7.7)			4 (13.3)	
Autoimmune disease		2 (50.0)			-			-	
Glomerulonephritis		-			-			3 (10.0)	
Others		1 (25.0)			7 (53.8)			7 (23.3)	

Data are presented as median (interquartile range) or as number (percentage).
SLKT, simultaneous liver-kidney transplantation; DBD, donation after brain death; DCD, donation after circulatory death; HBV, hepatitis B virus; HCV, hepatitis C virus; KT, kidney transplantation; LT, liver transplantation; LTA, liver transplantation alone; MELD, model for end-stage liver disease; NASH, nonalcoholic steatohepatitis; PBC, primary biliary cholangitis; PSC, primary sclerosing cholangitis; RRT, renal replacement therapy.

Table 3. Cause of graft failure in LTA and SLKT patients stratified by pretransplant renal function

	Stage 3b		Stage 4		Stage 5 or RRT	
	LTA (n=40)	SLKT (n=4)	LTA (n=32)	SLKT (n=13)	LTA (n=16)	SLKT (n=30)
Cause of liver graft failure						
Death with functioning graft	3 (7.5)	-	2 (6.3)	-	1 (6.3)	3 (10.0)
Acute rejection	1 (2.5)	-	-	-	-	-
Chronic rejection	1 (2.5)	-	1 (3.1)	-	1 (6.3)	-
Primary nonfunction	1 (2.5)	-	2 (6.3)	1 (7.7)	2 (12.5)	1 (3.3)
Infection	1 (2.5)	-	3 (9.4)	-	2 (12.5)	1 (3.3)
Recurrent disease	1 (2.5)	-	-	-	-	1 (3.3)
Nonanastomotic biliary stricture	3 (7.5)	-	-	-	-	-
Hemorrhage	-	-	1 (3.1)	-	-	-
Thrombosis	-	-	1 (3.1)	1 (7.7)	-	2 (6.7)
De novo malignancy	-	-	1 (3.1)	-	-	1 (3.3)
Other	2 (5.0)	-	-	1 (7.7)	2 (12.5)	1 (3.3)
Cause of kidney graft failure						
Death with functioning graft		1 (25.0)		2 (15.4)		7 (23.3)
Primary nonfunction		-		-		1 (3.3)
Recurrent disease		-		-		1 (3.3)
Thrombosis		-		1 (7.7)		-
Other		-		1 (7.7)		3 (10.0)

LTA, liver transplantation alone; SLKT, simultaneous liver-kidney transplantation; RRT, renal replacement therapy.



Chapter 9

Simultaneous liver-kidney versus liver transplantation categorized by pretransplant eGFR: Impact of the 2017 OPTN policy

Yitian Fang[*], Sarah Bouari[*], Jacqueline van de Wetering, Caroline M. den Hoed, Ron W.F. de Bruin, Robert J. Porte, Wojciech G. Polak, Robert C. Minnee

[*] Authors contributed equally

Transplantation, 2026

Abstract

Background Simultaneous liver-kidney transplantation (SLKT) has increased substantially in the United States since adoption of the MELD-based allocation, now comprising 9-10% of liver transplants. The survival benefit of SLKT compared with liver transplantation alone (LTA) remains uncertain.

Methods Using the OPTN/UNOS registry, we analyzed 63,407 adult liver transplants (57,780 LTA; 5,627 SLKT) performed between 2010 and 2019. Patient survival was evaluated across pretransplant eGFR categories and according to transplant era before and after implementation of the 2017 OPTN policy.

Results Among patients with pretransplant eGFR ≥30 ml/min/1.73 m^2, SLKT conferred no survival benefits, and LTA recipients achieved comparable or better long-term outcomes. In contrast, SLKT significantly reduced mortality in patients with advanced renal dysfunction. For eGFR 15-29 ml/min/1.73 m^2, SLKT reduced 1-, 3-, and 5-year mortality by 25%, 15%, and 13%, respectively. For eGFR <15 ml/min/1.73 m^2, SLKT reduced 1-, 3-, 5-, and 10-year mortality by 32%, 24%, 22%, and 17%, respectively. Following implementation of the 2017 OPTN policy and "Safety Net" policies, SLKT procedures declined. The survival advantage of SLKT observed in the pre-policy era was not evident post-policy, with 1.4% of LTA recipients undergoing kidney after liver transplantation under "Safety Net" allocation priority.

Conclusions SLKT is associated with survival benefit in patients with severe renal dysfunction (eGFR <30 ml/min/1.73 m^2). Following implementation of the 2017 OPTN policy, this survival difference was no longer evident, and SLKT procedures were reduced without compromising survival. These findings support a stage-specific allocation strategy incorporating the "Safety Net" framework.

Introduction

Simultaneous liver-kidney transplantation (SLKT) provides a life-saving option for patients with both end-stage liver disease (ESLD) and end-stage renal disease (ESRD).[1] One of the major comorbidities of ESLD is portal hypertension which causes pooling of the portal blood in the splanchnic circulation. This reduces the effective circulating volume and increases the risk of renal dysfunction and acute kidney injury (AKI).[2] Patients with ESLD and decompensated cirrhosis are further at risk of developing chronic kidney disease (CKD) due to hepatorenal syndrome, hypoperfusion, parenchymal renal disease, and drug-induced nephrotoxicity.[3, 4]

SLKT has become the most common multiorgan transplantation in the United States, as classified by United Network for Organ Sharing (UNOS). It has been performed increasingly since the Organ Procurement and Transplant Network (OPTN) adopted the Model for End-stage Liver Disease (MELD) scoring system for organ allocation in 2002.[5, 6] Since impaired renal function contributes to higher MELD score, patients with concomitant renal injury are more likely to be prioritized for liver transplantation, thereby contributing to the rising frequency of SLKT procedures. In 1998, only 23 SLKTs were performed, accounting for 1.3% of all deceased donor liver transplants. However, the total number of SLKTs has now reached 700 per year, making approximately 9-10% of deceased liver transplants in the US.[7, 8]

Despite the steady increase, the limited supply of donor organs remains a challenge for both SLKT and single-organ transplants. Moreover, recent evidence suggests that SLKT does not fully mitigate the negative impact of pretransplant CKD on long-term survival, as systemic consequences of CKD, such as cardiovascular disease, metabolic complications, and frailty may be irreversible.[9] These concerns prompted the OPTN to restrict eligibility for SLKT in 2017.[6, 8, 10] Meanwhile, the new policy "Safety Net" was introduced to prioritize kidney allocation for patients who have undergone liver transplantation alone (LTA) but still rely on renal replacement therapy or exhibit persistent renal failure within one year after liver transplantation.[11, 12]

In the context of organ shortage and increasingly restrictive eligibility criteria, it remains unclear whether SLKT confers a survival advantage over LTA, and which patient

populations benefit the most. Moreover, the impact of the 2017 OPTN policy on survival outcomes among patients with renal dysfunction of varying severity remains inadequately characterized. To address this, we analyzed the national UNOS/OPTN registry data covering all deceased-donor LTA and SLKT procedures performed between 2010 and 2019. Our study aimed to clarify whether SLKT provides a survival benefit compared with LTA and to assess how the 2017 OPTN policy and "Safety Net" have influenced survival outcomes.

Methods

Study Population

This retrospective cohort study was conducted in accordance with the Strengthening the Reporting of Observational Studies in Epidemiology (STROBE) reporting guidelines and used data from UNOS/OPTN deceased donor registry. Institutional review board approval was waived because the study used de-identified, publicly available registry data in compliance with the UNOS data use agreement.

All adult recipients (≥18 years) deceased-donor liver transplantation performed in the United States between January 1, 2010, and December 31, 2019, were included. Patients with incomplete follow-up data were excluded. The remaining cohort was categorized according to transplant type as LTA or SLKT.

Renal Function Assessment

Pre- and posttransplant renal function were assessed using estimated glomerular filtration rate (eGFR), calculated with the 2021 Chronic Kidney Disease Epidemiology Collaboration (CKD-EPI) equation.[13] Pretransplant eGFR was derived from the most recent serum creatinine measurement available prior to transplantation. Patients receiving chronic dialysis before transplantation (defined as dialysis ≥3 months) were classified in the eGFR <15 ml/min/1.73 m^2 category to reflect end-stage renal dysfunction.

Data Collection

Recipient demographics and clinical characteristics were extracted from the UNOS/OPTN registry, including age, sex, body mass index (BMI), ethnicity, underlying liver and kidney disease, pretransplant renal function, laboratory MELD score, waiting list time, and transplant year. Donor variables included type (donation after brain death, DBD, or donation after circulatory death, DCD), donor age, and liver/kidney cold ischemia time.

Study Outcomes

The primary outcome was patient survival. Secondary outcomes included death-censored liver/kidney graft survival and posttransplant eGFR. Death-censored graft survival was defined as graft loss excluding patient death with a functioning graft. Posttransplant eGFR was assessed annually up to 10 years following transplant.

Statistical Analysis

Continuous variables were reported as medians with interquartile ranges (IQRs), and categorical variables as numbers with percentages. Baseline characteristics were compared using the Wilcoxon rank-sum test or chi-squared test, as appropriate. Kaplan-Meier curves with log-rank tests were used to evaluate patient and graft survival across groups, stratified by pretransplant eGFR. Cox proportional hazards models were used to evaluate the impact of SLKT on patient survival, adjusting for transplant period, recipient age, sex, ethnicity, underlying liver disease, donor age, donor type and cold ischemia time of liver graft as covariates, and tested using Schoenfeld residuals (**Table S1**, **Figure S1**).

To assess the impact of the 2017 OPTN policy change, patients with pretransplant eGFR <45 ml/min/1.73 m^2, those most affected by revised SLKT eligibility criteria, were stratified into two eras based on transplant date: pre-policy (January 1, 2010-August 9, 2017) and post-policy (August 10, 2017-December 31, 2019). Given the shorter follow-up in the post-policy cohort, survival analyses focused on 1-, 3, and 5-year outcomes. P-value <0.05 was considered statistically significant. Data processing, statistical analysis and data visualization were conducted using R (version 4.2.2).

Results



Figure 1. Annual transplant numbers and proportions of liver transplant alone (LTA) and simultaneous liver-kidney transplantation (SLKT) in the United States, 2010-2019.

Between 2010 and 2019, the UNOS/OPTN registry recorded a total of 63,407 deceased donor transplants, including 57,780 LTAs and 5,627 SLKTs, including 1,609 SLKTs after the 2017 OPTN policy implementation (August 10, 2017). Patients were followed up for a median of 5 years (IQR: 2.8-7.8) after transplantation. The annual number of LTA increased steadily over the past decade. The proportion of SLKT grew from 6.9% of total deceased donor liver transplants in 2010 to 10.3% in 2016, and dropped to 9% in 2019 after the 2017 OPTN policy restricted SLKT eligibility (**Figure 1**).

Baseline Characteristics

Baseline characteristics are summarized in **Table 1** and **Table S2**. SLKT recipients were slightly older (median 58 vs. 57 years, p<0.001), less frequently male (62.7% vs. 66.5%, p<0.001), and had lower BMI (median 26.7 vs. 28.1 kg/m², p<0.001). Ethnic distribution also differed between groups, with SLKT recipients more likely to be Hispanic (17.1% vs. 14.1%) or Black (15.1% vs. 8.9%), whereas White patients predominated in both groups (62.7% vs. 71.0%) (p<0.001). As expected, SLKT recipients presented lower pretransplant eGFR (18 vs. 68 mL/min/1.73 m², p<0.001) and higher MELD scores (29 vs. 21, p<0.001). DCD donors were less common in SLKT than LTA (4.8% vs. 6.5%, p<0.001).

Table 2 shows that the majority of LTA recipients had preserved renal function prior to transplantation, with 29.5% having a pretransplant eGFR ≥90 ml/min/1.73 m^2 and 29% having an eGFR of 60-89 ml/min/1.73 m^2, while only 3.6% were classified as having a pretransplant eGFR <15 ml/min/1.73 m^2. In contrast, SLKT recipients predominantly presented with advanced renal dysfunction, with 36.1% having an eGFR 15-29 ml/min/1.73

m^2 and 38.9% having an eGFR <15 ml/min/1.73 m^2, while a minority were in the early stages (2% with eGFR ≥90 and 3.7% with eGFR 60-89 ml/min/1.73 m^2).

Patient Survival

Patient survival stratified by pretransplant eGFR is shown in **Figure 2**. Among patients with preserved or mildly impaired renal function (eGFR ≥90, 60-89, and 45-59 ml/min/1.73 m^2), posttransplant survival following LTA was significantly higher than SLKT (p<0.001, p<0.001, and p=0.002, respectively; **Figure 2A-C**). In patients with pretransplant eGFR 30-44 ml/min/1.73 m^2, survival curves were similar (1-, 3-, 5-, and 10-year survival: 88.8%, 83.9%, 79.5%, and 70.4% for LTA vs. 90.5%, 84.2%, 80.5%, and 72.9% for SLKT, p=0.494; **Figure 2D**). In contrast, among patients with pretransplant eGFR 15-29 ml/min/1.73 m^2, survival curves favored SLKT during early follow-up but converged over time, with crossing observed at approximately 7.7 years posttransplant. One-, 3-, 5-, and 10-year survival was 88%, 82.2%, 78%, and 70.3% for LTA compared with 90.8%, 84.6%, 80.4%, and 68.8% for SLKT (p=0.245; **Figure 2E**). For patients with pretransplant eGFR <15 ml/min/1.73 m^2, SLKT provided significantly improved survival compared with LTA (1-, 3-, 5-, and 10-year survival: 85.8%, 80.6%, 76.6%, and 66% for LTA vs. 90.5%, 85.2%, 81.6%, and 69.9% for SLKT, p<0.001; **Figure 2F**).

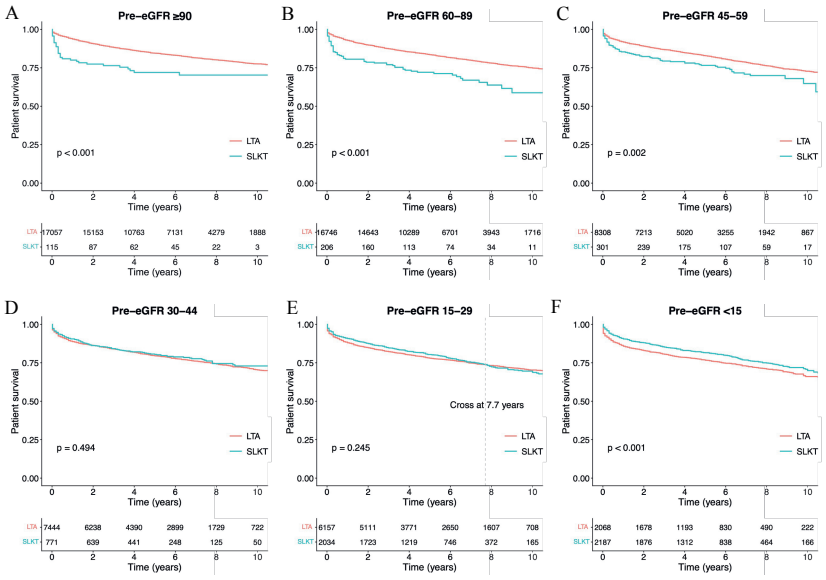


Figure 2. Patient survival after liver transplant alone (LTA) and simultaneous liver-kidney transplantation (SLKT) stratified by pretransplant eGFR.

Table 1. Baseline characteristics of LTA and SLKT recipients

	LTA (n=57780)	SLKT (n=5627)	p value
Age (year)	57 (50-63)	58 (51-63)	<0.001
Sex, male	38408 (66.5)	3528 (62.7)	<0.001
BMI (kg/m^2)	28.1 (24.5-32.4)	26.7 (23.3-31.2)	<0.001
Ethnicity			<0.001
White	41054 (71.0)	3526 (62.7)	
Hispanic	8167 (14.1)	964 (17.1)	
Black	5129 (8.9)	851 (15.1)	
Asian	2526 (4.4)	194 (3.5)	
Others	904 (1.6)	92 (1.6)	
MELD score	21 (13-31)	29 (23-36)	<0.001
Pre-eGFR (ml/min/1.73 m^2)	68 (42-96)	18 (11-29)	<0.001
Donor			<0.001
DBD	53997 (93.5)	5355 (95.2)	
DCD	3783 (6.5)	272 (4.8)	
Liver transplant			
Indication	31262 (54.1)	3892 (69.2)	<0.001
Liver cirrhosis	14977 (25.9)	520 (9.2)	
Hepatocellular carcinoma	4026 (7.0)	225 (4.0)	
Cholestatic liver disease	2280 (3.9)	83 (1.5)	
Acute liver failure	1486 (2.6)	179 (3.2)	
Retransplant	2279 (3.9)	354 (6.3)	
Metabolic disease	209 (0.4)	281 (5.0)	
Polycystic liver disease	1261 (2.2)	93 (1.6)	
Others			
Waiting list time (day)	89 (16-291)	72 (17-261)	0.004
Cold ischemia time (hour)	6.3 (5-8)	6.2 (5-8)	<0.001
Kidney transplant			
Indication			-
Hepatorenal syndrome	-	2526 (44.9)	
Diabetic kidney disease	-	1084 (19.3)	
Glomerulonephritis	-	392 (7.0)	
Interstitial kidney disease	-	355 (6.3)	
Hypertensive kidney disease	-	397 (7.1)	
Polycystic kidney disease	-	310 (5.5)	
Retransplant	-	124 (2.2)	
Metabolic disease	-	98 (1.7)	
Malignancy	-	14 (0.2)	
Others	-	327 (5.8)	
Waiting list time (day)	-	34 (8-150)	-
Cold ischemia time (hour)	-	10.3 (8-14)	-

Data are presented as median (interquartile range) or as number (percentage).
BMI, body mass index; DBD, donation after brain death; DCD, donation after circulatory death; LTA, liver transplant alone; MELD, Model for End-stage Liver Disease; Pre-eGFR, pretransplant estimated glomerular filtration rate; SLKT, simultaneous liver kidney transplant.

Table 2. Pretransplant eGFR distribution

Pre-eGFR (ml/min/1.73 m^2)	LTA (n=57780)	SLKT* (n=5627)
≥90	17057 (29.5)	115 (2.0)
60-89	16746 (29.0)	206 (3.7)
45-59	8308 (14.4)	301 (5.3)
30-44	7444 (12.9)	771 (13.7)
15-29	6157 (10.6)	2034 (36.1)
<15	2068 (3.6)	2187 (38.9)

* 13 (0.2%) missing data.
Pre-eGFR, pretransplant estimated glomerular filtration rate; LTA, liver transplant alone; SLKT, simultaneous liver kidney transplant.

Death-censored Graft Survival

Death-censored liver survival is presented in Figure S2. For patients with pretransplant eGFR ≥90, 60-89, 45-59, and 30-44 ml/min/1.73 m^2, liver survival did not differ significantly between LTA and SLKT (p=0.196, p=0.821, p=0.335, and p=0.423, respectively; **Figure S2A-D**). In contrast, SLKT was associated with significantly improved liver survival in patients with pretransplant eGFR 15-29 ml/min/1.73 m^2, 1-, 3-, 5-, and 10-year graft survival was 95.7%, 94.1%, 93%, and 92% for LTA versus 97.3%, 96.3%, 95.6%, and 94.1% for SLKT (p<0.001; **Figure S2E**). Similarly, in patients with pretransplant eGFR <15 ml/min/1.73 m^2, liver survival was significantly higher after SLKT than LTA. One-, 3-, 5-, and 10-year survival was 95.5%, 94.6%, 93.7%, and 91.1% for LTA versus 97.2%, 96.1%, 95.3%, and 92.7% for SLKT (p=0.028; **Figure S2F**).

Death-censored kidney survival was excellent overall in SLKT recipients, although modest differences were observed across pretransplant eGFR strata (p=0.049; **Figure S3**). At 1, 3, 5, and 10 years posttransplant, kidney survival ranged from 93.8 to 96.7%, 91.2 to 95.1%, 88 to 92.9%, and 83.8 to 88.8%, respectively, across all pretransplant eGFR categories.

Posttransplant Renal Function

Among patients remaining under follow-up at each time point, completeness of posttransplant renal function data was 95.5% at 6 months and 93.4% at 1 year, gradually declining to 76.7% at 5 years and 43.7% at 10 years (**Table S3**).

Posttransplant renal function is shown in **Figure S4**. Posttransplant renal function differed between groups across baseline eGFR strata. Among patients with baseline eGFR ≥90 ml/min/1.73m^2, eGFR values were slightly higher in the LTA group throughout follow-up. In contrast, in patients with pre-transplant eGFR <60 ml/min/1.73m^2, SLKT recipients demonstrated consistently higher median eGFR values compared with LTA recipients during long-term follow-up, with median differences of 7-12 ml/min/1.73m^2. The most pronounced separation was observed in patients with severely impaired renal function (eGFR <30 ml/min/1.73m^2).

Stage- and Time-dependent Survival Impact of SLKT versus LTA

We assessed the independent effect of SLKT versus LTA with cumulative 1-, 3-, 5-, and 10-year patient survival among patients with pretransplant eGFR <60 ml/min/1.73 m^2 using multivariable Cox regression models.

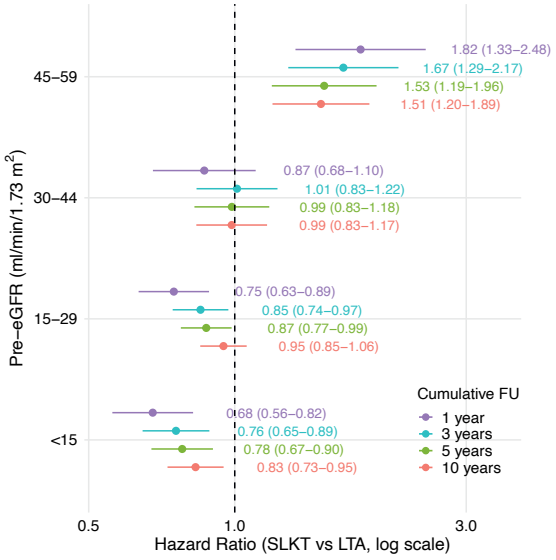


Figure 3. Multivariable Cox regression forest plot comparing patient survival after SLKT versus LTA stratified by pretransplant eGFR. Hazard ratios are adjusted for transplant period, recipient age, sex, ethnicity, underlying liver disease, donor age, donor type and liver graft cold ischemia time.

As shown in **Figure 3**, for patients with pretransplant eGFR 45-59 ml/min/1.73 m^2, SLKT was consistently associated with a significantly higher risk of mortality compared with LTA. Hazard ratios for cumulative mortality were 1.82 (95% CI 1.33-2.48, p<0.001) at 1 year, 1.67 (95% CI 1.29-2.17, p<0.001) at 3 years, 1.53 (95% CI 1.19-1.96, p<0.001) at 5 years, and 1.51 (95% CI 1.20-1.89, p<0.001) at 10 years. In patients with pretransplant eGFR 30-44 ml/min/1.73 m^2, no significant

differences in cumulative mortality were observed between SLKT and LTA at 1, 3, 5, or 10 years (p=0.244, p=0.911, p=0.864, and p=0.837, respectively). In contrast, for patients with pretransplant eGFR 15-29 ml/min/1.73 m^2, SLKT reduced cumulative mortality by 25% at 1 year (HR 0.75, 95% CI 0.63-0.89, p<0.001), 15% at 3 years (HR 0.85, 95% CI 0.74-0.97, p=0.017), and 13% at 5 years (HR 0.87, 95% CI 0.77-0.99, p=0.028), respectively, whereas no significant survival difference was observed at 10 years (p=0.333). For patients with pretransplant eGFR <15 ml/min/1.73 m^2, SLKT conferred a consistent survival benefit throughout the 10-year follow-up period. Compared with LTA, cumulative mortality was reduced by 32% at 1 year (HR 0.68, 95% CI 0.56-0.82, p<0.001), 24% at 3 years (HR 0.76, 95% CI 0.65-0.89, p<0.001), 22% at 5 years (HR 0.78, 95% CI 0.67-0.90, p<0.001), and 17% at 10 years (HR 0.83, 95% CI 0.73-0.95, p=0.004).

Impact of the 2017 OPTN Policy on Transplant Practice and Survival

As shown in **Figure 4**, implementation of the 2017 OPTN policy was associated with modest shifts in SLKT procedures across pretransplant eGFR strata. Compared with the pre-policy era, the proportion of SLKT recipients with preserved or mildly impaired renal function (pretransplant eGFR ⩾45 ml/min/1.73 m^2) decreased by 0.7% in the post-policy era. In contrast, the proportion of SLKT recipients with pretransplant eGFR <15 ml/min/1.73 m^2 increased by 0.5%. Smaller shifts were observed in intermediate strata, with a 0.4% increase among patients with eGFR 30-44 ml/min/1.73 m^2 and a 0.3% decrease among those with eGFR 15-29 ml/min/1.73 m^2.

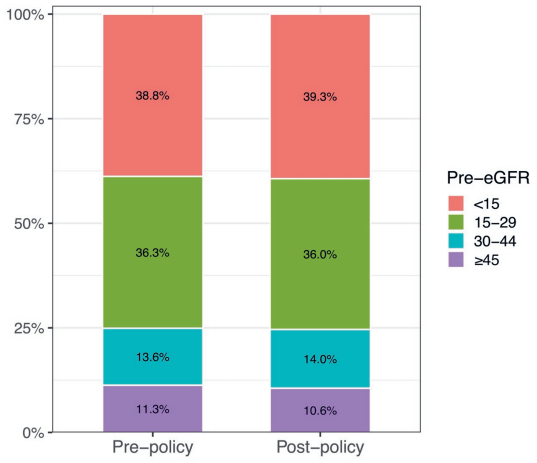


Figure 4. Distribution of SLKT stratified by pretransplant eGFR before and after implementation of the 2017 OPTN policy.

We further assessed the impact of OPTN policy change on patient survival among recipients with pretransplant eGFR <45 ml/min/1.73 m^2, the population most affected by the more stringent SLKT eligibility criteria (**Figure 5**). Patient survival following LTA and

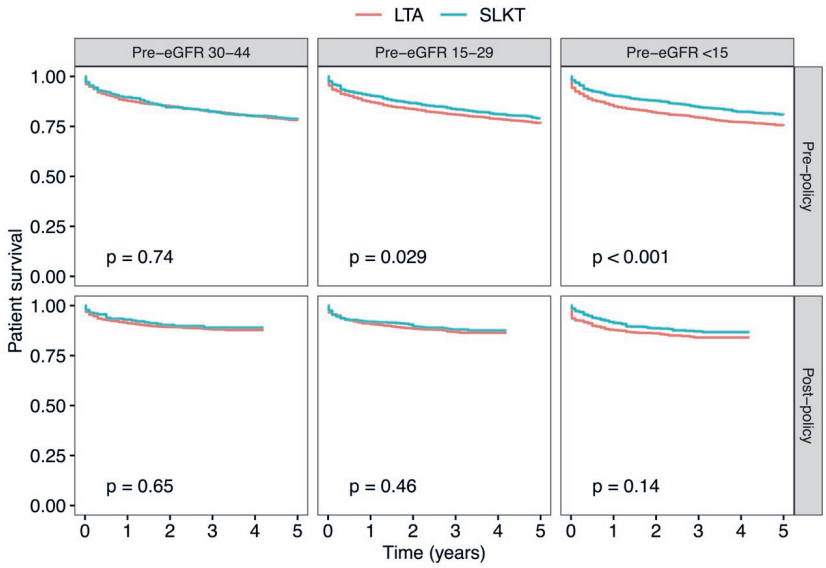


Figure 5. Comparison of patient survival after LTA versus SLKT before and after implementation of the 2017 OPTN policy.

SLKT was analyzed separately for the pre-policy and post-policy eras. Among patients transplanted with pretransplant eGFR 30-44 ml/min/1.73 m^2, no significant survival differences were observed between SLKT and LTA in either the pre-policy or post-policy periods (p=0.74 and p=0.65, respectively). In contrast, in the pre-policy era, SLKT was associated with a significant survival advantage among patients with more advanced renal dysfunction. Specifically, for patients with pretransplant eGFR 15-29 ml/min/1.73 m^2, 1-, 3-, and 5-year survival was 90.3%, 83.5%, and 79.1% after SLKT compared with 87.1%, 80.9%, and 76.5% after LTA (p=0.029). In patients with pretransplant eGFR <15 ml/min/1.73 m^2, 1-, 3-, and 5-year survival was 90.2%, 84.6%, and 80.8% after SLKT versus 85.1%, 79.4%, and 75.3% after LTA (p<0.001). However, after the revised OPTN policy implementation, these survival differences were no longer significant. In the post-policy era, patient survival did not differ significantly between SLKT and LTA among recipients with pretransplant eGFR 15-29 ml/min/1.73 m^2 or <15 ml/min/1.73 m^2 during the available follow-up period (p=0.46 and p=0.14, respectively).

Notably, in the post-policy era, 221 kidney after liver transplantation (KALT) procedures (1.4% of all LTAs) were recorded under the “Safety Net” allocation priority within one year post-LTA.

Discussion

Using the OPTN/UNOS national registry, we systematically compared outcomes of SLKT and LTA across strata of pretransplant renal function. Our findings demonstrate a clear stage- and time-dependent survival effect of SLKT. Among patients with pretransplant eGFR ≥30 ml/min/1.73 m^2, SLKT did not confer a survival advantage over LTA; instead, recipients undergoing LTA achieved comparable or better long-term survival. In contrast, SLKT was associated with significantly improved survival among patients with advanced renal dysfunction (pretransplant eGFR <30 ml/min/1.73 m^2), reducing 1-, 3-, and 5-year mortality by 25%, 15%, and 13% in those with eGFR 15-29 ml/min/1.73 m^2, and 32%, 24%, and 22% in those with eGFR <15 ml/min/1.73 m^2, respectively. This survival benefit attenuated after approximately 7.7 years posttransplant in patients with eGFR 15-29 ml/min/1.73 m^2, whereas a sustained benefit was observed through 10 years among those with eGFR <15 ml/min/1.73 m^2.

These findings extend prior evidence regarding the comparative effectiveness of SLKT and LTA in patients with renal dysfunction. In our previous systematic review and meta-analysis, SLKT recipients demonstrated improved liver graft survival compared with LTA recipients, despite comparable overall patient survival, suggesting potential benefit in selected populations.[14] However, limited studies have been able to identify patients of which extents of renal dysfunction can benefit from SLKT. Analyses from the UK national transplant registry reported that only patients dependent on renal replacement therapy experienced survival benefits from SLKT, with 5-year survival of 90.6% versus 71% following LTA.[15] Similarly, data from the Dutch Organ Transplantation Registry demonstrated improved survival with SLKT in patients with CKD stage 5 or receiving dialysis, with 5-year survival of 80.8% compared with 51.7% after LTA.[16] Our study refines these findings by demonstrating the stage-specific and time-dependent impact of SLKT, which provides a more granular basis for patient selection and may better align organ allocation with clinical benefit.

The 2017 OPTN policy restricted SLKT eligibility to candidates with sustained eGFR ≤60 ml/min/1.73m² for more than 90 days, and most recent GFR ≤30 mL/min/1.73m² or ongoing dialysis.[17] Meanwhile, the “Safety Net” policy ensures that LTA recipients who develop

persistent renal failure have priority for subsequent KALT.[18, 19] These complementary strategies are intended to balance appropriate dual-organ allocation and optimize kidney utilization given the prolonged deceased donor kidney waiting times (typically over three years).[20] Althuser et al.[19] found that after implementing "Safety Net" policies, the proportion of SLKT cases among total liver transplant recipients decreased from 10.2% to 9.0%, while the number of KALT procedures increased by 65% over 2.5 years. Cheng et al.[21] demonstrated that such policies improved organ utilization and liver transplant outcomes. International experience supports these findings. For example, in the Eurotransplant region, patients who require dialysis after the other organ transplant between 90 and 360 days will receive bonus points for a delayed kidney transplantation.[22, 23]

Consistent with the intent of this policy framework, both the number and proportion of SLKT procedures declined following implementation of the revised eligibility criteria. The survival advantage of SLKT observed among patients with pretransplant eGFR <30 ml/min/1.73 m^2 in the pre-policy era was no longer evident in the post-policy era. Under the more stringent SLKT policy, the proportion of LTA recipients increased by approximately 1%, suggesting that some patients with concurrent renal dysfunction who would previously have undergone SLKT instead received LTA. Despite inclusion of this potentially higher-risk population, post-policy survival remained comparable between LTA and SLKT recipients. This finding reflects recovery of reversible AKI after LTA, and timely KALT through the "Safety Net" priority allocation, which contributed to 1.4% LTA recipients within one year post-liver transplantation. Such findings are in line with the study by Cannon et al.[24] demonstrating that LTA patients with renal dysfunction who are protected by "Safety Net" achieve comparable 1-year survival to those not requiring kidney transplantation, and superior outcomes compared with SLKT listed patients undergoing LTA without subsequent KALT listing. Additionally, survival improved in both SLKT and LTA recipients during the post-policy era compared with the earlier period, likely reflecting broader advances in surgical technique, perioperative care, and posttransplant management rather than policy effects alone.

Several limitations must be addressed. First, pretransplant renal function may have been overestimated in a subset of patients. In patients with advanced cirrhosis, reduced muscle mass and lower serum creatinine levels can lead to overestimation of true renal function

when using creatinine-based CKD-EPI equations.[25] Prior studies have demonstrated that among liver disease patients with measured GFR <30 ml/min/1.73 m^2, CKD-EPI may overestimate true GFR by approximately 8.7 ml/min/1.73 m^2.[26] Accordingly, some patients categorized in this study as having pretransplant eGFR 30-44 ml/min/1.73 m^2 may have had true GFR <30 ml/min/1.73 m^2. In addition, the UNOS dataset does not capture acute dialysis at the time of transplantation. As a result, patients who underwent urgent pretransplant dialysis but subsequently had relatively low recorded serum creatinine may have been misclassified into higher eGFR strata (e.g., ≥60 ml/min/1.73 m^2), which may explain the presence of SLKT in patients with apparently preserved renal function. These factors may have reduced the accuracy of using a single eGFR value for renal function stratification. Importantly, because creatinine-based estimation in cirrhosis generally results in overestimation rather than underestimation of renal dysfunction, misclassification would most likely shift patients with more severe renal impairment into higher eGFR categories. Therefore, the observed survival benefit among patients categorized as eGFR <30 ml/min/1.73 m^2 is unlikely to be inflated and represents a conservative estimate. Nevertheless, future studies incorporating more accurate assessment of renal function in patients with liver disease, such as cystatin C-based equations or the Glomerular Filtration Rate Assessment in Liver Disease (GRAIL) model, are warranted to validate these findings.[26]

In conclusion, SLKT provides a survival benefit in patients with pretransplant eGFR <30 ml/min/1.73 m^2; however, this difference was no longer significant following implementation of the 2017 OPTN policy and "Safety Net" framework. Importantly, the revised policy was associated with reduced SLKT procedures without compromising patient survival, as post-policy LTA recipients achieved comparable outcomes to SLKT recipients. These findings highlight the critical role of pretransplant renal function in guiding organ allocation, supporting SLKT for patients with severe and irreversible renal dysfunction while favoring LTA for those with preserved or moderately impaired renal function, thereby optimizing organ utilization without sacrificing long-term patient survival.

Reference

1. Singal AK, Ong S, Satapathy SK, Kamath PS, Wiesner RH. Simultaneous liver kidney transplantation. Transpl Int. 2019;32(4):343-52.
2. Gines P, Schrier RW. Renal failure in cirrhosis. N Engl J Med. 2009;361(13):1279-90.
3. Tariq R, Singal AK. Management of Hepatorenal Syndrome: A Review. J Clin Transl Hepatol. 2020;8(2):192-9.
4. Ekser B, Goggins WC. Delayed kidney transplantation in combined liver-kidney transplantation. Curr Opin Organ Transplant. 2021;26(2):153-9.
5. Kamath PS, Wiesner RH, Malinchoc M, Kremers W, Therneau TM, Kosberg CL, et al. A model to predict survival in patients with end-stage liver disease. Hepatology. 2001;33(2):464-70.
6. Nadim MK, Sung RS, Davis CL, Andreoni KA, Biggins SW, Danovitch GM, et al. Simultaneous liver-kidney transplantation summit: current state and future directions. Am J Transplant. 2012;12(11):2901-8.
7. Nadim M, Sung, RS., Davis, CL., Andreoni, KA. Simultaneous Liver-Kidney Transplantation Summit: Current State and Future Directions. American Journal of Transplantation. 2012.
8. Ekser B, Contreras AG, Andraus W, Taner T. Current status of combined liver-kidney transplantation. Int J Surg. 2020;82S:149-54.
9. Cullaro G, Verna EC, Lee BP, Lai JC. Chronic Kidney Disease in Liver Transplant Candidates: A Rising Burden Impacting Post-Liver Transplant Outcomes. Liver Transpl. 2020;26(4):498-506.
10. Committee OUKT. Simultaneous Liver Kidney (SLK) Allocation Policy. 2015.
11. Formica RN, Aeder M, Boyle G, Kucheryavaya A, Stewart D, Hirose R, et al. Simultaneous Liver-Kidney Allocation Policy: A Proposal to Optimize Appropriate Utilization of Scarce Resources. Am J Transplant. 2016;16(3):758-66.
12. Asch WS, Bia MJ. New Organ Allocation System for Combined Liver-Kidney Transplants and the Availability of Kidneys for Transplant to Patients with Stage 4-5 CKD. Clin J Am Soc Nephrol. 2017;12(5):848-52.
13. Inker LA, Eneanya ND, Coresh J, Tighiouart H, Wang D, Sang Y, et al. New Creatinine- and Cystatin C-Based Equations to Estimate GFR without Race. N Engl J Med. 2021;385(19):1737-49.
14. Bouari S, Rijkse E, Metselaar HJ, van den Hoogen MWF, JNM IJ, de Jonge J, et al. A comparison between combined liver kidney transplants to liver transplants alone: A systematic review and meta-analysis. Transplant Rev (Orlando). 2021;35(4):100633.
15. Tinti F, Mitterhofer AP, Umbro I, Nightingale P, Inston N, Ghallab M, et al. Combined liver-kidney transplantation versus liver transplant alone based on KDIGO stratification of estimated glomerular filtration rate: data from the United Kingdom Transplant registry - a retrospective cohort study. Transpl Int. 2019;32(9):918-32.
16. Bouari S, Fang Y, van de Wetering J, de Meijer VE, Pol RA, Berger SP, et al. Simultaneous Liver-Kidney Transplantation versus Liver Transplantation in End-Stage Liver Disease Patients with Kidney Dysfunction. Eur Surg Res. 2026;67(1):46-55.
17. Samoylova ML, Wegermann K, Shaw BI, Kesseli SJ, Au S, Park C, et al. The Impact of the 2017 Kidney Allocation Policy Change on Simultaneous Liver-Kidney Utilization and Outcomes. Liver Transpl. 2021;27(8):1106-15.
18. Cullaro G, Verna EC, Emond JC, Orandi BJ, Mohan S, Lai JC. Early Kidney Allograft Failure After Simultaneous Liver-kidney Transplantation: Evidence for Utilization of the Safety Net? Transplantation. 2021;105(4):816-23.
19. Altshuler PJ, Shah AP, Frank AM, Glorioso J, Dang H, Shaheen O, et al. Simultaneous liver kidney allocation policy and the Safety Net: an early examination of utilization and outcomes in the United States. Transpl Int. 2021;34(6):1052-64.
20. Saran R, Li Y, Robinson B, Abbott KC, Agodoa LY, Ayanian J, et al. US Renal Data System 2015 Annual Data Report: Epidemiology of Kidney Disease in the United States. Am J Kidney Dis. 2016;67(3 Suppl 1):Svii, S1-305.
21. Cheng XS, Kim WR, Tan JC, Chertow GM, Goldhaber-Fiebert J. Comparing Simultaneous Liver-Kidney Transplant Strategies: A Modified Cost-Effectiveness Analysis. Transplantation. 2018;102(5):e219-e28.
22. Eurotransplant. Chapter 4 Kidney (ETKAS and ESP) 2025 [Available from: https://www.eurotransplant.org/wp-content/uploads/2025/03/H4-Kidney-2025.2-March-2025.pdf.
23. Bouari S, Polak WG, van de Wetering J, Metselaar HJ, JNM IJ, Minnee RC. Combined liver-kidney transplantation with delayed kidney implantation: A case report. Int J Surg Case Rep. 2023;106:108276.
24. Cannon RM, Goldberg DS, Eckhoff DE, Anderson DJ, Orandi BJ, Locke JE. Early Outcomes With the Liver-kidney Safety Net. Transplantation. 2021;105(6):1261-72.
25. Sherman DS, Fish DN, Teitelbaum I. Assessing renal function in cirrhotic patients: problems and pitfalls. Am J Kidney Dis. 2003;41(2):269-78.

26. Asrani SK, Jennings LW, Trotter JF, Levitsky J, Nadim MK, Kim WR, et al. A Model for Glomerular Filtration Rate Assessment in Liver Disease (GRAIL) in the Presence of Renal Dysfunction. Hepatology. 2019;69(3):1219-30.

Supplementary

Table S1. Univariable Cox regression analysis of recipient, donor, and transplant characteristics associated with posttransplant survival

	HR (95% CI)	p value
LTA	ref	
SLKT	0.997 (0.935-1.063)	0.922
Transplant period		
2010-2012	ref	
2013-2015	0.782 (0.737-0.830)	<0.001
2016-2019	0.600 (0.563-0.639)	<0.001
Age (year)	1.017 (1.015-1.020)	<0.001
Sex		
Female	ref	
Male	1.115 (1.060-1.173)	<0.001
Ethnicity		
White	ref	
Hispanic	0.867 (0.804-0.934)	<0.001
Black	1.214 (1.122-1.314)	<0.001
Asian	0.930 (0.805-1.075)	0.326
Others	1.002 (0.828-1.211)	0.986
Liver transplant indication		
Liver cirrhosis	ref	
Hepatocellular carcinoma	1.292 (1.208-1.382)	<0.001
Cholestatic liver disease	0.768 (0.683-0.863)	<0.001
Acute liver failure	0.896 (0.785-1.022)	0.102
Retransplant	0.716 (0.605-0.847)	<0.001
Metabolic disease	1.664 (1.519-1.822)	<0.001
Polycystic liver disease	0.451 (0.325-0.626)	<0.001
Others	1.395 (1.164-1.673)	<0.001
MELD score		
<15	ref	
15-25	0.937 (0.846-1.038)	0.215
>25	0.954 (0.866-1.051)	0.342
Pre-eGFR (ml/min/1.73m^2)		
45-59	ref	
30-44	1.143 (1.070-1.221)	<0.001
15-29	1.196 (1.120-1.276)	<0.001
<15	1.212 (1.121-1.310)	<0.001
Donor age (year)	1.007 (1.005-1.008)	<0.001
Donor type		
DBD	ref	
DCD	1.117 (1.003-1.243)	0.043
Cold ischemia time (hour)	1.019 (1.010-1.028)	<0.001

DBD, donation after brain death; DCD, donation after circulatory death; LTA, liver transplant alone; MELD, Model for End-stage Liver Disease; Pre-eGFR, pretransplant estimated glomerular filtration rate; SLKT, simultaneous liver kidney transplant.

Table S2. Kidney transplant indication categorized by pretransplant eGFR

Pre-eGFR (ml/min/1.73 m^2)	≥90 (n=146)	60-89 (n=261)	45-59 (n=429)	30-44 (n=1114)	15-29 (n=3035)	<15 (n=3371)
Hepatorenal syndrome	86 (58.9)	145 (55.6)	231 (53.8)	502 (45.1)	1305 (43)	1078 (32)
Diabetic kidney disease	15 (10.3)	29 (11.1)	61 (14.2)	197 (17.7)	566 (18.6)	684 (20.3)
Glomerulonephritis	4 (2.7)	13 (5.0)	27 (6.3)	94 (8.4)	250 (8.2)	333 (9.9)
Interstitial kidney disease	13 (8.9)	31 (11.9)	30 (7.0)	98 (8.8)	273 (9.0)	238 (7.1)
Hypertensive kidney disease	6 (4.1)	10 (3.8)	22 (5.1)	63 (5.7)	217 (7.1)	304 (9.0)
Polycystic kidney disease	2 (1.4)	4 (1.5)	10 (2.3)	34 (3.1)	99 (3.3)	283 (8.4)
Retransplant	5 (3.4)	5 (1.9)	12 (2.8)	22 (2.0)	85 (2.8)	152 (4.5)
Metabolic disease	2 (1.4)	-	3 (0.7)	6 (0.5)	34 (1.1)	99 (2.9)
Malignancy	1 (0.7)	1 (0.4)	1 (0.2)	5 (0.4)	5 (0.2)	6 (0.2)
Others	12 (8.2)	23 (8.8)	32 (7.5)	93 (8.3)	201 (6.6)	194 (5.8)

Pre-eGFR, pretransplant estimated glomerular filtration rate.

Table S3. Risk-set-adjusted completeness of posttransplant eGFR measurements

Follow-up time	Patients at risk	eGFR available	Completeness (%)
6 months	59615	56937	95.5
1 year	58182	54345	93.4
2 years	54773	46392	84.7
3 years	46213	38228	82.7
4 years	38760	30965	79.9
5 years	31765	24371	76.7
6 years	25535	18933	74.1
7 years	19926	14029	70.4
8 years	15075	9837	65.3
9 years	10636	6103	57.4
10 years	6541	2860	43.7

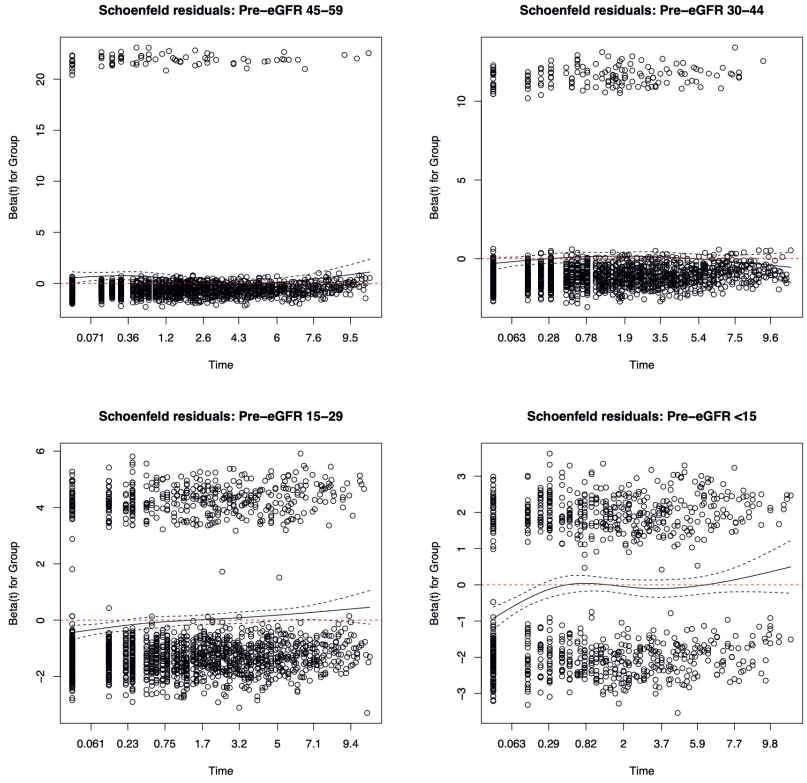


Figure S1. Schoenfeld residual plots for SLKT versus LTA stratified by pretransplant eGFR. The solid line represents a smoothed fit of the residuals over time (with confidence intervals), and the dashed red line indicates zero. A stable, near-horizontal trend around zero suggests that the proportional hazards assumption holds for the variable (SLKT versus LTA) in each pretransplant eGFR subgroup.

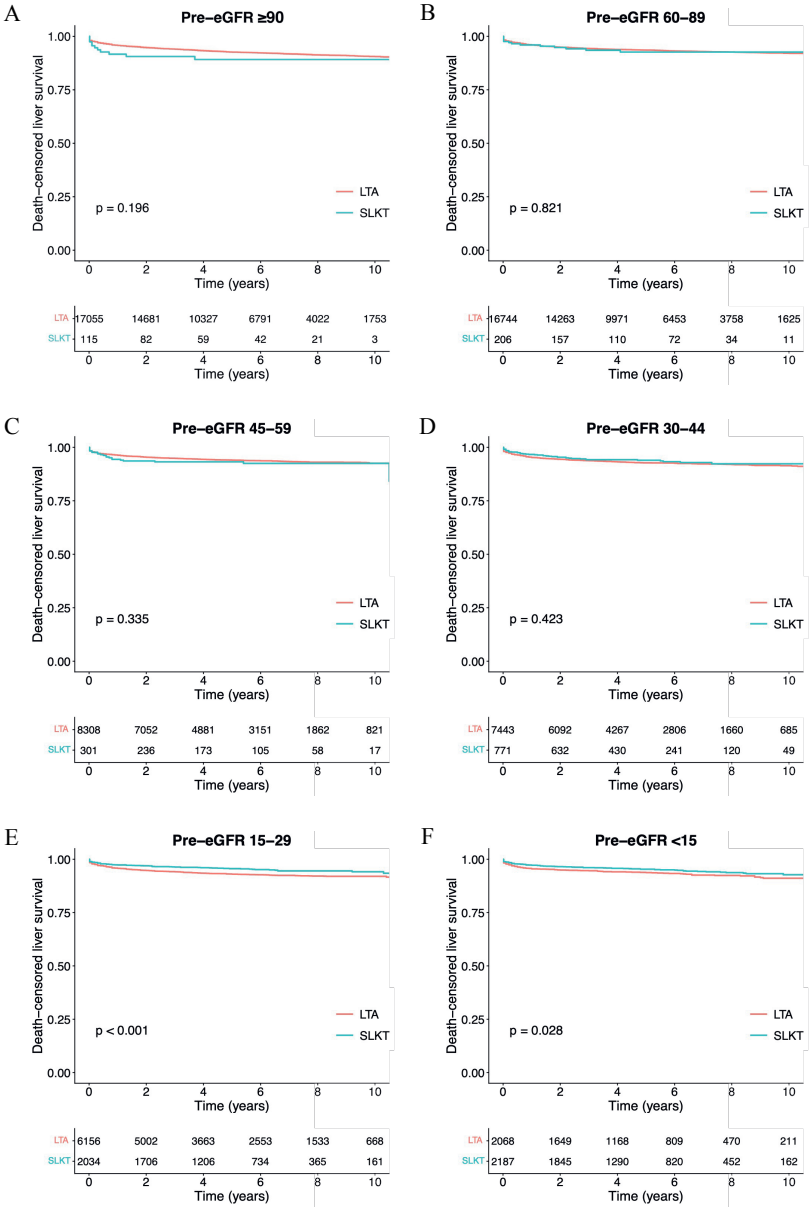


Figure S2. Death-censored liver graft survival after liver transplant alone (LTA) and simultaneous liver-kidney transplantation (SLKT) stratified by pretransplant eGFR.

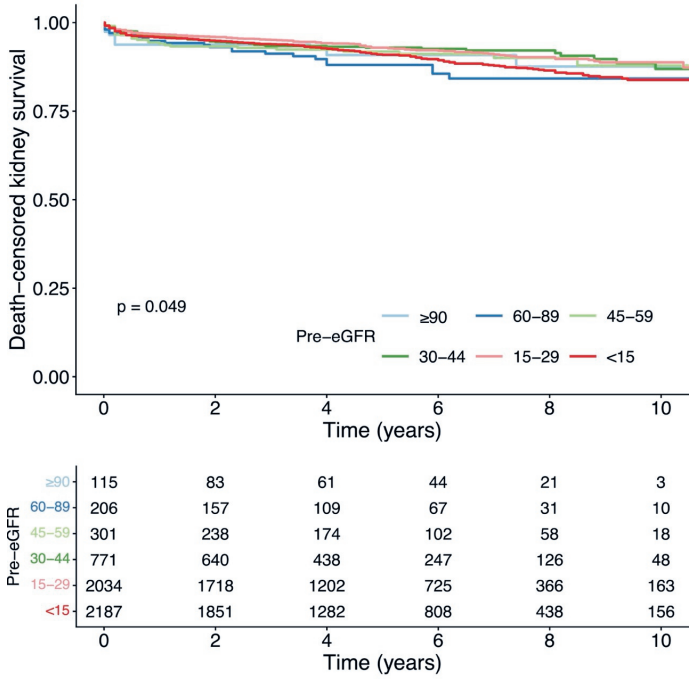


Figure S3. Death-censored kidney graft survival after simultaneous liver-kidney transplantation (SLKT) stratified by pretransplant eGFR.

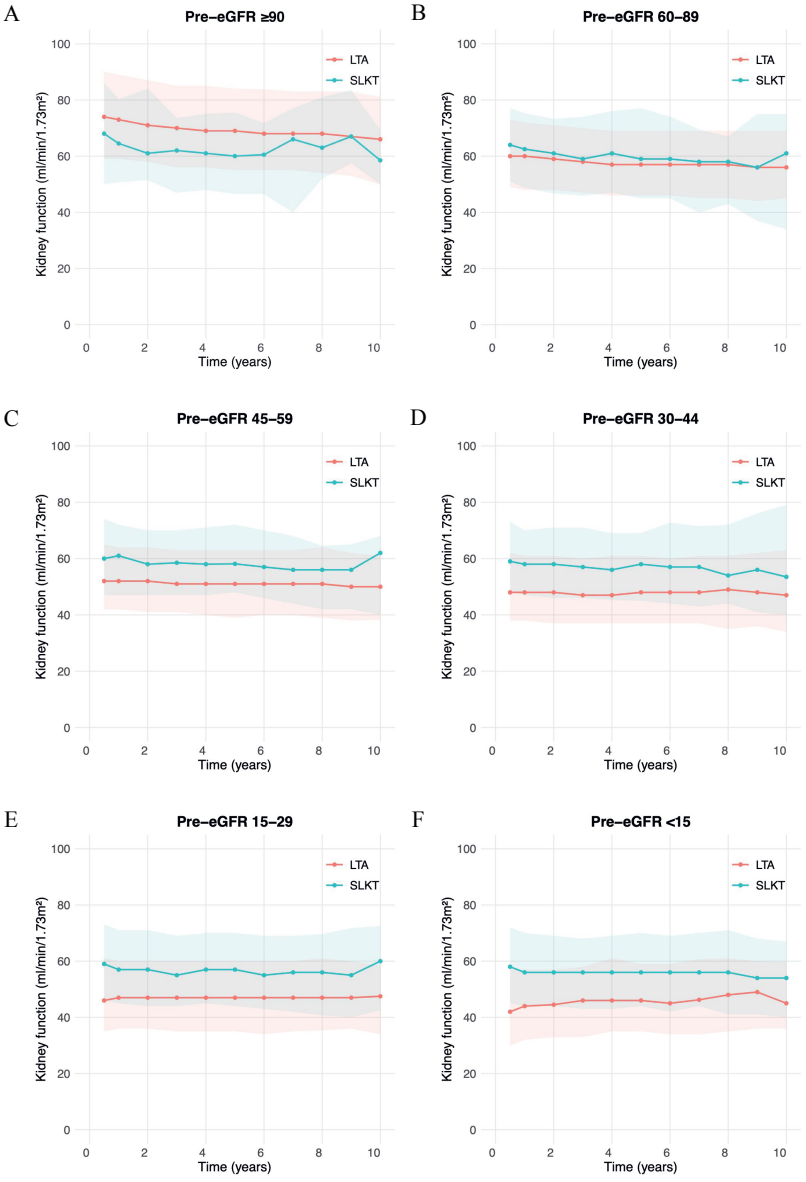
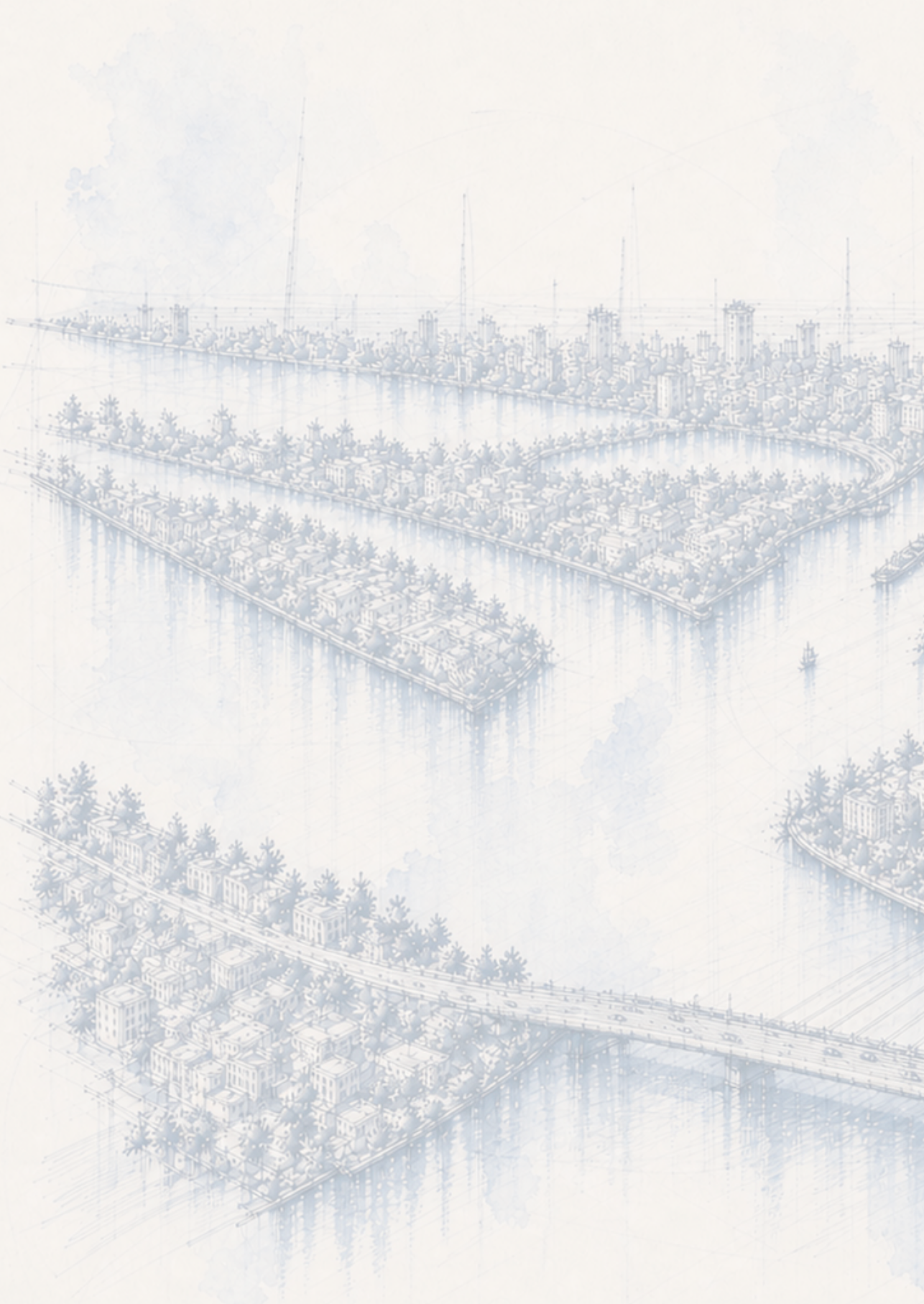


Figure S4. Posttransplant eGFR in LTA and SLKT recipients stratified by pretransplant eGFR.



Chapter 10

Treatment of renal artery aneurysm by ex-situ repair and autotransplantation: a nationwide cohort study

Yitian Fang, Hendrikus J.A.N. Kimenai, Ron W.F. de Bruin, Dorottya K. de Vries, Bart-Jeroen Petri, Michiel C. Warlé, Ignace F.J. Tielliu, Jorinde van Laanen, Mirza M. Idu, Robert A. Pol, Robert C. Minnee, Dutch Kidney Transplant Study Group

European Surgical Research, 2024

Abstract

Introduction Renal artery aneurysm (RAA) is a rare vascular disease with a mortality rate of up to 80% upon rupture. This study aims to investigate the safety and efficacy of ex-situ repair and autotransplantation for endovascularly untreatable RAA.

Methods A retrospective nationwide cohort study was conducted in RAA patients undergoing ex-situ repair and autotransplantation in the Netherlands. Surgical techniques, postoperative complications, and graft outcomes were assessed.

Results Ex-situ repair was performed in 9 patients with 11 RAAs. Eight RAAs were located at the first bifurcation, one on the main trunk, one on the first branch, and one on the second branch. Nephrectomy was performed via laparoscopy (n=7), robotic-assisted laparoscopy (n=1) and laparotomy (n=1). Postoperative complications were recorded in four patients, including bowel obstruction, delirium, pneumonia and hydronephrosis due to double-J dislocation. Median estimated glomerular filtration rate (eGFR) was 83 ml/min/1.73m^2 pretransplant and 88 ml/min/1.73m^2 posttransplant. By an average follow-up of 32 months, two patients had died due to lung adenocarcinoma and stroke, while all autotransplanted kidneys had good patency and remained functional.

Conclusions Ex-situ repair and autotransplantation are safe and feasible for endovascularly untreatable RAA cases. Larger cohorts with longer follow-up periods are necessary to further evaluate the role of this surgical approach.

Introduction

Renal artery aneurysm (RAA) is a rare vascular disease, with an incidence of 0.1% in the general population.[1, 2] Most aneurysms are small, asymptomatic, and diagnosed incidentally during examinations for other purposes.[3] When symptomatic, RAA patients present hypertension, flank pain, hematuria, or urinary collecting system obstruction. Complications of RAA include rupture, distal embolization, infarction, arterial dissection, and renal failure.[2]

The indications for RAA treatment include symptomatic patients, women who are pregnant or of childbearing age, and aneurysms with a diameter greater than 2 cm.[2] Treatment strategies include endovascular and surgical repair, depending on the aneurysm size, morphology, and location. Surgical repair, including in-situ repair and ex-situ repair, is indicated for complex aneurysms or those located at the bifurcation or distal branches. Additionally, nephrectomy remains a treatment option if other approaches fail.

Existing literature comparing endovascular and surgical techniques focus on in-situ repair, although outcomes of ex-situ repair might be superior.[4] Since Gallagher et al.[3] reported the first case series of ex-situ repair and autotransplantation, clinical features and outcomes of this technique have been reported through small case series.[5-8] Herein, we present a nationwide cohort study of 11 ex-situ RAA repairs with autotransplantation in nine patients, including one patient with three concomitant aneurysms.

Methods

A nationwide cohort study was conducted via the Dutch Kidney Transplant Study Group between January 2016 and December 2023. To identify RAA patients who underwent ex-situ repair and autotransplantation, a national survey was conducted across all transplant centers qualified to perform kidney transplantation. Demographics, surgical records and follow-ups were collected from electronic medical records by the operating surgeons.

The decision of ex-situ repair and autotransplantation was made based on the collective expertise of the medical team and patient's willingness. A comprehensive multidisciplinary

meeting was organized to discuss possible treatment strategies, and these options were extensively discussed with the patient.

Primary outcome measure was the success of the procedures, defined by graft patency and renal function preservation. Secondary outcome measures included operative time, hospital stay and postoperative complications, classified according to the Clavien-Dindo classification.

Surgical Techniques

The surgical procedure involves nephrectomy, ex-situ aneurysm repair, and autotransplantation.

Nephrectomy

Nephrectomy was performed using a laparoscopic, robotic-assisted laparoscopic, or laparotomy technique. Laparotomy was performed in a single case where the RAA was in a transplanted kidney in the iliac fossa.

Nephrectomy was performed following the standard procedure for donor nephrectomy according to international guidelines.[9] For robotic-assisted laparoscopic nephrectomy, the da Vinci Xi surgical system was used. Port placement is shown as **Figure 1**. The kidney was extracted using a specimen retrieval bag through the modified Gibson incision, flushed with cold University of Wisconsin (UW) solution and stored on ice for aneurysm repair.

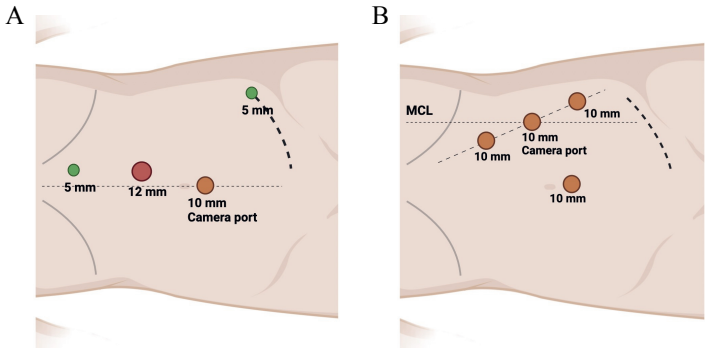


Figure 1. Port placement of (A) laparoscopic nephrectomy and (B) robotic-assisted laparoscopic nephrectomy (left-sided). MCL, midclavicular line.

Ex-situ Repair and Autotransplantation

Various techniques used for the reconstruction of renal arteries were depicted in **Figure 2**. The type of suture most commonly used was 6-0 or 7-0 prolene, depending on the size of the artery or arterial branches. In all cases optical magnification (typically using surgical loupes at 2.5× to 4×) was required to ensure precise anastomosis.

Kidney autotransplantation was performed in heterotopic position through the kidney extraction incision (Gibson incision). For kidneys with multiple arterial branches, a side-to-side anastomosis was performed following an end-to-side anastomosis to the external iliac artery. The choice of technique was thus tailored based on the length and number of the remaining renal arteries and the patient's specific anatomy.

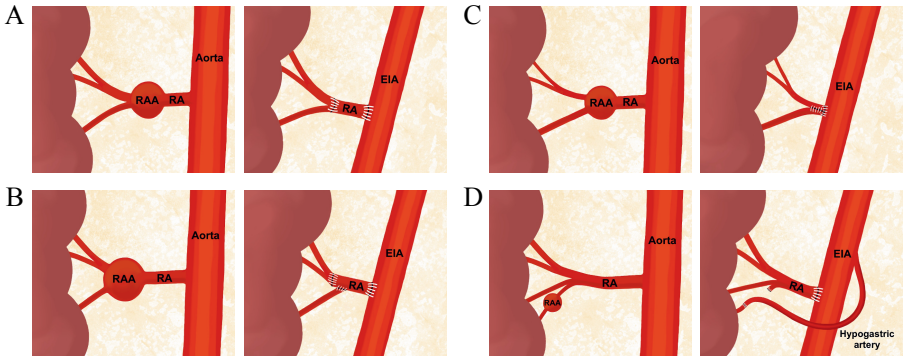


Figure 2. Schematic drawings depicting different RAAs (left) and reconstruction (right). A. For aneurysms involving a single artery, segmental resection and end-to-end anastomosis was performed, provided this could be carried out without tension. B. For aneurysms located in the first bifurcation, the larger arterial branch was anastomosed end-to-end to the main renal artery, and the smaller one was anastomosed end-to-side to the main artery after aneurysmectomy. C. For aneurysms involving two similar-sized arteries, ends of the two vessels were sutured side-to-side to form a co-adaptive patch. D. When the residual artery was of insufficient length after aneurysmectomy, the hypogastric artery was used to bridge the defect via end-to-end anastomosis. EIA, external iliac artery; RA, renal artery; RAA, renal artery aneurysm.

Results

Ex-situ repair was performed in 9 patients (8 female and 1 male) with a median age of 61 years (**Table 1**). Seven patients had additional comorbidities, including hypertension (n=5), aortic valve replacement (n=2), and chronic obstructive pulmonary disease (n=1). Six patients were asymptomatic, with RAAs discovered incidentally by CT scans performed for other conditions. Three patients were symptomatic, presenting with flank pain that

prompted the initial diagnostic CT scan. One patient had a solitary kidney, and another had a history of kidney transplantation. Preoperative blood pressures ranged from 125 to 180 mmHg systolic and 75 to 110 mmHg diastolic. Estimated glomerular filtration rate (eGFR) was 47 ml/min/1.73m^2 in the transplant recipient and 83 ml/min/1.73m^2 (range 70-94) in the other patients.

Table 1. Demographic characteristics of patients with ex-situ renal artery aneurysm

Characteristics	
Age (yr), median (range)	61 (51-68)
Sex, n (%)	
Male	1 (11)
Female	8 (89)
BMI (kg/m^2), median (range)	26 (17-30)
ASA classification, median (range)	2 (1-3)
Symptoms, n (%)	
Asymptomatic	6 (67)
Flank pain	3 (33)
Aneurysm characteristics[a]	
Left, n (%)	7 (64)
Right[b], n (%)	4 (36)
Size (cm), median (range)	2.7 (0.8-7.4)
Location, n (%)	
First bifurcation	8 (73)
Main trunk	1 (9)
First branch	1 (9)
Second branch	1 (9)
Prior treatment, n (%)	
Untreated	8 (89)
Coil embolization	1 (11)

[a] Variables are based on the number of aneurysms.

[b] This variable includes the kidney graft in the right iliac fossa.

RAAs were located on the left side in five cases. One patient had multiple aneurysms, including a large aneurysm with a diameter of 7.4 cm and two smaller ones. The remaining patients had single aneurysms greater than 2 cm. One patient underwent unsuccessful coil embolization before surgical intervention, while the others were untreated before the final treatment.

Most nephrectomies were performed laparoscopically (n=8), with one patient undergoing robotic-assisted nephrectomy. The kidney transplant recipient underwent a transplantectomy through laparotomy prior to ex-situ repair and retransplantation.

The majority of RAAs (73%) were located at the first bifurcation of the renal artery, while the remaining were located in the main trunk (n=1), first branch (n=1), and second branch of the anterior renal artery (n=1). All aneurysms were saccular. After aneurysmectomy, a combined end-to-end and end-to-side arterial anastomosis was performed in four cases. The hypogastric artery was used to bridge the arterial defect in two cases and direct end-to-end anastomosis was performed in two cases. A side-to-side coadaptation was performed for implantation in one case. In the case of aneurysm located in the main trunk, it was in close proximity to the first bifurcation of superior and inferior arterial branches, making endovascular treatment not possible without sacrificing one of the branches.

The median operative time was 5.5 hours (range 3-9), with median warm ischemia time (WIT) of 23 minutes (range 13-33) and estimated blood loss of 300 ml (range 100-550). The median length of hospital stay was 8 days (range 6-85), with the 85-day stay attributed to pneumonia. Four patients had postoperative complications, including postoperative delirium, bowel obstruction, pneumonia (grade II), and hydronephrosis due to double-J dislocation (grade IIIa).

At a mean follow-up of 32 months, postoperative eGFR was 31 ml/min/1.73m^2 in the patient with kidney transplant history. The renal function of other patients was stable, with an average eGFR of 88 ml/min/1.73m^2 (range 63-93). No patient required temporary dialysis. Renal duplex ultrasonography confirmed good arterial patency in all patients. Representative pre- and postoperative CT scans are shown in **Figure 3**. Postoperative blood pressures ranged from 110 to 150 mmHg systolic and 60 to 95 mmHg diastolic. Three patients had an improvement in blood pressure control, with a decrease of 11 to 35 mmHg systolic and 19 to 25 mmHg diastolic. Both asymptomatic and symptomatic patients achieved excellent graft patency. However, asymptomatic patients exhibited better postoperative renal function and a lower frequency of complications. By the end of follow-up, two patients died due to lung adenocarcinoma and stroke, both with a functioning autotransplanted kidney.

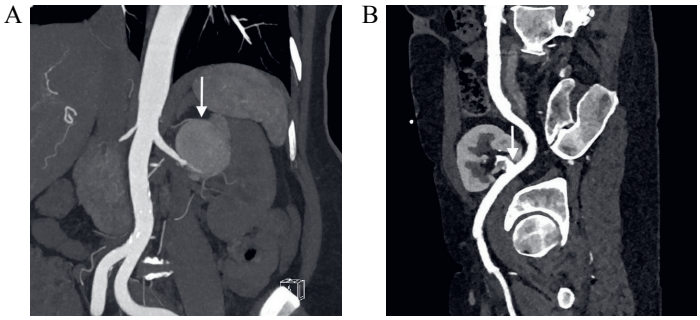


Figure 3. (A) Preoperative computed tomography scan showing a 7.4 cm saccular renal artery aneurysm at the first bifurcation of the left kidney. (B) Postoperative computed tomography scan showing the kidney reimplanted in the right iliac fossa after ex-situ aneurysm repair and arterial reconstruction.

Discussion

In our cohort, RAA predominantly affects individuals in their middle to older age (range 51-68 years) and females (89%). This aligns with existing literature showing a typical presentation in their sixth decade and associated with fibromuscular dysplasia which is more prevalent in females.[2] Additionally, 67% of patients were asymptomatic at diagnosis, which aligns with previous studies reporting symptomatic presentation in 4%-23% of cases. Hypertension is often the primary cardiovascular risk factor, as 56% of patients were observed with hypertension.

Although endovascular RAA repair has gained acceptance for treating proximal aneurysms at the main renal trunk, studies have reported 8-17% of the patients undergoing endovascular repair experienced aneurysm reperfusion, with 4.4% requiring a secondary procedure.[10, 11] In more complex cases, endovascular intervention results in high incidences of postembolization syndrome and segmental renal ischemia. Consequently, in these cases surgical treatment remains the gold standard.

To ensure adequate blood flow, different arterial reconstruction techniques have been applied. Previous studies have reported the use of the saphenous vein or gonadal vein as interposition grafts between the arterial stump and iliac artery.[3, 5, 6] These vein grafts are ease for harvest and flexible. However, due to the inherent structural and functional limitations, vein grafts carry a higher risk of occlusion, intimal hyperplasia and aneurysms

when exposed to arterial pressures.[12] Harvesting the hypogastric artery is more complex and invasive compared to the vein graft, but it provides long-term durability and patency, making it ideal for high-pressure arterial systems. However, the long-term risk of buttock claudication should be monitored.

One patient in our cohort underwent robotic-assisted nephrectomy, which is a promising alternative to traditional laparoscopic surgery. Compared to laparoscopic nephrectomy, robotic-assisted nephrectomy shows similar postoperative complications but shorter hospital stay.[13, 14] For complex vascular anastomoses, robotic surgery has proven superior over traditional laparoscopic surgery as it allows for a more ergonomic approach and recreates the hand-eye coordination that is lost in laparoscopic surgery.[15] For nephrectomy, larger cohort studies are warranted to investigate if robotic-assisted nephrectomy can reduce the morbidity and improve outcome.

The choice between in-situ and ex-situ repair remains open. Recent studies of in-situ RAA repair have reported durations of surgery of 3-6 hours, WIT of 10-60 minutes, and blood loss of 25-400 ml.[15, 16] We reported a longer surgery duration and more blood loss but a shorter WIT. Despite the longer surgery duration, ex-situ repair offers several advantages. Firstly, although intracorporeal transarterial renal hypothermia is performed during in-situ repair,[16, 17] complex cases still require longer WIT. Secondly, extracorporeal flushing with cold preservation solution ensures better protection, while renal cortex remains around 20°C under intracorporeal hypothermic perfusion during in-situ repair.[18] Additionally, the extensive expertise required for in-situ repair limits its widespread adoption.

In our study, all cases involved transection of the ureter. Autotransplantation without transection is another option, in which the renal vessels are anastomosed with the ureter intact.[5, 7, 19] Nephrectomy without ureteral transection avoids the complications related to ureteroneocystostomy. However, resecting the ureter simplifies the graft cooling and arterial reconstruction, as these procedures are conducted on the back table, instead of on the patient's skin during surgery. To our knowledge, no studies to date have compared the clinical outcomes of ex-situ repair with and without ureter transection.

RAA is associated with impaired renal function and hypertension due to renal artery compression, microembolization in the distal renal parenchyma, and hemodynamic changes

from turbulent blood flow in the aneurysm.[20] Our results demonstrated a mild improvement in renal function following ex-situ repair and autotransplantaion. Three out of five patients exhibited improved blood pressure, while two patients had no significant improvement. Such different therapeutic effects are also reported in other studies.[3, 5, 8] Our findings suggest that successful surgical revascularization plays an important role in improving renal hemodynamics. However, for non-renovascular hypertension, the impact of aneurysm repair is limited, consistent with observations from in-situ RAA repair studies.[17]

Another option for RAA patients necessitating nephrectomy is to donate the removed kidney. The study by Ceuppens et al.[21] shows that patients with benign kidney disorders, including RAAs, can successfully donate kidneys as unspecified donors following nephrectomy. Before considering donation, it is important to ensure the individual has sufficient renal function in the remaining kidney and no contraindications to donation. For RAA patients, the presence of multiple arterial aneurysms and the potential risk of aneurysm development in the remaining kidney should be carefully assessed. All ethical and medical considerations must be addressed, and patients should be fully informed about the risks, benefits, and the need for regular post-donation follow-up.

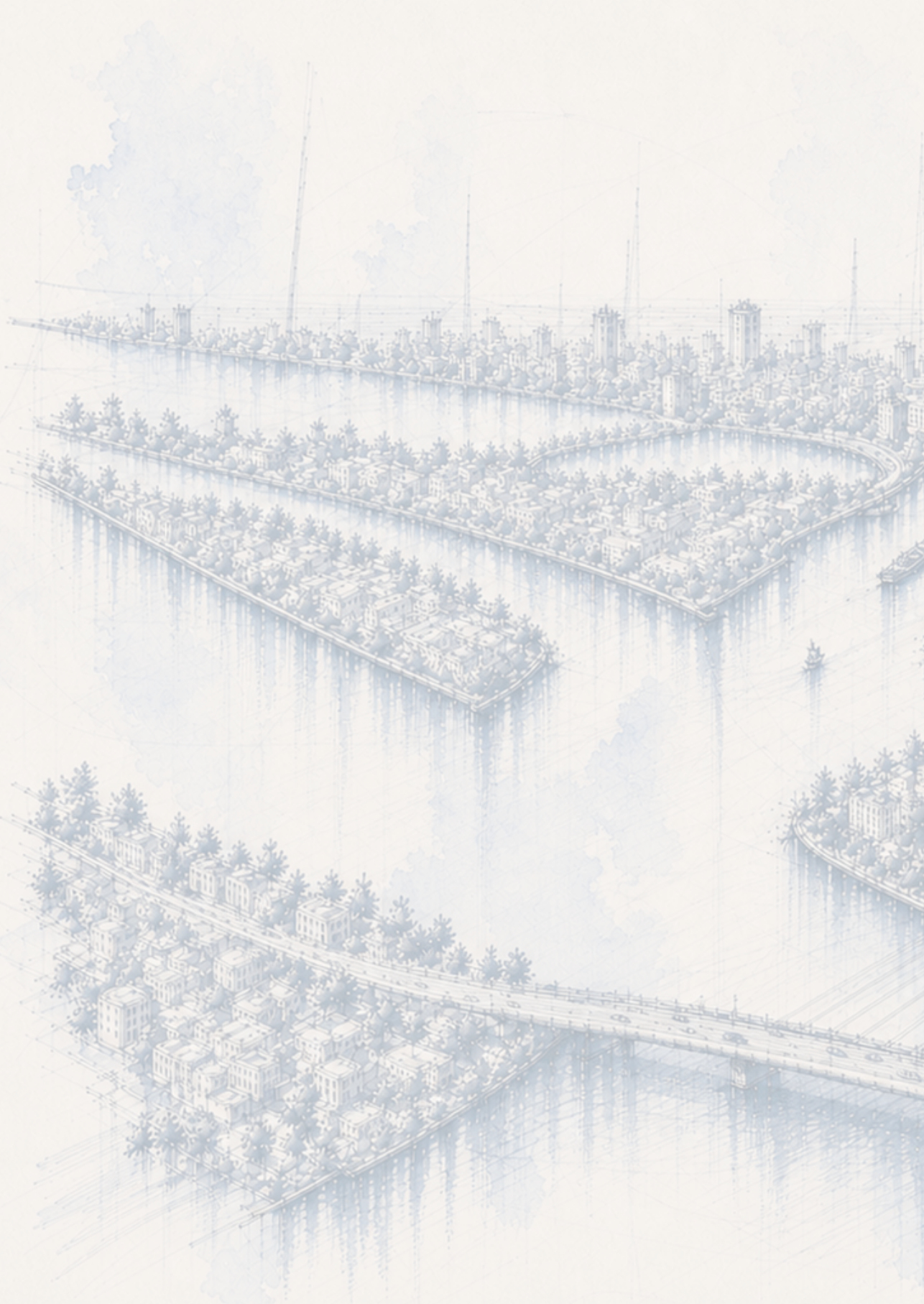
Given the technical complexity and low frequency of ex-situ repair for RAAs, we recommend that these procedures be performed in specialized transplant centers. These centers should have a multidisciplinary team comprising experienced transplant and vascular surgeons, as well as nephrologists. Additionally, we propose conducting such nationwide survey at regular intervals (i.e. every five years). This approach would not only help to enlarge the cohort size but would also enable the prolongation of follow-ups, thereby improving data integrity and providing a more comprehensive understanding of long-term outcomes.

Conclusion

In this study, we reported surgical techniques and clinical outcomes of ex-situ RAA repair and autotransplantation based on a nationwide cohort. As a supplement to in-situ repair, ex-situ repair and autotransplantation are safe and feasible for endovascularly untreatable RAAs. The limited follow-up and sample size require larger studies to validate its therapeutic efficacy.

Reference

1. Henke PK, Cardneau JD, Welling TH, 3rd, Upchurch GR, Jr., Wakefield TW, Jacobs LA, et al. Renal artery aneurysms: a 35-year clinical experience with 252 aneurysms in 168 patients. Ann Surg. 2001;234(4):454-62; discussion 62-3.
2. Coleman DM, Stanley JC. Renal artery aneurysms. J Vasc Surg. 2015;62(3):779-85.
3. Gallagher KA, Phelan MW, Stern T, Bartlett ST. Repair of complex renal artery aneurysms by laparoscopic nephrectomy with ex vivo repair and autotransplantation. J Vasc Surg. 2008;48(6):1408-13.
4. Barrionuevo P, Malas MB, Nejim B, Haddad A, Morrow A, Ponce O, et al. A systematic review and meta-analysis of the management of visceral artery aneurysms. J Vasc Surg. 2019;70(5):1694-9.
5. Laser A, Flinn WR, Benjamin ME. Ex vivo repair of renal artery aneurysms. J Vasc Surg. 2015;62(3):606-9.
6. Contarini E, Takagi K, Kimenai H, Ijzermans JNM, Furian L, Rigotti P, et al. Kidney Autotransplantation for Renal Artery Aneurysm: Case Series and a Systematic Review. Ann Vasc Surg. 2021;77:349 e5- e18.
7. Lacroix H, Bernaerts P, Nevelsteen A, Hanssens M. Ruptured renal artery aneurysm during pregnancy: successful ex situ repair and autotransplantation. J Vasc Surg. 2001;33(1):188-90.
8. Machado M, Machado R, Almeida R. Renal Autotransplantation for The Treatment of Renal Artery Aneurysm. Ann Vasc Surg. 2022;79:226-32.
9. Bishoff JT, Kavoussi LR. Atlas of laparoscopic and robotic urologic surgery. Fourth edition. ed. Philadelphia, PA: Elsevier; 2023. xiii, 353 pages p.
10. Kok HK, Asadi H, Sheehan M, Given MF, Lee MJ. Systematic Review and Single-Center Experience for Endovascular Management of Visceral and Renal Artery Aneurysms. J Vasc Interv Radiol. 2016;27(11):1630-41.
11. Robinson WP, 3rd, Bafford R, Belkin M, Menard MT. Favorable outcomes with in situ techniques for surgical repair of complex renal artery aneurysms. J Vasc Surg. 2011;53(3):684-91.
12. Gaudino M, Benedetto U, Fremes S, Biondi-Zoccai G, Sedrakyan A, Puskas JD, et al. Radial-Artery or Saphenous-Vein Grafts in Coronary-Artery Bypass Surgery. N Engl J Med. 2018;378(22):2069-77.
13. Cohen AJ, Williams DS, Bohorquez H, Bruce DS, Carmody IC, Reichman T, et al. Robotic-assisted laparoscopic donor nephrectomy: decreasing length of stay. Ochsner J. 2015;15(1):19-24.
14. Windisch OL, Matter M, Pascual M, Sun P, Benamran D, Buhler L, et al. Robotic versus hand-assisted laparoscopic living donor nephrectomy: comparison of two minimally invasive techniques in kidney transplantation. J Robot Surg. 2022;16(6):1471-81.
15. Giulianotti PC, Bianco FM, Addeo P, Lombardi A, Coratti A, Sbrana F. Robot-assisted laparoscopic repair of renal artery aneurysms. J Vasc Surg. 2010;51(4):842-9.
16. Abreu AL, Medina LG, Chopra S, Gill K, Cacciamani GE, Azhar RA, et al. Robotic Renal Artery Aneurysm Repair. Eur Urol. 2020;78(1):87-96.
17. Pfeiffer T, Reiher L, Grabitz K, Grunhage B, Hafele S, Voiculescu A, et al. Reconstruction for renal artery aneurysm: operative techniques and long-term results. J Vasc Surg. 2003;37(2):293-300.
18. Liu F, Yuan H, Li X, Ma X, Wang M. Application of Hypothermic Perfusion via a Renal Artery Balloon Catheter During Robot-assisted Partial Nephrectomy and Effect on Renal Function. Acad Radiol. 2019;26(8):e196-e201.
19. Duprey A, Chavent B, Meyer-Bisch V, Varin T, Albertini JN, Favre JP, et al. Editor's Choice - Ex vivo Renal Artery Repair with Kidney Autotransplantation for Renal Artery Branch Aneurysms: Long-term Results of Sixty-seven Procedures. Eur J Vasc Endovasc Surg. 2016;51(6):872-9.
20. Chaer RA, Abularrage CJ, Coleman DM, Eslami MH, Kashyap VS, Rockman C, et al. The Society for Vascular Surgery clinical practice guidelines on the management of visceral aneurysms. J Vasc Surg. 2020;72(1S):3S-39S.
21. Ceuppens S, Kimenai H, Klop KWJ, Zuidema WC, Betjes MGH, Weimar W, et al. Unspecified live kidney donation by urological patients. World J Transplant. 2020;10(8):215-22.



Chapter 11

Machine Learning-Driven Assessment of Early Graft Function in Living Donor Kidney Transplantation Using Intraoperative Laser Speckle Contrast Imaging

Yitian Fang*, Li You*, Hendrikus J.A.N. Kimenai, Miao-Ping Chien, Frank J.M.F. Dor, Ron W.F. de Bruin, Robert C. Minnee

* Authors contributed equally.

Submitted.

Abstract

Laser speckle contrast imaging (LSCI) enables real-time, non-contact assessment of renal microcirculation and may provide complementary value for predicting early graft dysfunction after living donor kidney transplantation (LDKT). We performed intraoperative LSCI in 110 LDKT recipients at Erasmus Medical Center. Early graft function was assessed by estimated glomerular filtration rate at 1 week and classified as ≥ 30 or < 30 mL/min/1.73 m². Two feature sets were evaluated across four machine learning algorithms (support vector machine [SVM], logistic regression, random forest [RF], and XGBoost): Clinical Model and Combined Model integrating clinical variables with convolutional neural network (CNN)-derived LSCI features. The Combined Model consistently outperformed the Clinical Model. SVM achieved higher accuracy (0.89 [95% CI, 0.85-0.92] vs. 0.79 [0.75-0.84]) and logistic regression showed higher recall (0.86 [0.83-0.88] vs. 0.76 [0.74-0.79]). On independent testing, Combined Models maintained better performance, with SVM achieving the highest F1 score (0.60 [0.50-0.71]) and RF the highest recall (0.88 [0.50-1.00]). Grad-CAM confirmed physiologically relevant CNN-derived feature localization. LSCI also detected and guided correction of vascular complications intraoperatively. Integrating intraoperative LSCI features with clinical variables significantly improves prediction of early low eGFR after LDKT and offers additional intraoperative diagnostic value. Multicenter validation is warranted to confirm generalizability.

Introduction

Living donor kidney transplantation (LDKT) provides superior graft survival compared to deceased donor kidney transplantation.[1] However, a subset of 5-12% LDKT recipients develop early graft dysfunction, which may negatively impact long-term outcome if not promptly identified.[2]

Early graft function is influenced by a complex interplay of donor, recipient, and surgical factors. Previous studies have investigated a range of clinical predictors, including demographic characteristics, injury biomarkers, circulating anti-HLA antibody specificities and concentrations, and allograft pathology information to identify patients at risk of early graft loss and delayed graft function.[3-6] While these parameters are informative, their predictive accuracy remains limited, particularly in the intraoperative setting where real-time risk assessment could guide immediate clinical decision-making.

Laser speckle contrast imaging (LSCI) is an emerging optical technique that enables non-invasive, non-contact, and contrast-free visualization of tissue microcirculation in real-time. By capturing dynamic speckle patterns generated by moving red blood cells, LSCI offers a semi-quantitative measure of renal cortical microcirculation. Due to the strong correlation between renal cortical microcirculation and kidney function, LSCI holds valuable functional insight into graft function beyond macroscopic inspection.[7]

With the rise of artificial intelligence in medicine, machine learning (ML) and deep learning approaches have demonstrated substantial potential in supporting clinical decision-making. In particular, convolutional neural networks (CNNs) are a form of artificial neural networks that are able to extract and interpret high-dimensional features, which makes CNN ideal for image analysis.[8] When combined with traditional clinical prediction models, these CNN-derived imaging features may improve the performance of predictive models.

In this study, we aimed to investigate the value of intraoperative LSCI-derived imaging features, extracted using a CNN-based approach, in predicting early graft function following LDKT. We hypothesized that prediction models incorporating both clinical and LSCI data would outperform models based solely on clinical variables, thereby providing a more accurate tool for identifying early risk in LDKT recipients.

Methods

Study Design

A schematic overview of the study design is shown in **Figure 1**. This prospective, single-center cohort study enrolled 110 adult patients who underwent living donor kidney transplantation (LDKT) at Erasmus Medical Center between March 2023 and March 2025. Intraoperative LSCI measurements were performed after reperfusion during the transplant procedure.

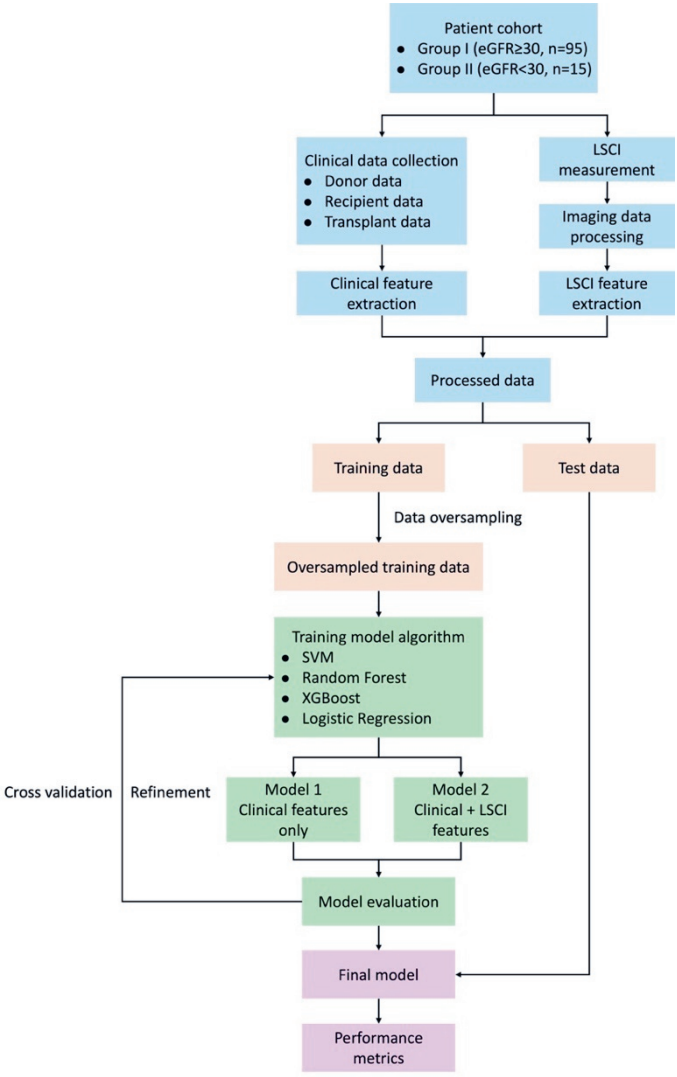


Figure 1. Flowchart for predicting early graft dysfunction in living donor kidney transplantation.

Estimated glomerular filtration rate (eGFR) was assessed one week post-transplant. Patients were classified into two groups based on early graft function. Patients with eGFR ≥ 30 mL/min/1.73m^2 were classified as Group I, whereas those with eGFR < 30 mL/min/1.73m^2 were classified as Group II. We selected the threshold of 30 mL/min/1.73 m^2 because an eGFR below this level represents severe early renal impairment and an indicator of poor early graft recovery in previous studies.[9, 10]

To assess the predictive value of intraoperative LSCI, we developed and compared two ML models with predefined feature sets:

(1) Clinical Model, which includes selected clinical variables only; and (2) Combined Model, which includes the same clinical features and CNN-derived LSCI features. Both ML models were trained and evaluated separately, and model performance was assessed using standard classification metrics.

Clinical Data Collection

To investigate the key prognostic determinants of early graft dysfunction, we included donor-related characteristics, recipient-related characteristics, and transplant data. The following parameters were collected for the construction of the early graft function prediction model: (1) donor age, sex, BMI, and predonation renal function; (2) recipient age, sex, BMI, cause of ESRD, and comorbidities; (3) transplant data including ABO compatibility, virtual panel reactive antibodies (vPRA), HLA-A/B/DR mismatch numbers, preemptive transplant status, warm ischemia time, and estimated intraoperative blood loss.

LSCI Measurement

LSCI was performed using the MoorO2Flo system (Moor Instruments Ltd., Axminster, UK) to assess renal microcirculation during the early reperfusion phase. All measurements were conducted after reperfusion with the kidney graft positioned in its final transplant orientation. Each recording lasted 10 seconds. To minimize ambient light interference, surgical lights were turned off and external light sources were blocked during measurement.

During data acquisition, real-time LSCI images were monitored by the surgical team. If abnormal perfusion patterns (e.g., focal hypoperfusion) were observed, transplant surgeons were informed to evaluate potential issues such as anastomotic stenosis, renal artery kinking or venous outflow problems. In such cases, a repeat LSCI acquisition was performed following intervention and included for analysis. Detailed working principle, protocol and quality control procedures of the LSCI measurements are described in **Supplementary Methods S1**.

LSCI Data Processing

The workflow of LSCI measurement, image processing, and feature extraction is illustrated in **Figure 2**.

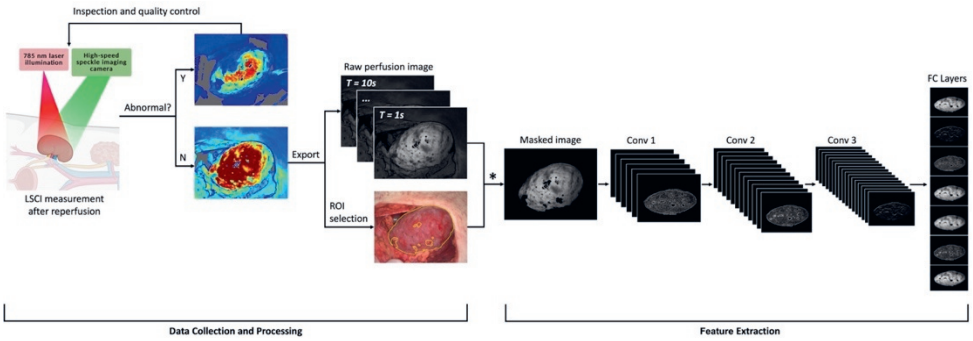


Figure 2. Workflow of LSCI measurement, image processing and feature extraction. LSCI was performed after reperfusion during kidney transplantation. If perfusion abnormalities were observed when real-time monitoring, repeat measurements were performed after corrective intervention and included in the analysis. For each patient, ten representative LSCI frames (one per second) were selected, and both raw perfusion and corresponding color images were exported. Using the color image as anatomical reference, the visible renal surface was manually delineated as the region of interest (ROI), excluding areas obscured by adipose tissue or surgical artifacts. This ROI was applied to the perfusion images to create masked images. The masked images were processed using a customized convolutional neural network (CNN) based on AlexNet architecture, consisting of three convolutional layers followed by two fully connected (FC) layers. The CNN extracted high-dimensional feature vectors from the images, which were subsequently used for predictive modeling.

For each patient, LSCI measurement was performed at a frame rate of 20 Hz over a duration of 10 seconds, resulting in a total of 201 frames per recording. For data analysis, 10 representative frames were selected-one from each second, corresponding to frames 20, 40, 60, ..., 200. From each selected frame, both the LSCI perfusion image and the corresponding colour image were exported.

Due to the limited measurement depth of LSCI (~0.3 mm), surface obstructions can interfere with accurate perfusion measurements.[11, 12] Using the color images as anatomical reference, the entire visible kidney surface was manually delineated as the region of interest (ROI), excluding areas obscured by adipose tissue or surgical artifacts such as cauterized clots. The defined ROI for each kidney was applied to the corresponding LSCI perfusion image to create a masked image.

LSCI Image Feature Extraction

The masked perfusion images were used as input for our CNN, which in this study, is based on a modified AlexNet architecture consisting of 3 convolutional layers followed by 2 fully connected layers.[13] Convolutional layers are used to iteratively extract LSCI image features, such as ROI shapes, textures, brightness, brightness gradient, colormaps, or abstract patterns that can describe other spatial structures. Let $f = \{f_1, f_2, \dots, f_n\}$ denote the sets of n features. Fully connected layers will make use of all extracted features and classify whether an image represents "Group I" (represented by 0 in a binary case) or "Group II" (represented by 1 in a binary case). The classification is done via a loss function $\mathcal{L}(f) \rightarrow 1$.

The supervised learning process is summarized as follows: (1) Each input image has a ground truth label. Let $I = \{I_1, I_2, \dots, I_m\}$ denote the set of m input images, and $L = \{L_1, L_2, \dots, L_m\}$ the set of corresponding ground truth labels, where $L_{i\in[1,m]} = 0\ or\ 1$. (2) CNN extracts a set of features $f = \{f_1, f_2, \dots, f_n\}$ from I and assigns weights $w = \{w_1, w_2, \dots, w_n\}$ to them. Initially, the weights are equal, and through learning the network adjusts these weights so that certain features become more important in predicting the output. (3) The weighted features are passed through a loss function to calculate a predicted label $\mathcal{L}(f, w)$. The loss function quantifies the difference between the predicted and ground truth labels and updates the weights accordingly. A full pass through all training images constitutes one epoch. In our set up, we trained the CNN for 50 epochs, meaning CNN scanning through all images I and update weights w for 50 times, which is a standard number of epochs to achieve stable performance.

Through supervised learning with AlexNet, we developed a CNN model that achieved a classification accuracy of 82%. This process yielded both features and their corresponding

weights, which reflect their relative importance in distinguishing between outcome classes. Features with positive weights ($w_i > 0$) were considered informative and selected for further analysis.

LSCI Image Feature Localization

The selected CNN features can be pinpointed back to the original LSCI data for sanity check. **Figure 3** illustrates feature localization using Gradient-weighted Class Activation Mapping (Grad-CAM) across two convolutional layers of the CNN trained on LSCI data. Grad-CAM generates class-specific heatmaps by backpropagating the gradients of the predicted class to the convolutional feature maps, thereby highlighting regions most influential for the network's decision.[14]

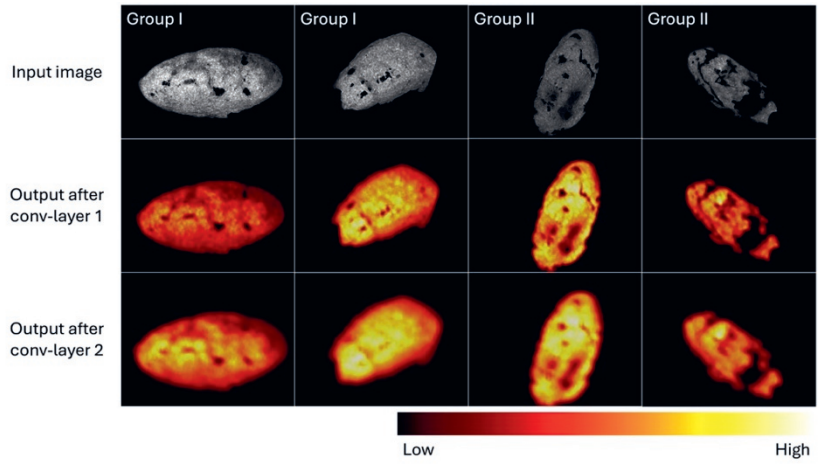


Figure 3. Visualizations of convolutional feature activations from the CNN trained on LSCI data acquired during kidney transplantation. The top row shows representative raw LSCI input images, labelled as either Group I or Group II. The second and third rows illustrate the Grad-CAM heatmaps from the first and second convolutional layers, respectively. The first layer activations are broadly distributed, reflecting low-level texture and contrast patterns, whereas the second layer activations become more refined and spatially focused. The highlighted regions (e.g., yellow region) indicate areas most influential in the network's decision.

The first row shows representative raw LSCI input images, categorized as stable or at-risk grafts. The second and third rows display the corresponding Grad-CAM heatmaps from the first and second convolutional layers, respectively. In the first layer, activations are distributed broadly and capture low-level texture and contrast variations. In contrast, the second layer produces more refined and spatially focused activations, highlighting regions

most discriminative for graft function classification. These visualizations indicate that CNN focused on physiologically relevant regions when making predictions.

Statistical Analysis

Continuous variables were described using medians with interquartile ranges (IQR), and categorical variables were described using number and percentages. Medians and proportions between groups were compared with the Mann–Whitney U test, or the x^2 test (or Fisher exact test if appropriate). Values of $P < 0.05$ were considered significant, and all tests were 2 tailed.

ML Model Development

We implemented ML models that can be applied to classify binary outcomes, referred to as ML classification models, including support vector machine (SVM) with a linear kernel, extreme gradient boosting (XGBoost), random forest (RF), and logistic regression (LR). Each ML model is detailed in the **Supplementary Methods S2**.

All predictor variables were centered and scaled. The full cohort was randomly split into training (70%) and test (30%) sets using stratified sampling. The test set (30%) serves as unseen data to the trained model, used to examine the robustness of model training.

For training set, the Synthetic Minority Oversampling Technique (SMOTE) was applied to address class imbalance before model fitting. Predictor variables were selected based on the concordance index (C-index) of each variable with respect to the outcome using original dataset, which quantifies the variable discriminatory ability. Variables with a C-index > 0.6 or < 0.4 were included in subsequent model development. Model training was conducted on the SMOTE-balanced training dataset. ML was performed using 5-fold cross-validation with a grid search strategy, with 4 folds used to train the model and the left-out fold used to evaluate the model's performance.

Model Evaluation

Each model was trained and evaluated over 30 independent iterations with different random stratified splits to ensure performance robustness. In each iteration, the best-performing

parameter combination was identified based on cross-validated AUC within the SMOTE-balanced training set. The final tuned model was then evaluated on the held-out test data for external validation. Performance metrics (accuracy, precision, recall, and F1 score) were calculated separately for the training and test datasets and summarized across iterations.

Results

Participant Characteristics

A total of 110 LDKT patients were enrolled in the study, including 95 (83%) cases in Group I and 15 (17%) in Group II. Baseline characteristics stratified by graft function are displayed in **Table 1**. Compared to Group I, patients in Group II received kidneys from older donors (median 64 [IQR 56-68] vs. 55 (47-64) years; p=0.027) with lower donor pre-donation eGFR (74 [70-83] vs. 87 [76-97] ml/min/1.73m^2; p=0.011). Patients in Group II had significantly higher BMI (29.2 [25.6-32.7] vs. 25.5 [23.5-28.0] kg/m^2; p=0.022), and were more likely to have cardiovascular disease (60.0% vs. 26.3%; p=0.015), and higher intraoperative blood loss (250 [200-375] vs. 100 [100-200] mL; p<0.001).

Intraoperative Detection of Vascular Complications

In our cohort, two cases of perfusion abnormalities were identified intraoperatively using LSCI. The first case demonstrated extensive cortical hypoperfusion caused by anastomotic stenosis following arterial reconstruction due to dual renal artery branches. The anastomosis was uncoupled and reconstructed, after which repeat LSCI confirmed restoration of perfusion (**Figure S1A**). The second case showed localized perfusion deficiency after reperfusion, which was attributed to renal artery kinking. Adjustment of the graft position corrected the defect, and subsequent LSCI imaging confirmed satisfactory cortical perfusion (**Figure S1B**).

Table 1. Cohort's characteristics

	Group I (n=95)	Group II (n=15)	P value
Donor characteristics			
Age, yr, median (IQR)	55 (47-64)	64 (56-68)	0.027
Male sex, n (%)	42 (42.2)	7 (46.7)	1.000
BMI, median (IQR)	26.1 (23.8-28.1)	26.5 (23.4-28.0)	0.764
Serum creatinine, µmol/l, median (IQR)	76 (69-87)	80 (71-92)	0.278
eGFR, ml/min per 1.73m^2, median (IQR)	87 (76-97)	74 (70-83)	0.011
Recipient characteristics			
Age, yr, median (IQR)	56 (47-66)	63 (53-69)	0.190
Male sex, n (%)	59 (62.1)	7 (46.7)	0.395
BMI, median (IQR)	25.5 (23.5-28.0)	29.2 (25.6-32.7)	0.022
End-stage renal disease causes, n (%)			0.274
Glomerular disease	24 (25.3)	2 (13.3)	
Vascular disease	20 (21.1)	6 (40.0)	
Diabetes	12 (12.6)	3 (20.0)	
Others	39 (41.1)	4 (26.7)	
Comorbidities, n (%)			
Cardiovascular disease	25 (26.3)	9 (60.0)	0.015
Diabetes	18 (18.9)	5 (33.3)	0.302
Hypertension	49 (51.6)	7 (46.7)	0.940
Transplant characteristics			
ABO-incompatible, n (%)	9 (9.5)	1 (6.7)	1.000
Preemptive, n (%)	58 (61.1)	8 (53.3)	0.777
Warm ischemia time, min, median (IQR)	18 (16-22)	20 (17-25)	0.256
Blood loss, mL, median (IQR)	100 (100-200)	250 (200-375)	<0.001
Immunologic parameters			
vPRA (%), median (IQR)	0 (0-24.3)	0 (0-2.5)	0.548
HLA-A/B mismatch number, median (IQR)	2 (2-3)	3 (2-3.5)	0.387
HLA-DR mismatch number, median (IQR)	1 (1-2)	1 (1-2)	0.394

BMI, body mass index; eGFR, estimated glomerular filtration rate; HLA, human leukocyte antigen; vPRA, virtual panel reactive antibody.

Variable Selection for Model Development

The C-index was calculated for each candidate variable to assess the individual predictive capability (**Figure S2**, **S3**). Variables with a C-index > 0.6 or < 0.4 were selected for model development, indicating strong discriminatory power in either direction.

For the Clinical Model, the following variables were selected for ML model development: donor age, donor pre-donation eGFR, recipient age, BMI, history of cardiovascular disease, and estimated intraoperative blood loss. For the Combined Model, these six clinical variables were supplemented with five LSCI-derived features to incorporate quantitative perfusion information (**Figure 4**).

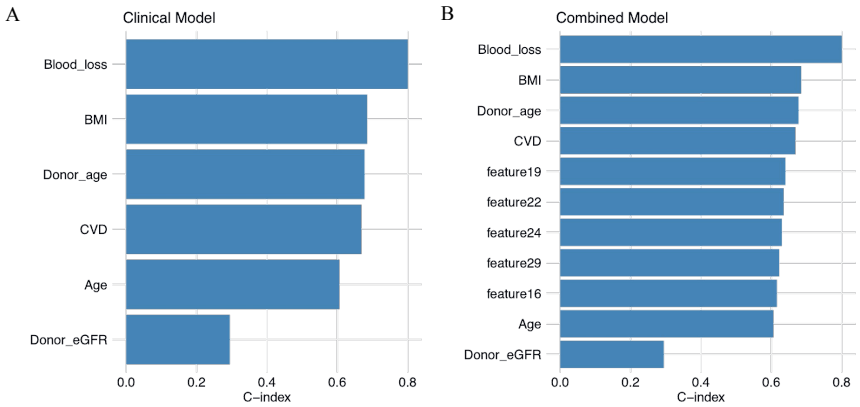


Figure 4. Variables selected for machine learning model development based on concordance index (C-index). (A) Variables selected for the Clinical Model and (B) for the Combined Model. Features with a C-index > 0.6 or < 0.4 were retained for model development. The Combined Model includes the same clinical variables as the Clinical Model along with additional LSCI-derived features.

ML Model Performance

Model performance was assessed using classification metrics as shown in **Figure 5**. Across all metrics (accuracy, precision, recall, and F1 score), the Combined Model consistently outperformed the Clinical Model during training, regardless of the ML algorithm used. For example, SVM achieved higher accuracy with combined features (0.89 [0.85-0.92] vs. 0.79 [0.75-0.84]; **Figure 5A**, left), while LR yielded a higher recall in the Combined Model (0.86 [0.83-0.88] vs. 0.76 [0.74-0.79], **Figure 5C**, left).

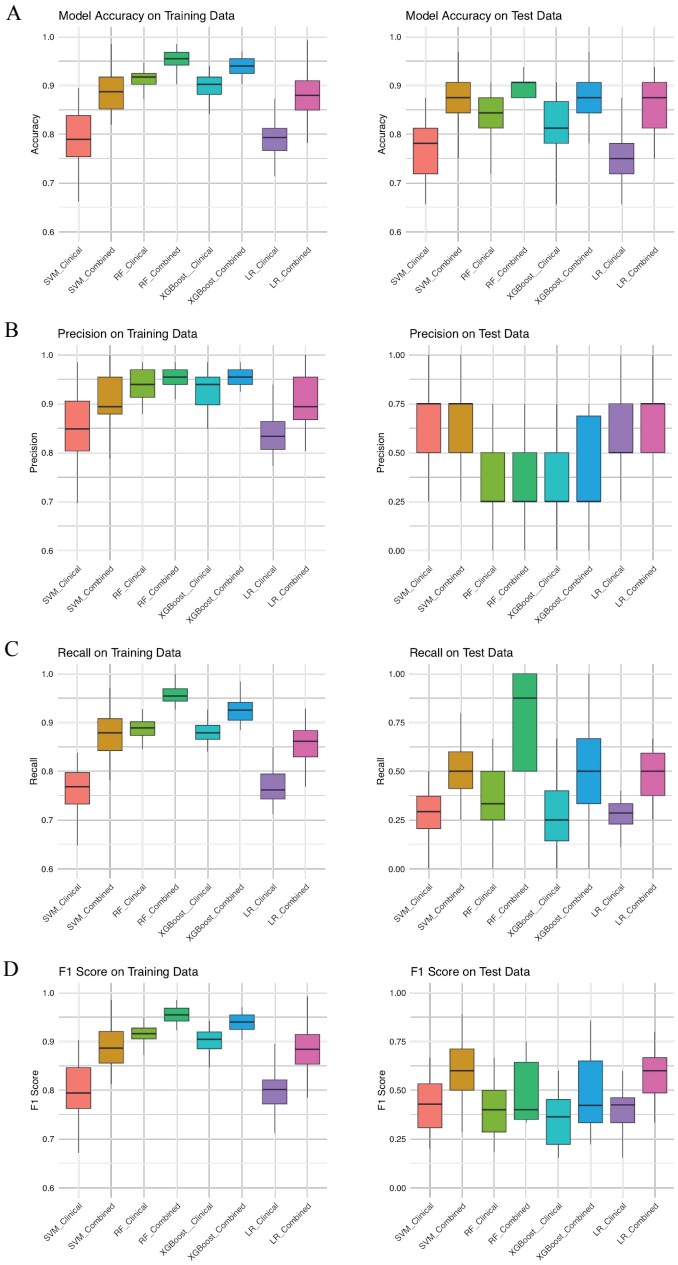


Figure 5. Prediction performance of classification models on SMOTE-balanced training and independent test data. Boxplots show the distribution of (A) accuracy, (B) precision, (C) recall, and (D) F1 score for eight classification models across 30 repeated stratified train/test splits. Each model was trained and cross-validated using SMOTE-balanced training data (left) and tested in an independent test data (right). Models include support vector machine (SVM), random forest (RF), extreme gradient boosting (XGBoost), and logistic regression (LR), each developed using either clinical variables only (Clinical) or combined clinical and LSCI features (Combined).

The prominent advantage of the Combined Model remained when applied on the unseen test dataset. All Combined Models achieved comparable accuracy (**Figure 5A**, right). SVM and LR achieved the highest precision, indicating stronger performance in identifying 'at-risk' cases (0.75 [0.50-0.75]; **Figure 5B**, right). In contrast, RF exhibited the highest recall, suggesting greater sensitivity in detecting at-risk cases (0.88 [0.50-1.00] vs. 0.33 [0.25-0.50], **Figure 5C**, right). Among all models, SVM achieved the highest F1-score on the test set, demonstrating the best balance between precision and recall (0.60 [0.50-0.71], **Figure 5D**, right). Full performance metrics are provided in **Table S1** and **S2**.

Discussion

In this prospective study, we investigated the added value of intraoperative LSCI features, extracted using CNN, for predicting early graft dysfunction following LDKT. Our findings demonstrate that incorporating CNN-derived perfusion features from LSCI into ML models significantly improves predictive performance compared to using clinical variables alone.

Patients at risk of early graft dysfunction were characterized by higher donor age, reduced donor pre-donation eGFR, higher recipient BMI, increased prevalence of cardiovascular disease, and more intraoperative blood loss. These clinical variables were selected for model development based on their concordance with graft outcomes. When combined with LSCI-derived features, all ML models showed improved accuracy, precision, recall, and F1 score, both in training and independent test sets. Notably, the Combined Model achieved higher sensitivity in identifying at-risk grafts without compromising specificity, suggesting that LSCI-derived features provide meaningful, complementary insight into graft function recovery.

Previous studies have explored various biomarkers, either pretransplant in the donor, or posttransplant in the recipient, for their prognostic relevance. For example, elevated levels of donor-derived plasma mitochondrial DNA and urinary anaphylatoxin C5a have been associated with an increased risk of DGF.[15, 16] Similarly, biomarkers found in preservation fluid, such as cell-free miR-505-3p, glutathione S-transferase pi, and neutrophil gelatinase-associated lipocalin, have shown significant associations with posttransplant graft dysfunction.[5, 6, 17, 18] Posttransplant biopsies have also offered insights into graft viability. The presence of partial endothelial to mesenchymal transition and strong expression of

TGF-β1 in phenotypic changed endothelial cells have been associated poor graft function recovery.[19] However, these biomarkers typically represent isolated pathways and may not reflect the complete phenotype of the graft.

In parallel, predictive models leveraging large-scale clinical datasets have gained traction.[20-23] For instance, the iBOX prognostication system integrates functional, immunological, and histological parameters to predict long-term graft outcomes, and is being adopted in clinical practice.[3, 24] However, it is important to note that such models are specifically designed for predicting long-term outcomes and are not tailored to assess early graft function in the immediate posttransplant period. Other tools such as the Kidney Donor Risk Index and Kidney Donor Profile Index primarily focus on donor-related factors and are intended to estimate the overall quality of the donor organ prior to transplantation.[25-27] While valuable for organ allocation and long-term risk stratification, these tools lack the ability to capture intraoperative dynamics that may critically impact graft function.

Therefore, complementary strategies, such as intraoperative imaging and machine learning-based integration of perfusion and clinical data, are needed to enhance early risk stratification. Various imaging modalities, such as Doppler ultrasound, indocyanine green fluorescence angiography, photoacoustic imaging, and MRI, have been investigated to assess graft function in transplantation or machine perfusion settings.[28-32] However, these techniques are either operator-dependent or require the use of contrast agents. In contrast, LSCI is non-contact, contrast-free, and real-time, making it well suited for surgical workflows. Importantly, the developed tool is practical to apply in the clinical setting. Donor and recipient characteristics are routinely collected before transplantation, and LSCI acquisition requires only 10 seconds of recording under standardized conditions. Once LSCI images are processed by the pre-trained CNN model, feature extraction and risk prediction can be performed within seconds. Therefore, for a new patient, all required inputs can be rapidly obtained and integrated into the ML model, allowing near real-time prediction of early graft function without delaying decision-making.

To our knowledge, this is the first study to apply intraoperative LSCI and ML classification on early graft function prediction in kidney transplantation. The use of CNN enabled the extraction of high-dimensional, abstract image features that represent spatial perfusion

patterns, allowing ML algorithms to capture complex associations between intraoperative microcirculation and graft function. These CNN-derived features provided a nuanced characterization of microvascular heterogeneity, likely reflecting subtle hemodynamic abnormalities that precede clinically measurable dysfunction. To enhance interpretability, Grad-CAM was used to map class-specific activations back onto the original LSCI images, thereby identifying the most influential regions for classification. This confirmed that the CNN focused on physiologically relevant areas of the graft, differentiating stable from at-risk cases. Together, the integration of LSCI, CNN feature learning, and Grad-CAM visualization provides a novel and interpretable framework for intraoperative graft function assessment in kidney transplantation.

Moreover, our study highlights the added clinical utility of LSCI in detecting intraoperative vascular complications. In two cases, abnormal perfusion patterns identified by LSCI revealed anastomotic stenosis and arterial kinking, both of which were promptly corrected, with restoration of cortical perfusion confirmed by repeat imaging. These findings highlight the ability of LSCI to provide immediate intraoperative feedback, facilitating timely surgical (re-)intervention and potentially reducing postoperative complications.

Despite these promising strengths, several limitations should be acknowledged. First, the sample size was limited in Group II, although we employed SMOTE to mitigate class imbalance in the training phase and performed repeated validations to ensure robustness. Second, LSCI measurements, while standardized in this study, may be affected by variations in kidney exposure, lighting conditions, or technical factors. Although we implemented strict quality control protocols, broader generalizability requires validation across institutions. Third, while CNNs offer powerful feature extraction capabilities, the interpretability of these features remains limited. Lastly, the use of eGFR at one week posttransplant as a surrogate for early graft function is practical and commonly adopted, but it may not fully capture long-term graft outcomes. Follow-up studies linking early perfusion profiles with long-term graft survival would further validate the clinical relevance of LSCI-guided risk stratification. Also, follow-up studies should also explore the value of LSCI in deceased donor kidney transplantation as it is associated with a higher incidence of early graft dysfunction or delayed graft function compared to LDKT.

In conclusion, our findings suggest that CNN-extracted LSCI features, when integrated with clinical variables and analyzed using ML models, significantly improves the prediction of low one-week eGFR (< 30 mL/min/1.73m²) in LDKT. This integrative strategy has the potential to support posttransplant decision-making and improve transplant outcomes. Further validation in larger, multicenter cohorts is warranted to confirm the generalizability and clinical utility of this approach.

References

1. Baid-Agrawal S, Frei UA. Living donor renal transplantation: recent developments and perspectives. Nat Clin Pract Nephrol. 2007;3(1):31-41.
2. van de Laar SC, de Weerd AE, Bemelman FJ, Idu MM, de Vries APJ, Alwayn IPJ, et al. Favorable Living Donor Kidney Transplantation Outcomes within a National Kidney Exchange Program. Clin J Am Soc Nephro. 2025;20(3):440-50.
3. Loupy A, Aubert O, Orandi BJ, Naesens M, Bouatou Y, Raynaud M, et al. Prediction system for risk of allograft loss in patients receiving kidney transplants: international derivation and validation study. BMJ. 2019;366:l4923.
4. Naesens M, Lerut E, Emonds MP, Herelixka A, Evenepoel P, Claes K, et al. Proteinuria as a Noninvasive Marker for Renal Allograft Histology and Failure: An Observational Cohort Study. Journal of the American Society of Nephrology. 2016;27(1):281-92.
5. van den Akker EK, Hesselink DA, Manintveld OC, JN IJ, de Bruijn RW, Dor FJ. Neutrophil Gelatinase-Associated Lipocalin, but Not Kidney Injury Marker 1, Correlates with Duration of Delayed Graft Function. Eur Surg Res. 2015;55(4):319-27.
6. Nielsen MB, Krogstrup NV, Nieuwenhuijs-Moeke GJ, Oltean M, Dor F, Jespersen B, et al. P-NGAL Day 1 predicts early but not one year graft function following deceased donor kidney transplantation - The CONTEXT study. PLoS One. 2019;14(2):e0212676.
7. Fang Y, van Ooijen L, Ambagtsheer G, Nikolaev AV, Clahsen-van Groningen MC, Dankelman J, et al. Real-time laser speckle contrast imaging measurement during normothermic machine perfusion in pretransplant kidney assessment. Lasers Surg Med. 2023;55(8):784-93.
8. LeCun Y, Bengio Y, Hinton G. Deep learning. Nature. 2015;521(7553):436-44.
9. National Kidney F. K/DOQI clinical practice guidelines for chronic kidney disease: evaluation, classification, and stratification. Am J Kidney Dis. 2002;39(2 Suppl 1):S1-266.
10. Oliva-Damaso N, Delanaye P, Oliva-Damaso E, Payan J, Glassock RJ. Risk-based versus GFR threshold criteria for nephrology referral in chronic kidney disease. Clin Kidney J. 2022;15(11):1996-2005.
11. O'Doherty J, McNamara P, Clancy NT, Enfield JG, Leahy MJ. Comparison of instruments for investigation of microcirculatory blood flow and red blood cell concentration. J Biomed Opt. 2009;14(3):034025.
12. Eriksson S, Nilsson J, Sturesson C. Non-invasive imaging of microcirculation: a technology review. Med Devices (Auckl). 2014;7:445-52.
13. Krizhevsky A, Sutskever I, Hinton GE. ImageNet Classification with Deep Convolutional Neural Networks. Commun Acm. 2017;60(6):84-90.
14. Selvaraju RR, Cogswell M, Das A, Vedantam R, Parikh D, Batra D. Grad-CAM: Visual Explanations from Deep Networks via Gradient-based Localization. Ieee I Conf Comp Vis. 2017:618-26.
15. Han F, Wan SG, Sun QP, Chen N, Li H, Zheng LL, et al. Donor Plasma Mitochondrial DNA Is Correlated with Posttransplant Renal Allograft Function. Transplantation. 2019;103(11):2347-58.
16. Schroppel B, Heeger PS, Thiessen-Philbrook H, Hall IE, Doshi MD, Weng FL, et al. Donor Urinary C5a Levels Independently Correlate With Posttransplant Delayed Graft Function. Transplantation. 2019;103(1):e29-e35.
17. Roest HP, Ooms LSS, Gills AJM, IJzermans JNM, Looijenga LHJ, Dorssers LCJ, et al. Cell-free MicroRNA miR-505-3p in Graft Preservation Fluid Is an Independent Predictor of Delayed Graft Function After Kidney Transplantation. Transplantation. 2019;103(2):329-35.
18. Hall IE, Bhangoo RS, Reese PP, Doshi MD, Weng FL, Hong K, et al. Glutathione S-transferase iso-enzymes in perfusate from pumped kidneys are associated with delayed graft function. Am J Transplant. 2014;14(4):886-96.
19. Xu-Dubois YC, Ahmadpoor P, Brocheriou I, Louis K, Arzouk Snanoudj N, Rouvier P, et al. Microvasculature partial endothelial mesenchymal transition in early posttransplant biopsy with acute tubular necrosis identifies poor recovery renal allografts. Am J Transplant. 2020;20(9):2400-12.
20. Bae S, Massie AB, Caffo BS, Jackson KR, Segev DL. Machine learning to predict transplant outcomes: helpful or hype? A national cohort study. Transpl Int. 2020;33(11):1472-80.
21. Ramspek CL, El Moumni M, Wali E, Heemskerk MBA, Pol RA, Crop MJ, et al. Development and external validation study combining existing models and recent data into an up-to-date prediction model for evaluating kidneys from older deceased donors for transplantation. Kidney International. 2021;99(6):1459-69.
22. Taherkhani N, Sepehri MM, Khasha R, Shafaghi S. Determining the Level of Importance of Variables in Predicting Kidney Transplant Survival Based on a Novel Ranking Method. Transplantation. 2021;105(10):2307-15.

23. Truchot A, Raynaud M, Kamar N, Naesens M, Legendre C, Delahousse M, et al. Machine learning does not outperform traditional statistical modelling for kidney allograft failure prediction. Kidney Int. 2023;103(5):936-48.
24. Klein A, Loupy A, Stegall M, Helantera I, Kosinski L, Frey E, et al. Qualifying a novel clinical trial endpoint (iBOX) predictive of long-term kidney transplant outcomes. Am J Transplant. 2023;23(10):1496-506.
25. Rao PS, Schaubel DE, Guidinger MK, Andreoni KA, Wolfe RA, Merion RM, et al. A comprehensive risk quantification score for deceased donor kidneys: the kidney donor risk index. Transplantation. 2009;88(2):231-6.
26. Massie AB, Luo X, Chow EK, Alejo JL, Desai NM, Segev DL. Survival benefit of primary deceased donor transplantation with high-KDPI kidneys. Am J Transplant. 2014;14(10):2310-6.
27. Massie AB, Leanza J, Fahmy LM, Chow EK, Desai NM, Luo X, et al. A Risk Index for Living Donor Kidney Transplantation. Am J Transplant. 2016;16(7):2077-84.
28. Lau NS, Ly M, Liu K, Majumdar A, McCaughan G, Crawford M, et al. Current and Potential Applications for Indocyanine Green in Liver Transplantation. Transplantation. 2022;106(7):1339-50.
29. Fang Y, Nikolaev AV, Essers J, Ambagtsheer G, Clahsen-van Groningen MC, Minnee RC, et al. Enhancing Kidney Quality Assessment: Power Doppler During Normothermic Machine Perfusion. Artif Organs. 2025;49(7):1132-40.
30. Ietto G, Iori V, Inversini D, Parise C, Zani E, Iovino D, et al. Indocyanine Green Angiography for Quality Assessment of Renal Graft Before Transplantation: A Pilot Study. Exp Clin Transplant. 2023;21(2):110-5.
31. Nikolaev AV, Fang Y, Essers J, Panth KM, Ambagtsheer G, Clahsen-van Groningen MC, et al. Pre-transplant kidney quality evaluation using photoacoustic imaging during normothermic machine perfusion. Photoacoustics. 2024;36:100596.
32. Hamelink TL, Ogurlu B, Pamplona CC, Castelein J, Bennedsgaard SS, Qi H, et al. Magnetic resonance imaging as a noninvasive adjunct to conventional assessment of functional differences between kidneys in vivo and during ex vivo normothermic machine perfusion. Am J Transplant. 2024.

Supplementary

Methods S1: Laser Speckle Contrast Imaging (LSCI) Measurement Procedures

S1.1 Basic principle of LSCI

When scattering tissue is illuminated with a coherent near-infrared laser, the scattered light interferes and produces a random speckle pattern, which is detected by a high-speed camera. The motion of red blood cells (RBCs) causes temporal fluctuations in this speckle pattern. Faster RBC motion results in faster speckle fluctuations and lower speckle contrast.

In spatial mode, a kernel size of 5×5 pixels is used to calculate the speckle contrast *K* using the equation:

$K = \frac{\sigma}{\langle I \rangle}$ (1),

where σ is the standard deviation of pixel intensity *I*, and $\langle I \rangle$ is the mean intensity within the kernel. In this mode, the basic formula for LSCI measurement of renal perfusion (Flux) is $Flux \propto \left(\frac{\langle I \rangle}{\sigma}\right)^2$ (2), and measured in perfusion unit (PU).

Higher RBC velocities lead to lower *K* and higher Flux values. As speckle patterns fluctuate rapidly with fast RBC motion, the camera's exposure time averages the signal, resulting in a reduced intensity variance (σ) and thus lower contrast.

S1.2 LSCI Measurement Settings

All LSCI measurements were conducted using the MoorO$_2$Flo system (Moor Instruments Ltd., Axminster, UK), with a laser wavelength of 785 nm. The system was set to an exposure time of 20 ms and a spatial resolution of 3.9 μm per pixel. Measurements were performed peri-transplant during the reperfusion phase, ~15 minutes after vascular anastomosis, once perfusion of was stable. The kidney was positioned in its final transplant orientation. To eliminate external interference, ambient light was blocked by turning off surgical lights and closing window shades.

S1.2.1 Measurement Distance

As the distance between the camera and the sample increases, the speckle size increases. If the speckle size becomes larger than the camera pixel size, the speckle contrast artificially increases, leading to an overestimation of *K* and an underestimation of flux. To ensure consistency, a working distance of ~20 cm was maintained to keep the kidney fully in the field of view.

S1.2.2 Camera Gain

Higher camera gain leads to overestimation of RBC velocity, while lower gain leads to the loss of low velocity. A fixed gain of ~150 was used across all measurements to standardize results.

S1.2.3 LED Brightness

Higher brightness leads to overestimation of flux. Brighter illumination increases $\langle I \rangle$ (mean intensity), therefore increases Flux. LED brightness was kept constant during all measurements.

S1.2.4 Measurement Frequency

High frequency is suitable for faster-moving RBCs and low frequency for slower RBCs. As a frequency of 20 Hz is commonly used for low to moderate velocities, all measurements were performed at the rate of 20 Hz. Each measurement lasted for 10 seconds.

S1.3 Quick Start Guide

1. Make sure the system is turned on and that all leads are properly connected.
2. Open the **moorO2Flo Measurement** software.
3. Select the **Setup** tab and open the **Video Preview** window to position the camera to make sure the kidney is in the field of view.
4. Select the **Setup** tab and open the **System Setup** window to adjust the following settings:
    - Adjust the **Zoom** setting to make sure the whole kidney is the field of view.
    - Adjust the **Focus** setting to make sure the focus is on the subject. **Auto Focus** may be unsuccessful and manual adjustment may be required.
    - Adjust the **Camera Gain** to 150.
    - Adjust the **LED Brightness** to achieve an optimal brightness. For manual adjustment always set the camera gain first before adjusting LED brightness.

5. Select the **Image Settings** tab and configure the following settings:
    - **High resolution** processing mode (576×748 pixels).
    - **Frame rate**: **Frequency**, 20 Hz.
    - Duration: **Fixed duration**, 10 s.

6. Close the System Setup window with the **OK** button.
7. Start the measurement by clicking **Start measurement** on the toolbar. Measurement should start immediately and the perfusion.
8. Once the set duration ends, the measurement will stop automatically. Click **Save As** to save the measurement data.

S1.4 Real-Time Monitoring and Quality Control

During LSCI acquisition, real-time renal perfusion was assessed. If abnormal perfusion patterns were detected, the transplant surgeons were notified to assess potential issues such as anastomotic stenosis or renal artery kinking. If any adjustments were made that may affect renal perfusion, another LSCI measurement would be performed included for further analysis.

Methods S2: Description of the Machine Learning Classification Models

S2.1 Support Vector Machine

Support Vector Classification is a supervised machine learning algorithm derived from classical Support Vector Machine (SVM) framework, designed to solve binary classification problems by finding the optimal separating hyperplane that maximizes the margin between two classes. The C-SVC formulation incorporates a regularization

parameter **C**, which balances the trade-off between maximizing the margin and minimizing classification errors (soft-margin SVM).

In this study, linear kernel (LK-SVM) was applied.

The linear kernel computes the similarity between two input vectors x_i and x_j using a simple dot product: $K(x_i, x_j) = x_i^T x_j$

This kernel assumes that the classes can be separated by a linear decision boundary. It does not require additional hyperparameters beyond the regularization parameter **C**, making it suitable for high-dimensional data or cases where the relationship between variables and outcome is approximately linear.

S2.2 Classification Random Forest

Classification Random Forest is a supervised machine learning method derived from the decision tree algorithm, designed to enhance prediction accuracy and reduce overfitting. It achieves this by constructing a large number of decision trees during training and aggregating their predictions to produce a final classification outcome.

Each individual tree in the forest is trained on a bootstrap sample, randomly drawn with replacement, from the original training dataset. To introduce further randomness and reduce correlation among trees, only a random subset of predictors is considered at each node when determining the best split.

Given a training set $D = \{(x_1, y_1), (x_2, y_2), \dots, (x_n, y_n)\}$, where x_i represents the feature vector and $y_i \in \{0, 1\}$ is the class label ("Stable" = 0, "High-risk" = 1), the algorithm proceeds as follow:

For b = 1 to B (e.g., 500 trees)

- Bootstrap sample D_b is drawn from D.
- A decision tree T_b is trained on D_b. m candidate predictors are selected at each node of the tree, and the split is made based on the Gini impurity.

For a new observation x, the forest predicts the class $\hat{y}$ by majority vote

- $\hat{y} = majority\ vote\{T_b(x)\}_{b=1}^{B}$

Split Rule

At each node, the algorithm evaluates candidate splits using the Gini impurity criterion, defined as: $G(t) = 1 - \sum_{k=1}^{K} {p_k}^2$, where $G(t)$ is the Gini impurity of node t, K is the number of classes (in binary classification, $K = 2$), p_k is the proportion of samples of class k in node t. The split that achieves the maximum reduction in impurity (i.e., the largest decrease in $G(t)$) is selected.

In this study, a Classification Random Forest was used to predict binary graft outcomes ("Stable" vs. "At-risk") based on a combination of clinical and LSCI-derived features. The model was implemented using the "randomForest" package in R with the following parameters:

Number of trees (B) = 500

Features considered at each split $(m) = \sqrt{p}$, the default setting for classification.

S2.3 Extreme Gradient Boosting

Extreme Gradient Boosting (XGBoost) is a scalable and efficient implementation of gradient boosting machines, designed for supervised learning tasks including classification and regression. It builds an ensemble of decision trees sequentially, where each new tree is trained to correct the errors made by the previous ones. XGBoost

improves upon traditional gradient boosting by introducing optimized regularization, parallel processing, and handling of missing values, which enhances both model performance and computational speed.

In XGBoost, the model minimizes a regularized objective function that combines a loss term $L(\phi)$ (e.g., logistic loss for binary classification) and a regularization term $\Omega(f)$ to control model complexity: $L(\phi) = \sum_{i=1}^{n} l(y_i, \hat{y}_i) + \sum_{k=1}^{K} \Omega(f_k)$, where $\Omega(f) = \gamma T + \frac{1}{2}\lambda \sum_{j=1}^{T} {w_j}^2$,

$l(y_i, \hat{y}_i)$ is the loss function (e.g., log-loss),

f_k is the function (tree) added at boosting iteration k,

T is the number of leaves in the tree,

w_j are the leaf weights,

γ and λ are regularization parameters.

The model uses second-order gradient information (both first and second derivatives of the loss function) to guide tree construction and split evaluation, enabling more precise and efficient optimization.

S2.4 Logistic Regression

Logistic regression is a supervised machine learning algorithm commonly used for binary classification problems, where the outcome variable has two possible classes. It models the probability that a given input belongs to a particular class by applying the logistic (sigmoid) function to a linear combination of input features. The resulting output is a value between 0 and 1, interpreted as the probability of class membership.

In this study, we applied a binary logistic regression model to predict early graft dysfunction which required no hyperparameters. For classification, a default decision threshold of 0.5 was applied to the predicted probabilities. Cases with predicted probability $\geqslant$ 0.5 were classified as "At-risk", and those with probabilities < 0.5 were classified as "Stable".

Table S1. Performance metrics of the ML models for early graft function classification in the oversampled train data

Modeling	Accuracy	Sensitivity (Recall)	Specificity	Precision (PPV)	NPV	F1 score	AUC (ROC)
SVM							
Clinical	0.79 (0.75-0.84)	0.77 (0.73-0.80)	0.83 (0.79-0.89)	0.85 (0.80-0.91)	0.83 (0.79-0.89)	0.79 (0.76-0.85)	0.84 (0.81-0.88)
Combined	0.89 (0.85-0.92)	0.88 (0.84-0.91)	0.89 (0.88-0.95)	0.89 (0.88-0.95)	0.89 (0.88-0.95)	0.89 (0.86-0.92)	0.94 (0.91-0.96)
RF							
Clinical	0.92 (0.90-0.92)	0.89 (0.87-0.90)	0.94 (0.91-0.97)	0.94 (0.91-0.97)	0.94 (0.91-0.97)	0.92 (0.91-0.93)	0.97 (0.96-0.98)
Combined	0.95 (0.94-0.97)	0.95 (0.94-0.97)	0.96 (0.94-0.97)	0.95 (0.94-0.97)	0.96 (0.94-0.97)	0.95 (0.94-0.97)	0.99 (0.98-0.99)
XGBoost							
Clinical	0.90 (0.88-0.92)	0.88 (0.87-0.89)	0.94 (0.90-0.95)	0.94 (0.90-0.95)	0.94 (0.90-0.95)	0.90 (0.88-0.92)	0.96 (0.95-0.97)
Combined	0.94 (0.92-0.95)	0.93 (0.90-0.94)	0.95 (0.94-0.97)	0.95 (0.94-0.97)	0.95 (0.94-0.97)	0.94 (0.92-0.95)	0.98 (0.98-0.99)
LR							
Clinical	0.79 (0.77-0.81)	0.76 (0.74-0.79)	0.82 (0.79-0.86)	0.83 (0.81-0.86)	0.82 (0.79-0.86)	0.80 (0.77-0.82)	0.84 (0.82-0.87)
Combined	0.88 (0.85-0.91)	0.86 (0.83-0.88)	0.89 (0.87-0.95)	0.89 (0.87-0.95)	0.89 (0.87-0.95)	0.88 (0.85-0.91)	0.92 (0.91-0.94)

Data are presented as median (interquartile range).
AUC, area under the curve; ML, machine learning; NPV, negative predictive value; PPV, positive predictive value; RF, random forest; ROC, receiver operating characteristic; SVM, support vector machine; XGBoost, extreme gradient boosting.

Table S2. Performance metrics of the ML models for early graft function classification in the test data

Modeling	Accuracy	Sensitivity (Recall)	Specificity	Precision (PPV)	NPV	F1 score	AUC (ROC)
SVM							
Clinical	0.77 (0.72-0.80)	0.29 (0.21-0.37)	0.95 (0.91-0.96)	0.75 (0.50-0.75)	0.95 (0.91-0.96)	0.43 (0.31-0.53)	0.79 (0.72-0.89)
Combined	0.88 (0.84-0.91)	0.50 (0.41-0.60)	0.96 (0.93-0.96)	0.75 (0.50-0.75)	0.96 (0.93-0.96)	0.60 (0.50-0.71)	0.84 (0.81-0.95)
RF							
Clinical	0.84 (0.81-0.88)	0.33 (0.25-0.50)	0.90 (0.89-0.93)	0.25 (0.25-0.50)	0.90 (0.89-0.93)	0.40 (0.29-0.50)	0.77 (0.72-0.85)
Combined	0.91 (0.88-0.91)	0.88 (0.50-1.00)	0.90 (0.90-0.93)	0.25 (0.25-0.50)	0.90 (0.90-0.93)	0.40 (0.35-0.64)	0.90 (0.77-0.96)
XGBoost							
Clinical	0.81 (0.78-0.87)	0.25 (0.14-0.40)	0.89 (0.88-0.92)	0.25 (0.25-0.50)	0.89 (0.88-0.92)	0.36 (0.22-0.45)	0.76 (0.66-0.83)
Combined	0.88 (0.84-0.91)	0.50 (0.33-0.67)	0.90 (0.90-0.95)	0.25 (0.25-0.69)	0.90 (0.90-0.95)	0.42 (0.33-0.65)	0.84 (0.72-0.88)
LR							
Clinical	0.75 (0.72-0.78)	0.29 (0.23-0.33)	0.93 (0.91-0.96)	0.50 (0.50-0.75)	0.93 (0.91-0.96)	0.42 (0.33-0.46)	0.78 (0.69-0.88)
Combined	0.88 (0.81-0.91)	0.50 (0.38-0.59)	0.96 (0.93-0.96)	0.75 (0.50-0.75)	0.96 (0.93-0.96)	0.60 (0.49-0.67)	0.82 (0.79-0.92)

Data are presented as median (interquartile range).
AUC, area under the curve; ML, machine learning; NPV, negative predictive value; PPV, positive predictive value; RF, random forest; ROC, receiver operating characteristic; SVM, support vector machine; XGBoost, extreme gradient boosting.

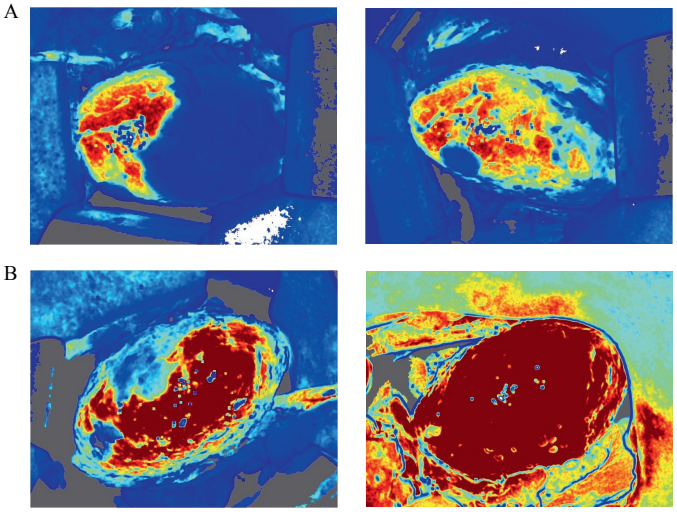


Figure S1. Representative LSCI images of cases showing intraoperative abnormalities and improved renal cortical perfusion after intervention. (A) The kidney required arterial reconstruction due to the dual donor renal artery branches without a patch. LSCI revealed extensive perfusion deficiency in the upper pole after reperfusion (left). The arterial anastomosis was reconstructed, and the LSCI demonstrated improved perfusion (right); (B) LSCI revealed a localized perfusion defect after reperfusion (left). Intraoperative assessment identified artery kinking, which was corrected by adjusting graft position. Subsequent LSCI imaging confirmed adequate perfusion (right).

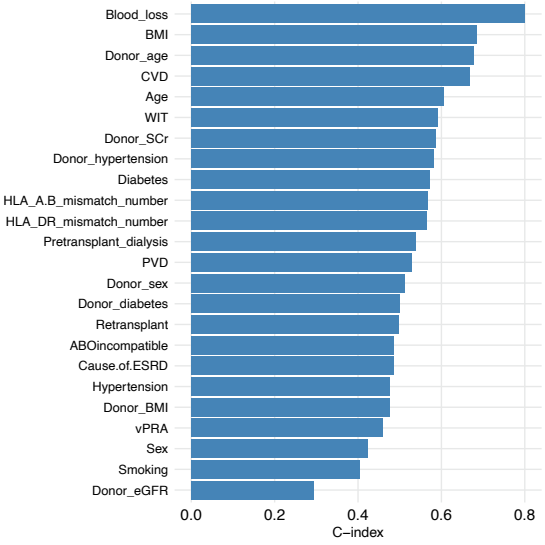


Figure S2. Concordance index (C-index) of all candidate predictor variables used for Clinical Model development. Each bar represents the C-index of a single variable in discriminating between "Stable" and "High-risk" graft outcomes.

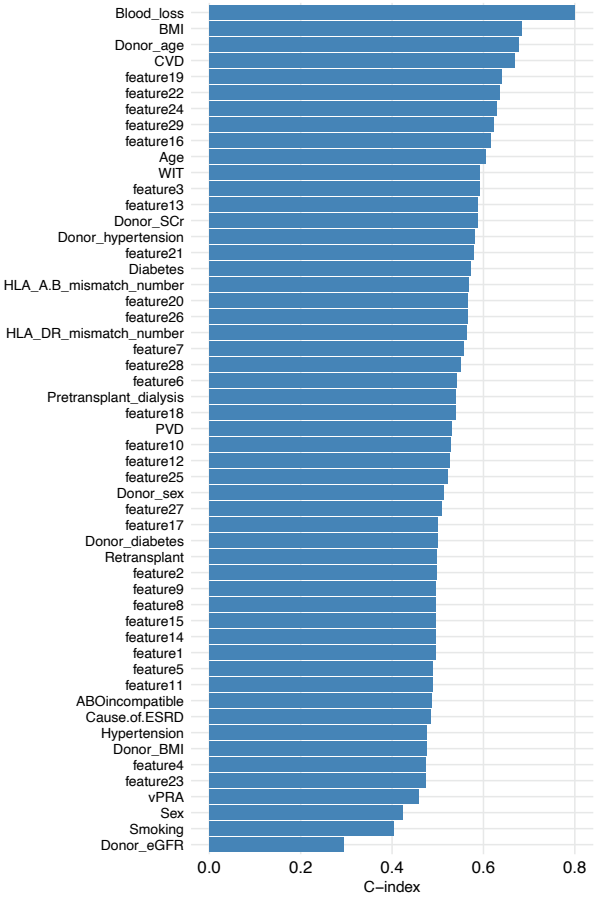
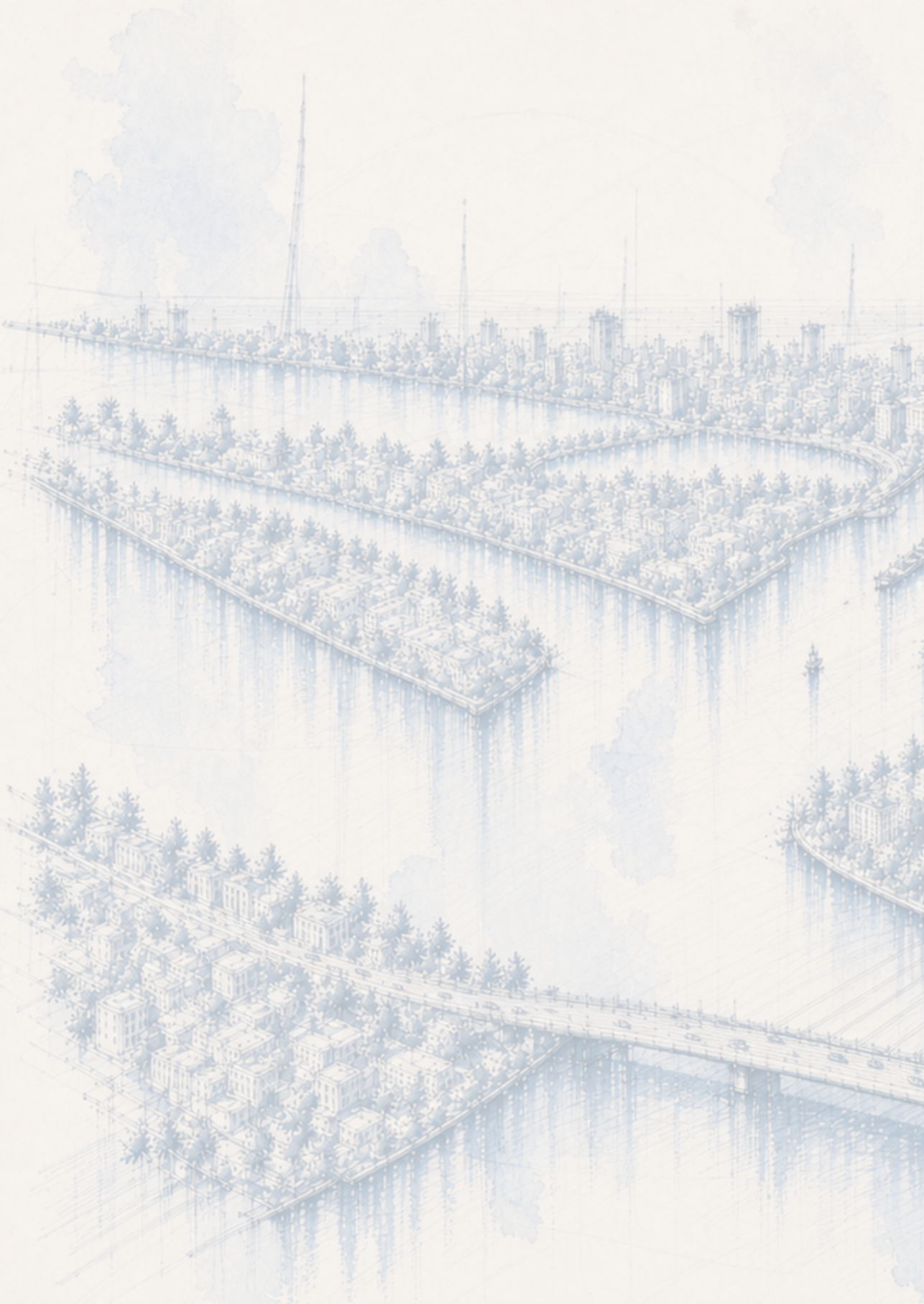
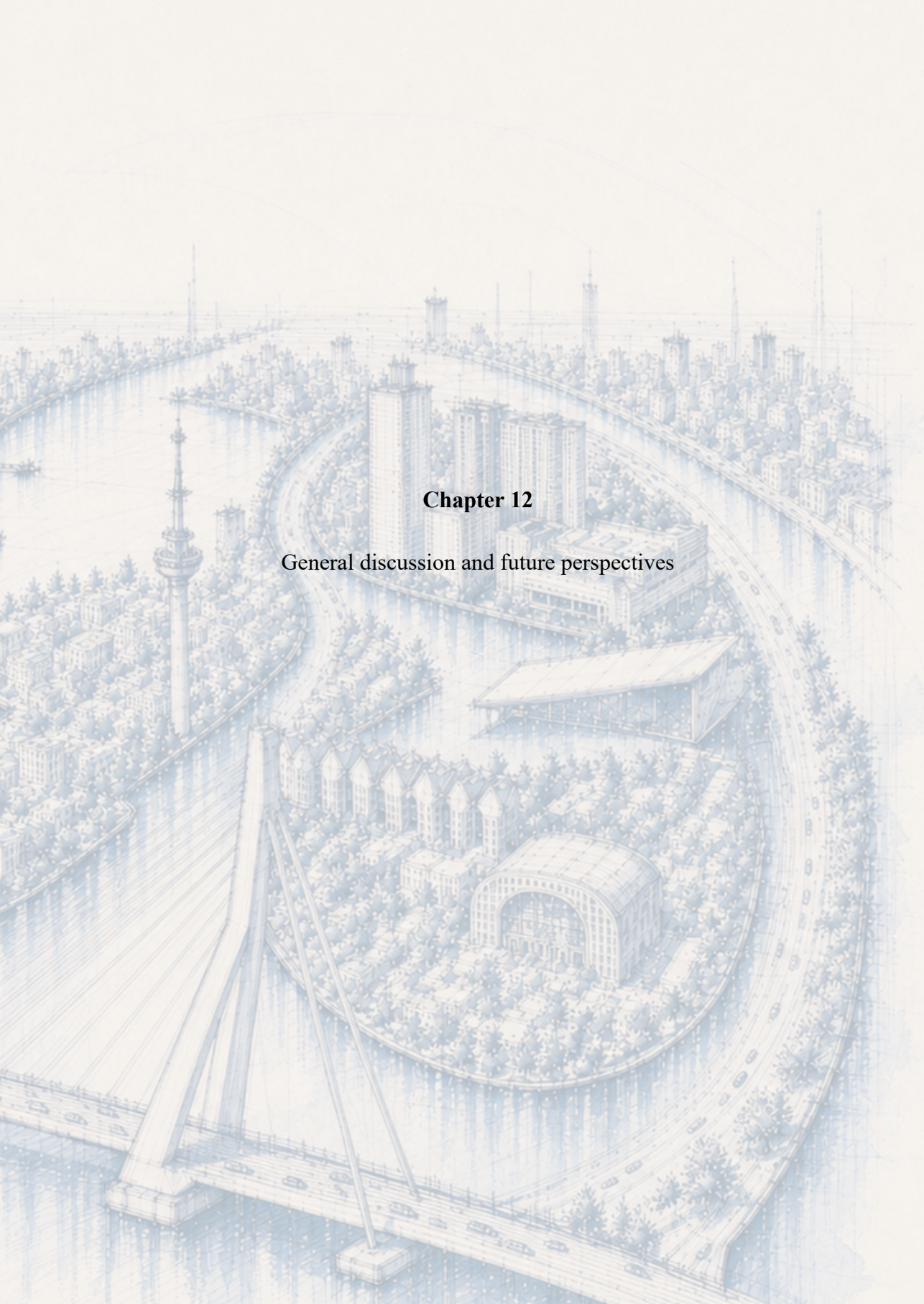


Figure S3. Concordance index (C-index) of all candidate predictor variables used for Combined Model development. Each bar represents the C-index of a single variable in discriminating between "Stable" and "High-risk" graft outcomes.





Chapter 12

General discussion and future perspectives

Discussion and Future Perspectives

Kidney transplantation remains the only definitive treatment that improves both survival and quality of life in end-stage renal disease (ESRD) patients.[1-3] Meanwhile, a persistent global shortage of donor organs limits the access to this life-saving therapy. These facts demand a dual approach: safely extending recipient eligibility criteria to include more patients who can benefit from transplantation, and enhancing the utilization of marginal donor kidneys, all while preserving residual renal function in susceptible population whenever possible. **Part I** of this thesis focuses on pre-clinical research using normothermic machine perfusion (NMP) as a dynamic assessment platform, which allows novel imaging techniques and perfusion parameters to guide transplantability decisions. **Part II** focuses on clinical research, examining transplant outcomes in high-risk recipients and exploring the potential of imaging techniques for early identification of adverse outcomes

Optimizing Transplant Eligibility Criteria

Historically, transplant eligibility criteria have been conservative, excluding individuals with significant comorbidities due to surgical risks, posttransplant complications, and inferior long-term survival.[4-9] However, with ongoing advances in surgical techniques and posttransplant management, these boundaries are being reassessed, providing opportunities to optimize transplant criteria to previously excluded populations.

Patients with obesity have reduced access to kidney transplantation despite obesity not being an absolute contraindication.[10] Ideally, bariatric surgery should be performed during the early stages of chronic kidney disease (CKD), as it is associated with remission of albuminuria and improved renal function.[11] However, in ESRD patients, bariatric surgery helps improve transplant candidacy by stable weight loss, but not renal function.[12] Pretransplant bariatric surgery may also prolong time on dialysis while awaiting weight loss and recovery. **Chapter 6** demonstrates that kidney transplantation is safe and feasible in ESRD patients with obesity, regardless of whether bariatric surgery is performed before or after transplantation. Both surgical sequences can achieve favorable patient and graft survival, with acceptable rates of postoperative complications. These findings support a flexible and individual approach, allowing tailored surgical sequencing based on individual risk profiles and surgeon expertise.

Aortoiliac atherosclerotic stenosis is commonly observed in ESRD patients and considered as a relative contraindication.[13] In **Chapter 7**, we investigated the impact of aortoiliac stenosis on long-term transplant outcomes using the Trans-Atlantic Inter-Society Consensus (TASC) II classification.[14] Our findings revealed that compared to remaining on dialysis, kidney transplantation effectively prolongs survival and improves the quality of life in patients with TASC A/B stenosis.[15, 16] For patients with TASC C/D stenosis, kidney transplantation distinctly improves quality of life but does not translate into survival benefits, suggesting that careful patient selection and individualized counseling are essential. Meanwhile, the presence of vascular stenosis did not adversely affect graft survival or function.

Patients with concurrent end-stage liver disease and CKD represent another challenge for transplant decision-making in the context of persistent organ shortage. One key question is whether simultaneous liver-kidney transplantation (SLKT) offers a survival advantage over liver transplantation alone (LTA), and how pretransplant renal function should guide organ allocation. Using data from the Dutch Organ Transplantation Registration and the Organ Procurement and Transplant Network (OPTN)/United Network for Organ Sharing (UNOS) registry, **Chapter 8** and **9** demonstrate that in patients with mild to moderate CKD, liver transplantation alone achieves comparable patient and liver graft survival to SLKT. In contrast, for patients with advanced CKD or on dialysis, SLKT provides significant survival benefits, particularly during the first decade after transplantation. These findings highlight the critical role of pretransplant renal function in transplant strategy, supporting SLKT for patients with severe or irreversible renal impairment while reserving LTA for those with preserved renal function, thereby optimizing organ utilization while maintaining long-term outcomes.

Preservation Strategy for High-Risk Kidneys

Among preservation techniques, NMP has emerged as a particularly promising strategy for evaluating and potentially reconditioning high-risk kidneys. By providing a near-physiological environment, NMP enables real-time functional assessment, cellular metabolic recovery and adenosine triphosphate (ATP) synthesis. Despite these advantages,

its implementation requires clinically certified devices, disposables and trained perfusionists. These factors limit its routine application compared to SCS or HMP.

One of the key questions is which donor kidney should undergo NMP. Currently, this decision largely depends on institutional protocols, experience of surgeons and researchers, and organ-specific conditions. Existing literature highlights diverse applications of NMP. Hosgood et al.[17, 18] performed NMP on controlled donation after circulatory death (DCD) kidneys that were deemed suitable for transplantation. Minor et al.[19] applied controlled rewarming and NMP on an expanded criteria donors (ECD) kidney with a high Kidney Donor Risk Index. Rijkse et al.[20] applied 2-hour NMP on both donation after brain death (DBD) and DCD kidneys in the Eurotransplant Senior Program. Additionally, Hosgood et al.[21] also reported that 5 out of 10 initially declined kidneys were successfully transplanted based on the quality assessment during 1-hour NMP.

Nonetheless, short-duration NMP (typically 1-2 hours) has not yet demonstrated significant improvements in post-transplant outcomes in these marginal grafts.[18] Therefore, the clinical utility of NMP should be justified by clear benefits, which is safely improving the utilization of high-risk kidneys, that outweigh the added costs and time. Currently, NMP should primarily target at the kidneys of uncertain transplantability, typically the ECD kidneys that an objective assessment may facilitate safe transplantation and reduce unnecessary discards.

The next challenge is to define standardized criteria to determine kidney transplantability based on NMP parameters. As described in **Chapter 1**, a wide range of parameters can inform this decision, including perfusion dynamics, functional biomarkers, and cellular biomarkers.[21-26] For example, Hosgood et al.[21, 22] developed a quality assessment score based on one-hour NMP data including macroscopic perfusion, renal blood flow, and urine production.

However, it is important to emphasize that the use of different perfusion devices and protocols can substantially influence observations during NMP in terms of perfusion parameters and functional markers.[27] **Chapter 5** demonstrates how kidneys with similar baseline characteristics can exhibit different performance depending on arterial perfusion pressure. This finding shows that raising perfusion pressure to physiological levels may

improve function in kidneys with borderline viability, underscoring the need for optimizing perfusion protocols that balance restoration of function with minimization of injury.

To fully realize the potential of NMP, it is essential to move toward standardized protocols and evidence-based transplantability criteria, ideally supported by large clinical transplant data. Such standardization will enable better comparison across studies, improve clinical decision-making, and allow more equitable access to advanced preservation strategies.

Medical Imaging in Machine Perfusion

Medical imaging techniques hold the potential to better understand intrarenal physiological processes, providing valuable insight through imaging-derived biomarkers of organ function and injury.

While imaging modalities such as ultrasound, computed tomography (CT), and magnetic resonance imaging (MRI) are widely used in clinical practice to evaluate vascular anatomy pre-transplant and vascular patency post-transplant, their application during NMP for real-time kidney quality assessment remains largely in the exploratory phase.

Recent studies have explored the feasibility of integrating imaging into NMP protocols. Schutter et al.[28] and Hamelink et al.[29] demonstrated the potential of MRI to monitor dynamic redistribution of perfusion in the renal cortex and medulla. Thompson et al.[30] applied contrast-enhanced ultrasound (CEUS), which uses inert gas-filled microbubbles as contrast agents, to assess microvascular perfusion during NMP. Based on ionizing radiation imaging, Valenzuela et al.[31] utilized fluoroscopy in perfused porcine kidneys to quantify anatomical dimensions in the main renal arteries. Additionally, Heeman et al.[32] reported the use of side-stream dark-field (SDF) imaging and laser speckle contrast imaging (LSCI) to measure renal blood flow in a porcine NMP model.

Moreover, **Chapter 2** explores the use of LSCI in assessing renal cortical perfusion, and compares dual- versus single-sided measurements to determine added diagnostic value. **Chapter 3** introduces the utility of photoacoustic (PA) imaging in measuring renal cortical oxygenation and examining correlations with markers of kidney viability. **Chapter 4**

describes the feasibility of Power Doppler (PD) imaging in visualizing renal cortical circulation, even in kidneys of low blood flow.

Given the unique strengths of each modality, medical imaging should be considered for routine implementation. However, the selection of the most suitable imaging modality should be tailored to the characteristics and clinical context of the donor kidney. LSCI is non-contact, non-invasive, and broadly applicable to all kidneys undergoing NMP. It is especially valuable for kidneys with high intrarenal resistance, suspected perfusion insufficiency, or vascular anatomical abnormalities, as it can semi-quantify perfusion heterogeneity and guide potential interventions. PA imaging offers molecular-level information by quantifying tissue-specific components. For example, the ratio of oxygenated to deoxygenated hemoglobin can be used to assess viability in kidneys with prolonged warm ischemia. PA can also detect collagen components, enabling non-invasive assessment of renal fibrosis and transplant suitability. PD imaging allows for high-resolution visualization of renal cortical vasculature under low-flow conditions, making it valuable in marginal kidneys or those with suspected microvascular dysfunction, where conventional flow metrics may be inadequate. Ultimately, incorporating targeted imaging modalities during NMP has the potential to support clinical decision-making, increase the utilization of marginal grafts, and improve transplant outcomes.

Prolonged Machine Perfusion for Kidney Repair

Kidney NMP has been safely translated into clinical practice by several studies. All applications, however, are thus far limited to short perfusion durations (1-2 hours).[18, 21, 33, 34] To fully leverage NMP's potential as a platform for therapeutic delivery and organ repair, prolonged NMP is required.

In preclinical settings, Weissenbacher et al.[35, 36] demonstrated the feasibility of 24-48 hours of NMP in discarded human kidneys using red cell-based perfusate. Despite this progress, extended NMP introduces new challenges and safety concerns. For example, endothelial injury has been observed during NMP longer than 6 hours and may adversely affect transplant outcomes.[37] Arykbaeva et al.[38] identified progressive hemolysis during prolonged NMP, which leads to oxidative stress and toxic accumulation of hemolysis byproducts, compromising graft viability.

Nevertheless, prolonged NMP remains a promising therapeutic window for ex vivo organ conditioning, enabling localized drug delivery while avoiding systemic toxicity. For example, Bagul et al.[39] reported that carbon monoxide supplementation in the perfusate exhibited protective effects against ischemia reperfusion injury in a porcine kidney reperfusion model. For cellular therapy, administration of mesenchymal stromal cells (MSCs) were found to be safe, with MSCs surviving and accumulating in glomerular capillaries in porcine kidney NMP model.[40, 41] Furthermore, ex vivo perfusion of DCD kidneys with human MSCs for 24 hours has been shown to enhance renal regeneration.[42] Thompson et al.[30] also explored the use of multipotent adult progenitor cells (MAPCs) to reduce ischemia reperfusion injury during ex vivo kidney perfusion. Tietjen et al.[43] reported the use of polymeric nanoparticles as drug delivery vehicles to the vascular endothelial cells during NMP, allowing for sustained and localized drug release.

Beyond normothermic strategies, alternative approaches such as subzero and ultralow-temperature preservation have emerged as promising methods to extend organ preservation duration. Sharma et al.[44] reported the successful rewarming of rat kidneys with preserved morphology and good viability which was preserved at -150 °C with cryoprotective agents and silica-coated iron oxide nanoparticles. Loftin et al.[45] demonstrated that kidneys preserved at -5°C for 72 hours using peptoid anti-icing agents were able to restore normal renal function after autotransplantation in a porcine model. These supercooling and cryopreservation approaches serves as promising alternatives to NMP, potentially enabling longer preservation duration. However, their therapeutic safety and efficacy remain to be further validated.

While prolonged NMP offers a unique platform for organ repair and therapeutic intervention, it requires further refinement to mitigate associated risks. Continued development and validation of therapeutic strategies, along with optimization of perfusion protocols, will be critical to translating prolonged machine perfusion into routine clinical practice.

Combined Organ Perfusion

In addition to extending the duration of NMP, combined organ perfusion has emerged as a promising strategy to improve donor graft quality.

Compared to solitary organ perfusion, combing multiple organs in one perfusion circuit not only reduces the need of labor, equipment, and costs, but also helps to restore physiological homeostasis, thereby contributing to improved organ preservation and reconditioning.

In standard solitary NMP, the organ is perfused in isolation, allowing for objective assessment of function and application of regenerative therapies. However, the absence of supporting organ systems in solitary perfusion may limit the physiological fidelity of the environment, potentially compromising organ quality. For example, the liver is a crucial metabolic hub that plays a crucial role in detoxification, protein synthesis, and metabolic regulation. Incorporating the liver into a kidney perfusion circuit may prolong renal viability by mitigating the accumulation of toxic metabolites in the system. On the other hand, the kidney plays an important role in electrolyte balance and excretion of metabolic waste products, which in turn can support liver function during NMP.

In clinical practice, normothermic regional perfusion (NRP), which involves in situ machine perfusion of a portion of the donor's body using extracorporeal organ support, has shown increased graft utilization and improved outcomes in DCD transplantation.[46-51]

In preclinical settings, several studies have demonstrated the feasibility and advantages of combined liver-kidney NMP. Compared to solitary liver NMP, combined liver-kidney perfusion has been associated with a more favorable biochemical milieu, improved regenerative capability and reduced biliary epithelium injury and inflammatory cytokine release.[52, 53] Similarly, when compared to solitary kidney NMP, combined liver kidney NMP has shown lower lactate level, less severe renal tubular epithelium vacuolization, and reduced expression of renal pro-inflammatory factors.[54]

Furthermore, the sequence in which organs are subjected into the perfusion circuit also impacts perfusion dynamics and metabolic stability. For example, a kidney-first perfusion sequence has been shown to produce more stable and physiologically aligned parameters, such as urine output, glucose, pH, lactate, and electrolyte balance, when compared to a liver-first modality.[55]

We have recently initiated experimental combined liver-kidney NMP, and results are expected later this year. This strategy holds the potential to salvage marginal kidneys and

livers that are currently deemed unsuitable for transplantation. While early data are encouraging, further investigation is needed to determine whether combined machine perfusion can reliably improve donor organ quality and translate into improved long-term outcomes.

Organ Hub: A Centralized Strategy for Organ Preservation and Translational Research

With the continuous advancement of machine perfusion technologies, the concept of Organ Hub has gained increasing interest as a transformative shift in the logistics, preservation, and organ management. Currently, the role of organ hubs is largely limited to facilitating organ donation and allocation.[56] Machine perfusion and organ quality assessment are predominantly performed at individual transplant centers, which is under time constraints and with variable access to perfusion devices and protocols.

In the future perspective, the Organ Hub envisions a centralized facility equipped with high-capacity machine perfusion systems capable of simultaneously perfusing, assessing, and reconditioning multiple organs. This model offers several clinical and logistical advantages. Standardized perfusion protocols, quality assessment criteria, and decision-making algorithms can reduce inter-institutional variability and support objective and reproducible quality assessments. Concentrating specialized personnel and advanced technologies, including real-time imaging, molecular diagnostics, and ex vivo therapeutic interventions, would also enable complex organ repair strategies that are difficult to implement consistently across all transplant centers. In this way, organ hubs have the potential to improve organ utilization while reducing procedural redundancy and enhancing cost-effectiveness at the system level.

Beyond its clinical role, the Organ Hub could serve as a unique infrastructure for translational research. Rather than each transplant center's independent work, centralized hubs could coordinate research efforts, thereby reducing unnecessary consumption of donor organs and perfusion resources, and accelerating the generation of robust evidence. Such a collaborative framework would also facilitate harmonization of study protocols, improve reproducibility, and enhance comparability across institutions.

Importantly, the Organ Hub would enable the establishment of large-scale databases integrating donor characteristics, perfusion parameters, multimodal imaging, omics profiles, therapeutic interventions, and post-transplant outcomes. These comprehensive datasets are essential for developing and externally validating artificial intelligence models for organ quality assessment and outcome prediction. Such high-quality multicenter data would further support precision transplantation by enabling individualized organ-recipient matching and evidence-based clinical decision-making.

Significant challenges must be addressed before this vision can be realized. Further technological refinement are required to improve the reliability of machine perfusion systems, while efficient transportation networks must ensure timely delivery of organs to and from centralized facilities. In addition, substantial investment in infrastructure, harmonized regulatory frameworks, and standardized operating procedures will be necessary to enable collaboration across transplant centers and national organ allocation systems.

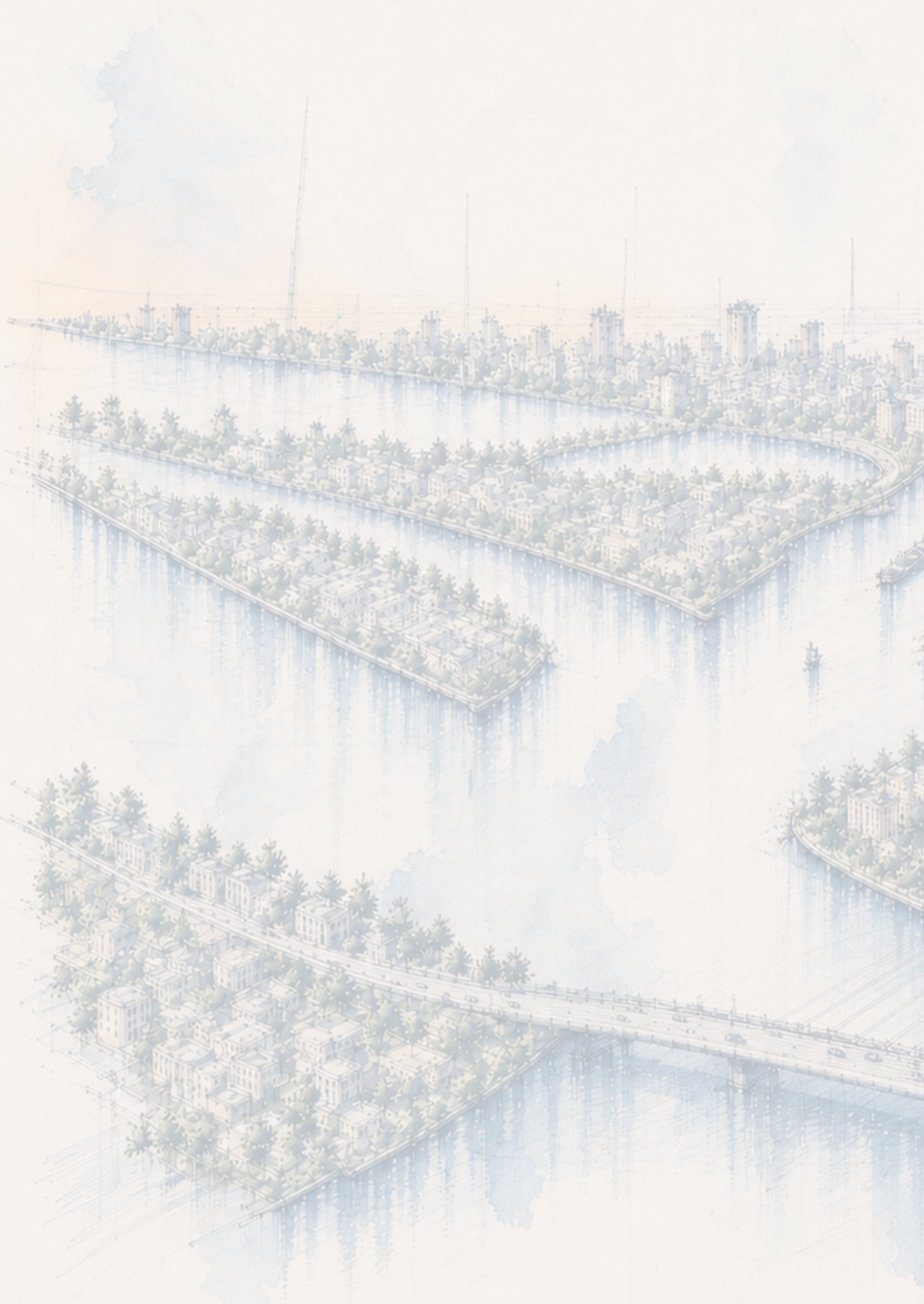
Nevertheless, the Organ Hub represents more than a logistical innovation. It provides a platform for integrating clinical care, technological innovation, and collaborative research. As machine perfusion evolves from a preservation technique toward a platform for organ repair, regeneration, and precision assessment, Organ Hubs are likely to become key drivers of future transplantation research and practice, bringing the field closer to the vision of "one organ for life."

Reference

1. Tonelli M, Wiebe N, Knoll G, Bello A, Browne S, Jadhav D, et al. Systematic review: kidney transplantation compared with dialysis in clinically relevant outcomes. Am J Transplant. 2011;11(10):2093-109.
2. Boenink R, Astley ME, Huijben JA, Stel VS, Kerschbaum J, Ots-Rosenberg M, et al. The ERA Registry Annual Report 2019: summary and age comparisons. Clin Kidney J. 2022;15(3):452-72.
3. Hussien H, Apetrii M, Covic A. Health-related quality of life in patients with chronic kidney disease. Expert Rev Pharmacoecon Outcomes Res. 2021;21(1):43-54.
4. Lafranca JA, JN IJ, Betjes MG, Dor FJ. Body mass index and outcome in renal transplant recipients: a systematic review and meta-analysis. BMC Med. 2015;13:111.
5. Aalten J, Christiaans MH, de Fijter H, Hene R, van der Heijde JH, Roodnat J, et al. The influence of obesity on short- and long-term graft and patient survival after renal transplantation. Transpl Int. 2006;19(11):901-7.
6. Ozcelik A, Treckmann J, Paul A, Witzke O, Sotiropoulos G, Nadalin S, et al. Results of kidney transplantation with simultaneous implantation of vascular graft. Transplant Proc. 2007;39(2):509-10.
7. Tsivian M, Neri F, Nardo B, Bertelli R, Cavallari G, Fuga G, et al. Aortoiliac surgery concomitant with kidney transplantation: a single center experience. Clin Transplant. 2009;23(2):164-7.
8. Liew YP, Bartholomew JR, Demirjian S, Michaels J, Schreiber MJ, Jr. Combined effect of chronic kidney disease and peripheral arterial disease on all-cause mortality in a high-risk population. Clin J Am Soc Nephrol. 2008;3(4):1084-9.
9. Rajagopalan S, Dellegrottaglie S, Furniss AL, Gillespie BW, Satayathum S, Lameire N, et al. Peripheral arterial disease in patients with end-stage renal disease: observations from the Dialysis Outcomes and Practice Patterns Study (DOPPS). Circulation. 2006;114(18):1914-22.
10. Lassalle M, Fezeu LK, Couchoud C, Hannedouche T, Massy ZA, Czernichow S. Obesity and access to kidney transplantation in patients starting dialysis: A prospective cohort study. PLoS One. 2017;12(5):e0176616.
11. Cohen RV, Pereira TV, Aboud CM, Petry TBZ, Lopes Correa JL, Schiavon CA, et al. Effect of Gastric Bypass vs Best Medical Treatment on Early-Stage Chronic Kidney Disease in Patients With Type 2 Diabetes and Obesity: A Randomized Clinical Trial. JAMA Surg. 2020;155(8):e200420.
12. Kassam AF, Mirza A, Kim Y, Hanseman D, Woodle ES, Quillin RC, 3rd, et al. Long-term outcomes in patients with obesity and renal disease after sleeve gastrectomy. Am J Transplant. 2020;20(2):422-9.
13. Chadban SJ, Ahn C, Axelrod DA, Foster BJ, Kasiske BL, Kher V, et al. Summary of the Kidney Disease: Improving Global Outcomes (KDIGO) Clinical Practice Guideline on the Evaluation and Management of Candidates for Kidney Transplantation. Transplantation. 2020;104(4):708-14.
14. Norgren L, Hiatt WR, Dormandy JA, Nehler MR, Harris KA, Fowkes FG, et al. Inter-Society Consensus for the Management of Peripheral Arterial Disease (TASC II). J Vasc Surg. 2007;45 Suppl S:S5-67.
15. Eknoyan G, Beck GJ, Cheung AK, Daugirdas JT, Greene T, Kusek JW, et al. Effect of dialysis dose and membrane flux in maintenance hemodialysis. N Engl J Med. 2002;347(25):2010-9.
16. Bourrier M, Ferguson TW, Embil JM, Rigatto C, Komenda P, Tangri N. Peripheral Artery Disease: Its Adverse Consequences With and Without CKD. Am J Kidney Dis. 2020;75(5):705-12.
17. Hosgood SA, Saeb-Parsy K, Wilson C, Callaghan C, Collett D, Nicholson ML. Protocol of a randomised controlled, open-label trial of ex vivo normothermic perfusion versus static cold storage in donation after circulatory death renal transplantation. BMJ Open. 2017;7(1):e012237.
18. Hosgood SA, Callaghan CJ, Wilson CH, Smith L, Mullings J, Mehew J, et al. Normothermic machine perfusion versus static cold storage in donation after circulatory death kidney transplantation: a randomized controlled trial. Nat Med. 2023;29(6):1511-9.
19. Minor T, von Horn C, Gallinat A, Kaths M, Kribben A, Treckmann J, et al. First-in-man controlled rewarming and normothermic perfusion with cell-free solution of a kidney prior to transplantation. Am J Transplant. 2020;20(4):1192-5.
20. Rijkse E, de Jonge J, Kimenai H, Hoogduijn MJ, de Bruin RWF, van den Hoogen MWF, et al. Safety and feasibility of 2 h of normothermic machine perfusion of donor kidneys in the Eurotransplant Senior Program. BJS Open. 2021;5(1).
21. Hosgood SA, Thompson E, Moore T, Wilson CH, Nicholson ML. Normothermic machine perfusion for the assessment and transplantation of declined human kidneys from donation after circulatory death donors. Br J Surg. 2018;105(4):388-94.
22. Hosgood SA, Barlow AD, Hunter JP, Nicholson ML. Ex vivo normothermic perfusion for quality assessment of marginal donor kidney transplants. Br J Surg. 2015;102(11):1433-40.
23. Kaths JM, Hamar M, Echeverri J, Linares I, Urbanellis P, Cen JY, et al. Normothermic ex vivo kidney perfusion for graft quality assessment prior to transplantation. Am J Transplant. 2018;18(3):580-9.

24. Hosgood SA, Brown RJ, Nicholson ML. Advances in Kidney Preservation Techniques and Their Application in Clinical Practice. Transplantation. 2021;105(11):E202-E14.
25. Woud WW, Merino A, Hoogduijn MJ, Boer K, van den Hoogen MWF, Baan CC, et al. Nanoparticle Release by Extended Criteria Donor Kidneys During Normothermic Machine Perfusion. Transplantation. 2019;103(5):e110-e1.
26. Rigalli JP, Barros ER, Sommers V, Bindels RJM, Hoenderop JGJ. Novel Aspects of Extracellular Vesicles in the Regulation of Renal Physiological and Pathophysiological Processes. Front Cell Dev Biol. 2020;8:244.
27. Lantinga VA, Arykbaeva AS, Spraakman NA, Blom EWP, Huijink TM, de Vries DK, et al. Impact of device variability and protocol differences on kidney function during normothermic machine perfusion: A comparative study using porcine and human kidneys. Artif Organs. 2025;49(1):93-107.
28. Schutter R, Lantinga VA, Hamelink TL, Pool MBF, van Varsseveld OC, Potze JH, et al. Magnetic resonance imaging assessment of renal flow distribution patterns during ex vivo normothermic machine perfusion in porcine and human kidneys. Transpl Int. 2021;34(9):1643-55.
29. Hamelink TL, Ogurlu B, Pamplona CC, Castelein J, Bennedsgaard SS, Qi H, et al. Magnetic resonance imaging as a noninvasive adjunct to conventional assessment of functional differences between kidneys in vivo and during ex vivo normothermic machine perfusion. Am J Transplant. 2024.
30. Thompson ER, Bates L, Ibrahim IK, Sewpaul A, Stenberg B, McNeill A, et al. Novel delivery of cellular therapy to reduce ischemia reperfusion injury in kidney transplantation. Am J Transplant. 2021;21(4):1402-14.
31. Valenzuela TF, Schinstock E, Kohnle S, Latib A, Bliagos D, Tunev S, et al. Preclinical research performed on reanimated/perfused swine kidneys: The Visible Kidney methodologies. Physiol Rep. 2023;11(5):e15630.
32. Heeman W, Maassen H, Calon J, van Goor H, Leuvenink H, van Dam GM, et al. Real-time visualization of renal microperfusion using laser speckle contrast imaging. J Biomed Opt. 2021;26(5).
33. Rijkse E, de Jonge J, Kimenai HJAN, Hoogduijn MJ, de Bruin RWF, van den Hoogen MWF, et al. Safety and feasibility of 2 h of normothermic machine perfusion of donor kidneys in the Eurotransplant Senior Program. Bjs Open. 2021;5(1).
34. Mazilescu LI, Urbanellis P, Kim SJ, Goto T, Noguchi Y, Konvalinka A, et al. Normothermic Ex Vivo Kidney Perfusion for Human Kidney Transplantation: First North American Results. Transplantation. 2022;106(9):1852-9.
35. Weissenbacher A, Lo Faro L, Boubriak O, Soares MF, Roberts IS, Hunter JP, et al. Twenty-four-hour normothermic perfusion of discarded human kidneys with urine recirculation. Am J Transplant. 2019;19(1):178-92.
36. Weissenbacher A, Messner F, Gasteiger S, Soleiman A, Ofner D, Schneeberger S. Forty-eight hours of normothermic kidney preservation applying urine recirculation. Artif Organs. 2022;46(4):710-4.
37. Huijink TM, van 't Hof CJ, van Furth LA, de Haan NA, Maassen H, Venema LH, et al. Loss of Endothelial Glycocalyx During Normothermic Machine Perfusion of Porcine Kidneys Irrespective of Pressure and Hematocrit. Transplant Direct. 2023;9(8):e1507.
38. Arykbaeva AS, Lerink LJS, Vos J, Engelse MA, van Kooten C, de Korte D, et al. Red blood cells as oxygen carrier during normothermic machine perfusion of kidney grafts: Friend or foe? American Journal of Transplantation. 2024;24(7):1172-9.
39. Bagul A, Hosgood SA, Kaushik M, Nicholson ML. Carbon monoxide protects against ischemia-reperfusion injury in an experimental model of controlled nonheartbeating donor kidney. Transplantation. 2008;85(4):576-81.
40. Pool M, Eertman T, Parraga JS, 't Hart N, Roemeling-van Rhijn M, Eijken M, et al. Infusing Mesenchymal Stromal Cells into Porcine Kidneys during Normothermic Machine Perfusion: Intact MSCs Can Be Traced and Localised to Glomeruli. International Journal of Molecular Sciences. 2019;20(14).
41. Lohmann S, Pool MBF, Rozenberg KM, Keller AK, Moers C, Moldrup U, et al. Mesenchymal stromal cell treatment of donor kidneys during ex vivo normothermic machine perfusion: A porcine renal autotransplantation study. Am J Transplant. 2021;21(7):2348-59.
42. Brasile L, Henry N, Orlando G, Stubenitsky B. Potentiating Renal Regeneration Using Mesenchymal Stem Cells. Transplantation. 2019;103(2):307-13.
43. Tietjen GT, Hosgood SA, DiRito J, Cui J, Deep D, Song E, et al. Nanoparticle targeting to the endothelium during normothermic machine perfusion of human kidneys. Sci Transl Med. 2017;9(418).
44. Sharma A, Rao JS, Han Z, Gangwar L, Namsrai B, Gao Z, et al. Vitrification and Nanowarming of Kidneys. Adv Sci (Weinh). 2021;8(19):e2101691.
45. Loftin A, Guo YN, Kim H, Zhang YC, Drivas E, Rosenberg A, et al. First successful preclinical transplantation following extended subzero porcine kidney preservation with nature inspired cryoprotectants. Transplantation. 2024;108(9s).

46. Oniscu GC, Randle LV, Muiesan P, Butler AJ, Currie IS, Perera MT, et al. In situ normothermic regional perfusion for controlled donation after circulatory death--the United Kingdom experience. Am J Transplant. 2014;14(12):2846-54.
47. Watson CJE, Hunt F, Messer S, Currie I, Large S, Sutherland A, et al. In situ normothermic perfusion of livers in controlled circulatory death donation may prevent ischemic cholangiopathy and improve graft survival. Am J Transplant. 2019;19(6):1745-58.
48. Hessheimer AJ, Coll E, Torres F, Ruiz P, Gastaca M, Rivas JI, et al. Normothermic regional perfusion vs. super-rapid recovery in controlled donation after circulatory death liver transplantation. J Hepatol. 2019;70(4):658-65.
49. Muller X, Rossignol G, Damotte S, Gregoire A, Matillon X, Morelon E, et al. Graft utilization after normothermic regional perfusion in controlled donation after circulatory death-a single-center perspective from France. Transpl Int. 2021;34(9):1656-66.
50. Gaurav R, Butler AJ, Kosmoliaptsis V, Mumford L, Fear C, Swift L, et al. Liver Transplantation Outcomes From Controlled Circulatory Death Donors: SCS vs in situ NRP vs ex situ NMP. Ann Surg. 2022;275(6):1156-64.
51. Bekki Y, Croome KP, Myers B, Sasaki K, Tomiyama K. Normothermic Regional Perfusion Can Improve Both Utilization and Outcomes in DCD Liver, Kidney, and Pancreas Transplantation. Transplant Direct. 2023;9(3):e1450.
52. Chung WY, Gravante G, Al-Leswas D, Alzaraa A, Sorge R, Ong SL, et al. The autologous normothermic ex vivo perfused porcine liver-kidney model: improving the circuit's biochemical and acid-base environment. Am J Surg. 2012;204(4):518-26.
53. He X, Ji F, Zhang Z, Tang Y, Yang L, Huang S, et al. Combined liver-kidney perfusion enhances protective effects of normothermic perfusion on liver grafts from donation after cardiac death. Liver Transpl. 2018;24(1):67-79.
54. Li F, Zhang Y, Ruan H, He Y, Zhan L, Chen S, et al. Addition of a liver to the normothermic perfusion circuit reduces renal pro-inflammatory factors. Artif Organs. 2023;47(11):1732-41.
55. Chung WY, Gravante G, Eltweri A, Sorge R, Ong SL, Pollard C, et al. The "kidney-liver" multiorgan ex vivo perfused model improves the circuit's biochemical milieu during perfusion compared to the "liver-kidney" counterpart. J Artif Organs. 2015;18(2):151-61.
56. ODT Hub 2017 [Available from: https://www.odt.nhs.uk/odt-structures-and-standards/odt-hub-programme/odt-hub/.





APPENDICES

Summary

In the absence of fully mature xenotransplantation and artificial organ technologies, kidney transplantation remains the optimal treatment for patients with end-stage renal disease (ESRD). To address the persistent organ shortage and improve patient prognosis, three strategies are crucial: extending recipient eligibility to include more patients who may benefit from transplantation, increasing the utilization of marginal donor kidneys through objective assessment, and preserving residual renal function in patients with chronic kidney disease (CKD) to delay or avoid transplantation.

Part I Organ Quality Assessment during Machine Perfusion

In **Chapter 2**, we explored the utility of laser speckle contrast imaging (LSCI) for assessing renal microcirculation in a porcine normothermic machine perfusion (NMP) model. LSCI enabled visualization and semi-quantification of renal cortical perfusion and ischemia, with LSCI flux showing a linear correlation with renal blood flow. After we induced renal artery branch occlusion, the overall ischemic area percentage of the ventral and dorsal sides was comparable, but heterogenous patterns between the two aspects were observed by LSCI measurements. Dual-side LSCI measurements are of added value compared to single aspect measurement and renal function markers, as no significant difference was found in creatinine clearance, fractional excretion of sodium, total sodium reabsorption and histological damage before and after renal artery occlusion.

In **Chapter 3**, we monitored renal cortical oxygenation (sO_2) using photoacoustic (PA) imaging during NMP in 22 porcine kidneys. Based on renal function and viability biomarkers, the kidneys were categorized into “non-functional” and “functional” groups. PA-derived sO_2 levels effectively differentiated between functional and non-functional kidneys. The non-functional kidneys can be detected with a cut-off value of $sO_2 < 39\%$, with the sensitivity and specificity of 80% and 85%, respectively. sO_2 correlated with renal blood flow and oxygen consumption in all kidneys. In functional kidneys, sO_2 also correlated with creatinine clearance, supporting PA imaging as a potential non-invasive viability biomarker.

In **Chapter 4**, we investigated the role of Power Doppler (PD) in kidney quality assessment during NMP. PD-derived metrics, including vascularization index (VI), flow index (FI), and vascularization flow index (VFI) were calculated. FI and VFI moderately correlated with creatinine clearance, while VI strongly correlated with oxygen consumption. At 120 minutes of NMP, these metrics demonstrated high diagnostic accuracy in distinguishing between kidneys with higher and lower viability. Cutoff values of 17% for VI, 50 a.u. for FI, and 9 a.u. for VFI provided 100% specificity and 73% sensitivity in identifying kidneys with low viability, with an overall diagnostic accuracy of 82%. PD imaging can be a valuable alternative to RBF during NMP for kidney quality assessment.

Kidneys from donation after circulatory death (DCD) donors are associated with great ischemic injury and high intrarenal resistance (IRR), making them deemed unsuitable for transplantation due to poor functional performance during NMP. In **Chapter 5**, we evaluated how different perfusion pressures impacted function and injury of marginal kidneys during NMP. Twenty-seven porcine kidneys were subjected to 60 minutes of warm ischemia to induce high IRR mimicking DCD conditions. These kidneys were randomized to 75 mmHg (subphysiological), 95 mmHg (physiological), and 115 mmHg (high physiological) perfusion pressures for 2-hour NMP. For kidneys with high IRR, both 95 mmHg and 115 mmHg perfusion pressures enable an early improvement in renal hemodynamics and function compared to 75 mmHg during NMP, while a high physiological perfusion can cause additional injury. Therefore, physiological perfusion pressure (95 mmHg) strikes a balance between functional recovery and safety, offering a strategy to improve perfusion performance of marginal kidneys that might otherwise be discarded.

Part II Clinical Practice in Kidney Transplantation

In **Chapter 6**, we assessed the safety and feasibility of kidney transplantation in ESRD patients with obesity, and explored the optimal timing of bariatric surgery (BS) in patients who required both BS and KT. This retrospective cohort including 22 patients in the KT first group and 34 in the BS first group showed that both patient and graft survival were favorable and comparable between the KT first and the BS first groups (100% versus 90.5%; 90.9% versus 81.0%). Both pre- and post-transplant BS can achieve favorable weight loss

and acceptable rates of postoperative complications. Different conditions of each transplant candidate should be considered in detail. For patients with high risk of transplantation due to obesity, BS should be considered prior to KT.

In **Chapter 7**, we examined the safety and efficacy of kidney transplantation in patients with aortoiliac atherosclerotic stenosis, which is stratified by the Trans-Atlantic Inter-Society Consensus (TASC) II classification. Propensity score matched data of 131 patients with aortoiliac stenosis and 524 without stenosis showed that patient survival and posttransplant vascular complication were significantly lower in the stenosis group compared to the non-stenosis group. However, death-censored graft survival and graft function were comparable. Aortoiliac atherosclerotic stenosis significantly impacts patient survival but not graft survival. Patients with TASC A/B stenosis have prolonged survival and enhanced quality of life through kidney transplantation. However, for patients with TASC C/D stenosis, kidney transplantation improves quality of life without bringing survival benefits.

In **Chapter 8**, we investigated the additional benefit of simultaneous liver-kidney transplantation (SLKT) in end-stage liver disease patients with concurrent kidney dysfunction compared to liver transplantation alone (LTA) using the Dutch Organ Transplantation Registration data. A retrospective cohort of 52 SLKT and 829 LTA recipients showed that for patients with CKD stage 3b and 4, LTA provides comparable patient and liver graft survival to SLKT. However, for those with CKD stage 5 or on dialysis, SLKT significantly improves survival outcomes. Meanwhile, primary etiology of liver disease and kidney dysfunction severity should be considered when determining SLKT eligibility.

In **Chapter 9**, we further assessed whether SLKT provides a survival benefit compared with LTA across different pretransplant eGFRs and evaluated the impact of the 2017 Organ Procurement and Transplant Network (OPTN) policy change. We retrospectively compared the transplant outcomes of 57,780 LTAs and 5,627 SLKTs using the OPTN/United Network for Organ Sharing (UNOS) registry data. Among patients with pretransplant eGFR ≥30 ml/min/1.73 m^2, SLKT conferred no survival benefits, as LTA recipients achieved comparable or superior long-term survival. In contrast, for patients with pretransplant eGFR

<30 ml/min/1.73 m^2, SLKT significantly reduced posttransplant mortality. Following the 2017 OPTN policy introducing stricter SLKT eligibility and "Safety Net" for kidney-after-liver transplantation, the survival advantage of SLKT observed in the pre-policy era was not evident, with 1.4% of LTA recipients undergoing kidney after liver transplantation under "Safety Net" allocation priority, suggesting that the new policy appears to optimize organ allocation by reducing unnecessary SLKTs while maintaining favorable outcomes.

In **Chapter 10**, we investigated the safety and efficacy of ex-situ repair followed by autotransplantation in patients with renal artery aneurysms (RAAs) unsuitable for endovascular treatment. We retrospectively analyzed a Dutch cohort of 9 patients with 11 RAAs undergoing ex-situ repair and autotransplantation. Eight RAAs were located at the first bifurcation, one on the main trunk, one on the first branch, and one on the second branch. Nephrectomy was performed via laparoscopy (n=7), robotic-assisted laparoscopy (n=1) and laparotomy (n=1). Postoperative complications were recorded in four (44%) patients, including bowel obstruction, delirium, pneumonia and hydronephrosis due to double-J dislocation. Median estimated glomerular filtration rate (eGFR) was 83 ml/min/1.73m^2 pretransplant and 88 ml/min/1.73m^2 posttransplant. By an average follow-up of 32 months, all autotransplanted kidneys had good patency and remained functional. These findings suggest that ex-situ repair with autotransplantation is safe and feasible option for complex RAAs when endovascular intervention is not possible.

In **Chapter 11**, we evaluated the predictive value of intraoperative LSCI-derived imaging features, extracted using a convolutional neural network (CNN), for early graft function after LDKT. We performed intraoperative LSCI in 110 LDKTs, with early graft function defined by eGFR at 1 week. Across multiple machine learning algorithms, models integrating clinical variables with CNN-derived LSCI features consistently outperformed the clinical-only models in both training and testing datasets. CNN attention maps demonstrated physiologically relevant feature localization, and intraoperative LSCI additionally enabled detection and correction of vascular complications, highlighting its potential to enhance both perioperative decision-making and early graft outcome prediction.

Samenvatting

Omdat xenotransplantatie- en kunstorgaan technologieën nog niet klinisch toepasbaar zijn blijft humane niertransplantatie de optimale behandeling voor patiënten met eindstadium nierfalen (ESRD). Om het aanhoudende tekort aan donororganen te verminderen en de prognose van patiënten te verbeteren, zijn drie strategieën van cruciaal belang: het verruimen van de transplantatiecriteria om meer geschikte patiënten toegang te geven tot transplantatie, het vergroten van het gebruik van marginale donornieren op basis van objectieve kwaliteitsbeoordeling, en het behouden van resterende nierfunctie bij patiënten met chronische nierschade (CKD) om transplantatie uit te stellen of te voorkomen.

Deel I Beoordeling van de orgaankwaliteit tijdens machineperfusie

In **Hoofdstuk 2** hebben we de bruikbaarheid van laser speckle contrast imaging (LSCI) onderzocht voor het beoordelen van de renale microcirculatie tijdens normotherme machineperfusie (NMP) van varkensnieren. LSCI maakte visualisatie en semi-kwantificatie van renale corticale perfusie en ischemie mogelijk, waarbij de LSCI-flux een lineaire correlatie vertoonde met de renale bloedstroom. Nadat we een occlusie van een tak van de nierslagader hadden geïnduceerd, was het totale percentage ischemische gebieden aan de ventrale en dorsale zijde vergelijkbaar, maar werden er heterogene patronen tussen de twee zijden waargenomen door middel van LSCI-metingen. LSCI-metingen aan beide zijden bieden toegevoegde waarde ten opzichte van metingen aan één zijde en bepalen van nierfunctiemarkers, aangezien er geen significant verschil werd gevonden in creatinineklaring, fractionele natriumuitscheiding, totale natriumreabsorptie en histologische schade vóór en na occlusie van de nierslagader.

In **Hoofdstuk 3** hebben we de zuurstofverzadiging (sO2) van de niercortex gemeten met behulp van fotoakoestische (PA) beeldvorming tijdens NMP in 22 varkensnieren. Op basis van biomarkers voor nierfunctie en vitaliteit werden de nieren ingedeeld in "niet-functionele" en "functionele" groepen. PA-afgeleide sO2-waarden maakten effectief onderscheid tussen functionele en niet-functionele nieren. Niet-functionele nieren kunnen worden gedetecteerd met een grenswaarde van sO2 < 39%, met een sensitiviteit en specificiteit van respectievelijk 80% en 85%. sO2 correleerde met de renale bloedstroom

en het zuurstofverbruik in alle nieren. In functionele nieren correleerde sO2 ook met de creatinineklaring, wat PA-beeldvorming ondersteunt als een potentiële niet-invasieve biomarker voor vitaliteit.

In **Hoofdstuk 4** onderzochten we de rol van Power Doppler (PD) bij de beoordeling van de vitaliteit van de nier tijdens NMP. PD-afgeleide parameters, waaronder de vascularisatie-index (VI), de flow-index (FI) en de vascularisatie-flow-index (VFI), werden berekend. FI en VFI correleerden matig met de creatinineklaring, terwijl VI sterk correleerde met het zuurstofverbruik. Na 120 minuten NMP lieten deze parameters een hoge diagnostische nauwkeurigheid zien bij het onderscheiden van nieren met een hogere en lagere vitaliteit. Grenswaarden van 17% voor VI, 50 a.u. voor FI en 9 a.u. voor VFI werden gehanteerd. VFI leverde een specificiteit van 100% en een sensitiviteit van 73% op bij het identificeren van nieren met een lage vitaliteit, met een algehele diagnostische nauwkeurigheid van 82%. PD-beeldvorming kan een waardevol alternatief zijn voor RBF tijdens NMP voor de beoordeling van de kwaliteit van de nier.

Nieren van donoren na circulatiestilstand (DCD) worden vaak gekenmerkt door ischemische schade en een hoge intrarenale weerstand (IRR), waardoor ze ongeschikt worden geacht voor transplantatie vanwege slechte functionele prestaties tijdens NMP. In **Hoofdstuk 5** hebben we onderzocht hoe verschillende perfusiedrukken de functie en schade van marginale nieren tijdens NMP beïnvloeden. Zevenentwintig varkensnieren werden gedurende 60 minuten blootgesteld aan warme ischemie om een hoge IRR te induceren, vergelijkbaar met DCD-omstandigheden. Deze nieren werden willekeurig toegewezen aan perfusiedrukken van 75 mmHg (subfysiologisch), 95 mmHg (fysiologisch) en 115 mmHg (hoogfysiologisch) gedurende 2 uur NMP. Bij nieren met een hoge IRR maken zowel perfusiedrukken van 95 mmHg als 115 mmHg een vroege verbetering van de renale hemodynamiek en functie mogelijk in vergelijking met 75 mmHg tijdens NMP, terwijl een hoge fysiologische perfusiedruk extra schade kan veroorzaken. Daarom biedt de fysiologische perfusiedruk (95 mmHg) een evenwicht tussen functioneel herstel en veiligheid, en een strategie om de perfusieprestaties van marginale nieren te verbeteren die anders zouden worden afgekeurd.

Deel II Klinisch praktijk naar niertransplantatie

In **Hoofdstuk 6** hebben we de veiligheid en haalbaarheid van niertransplantatie bij ESRD-patiënten met obesitas, en de optimale timing van bariatrische chirurgie (BS) onderzocht. Deze retrospectieve cohortstudie, met 22 patiënten in de KT-eerst-groep en 34 in de BS-eerst-groep, toonde aan dat zowel de overleving van de patiënt als die van het transplantaat gunstig en vergelijkbaar was tussen de KT-eerst- en de BS-eerst-groep (100% versus 90.5%; 90.9% versus 81.0%). Zowel pre- als posttransplantatie-BS kan leiden tot gunstig gewichtsverlies en acceptabele percentages postoperatieve complicaties. Bij de beslissing welke ingreep eerst uitgevoerd dient te worden, dienen individuele patient kenmerken zorgvuldig afgewogen te worden afgewogen. Voor patiënten met een hoog transplantatierisico als gevolg van obesitas moet BS worden overwogen vóór KT.

In **Hoofdstuk 7** hebben we de veiligheid en effectiviteit van niertransplantatie onderzocht bij patiënten met aorto-iliacale atherosclerotische stenose, ingedeeld volgens de Trans-Atlantic Inter-Society Consensus (TASC) II-classificatie. Gegevens van 131 patiënten met aorto-iliacale stenose en 524 patiënten zonder stenose, verkregen met behulp van propensity score matching, toonden aan dat de patient overleving en de vasculaire complicaties na transplantatie significant lager waren in de groep met stenose vergeleken met de groep zonder stenose. De overleving van het transplantaat (gecorrigeerd voor overlijden) en de transplantaatfunctie waren echter vergelijkbaar. Atherosclerotische stenose van de aorta-iliacale vaten heeft een significant effect op de overleving van de patiënt, maar niet op de overleving van het transplantaat. Patiënten met TASC A/B-stenose hebben een langere overleving en een verbeterde kwaliteit van leven na niertransplantatie. Bij patiënten met TASC C/D-stenose verbetert niertransplantatie echter de kwaliteit van leven zonder een overlevingsvoordeel te bieden.

In **Hoofdstuk 8** onderzochten we het extra voordeel van gelijktijdige lever-niertransplantatie (SLKT) bij patiënten met eindstadium leverfalen en gelijktijdige nierfunctiestoornis, vergeleken met levertransplantatie alleen (LTA), met behulp van gegevens uit het Nederlandse Orgaantransplantatie Register. Een retrospectieve cohortstudie met 52 SLKT- en 829 LTA-ontvangers toonde aan dat LTA bij patiënten met CKD-stadium 3b en 4 een vergelijkbare overleving van de patiënt en het levertransplantaat

biedt als SLKT. Bij patiënten met CKD-stadium 5 of dialysepatiënten verbetert SLKT de overleving echter significant. De primaire oorzaak van de leverziekte en de ernst van de nierfunctiestoornis moeten in overweging worden genomen bij het bepalen van de geschiktheid voor SLKT.

In **Hoofdstuk 9** beoordeelden we verder of SLKT een overlevingsvoordeel biedt ten opzichte van LTA in verschillende eGFR-waarden vóór de transplantatie en evalueerden we de impact van de beleidswijziging van het Organ Procurement and Transplant Network (OPTN) uit 2017. We hebben retrospectief de transplantatieresultaten van 57,780 levertransplantaties (LTA's) en 5,627 gelijktijdige lever-niertransplantaties (SLKT's) vergeleken met behulp van de OPTN/United Network for Organ Sharing (UNOS)-registergegevens. Bij patiënten met een eGFR ≥30 ml/min/1.73 m^2 vóór de transplantatie bood SLKT geen overlevingsvoordeel, aangezien LTA-ontvangers een vergelijkbare of betere overleving op lange termijn bereikten. Daarentegen verminderde SLKT de posttransplantatiemortaliteit significant bij patiënten met een eGFR <30 ml/min/1.73 m^2 vóór de transplantatie. Na de invoering van het OPTN-beleid in 2017, dat strengere SLKT-criteria en een "vangnet" voor nieren na levertransplantatie introduceerde, was het overlevingsvoordeel van SLKT dat vóór de beleidswijziging werd waargenomen niet langer evident. Slechts 1,4% van de LTA-ontvangers onderging een niertransplantatie na levertransplantatie met voorrang binnen het "vangnet". Dit suggereert dat het nieuwe beleid de orgaanallocatie lijkt te optimaliseren door onnodige SLKT's te verminderen en tegelijkertijd gunstige resultaten te behouden.

In **Hoofdstuk 10** onderzochten we de veiligheid en werkzaamheid van ex-situ herstel gevolgd door autotransplantatie bij patiënten met aneurysma's van de nierarterie (RAA's) die niet geschikt waren voor endovasculaire behandeling. We analyseerden retrospectief een Nederlands cohort van 9 patiënten met 11 RAA's die een ex-situ reparatie en autotransplantatie ondergingen. Acht RAA's bevonden zich bij de eerste bifurcatie, één op de hoofdstam, één op de eerste tak en één op de tweede tak. Nefrectomie werd uitgevoerd via laparoscopie (n=7), robot geassisteerde laparoscopie (n=1) en laparotomie (n=1). Vier (44%) patiënten ontwikkelden postoperatieve complicaties, waaronder darmobstructie, delirium, longontsteking en hydronefrose als gevolg van dislocatie van een dubbel-J-stent. De mediane geschatte glomerulaire filtratiesnelheid (eGFR) was 83 ml/min/1.73m^2 vóór de

transplantatie en 88 ml/min/1.73m^2 ná de transplantatie. Na een gemiddelde follow-up van 32 maanden waren de vaten van alle auto getransplanteerde nieren goed doorgankelijk en functioneel. Deze bevindingen suggereren dat ex-situ reparatie met autotransplantatie een veilige en haalbare optie is voor complexe RAA's wanneer endovasculaire interventie niet mogelijk is.

In **Hoofdstuk 11** hebben we de voorspellende waarde geëvalueerd van intraoperatieve LSCI-afgeleide beeldkenmerken, geëxtraheerd met behulp van een convolutioneel neuraal netwerk (CNN), voor de vroege transplantaatfunctie na LDKT. We hebben intraoperatieve LSCI uitgevoerd bij 110 LDKT's, waarbij de vroege transplantaatfunctie werd gedefinieerd door de eGFR na 1 week. Bij meerdere machine learning-algoritmen presteerden modellen die klinische variabelen integreerden met CNN-afgeleide LSCI-kenmerken consequent beter dan de modellen die alleen klinische gegevens gebruikten, zowel in de trainings- als in de testdatasets. CNN-aandachtskaarten lieten fysiologisch relevante kenmerk lokalisatie zien, en intraoperatieve LSCI maakte bovendien de detectie en correctie van vasculaire complicaties mogelijk, wat het potentieel ervan benadrukt om zowel de perioperatieve besluitvorming als de vroege voorspelling van de uitkomst van de transplantatie te verbeteren.

List of Publications

1. **Fang Y**, Bouari S, Hoogduijn MJ, Ijzermans JNM, de Bruin RWF, Minnee RC. Therapeutic efficacy of extracellular vesicles to suppress allograft rejection in preclinical kidney transplantation models: A systematic review and meta-analysis. Transplant Rev (Orlando). 2022 Dec;36(4):100714.

2. **Fang Y**, Outmani L, de Joode AAE, Kimenai HJAN, Roodnat JI, 't Hart JWH, Biter UL, Klaassen RA, de Bruin RWF, IJzermans JNM, Pol RA, Minnee RC. Bariatric surgery before and after kidney transplant: a propensity score-matched analysis. Surg Obes Relat Dis. 2023 May;19(5):501-509.

3. **Fang Y**, van Ooijen L, Ambagtsheer G, Nikolaev AV, Clahsen-van Groningen MC, Dankelman J, de Bruin RWF, Minnee RC. Real-time laser speckle contrast imaging measurement during normothermic machine perfusion in pretransplant kidney assessment. Lasers Surg Med. 2023 Oct;55(8):784-793.

4. **Fang Y**, Moelker A, den Hoed CM, Porte RJ, Minnee RC, Boehnert MU. Outflow obstruction after living donor liver transplantation managed with a temporary vena cava filter: A case report. Int J Surg Case Rep. 2023 Nov;112:108981.

5. **Fang Y**, Hamm JJM, den Hartog FPJ, Kimenai HJAN, de Bruin RWF, Minnee RC. Safety and efficacy of kidney transplantation in patients with aortoiliac stenosis: a retrospective cohort study. Int J Surg. 2024 Feb 1;110(2):992-999.

6. Nikolaev AV*, **Fang Y***, Essers J, Panth KM, Ambagtsheer G, Clahsen-van Groningen MC, Minnee RC, van Soest G, de Bruin RWF. Pre-transplant kidney quality evaluation using photoacoustic imaging during normothermic machine perfusion. Photoacoustics. 2024 Feb 9;36:100596.

7. **Fang Y***, Nikolaev AV*, Essers J, Ambagtsheer G, Clahsen-van Groningen MC, Minnee RC, de Bruin RWF, van Soest G. Enhancing Kidney Quality Assessment: Power Doppler During Normothermic Machine Perfusion. Artif Organs. 2025 Jul;49(7):1132-1140.

8. **Fang Y**, Kimenai HJAN, de Bruin RWF, de Vries DK, Petri BJ, Warlé MC, Tielliu IFJ, van Laanen J, Idu MM, Pol RA, Minnee RC; Dutch Kidney Transplant Study Group. Treatment of Renal Artery Aneurysm by ex situ Repair and Autotransplantation: A Nationwide Cohort Study. Eur Surg Res. 2024;65(1):123-129.

9. **Fang Y**, Ambagtsheer G, Xia L, Clahsen-van Groningen MC, Minnee RC, de Bruin RWF. Physiological arterial pressure improves renal performance during normothermic machine perfusion in a porcine kidney DCD model. Heliyon. 2025 Jan 10;11(2):e41610.

10. **Fang Y**, Westenberg LB, Hamm JJM, van de Wetering J, Bakker SJL, de Bruin RWF, Pol RA, Minnee RC. Impact of Donor and Recipient Sex on Long-Term Outcomes Following Living Donor Kidney Transplantation: A Retrospective Dual-Center Study. Clin Transplant. 2025 Oct;39(10):e70335.

11. Bouari S*, **Fang Y***, van de Wetering J, de Meijer VE, Pol RA, Berger SP, Polak WG, Blokzijl H, de Vries APJ, Coenraad MJ, Lam HD, de Vries DK, Porte RJ, den Hoed CM, IJzermans JNM, Minnee RC. Simultaneous Liver-Kidney Transplantation versus Liver Transplantation in End-Stage Liver Disease Patients with Kidney Dysfunction. Eur Surg Res. 2026;67(1):46-55.

12. **Fang Y***, Bouari S*, van de Wetering J, den Hoed CM, de Bruin RWF, Porte RJ, Polak WG, Minnee RC. Simultaneous Liver-kidney Versus Liver Transplantation Categorized by Pretransplant eGFR: Impact of the 2017 OPTN Policy. Transplantation. 2026 Jun 30.

13. Li S*, **Fang Y***, Minnee RC, de Bruin RWF, Hoogduijn MJ. Mesenchymal stromal cell derived membrane particles improve metabolic activity and functional performance during porcine kidney normothermic machine perfusion. Am J Nephrol.

14. Minnee RC, Sakamoto S, Fukuda A, Uchida H, Hirukawa K, Honda M, Okumura S, Ito T, Yilmaz TU, **Fang Y**, Ikegami T, Lee KW, Kasahara M; Vanguard Multi-Center Study of International Living Donor Liver Transplantation Group. Long-Term Outcomes of Living Donor Liver Transplantation for Methylmalonic Acidemia. Pediatr Transplant. 2024 Sep;28(6):e14834.

15. Lin H, Bousnina K, Slagter JS, **Fang Y**, Cristoferi I, Garrelds IM, Danser AHJ, Reinders MEJ, Minnee RC, Hoogduijn MJ. (Pro)renin, Erythropoietin, Vitamin D and Urodilatin Release From Human Donor Kidneys During Normothermic Machine Perfusion: Predictors of Early Post-Transplant Outcome? Clin Transplant. 2025 May;39(5):e70163.

16. Yan H, **Fang Y**, van de Wetering J, Kimenai HJAN, de Bruin RWF, Minnee RC. Effect of donor body weight on en bloc pediatric kidney transplantation in adults: A systematic review and meta-analysis. Transplant Rev (Orlando). 2025 Jul;39(3):100918.

17. Li S, Tejeda-Mora H, Slagter JS, Hullegie-Peelen DM, Cristoferi I, **Fang Y**, Bouari S, Schumacher D, Babler A, Schreibing F, Anslinger T, Reinders MEJ, Kramann R, Minnee RC, Hoogduijn MJ. Cellular Responses During Kidney Normothermic Machine Perfusion Reflect Graft Outcomes. Kidney Int Rep. 2025 Aug 20;10(11):4012-4026.

18. Czogalla J, Hausmann F, Lagies S, Gies SE, Christiansen S, Kaiser N, Haas F, Okabayashi Y, Kylies D, Hofmann S, Franzin R, Sabra N, Bouari S, **Fang Y**, Ambagtsheer G, Edenhofer I, Chilla S, Mühlig AK, Zimmermann M, Wong MN, Yokoo T, Kretz O, Lindenmeyer M, Grahammer F, Hoogduijn MJ, de Bruin R, Kuehl M, Hänzelmann S, Kammerer B, Gesualdo L, Bonn S, Minnee RC, Huber TB, Puelles VG. Metabolite-enhanced normothermic machine perfusion improves kidney transplant viability. JCI Insight. 2025 Sep 23;10(18):e190185.

19. Slagter JS, Bouari S, Rijkse E, Cristoferi I, **Fang Y**, Papamanoli A, Stubbs A, de Jonge J, de Bruin RWF, van den Hoogen MWF, Hoogduijn MJ, Clahsen-van Groningen MC, Porte RJ, Kimenai HJAN, Minnee RC. Normothermic versus hypothermic machine perfusion in kidney transplantation: A randomized controlled trial. Am J Transplant. 2026 May;26(5):1070-1079.

* Equal co-first authorship.

Acknowledgments

Hora finita!

Looking back on the past five years, I feel an overwhelming sense of pride in completing this thesis and the journey it represents. Although only my name appears on the cover, this dissertation is by no means the achievement of one person alone. It is the result of the guidance, encouragement, generosity, and friendship of everyone who have accompanied me throughout this unforgettable journey. I would like to express my heartfelt appreciation to all of you.

Dr. de Bruin, Dear **Ron**, it has been a great privilege to have you as my promotor throughout my PhD journey. Thank you for your unwavering guidance, patience, and trust, not only in my scientific development but also in my life. Your expertise in transplantation research has shaped the way I approach scientific questions, teaching me to think independently, critically evaluate evidence, and solve problems with confidence.
One of my first surprises after arriving in the Netherlands came during our very first meeting, when you greeted me in Chinese. I was amazed by your familiarity with different parts of China, which instantly made me feel at home. Even more unexpectedly, we discovered that we share a passion beyond science: reptiles, and your knowledge in this field is truly on another level! Looking back, I realize that our discussions extended far beyond research, and I will always cherish those discussions and the unique connection we developed.

Dr. Minnee, Dear **Robert**, thank you for opening the door to my PhD journey in the Netherlands. Your positive response to my application marked the beginning of an unforgettable chapter in my life. I still remember my first week at Erasmus MC, when you introduced me to colleagues, showed me around the hospital and operating room, and made every effort to help me adapt to a completely new environment.
Your approachable personality quickly changed my preconceived image of a “strict supervisor”. Coming from similar backgrounds, we always had endless discussions about transplant surgery and organ donation. I am truly grateful for the opportunity to work together on the projects in kidney transplantation and machine perfusion. Your support, encouragement, and confidence in me have been invaluable throughout these years.

Professor Hesselink, **Professor Gijsen**, **Professor Baan**, **Professor van Soest**, **Dr. Pol**, **Dr. van de Wetering**, **Dr. Essers**, and **Dr. Dor**, I sincerely thank you for serving on my reading committee and/or PhD defense committee. I am truly honored that you have devoted your valuable time and expertise to evaluating my dissertation and participating in this important milestone of my academic journey.

Dear **Gisela**, you are the colleague I spent the most Monday mornings with over the past few years. Every Monday, we loaded your car with ice boxes, perfusion solutions, and all kinds of equipment, yet you never complained. Those early morning drives, filled with conversations and beautiful scenery, have become my favourite memory.
Beyond the laboratory, you are always an extraordinary mother. Balancing research work with life is never easy, and you have always managed it with remarkable dedication. Thank you for everything, and I wish you and your family all the happiness and in the future.

To the APOLLO Study team, **Elsaline**, **Dafsy**, **Iacopo**, and **Julia**, it was a pleasure working alongside you on the APOLLO study. This project demanded many long evenings and late nights, but those efforts were ultimately rewarded with a successful publication. Thank you for making such a demanding project both productive and memorable.

To all transplant surgeons, **Dr. Kimenai**, **Dr. Dor**, **Dr. Tran**, and **Dr. Kooreman**; fellows, **Joost**, **Karin**, and **Kantoku**; together with **nurses**, **anesthesiologists**, and **OR staff**, thank you for your support during intraoperative laser speckle contrast imaging measurements. Acquiring intraoperative imaging data would not have been possible without your patience, and seamless collaboration.

Dr. Kimenai, Dear **Diederik**, you showed me that an excellent surgeon does not have to fit the stereotype of being serious and distant. Your openness, enthusiasm, and genuine interest in people are undoubtedly among the qualities that make you highly regarded by both colleagues and patients.

To the **nurses** and **secretaries** from the Department of Nephrology and Vascular Surgery, thank you for your kindness, patience, and continuous support throughout my clinical studies. Although much of your work takes place behind the scenes, it was indispensable to the successful completion of my research.

Dear **Carola** and **Ilone**, sincerely thank you for your invaluable administrative support. Your efficiency, kindness, and willingness to help with administrative tasks allowed me to focus on my research.

To the liver perfusion group, **Dr. de Jonge**, **Jorke**, **Stef**, **Efrayim**, **Puck**, **Roberto**, **Colin**, **Peter**, and **Lisa**, I sincerely appreciate the guidance and support from everyone in the liver perfusion group. I wish your team continued success, exciting discoveries, and many more achievements in the years to come. Dear **Puck**, it was a pleasure to work with you on the combined machine perfusion project. I have always admired your openness, straightforward communication, and decisive approach to both research and teamwork.

To my (former) colleagues in Ee173, **Dimitri**, **Bastiaan**, **Ivo**, **Mathijs**, **Olivier**, **Annick**, **Floris**, **Vincent**, **Rudolf**, **Lucas**, and **Sarah**, you were among the very first colleagues I met in the Netherlands and the people with whom I shared the office for the longest time. Thank you for creating such a welcoming environment filled with laughter, interesting conversations, and unforgettable coffee breaks.

Dear **Professor Mahmoudi**, **Dr. Palstra**, **Tsung Wai**, and friends from Ee634, every visit to your office was filled with positive energy, and laughter. **Raquel**, **Shringar**, and **Chengcheng (程程)**, thank you for sharing unforgettable concert nights with me. Those evenings filled with great music, laughter, and friendship will always remain among my favourite memories. **Tonmoy**, **Liset**, **Zora**, and **Annefien**, thank you for standing beside us as witnesses of our partnership registration. Sharing such a special day with friends made it even more meaningful, and we hope the happiness will stay with all of you in the future.

Department of Pathology, **Dr. Clahsen-van Groningen**, **Dr. van den Bosch**, **Jody**, **Agni**, **Angelique**, and **Shazia**, thank you for the wonderful collaboration. Our project would not have been possible without your expertise, and willingness to support every new idea.

Dear **Marian**, every time I came to your office, you were always surrounded by slides, reports, and an endless list of tasks. I often felt slightly guilty interrupting your busy schedule just to ask, “Could you please have a quick look at my slides?” Yet, despite how busy you were, you never hesitated to help.

Dear **Jody**, what began as a research collaboration gradually developed into a genuine friendship. I have always admired your professionalism and dedication to your work. Every clinical sample we collected was handled with exceptional care. More importantly, I truly appreciate your commitment to our collaboration and your unwavering support. I sincerely hope that our ongoing study will soon reach a successful publication.

Dear **Haichen (海晨)**, I have had the privilege of witnessing you become increasingly confident, and develop your own research ideas. Spending so much time together, we gradually became friends and talked about almost anything, far beyond research itself. Thank you for sharing not only scientific discussions but also valuable life lessons that no textbook could ever teach. I am certain these lessons will continue to benefit me throughout my career and life.
One thing that has always impressed me is your devotion to your family. Seeing you video call your wife and child every day reminded me that family always comes first. I sincerely wish you every success in completing your PhD, and even more importantly, a happy and fulfilling life.

Dear **Marco**, it has been a pleasure working with you on the combined machine perfusion project. Beyond research, some of our favourite memories are food, beer, football, and countless enjoyable conversations. Thank you for introducing me to authentic Italian risotto and for sharing a little piece of Italian culture with me.
On a more serious note, I am truly happy to see you starting your own PhD journey. I have no doubt that you will achieve great things, and I wish you every success in the years ahead. Wherever life takes us, I will always be able to say with a smile, *"I have a good friend in Italy!"*

Dear **Ferry** and everyone at **Slagerij van Meurs**, few people outside transplantation research understand how much important science begins in places like yours. Thank you for generously providing the porcine organs that formed the foundation of my preclinical research. Without your support, a substantial part of this thesis would simply not have been possible.

To all my collaborators, science is never accomplished alone, and this thesis is the result of collaborations with many outstanding colleagues across different disciplines and institutions.

My sincere thanks go to **Professor van Soest**, **Dr. Pol**, **Dr. Hoogduijn**, **Professor Ijzermans**, **Professor Porte**, **Professor Dankelman**, **Dr. Roodnat**, **Karim**, **Dr. den Hoed**, **Abylaikhan**, **Dr. Polak**, **Julie**, **Professor de Meijer**, **Dr. Tielliu**, **Lisa**, **Christiaan**, **Kimberly**, **Liselotte**, **Professor Bakker**, **Dr. de Joode**, **Lisanne**, **Professor Alwayn**, **Dr. de Vries**, **Dr. Idu**, **Dr. Petri**, **Professor Warlé**, **Dr. van Laanen**, **Dr. Biter**, **Judith**, and **Dr. Klaassen**. Thank you for your expertise, generosity, and the many productive collaborations that made this thesis stronger.

Dr. Nikolaev, Dear **Anton**, working with you has been one of the most interesting interdisciplinary collaborations. Your "scientific rigor" of questioning every assumption and refining every detail is a quality that I have come to admire deeply, and one that undoubtedly makes you an outstanding scientist.

I am really delighted to see you find happiness outside academia as well. I sincerely wish you and **Rosie** (**煦**) a lifetime of happiness together, and I hope you continue enjoying Chinese culture, and perhaps becoming an honorary "Chinese son-in-law".

Dr. Tan, Dear **Raoul**, every time we meet, we somehow end up talking for hours, and 99% of those conversations are about fishing! I hope we will continue sharing many fishing stories, and hopefully a few unforgettable fishing trips in the years to come.

Beyond our shared hobby, I also want to thank you for everything you have done to support Chinese PhD students at Erasmus MC. Your efforts to improve their experience have made a real difference to many of us. I truly admire your generosity and dedication, and I know your kindness will continue to inspire many international students in the future.

To **all kidney transplant patients and living and deceased organ donors**, this thesis would not have been possible without your generosity, trust, and participation. Every clinical sample, every medical image, and every piece of data ultimately represents a person, a family, and a story.

To the donors and their families, your selfless decision to donate has given others a second chance at life while also advancing scientific knowledge that may benefit countless future

patients. I sincerely hope that the work presented in this thesis will, in some small way, contribute to improving transplantation for future generations of patients.

I would also like to thank the **Department of Surgery**, **Transplant Institute**, **Applied Molecular Imaging Erasmus MC (AMIE)**, **Triallab**, **Nederlandse Transplantatie Vereniging (NTV)**, **the Dutch Research Council (NWO)**, and **the Dutch Kidney Transplant Study Group** that supported my research through scientific collaboration, educational opportunities, conference participation, and financial sponsorship. Your continued commitment to advancing transplantation research has been invaluable to both my professional development and the completion of this thesis.

I gratefully acknowledge the **China Scholarship Council (国家留学基金委员会)** for providing me with the opportunity to pursue my doctoral studies in the Netherlands. This scholarship not only enabled my academic journey abroad but also opened the door to invaluable international collaborations, lifelong friendships, and experiences that have profoundly shaped both my professional career and personal life. I sincerely hope that the knowledge and experience I have gained during these years will allow me to contribute to the continued development of transplantation research and to strengthen scientific collaboration between China and the Netherlands.

Dear **Zhimao (志茂)**, **Yuan (誉菡)**, and **Duoduo (多多)**, thank you for bringing so much joy, delicious food, and wonderful companionship into our lives. It was a great honor to witness your wedding in Prague, the most important moment of your lives. I sincerely wish you both every success in your careers, a lifetime of happiness together, and hope that Duoduo grows up healthy, happy, and full of laughter.

Dear **Junfeng (黄老师)** and **Bingqi (胡老师)**, thank you for sharing so many relaxed and enjoyable moments with us. Watching the European Championship together, playing football, and talking about work and life brought so much joy and balance to those busy days. I wish you both every success and happiness, wherever life may take you and whatever challenges lie ahead.

Dear **Yahong (亚鸿师兄)** and **Yuwei (雨薇师姐)**, you have always been role models for us, both in research and in life. I am grateful for the opportunity to travel with you, explore France, and watch the Paris Saint-Germain match together. The beautiful places we visited and the laughter we shared will always remain treasured memories. I wish you continued success and fulfillment in both your careers and your lives.

Dear **Li (游历师姐)** and **Shengbing (圣冰)**, thank you for the enjoyable collaborations we shared. I learned a great deal from working with you, and through you I also discovered many wonderful places and delicious food in Rotterdam! I wish you both every success in your careers and a happy, fulfilling life.

Dear friends from the neighbouring lab (**Wenqiu (文秋师姐)**, **Ziyun (子芸)**, **Yihe (乙壑)**, **Jing (王婧)**, **Yu (蔡宇)**, and **Liang (贾亮)**), **Tsai-Ying**, **Liang (吴亮师兄)**, **Hui (林惠师姐)**, **Tingyue (廷跃师兄)**, **Peifen (培芬师姐)**, **Zhongli (忠丽师姐)**, **Can (灿哥)**, **Anyan (安延)**, **Maria**, **Zilong (子龙)**, **Bibi**, **Mason**, **Yingxia (英侠)**, **Xincheng (欣澄师妹)**, **Li (陈力)**, **Jie (刘洁)**, **Mengqi (梦琪)**, **Shuqi (书琦)**, and everyone from the **"EMC Athletes (EMC 的体育生们)" football group**, thank you for making my years in the Netherlands so memorable. Whether we were sharing meals, playing football, travelling together, or simply talking about life, celebrating successes, and sharing the challenges, you made life far away from home feel much warmer. I feel incredibly fortunate to have met all of you, and I am grateful that you have become such an important part of my life. I wish each of you a bright future, continued growth in the paths you are passionate about, and every happiness and success in the years to come.

我的硕士研究生导师**赵红川教授**，以及安徽医科大学第一附属医院器官移植中心（干三）的所有老师（**耿小平教授**，**黄帆主任**，**吴若林博士等**）、师兄弟，感谢你们一直以来对我的培养、帮助与鼓励。安徽医科大学是我医学梦想开始的地方，而器官移植中心（干三）则是我踏入器官移植领域的起点。在那里，我不仅学习了专业知识和外科技能，更学会了如何成为一名严谨、负责、有担当的医生。正是那段宝贵的经历，为我来到荷兰攻读博士、探索器官移植研究奠定了坚实的基础。

夏林，感谢你不远万里来到荷兰，与我们一起领略少女峰的壮丽雪景，欣赏佛罗伦萨的温柔落日。每次回国，你也总会带着我们去寻找那些藏在山水与烟火里的美好：塔川层林尽染的秋色，奇墅湖洒满晨光的湖面，秀里鱼灯点亮古村的夜晚……正因为有你的陪伴，这些旅程才拥有了更深的意义，也成为我们共同珍藏的回忆。期待未来还能与你一起探索更多未知的风景，书写更多值得铭记的故事。

感谢**我的家人**，以及**星语的父母**，感谢你们始终无条件地支持着我们人生中的每一个选择。无论我们身在何方，你们永远都是我们最坚强的后盾。在我们远离家乡、专注于学习和工作的这些年里，是你们默默承担起家庭中的一切，让我们少了一份牵挂，多了一份安心。你们给予我们的关爱与理解，早已超越了言语所能表达。

也感谢可爱的弟弟妹妹，以及国内的朋友们，你们让我们的大家庭始终充满欢声笑语，也让我们即使身处异国，依然能感受到熟悉与温暖。愿未来的日子里，我们都能健康平安，常伴彼此，共享更多幸福而珍贵的时光。

最后，我想把最深的感谢留给我的爱人，**星语**。从校园恋爱到博士毕业，我们携手走过十年的时光。十年间，我们一起走过山川湖海，看过无数次日出日落，分享成功的喜悦，也共同面对挫折与迷茫。无论顺境还是逆境，你始终陪伴在我身边，给予我最坚定的支持和最温暖的依靠。

我一直相信，爱情最美好的模样，是彼此尊重，相互支持，共同成长。从你的身上，我看到的不仅是热爱时尚、懂得生活的女孩，更是一位自信、坚韧、独立的女性。你不断追求自己的梦想，也始终鼓励我坚持自己的方向。我们不仅是生活中的伴侣，更是精神上的知己，是彼此最坚定的支持者。

我期待与你一起迎接未来的每一个十年，一起去更多的地方，看更多的风景，经历更多的人生。愿未来的每一天，我们都能像今天一样，坚定地站在彼此身边。

Roy in Rotterdam, 7 August 2026

方翊天于荷兰鹿特丹，2026 年 8 月 7 日

PhD Portfolio

Name	Yitian Fang
PhD period	2021-2026
Department	Surgery
Supervisors	Dr. R.W.F. de Bruin (promotor) Dr. R.C. Minnee (co-promotor)

Courses	**Year**	**ECTS**
Laboratory Animal Science	2022	4.0
Sex & Gender in Research	2023	0.3
Good research practices: improving my research with open science	2024	0.6
Basic Flow Cytometry Course	2025	0.1
Scientific Integrity	2026	0.3
Conferences and seminars		
Bootcongres, Leiden	2022	0.5
Wetenschapsdag heelkunde, Erasmus MC (oral)	2023	1.0
Bootcongres, Groningen (oral)	2023	1.0
NWO Innovation Festival, Utrecht (pitch)	2023	1.0
European Society for Organ Transplantation, Athens (poster)	2023	2.0
Wetenschapsdag heelkunde, Erasmus MC (oral)	2024	1.0
Bootcongres, Utrecht (poster)	2024	0.5
The Transplantation Society, Istanbul (oral)	2024	2.5
Wetenschapsdag heelkunde, Erasmus MC	2025	0.5
Bootcongres, Rotterdam (oral)	2025	1.0
European Society for Organ Transplantation, London (poster)	2025	2.0
Transplant Institute Day (oral)	2025	1.0

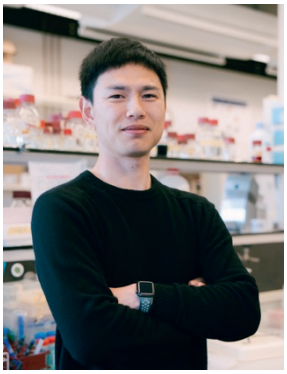
Teaching

Supervision master thesis (L. van Ooijen)	2022	5.0
Supervision master thesis (J. Hamm)	2023	2.5
Minor organ transplantation ‘machine perfusion’	2024-2025	0.6
Supervision bachelor systematic review	2025	0.5
Supervision systematic review (A. Sharmenov)	2025	2.5

Grant

NWO Open Mind	2023

About the Author



Yitian (Roy) Fang was born on August 24, 1995, in Pingwang, Suzhou, China. After completing high school in 2013, he began his medical education at Anhui Medical University through an integrated five-year bachelor's and three-year master's programme in clincal medicine.

In 2018, he started a three-year postgraduate training in HPB surgery and liver transplantation. During this period, he completed clinical rotations as a surgical resident and obtained certificates of practicing physician qualification and standardized residency training. He also completed his master's thesis, entitled *"A Single-Center Clinical Study of Multidrug-Resistant Bacterial Infections after Liver Transplantation"*.

In 2021, he was awarded the CSC scholarship and started his full-time PhD training at Erasmus MC, the Netherlands. His doctoral research focused on kidney transplantation and normothermic machine perfusion, with a particular interest in organ quality assessment and translational research in transplantation.

During his life outside of research, he had a passion for fishing. He became a member of HSV Groot Rotterdam and Verenigde Hengelsport Regio Dordecht. He enjoyed exploring diverse fishing opportunities. His PB catches include a 48cm perch, an 87cm zander, an 80cm pike from the Dutch waterways, and a 56cm largemouth bass from Lake Biwa.

Throughout his PhD training, he further developed his interest in transplantation and realized that his research experience and clinical background were a good fit in transplant surgery. Therefore, he will return to clinical practice as a HPB and transplant surgeon in the First Affiliated Hospital of Anhui Medical University.

